EXPERIMENTAL STUDIES OF ASTROCHEMICAL ION-ATOM AND ION-MOLECULE REACTIONS

A Thesis
Presented for the Degree
of Doctor of Philosophy in Chemistry
In the
University of Canterbury

by
Graham Bruce Ian Scott

University of Canterbury
1997

Some men see things as they are and say why? I dream of things that never were and say why not?

John F. Kennedy 1917-1963

This thesis is dedicated to Mum and Dad, who provided the raw materials, and to Murray and Kate, who "added value".

ABSTRACT

Data is presented for a number of ion-molecule and ion-atom reactions of likely relevance to the chemistry of interstellar clouds and planetary atmospheres. The measurements were made using a Selected Ion Flow Tube, (SIFT), operating at ambient temperatures, (300 ± 5 K), and at pressures between 0.30 - 0.35 Torr.

The reactivity of two $C_3H_3O^+$ isomers, namely protonated propynal, ($HC{\equiv}C\text{-}CHOH^+$), and the association product of $C_2H_3^+$ with CO, ($C_2H_3^+.CO$), were characterised in laboratory experiments. These measurements bracket the proton affinity of propynal between 759 and 736 kJ mol^{-1}. The proton affinity of propadienone is similarly constrained between 896 and 868 kJ mol^{-1}. In a complementary investigation, the $C_3H_3O^+$ potential surface was mapped using ab-initio calculations at the G2 level of theory. This combined experimental / theoretical study demonstrates that the condensation product between $C_2H_3^+$ and CO is C2-protonated propadienone, ($H_2C{=}CH\text{-}C{=}O$). Consequently, this finding indicates that propynal is *not* synthesised in the interstellar medium via the reaction of $C_2H_3^+$ with carbon monoxide.

The reactions between twenty-eight cations and molecular and atomic hydrogen were examined in a series of laboratory experiments. Most hydrocarbon cations react with H atoms by termolecular association or, alternatively, H atom transfer routes. In contrast, only unsaturated hydrocarbon cations tend to react with H_2 via H atom abstraction processes. There are fewer clear trends evident in the reactions between non-hydrocarbon ions and H atoms. If exothermic, H atom abstraction is almost always observed during reactions between non-hydrocarbon cations and H_2. Molecular and atomic hydrogen are both extremely plentiful in dense and diffuse interstellar clouds and these processes are therefore particularly relevant to the chemistry occurring within these objects.

Results are presented for the reaction of approximately thirty cations with molecular and atomic nitrogen. Most ions are unreactive with N_2, however atomic nitrogen is a more reactive neutral species. Small hydrocarbon cations react with N atoms by forming C-N bonds and eliminating H or H_2, while larger

$C_mH_n^+$ species react with this neutral by forming HCN and a fragment hydrocarbon ion. In general there are no obvious patterns to the reactivity of non-hydrocarbon cations with atomic nitrogen. These processes are pertinent both to interstellar chemistry and the aeronomy of nitrogenous planetary atmospheres.

The crucial reaction between H_3^+ and N has been measured for the first time in the laboratory and found to be rapid, ($k = 4.5 \times 10^{-10}$ cm^3 s^{-1}). This result offers an alternative, (and possibly more facile), synthetic route to ammonia in interstellar clouds.

Data is reported for the reaction of nineteen cations with O atoms, O_2 and NO. Small and medium sized hydrocarbon cations react with O atoms forming $C_mH_nO^+$ ions and an H or H_2 fragment, whilst larger $C_mH_n^+$ ions often react by C atom transfer forming CO and a smaller hydrocarbon ion. Most non-hydrocarbon cations examined were unreactive with atomic oxygen. Molecular oxygen is relatively unreactive with most ionic species, however many ions react with NO by charge transfer and / or termolecular association pathways. Nitric oxide, O_2 and O atoms are all present to varying degrees in interstellar clouds, hence the measurements presented here are applicable to the chemistry of these objects.

A number of preliminary experiments between ions and atomic carbon are detailed. The techniques for generating C atoms are described.

The research described in this thesis is pertinent to the many environments in which plasmas occur.

TABLE OF CONTENTS

ACKNOWLEDGEMENTS

Firstly, and primarily, I wish to acknowledge the tremendous assistance that I have received over the last 4 ½ years from my Supervisor, Dr Murray J. McEwan. Not only is Murray a dedicated and excellent scientist, but he is also an extremely likeable individual, and I have benefited greatly from our association. Murray only managed to bewilder me on one occasion and this was during the watching of a rugby test, when in an effort to placate a colleague's annoyed spouse he was heard to say "Rugby – I can take it or leave it!"

I wish also to thank my Associate Supervisor Dr Colin G. Freeman for his many efforts on my behalf. Dr Robert G.A.R. Maclagan has supervised all of the theoretical calculations that have been undertaken during this research and I am appreciative of his guidance.

David A. Fairley and Daniel B. Milligan assisted in gathering nearly all of the data presented in this thesis and I thank them both for their astute observations during the course of this work.

I would also like to take this opportunity to thank Professor David Smith and his colleague Dr Patrik Spanel for their marvellous efforts in helping to upgrade the SIFT instrument at the University of Canterbury during their visit to New Zealand in 1994. The expertise and timely advice provided by these distinguished scientists facilitated the collection of much of the data presented in this thesis.

I have also gained greatly by meeting and working alongside other eminent scientists who have visited the Chemistry Department over the course of my Ph. D. In particular I would like to mention the associations I have enjoyed with Professors Nigel G. Adams and Lucia M. Babcock, and Dr Vincent G. Anicich.

The technical staff of the mechanical, electronic and glassblowing workshops have been involved in maintaining and upgrading the SIFT instrument during the course of this research and I thank them for their labours. I should add that I have been rather impressed by the quality of work and the attention to detail demonstrated by the technicians undertaking the various projects.

I thank the University of Canterbury for the provision of a Doctoral Scholarship for the first three years of my Ph.D. Additionally the Marsden Fund provided some funding during the last ten months of the research and I thank them for this financial support.

I extend my thanks to Wendy Marsh for the preparation of some diagrams that have been incorporated into this thesis.

I would also like to acknowledge the marvellous efforts of Kathryn Hindmarsh, who proof-read this thesis. I should add that all remaining errors and omissions are my responsibility. Kate has been a wonderful friend, confidant and companion over the last 2 ½ years and I have greatly enjoyed our relationship.

Several individuals have come to be personal friends over the course of this Ph.D. and I thank them for their comradeship. At the risk of omitting one or two individuals I would like to name the following persons who fall into this category: Professor Leon F. Phillips, Dr Gregory T. Russell, Dr Bryce E. Williamson, Dr Andrew D. Abell, Dr Paul F. Wilson, Dr Glenn J. Foulds, and Hamish A. Struthers. Several of these individuals, including Professor Phillips, Dr Williamson and Dr Wilson, have also advised me on aspects of my research and I thank them for this input.

Finally I am very grateful to Mum and Dad and my brothers for their unstinting support during the period of my University studies. I have really appreciated it.

LIST OF TABLES

LIST OF FIGURES

PUBLICATIONS

The following publications are related to the research presented in this thesis:

Maclagan, R.G.A.R., McEwan, M.J., and Scott, G.B.I., *Chem. Phys. Lett.*, **240**, 185, (1995).
Ab-initio calculations related to the formation of propynal and propadienone in interstellar clouds.

Scott, G.B.I., Fairley, D.A., Freeman, C.G., Maclagan, R.G.A.R., and McEwan, M.J., *Int. J. Mass Spectrom. Ion Proc.*, **149/150**, 251, (1995).
The association reaction $C_2H_3^+$ + CO and interstellar propynal.

Scott, G.B., Fairley, D.A., Freeman, C.G., McEwan, M.J., Spanel, P., and Smith, D., *J. Chem. Phys.*, **106**, 3982, (1997).
Gas phase reactions of some positive ions with atomic and molecular hydrogen at 300 K.

Scott, G.B.I., Fairley, D.A., Freeman, C.G., McEwan, M.J., Adams, N.G., and Babcock, L.M., *J. Phys. Chem. A*, **101**, 4973, (1997).
$C_mH_n^+$ Reactions with H and H_2: An Experimental Study.

Scott, G.B.I., Fairley, D.A., Freeman, C.G., and McEwan, M.J., *Chem. Phys. Lett.*, **269**, 88, (1997).
The reaction H_3^+ + N: a laboratory measurement.

Scott, G.B.I., Freeman, C.G., and McEwan, M.J., *Mon. Not.,R. astr. Soc.*, **290**, 636, (1997).
The Interstellar Synthesis of Ammonia.

McEwan, M.J., Scott, G.B.I., and Anicich, V.G., *Int. J. Mass Spectrom. Ion Proc.*, In Press, (1997).
New Ion-Molecule Reactions for Titan's Ionosphere.

Scott, G.B.I., Freeman, C.G., Herbst, E., Adams, N.G., Babcock, L.M., and McEwan, M.J., *Astrophys. J.*, In Preparation, (1997).
Interstellar Hydrocarbon Ion-H Atom Chemistry.

Scott, G.B.I., Fairley, D.A., Freeman, C.G., and McEwan, M.J., In Preparation.
Gas phase reactions of some positive ions with atomic and molecular nitrogen at 300 K.

Scott, G.B.I., Fairley, D.A., Freeman, C.G., Anicich, V.G., and McEwan, M.J., In Preparation.
$C_mH_n^+$ Reactions with N and N_2: An Experimental Study.

Scott, G.B.I., Freeman, C.G., and McEwan, M.J., In Preparation.
Interstellar Hydrocarbon Ion-N Atom Chemistry.

Scott, G.B.I., Fairley, D.A., Freeman, C.G., Milligan, D.B., and McEwan, M.J., In Preparation.
Gas phase reactions of some positive ions with O atoms, O_2, and NO at 300 K.

Scott, G.B.I., Fairley, D.A., Freeman, C.G., Milligan, D.B., and McEwan, M.J., In Preparation.
$C_mH_n^+$ Reactions with O atoms, O_2, and NO: An Experimental Study.

Scott, G.B.I., Freeman, C.G., and McEwan, M.J., In Preparation.
Interstellar Hydrocarbon Ion-O Atom Chemistry.

CHAPTER 1.

INTRODUCTION.

1.1: The Significance of Ion-Neutral Reactions.

The chemistry of many natural plasmas may be largely characterised in terms of interactions between ions and neutral species. These reactions occur in regimes as diverse as flames, gas discharges, the Earth's ionosphere, planetary atmospheres and interstellar clouds.

The Dawn of the Field

Towards the end of the nineteenth century, researchers first noted the presence of charged species in both flames and gases that had been subjected to electrical discharges or high frequency radiation. A few years later, in 1905, Paul Langevin developed a theoretical treatment to describe the gas phase interaction between an ion and a neutral molecule. [1] Then in 1912 J.J. Thomson made the abstruse observation of the existence of an ion of mass three whilst irradiating hydrogen gas with cathode rays. [2] No cogent explanation of this experimental result was forthcoming for thirteen years until Lunn and Hogness [3] demonstrated that H_3^+ was the mysterious mass three species and had been formed by the reaction of ionised hydrogen with the parent molecular hydrogen, viz:

$$H_2^+ + H_2 \Rightarrow H_3^+ + H \qquad \textbf{(101)}$$

Later, in 1936, Eyring, Hirschfelder and Taylor [4] calculated a theoretical rate constant for this reaction but the value was not determined experimentally until 1957. [5] Indeed, the first experimental measurement of a rate coefficient for an ion-molecule reaction was made in 1952 by Tal'roze. [6] Shortly thereafter Stevenson and Schissler, (1955), [7] Field, Franklin and Lampe, (1956), [8] and Meisels, Hamill and Williams, (1956), [9] also measured rate constants for several ion-neutral processes.

The leisurely development of ion-molecule reaction kinetics in the first half of this century may be primarily attributed to two factors. Firstly the progress of mass spectrometry as an experimental technique did not gather momentum until the 1950s. Secondly, scientists were slow to recognise the critical importance of ion-molecule reactions in characterising the chemistry occurring in many systems.

Since the 1960s interest in ion-neutral chemistry has mushroomed. Initially the chemistry of the earth's ionosphere provided the focus for many scientists' efforts. A smaller number of workers also started to grapple with the complexities of flame chemistry. More recently, increasing numbers of astronomers, physicists and chemists have turned their attention to the chemistry occurring in the furthest recesses of the galaxy where new stars are being born in the interstellar molecular clouds. In the 1990s ion-neutral chemistry has matured into a well-established discipline at the confluence between chemistry, physics and astronomy.

1.2: Chemistry in the Interstellar Medium.

The largest chemical storerooms in the universe are the interstellar clouds. In 1937 the first entries were made in the inventory of interstellar species with the report of three simple diatomic molecules. Astronomers studying the optical spectra of distant stars had noticed absorption lines attributable to molecular species located between the stellar source and the terrestrial telescope. These initial entries in the chemical compendium were the compounds CH, CN and CH^+. [10, 11, 12] Today, well over one hundred different molecular species have been identified in the interstellar medium and more are being added to the list annually. [13] Since the first observations, scientists have attempted to address the origin of interstellar molecules. In the early 1970s two pioneering papers were published on gas phase ion molecule synthesis. [14, 15] These significant contributions explained the formation of many interstellar molecules and established a framework for future more rigorous, quantitative models. Gradually, over the ensuing two decades, a synergy between theory and experiment has enabled an elucidation of the observed abundances of many interstellar species. Complex synthetic reaction networks, [13, 16] which model the

chemical evolution of interstellar clouds, have been constructed but even at present levels of sophistication the synthetic route to CH^+ remains uncertain. A recent review article by Smith discusses synthetic pathways in the interstellar medium and illustrates how complex interstellar molecules are generated from simple precursor species. [17]

Physical Conditions in the Interstellar Medium

The interstellar medium consists of the interstellar void and interstellar clouds. The interstellar void is a quintessential nothingness, consisting of space with less than one particle per cubic centimetre. [19] In contrast, interstellar clouds, although tenuous, have densities ranging from 10^3 –10^{10} particles per cubic centimetre. [18-21] The temperature in these objects can vary markedly from 10 K up to 10^6 K in the protostellar regions where new stars are forming. [18-21] The largest interstellar clouds have a mass equivalent to 10^6 suns and may be 80 parsecs in diameter. [21] Interstellar clouds are primarily composed of gas with a small component of siliceous dust. [18] A flux of energetic cosmic rays bombard the interstellar clouds, dissociating and ionising the matter present. [18]

Chemical Constituents of Interstellar Clouds

Extraterrestrial chemistry bears little resemblance to the familiar processes that occur on Earth. In the terrestrial environment most matter is molecular, whereas in space atomic species are much more prevalent. [17] The overwhelming majority of compounds detected in interstellar clouds are organic. [17, 18] No branched chain molecules have been detected as yet and there also appears to be a paucity of inorganic metal rich species. [17, 18] Several ions have been observed, including H_3^+. [17, 22] Only polar molecules can be observed using standard radio astronomical techniques so there is certainly some observational bias present in the list of identified interstellar molecules. [18]

1.3: Generic Classes of Gas Phase Ion Reactions.

The salient features of gas phase chemical processes involving ions are described below. These reaction types are fundamental to an understanding of the chemistry occurring in tenuous plasmas such as interstellar clouds.

Binary Ion-Neutral Interactions

Ion-neutral reactions are considered to be major synthetic building blocks in the interstellar medium, facilitating the stepwise production of complex molecules from simple precursor reagents. Many ion-neutral reactions proceed on potential energy surfaces devoid of activation energy barriers, hence these processes ought to be facile even under the harsh physical conditions existing in the interstellar medium. Additionally, ion-neutral reactions frequently display rapid kinetics and significantly, often become even faster at the very low temperatures typical of interstellar clouds.

Ion-neutral reactions are classified as one of the following types of processes:

a. **Charge Transfer.** An example of a charge transfer reaction is: [23, 24]

$He^+ + CO \Rightarrow C^+ + O + He + 2.2\ eV$ **(102)**

$k_{(102)\ 300K} = (1.6 \pm 0.2) \times 10^{-9}\ cm^3\ s^{-1}$

These processes involve electron exchange and occur with both positive and negative ions. For positive ions, charge transfer only occurs when the ionisation potential, (IP), of the neutral is less than the recombination energy of the ion. Negative ion charge transfer requires that the EA of the neutral exceed the IP of the (negative) ion.

Charge transfer reactions may be dissociative, (as in reaction **(102)** above), or non-dissociative. The following reaction is illustrative of a non-dissociative charge transfer reaction involving anions: [25]

$ClO^- + NO_2 \Rightarrow NO_2^- + ClO + 0.1\ eV$ **(103)**

$k_{(103)\ 300K} = (3.2 \pm 1.6) \times 10^{-10}\ cm^3\ s^{-1}$

Ionisation potentials are much larger than electron affinities, hence positive ion charge exchange reactions are often considerably more exoergic, (and dissociative), than analogous reactions involving negative ions.

Charge transfer processes are typically fast with rate coefficients of about $10^{-9}\ cm^3\ s^{-1}$. Notable exceptions to this generalisation include the reactions between neon cations and H_2 or N_2, ($k_{Hydrogen} < 2 \times 10^{-14}\ cm^3\ s^{-1}$ [24, 26]; and $k_{Nitrogen} = (1.1 \pm 0.4) \times 10^{-13}\ cm^3\ s^{-1}$ [24, 27]).

b. **Proton Transfer.** An example of this class of reaction is: [24, 28]

$H_3^+ + H_2O \Rightarrow H_3O^+ + H_2 + 2.8\ eV$ **(104)**

$k_{(104)\ 300K} = (5.3 \pm 1.3) \times 10^{-9}\ cm^3\ s^{-1}$

In this example $\Delta E = 2.8$ eV = proton affinity (H_2O) - proton affinity (H_2).

These reactions are very efficient, ($k \approx 10^{-9} cm^3\ s^{-1}$), when significantly exothermic. [29] In cases where proton transfer is approximately thermoneutral, the rate coefficient reduces to ~ 50 % of the collision rate. In such a near thermoneutral interaction the intermediate complex has equivalent available phase space should it dissociate back to reactants or proceed on to products. [30] Rate constants for both the "forward" and "backward" reactions (k_f and k_r respectively) can often be measured in such systems and hence ΔG evaluated, [using $\Delta G = -RT \ln K = -RT \ln (k_f / k_r)$]. Moreover, it is often possible to monitor k_f/k_r over a range of temperatures and thereby calculate ΔH and ΔS for the proton transfer reaction. Alternatively, ΔH can be determined if ΔS is known, or can be evaluated in some way, and $K = k_f/k_r$ has been measured at a single temperature. This methodology has enabled the construction of a proton affinity scale. [31]

Often proton transfer occurs in competition with another channel such as charge transfer, eg. [24, 32]

$CH_4^+ + H_2S \Rightarrow H_3S^+ + CH_3 + 1.8\ eV \quad (0.55)$ **(105a)**

$\Rightarrow H_2S^+ + CH_4 + 2.1\ eV \quad (0.45)$ **(105b)**

$k_{(105)\ 300K} = (2.3 \pm 0.2) \times 10^{-9}\ cm^3\ s^{-1}$

The least exoergic channel is predominant.

Negative ions may also undergo proton transfer reactions, for example: [33]

$OH^- + HCN \Rightarrow CN^- + H_2O + 0.9\ eV$ **(106)**

$k_{(106)\ 297K} = (4.1 \pm 0.3) \times 10^{-9}\ cm^3\ s^{-1}$

c. **Hydrogen Atom Abstraction.** Typical examples of this type of process include: [24, 34]

$H_2^+ + H_2 \Rightarrow H_3^+ + H + 1.7\ eV$ **(107)**[a]

$k_{(107)\ 300K} = (2.0 \pm 0.2) \times 10^{-9}\ cm^3\ s^{-1}$

---

[a] Footnote added in proof: As shown by isotopic substitution experiments, process **(107)** is actually a composite proton transfer-H atom abstraction reaction, ie. both channels proceed with similar rate coefficients. [401, 402, 403]

and; [24, 35]

$NH_3^+ + H_2 \Rightarrow NH_4^+ + H + 0.9\ eV$ **(108)**

$k_{(108)\ 300K} = (4.4 \pm 0.9) \times 10^{-13}\ cm^3\ s^{-1}$

Reaction **(108)** is not atypical as H atom abstraction reactions often demonstrate slow kinetics. In the interstellar medium a sequence of H atom abstraction reactions with H_2 is thought to be responsible for the production of CH_3^+ from CH^+, the synthesis of NH_4^+ from NH^+, and the creation of H_3O^+ from OH^+.

d. **Carbon Insertion.** These reactions are usually rapid ($k \sim 10^{-9}\ cm^3\ s^{-1}$), commonly involve polyatomic hydrocarbon neutrals, and increase the length of the carbon chain eg. [24, 36]

$C^+ + C_2H_2 \Rightarrow C_3H^+ + H + \sim 2.2\ eV$ **(109)**

$k_{(109)\ 300K} = (2.6 \pm 0.3) \times 10^{-9}\ cm^3\ s^{-1}$

e. **Radiative Association.** Two examples of this class of reaction are detailed below: [37]

$C^+ + H_2 \Leftrightarrow CH_2^{+*} \Rightarrow CH_2^+ + h\nu$ **(110)**

$k_{(110)\ 230K} = 3 \times 10^{-17}\ cm^3\ s^{-1}$

and; [38]

$CH_3^+ + H_2O \Rightarrow CH_3^+.H_2O^*$ (or $CH_3OH_2^{+*}$?) **(111a)**

$CH_3^+.H_2O^*$ (or $CH_3OH_2^{+*}$?) $\Rightarrow CH_3^+.H_2O$ (or $CH_3OH_2^+$?) $+ h\nu$ **(111b)**

$k_{(111)\ 300K} < 1 \times 10^{-11}\ cm^3\ s^{-1}$

Only the collisionally stabilised three-body analogue (reaction **(112)** below) has been observed: [39]

$CH_3^+ + H_2O + M \Rightarrow CH_3^+.H_2O$ (or $CH_3OH_2^+$?) + M* (energy ≤ 2.9 eV) **(112)**

$k_{(112)\ 300K\ @\ 0.2 - 0.8\ Torr} = k_3 > 3 \times 10^{-26}\ cm^6\ s^{-1}$

Radiative association processes assemble large ions in a single step. Product ions are stabilised by emission of a photon and their conformation is often unknown. The emitted photon has yet to be observed experimentally in any system. The mechanism for radiative association envisages a stabilising vibrational transition in the intermediate complex, (usually, although not exclusively, [40, 41] within the ground electronic state), and concomitant photon emission in the infrared. The radiative lifetime of any vibrational transition is anticipated to be 10^{-2} - 10^{-3} seconds. Fragmentation of the vibrationally excited

complex, (unimolecular dissociation), will occur unless a photon with energy $h\nu$ > 3/2 k_bT is emitted.

Data on these reactions is gained from low pressure studies or from examination of analogous (termolecular) reactions where the product ion is stabilised via collisions with a bath gas.

The rate coefficients for such processes range from $k \sim 10^{-17}$ cm^3 s^{-1}, (diatomic reactants), to $k \sim 10^{-9}$ cm^3 s^{-1}, (interactions involving polyatomic species).

f. **Rearrangement Reactions.** The following example is illustrative of this type of process: [24, 32]

$CH^+ + H_2CO \Rightarrow CH_3^+ + CO + 5.5$ eV (0.3) **(113a)**

$\Rightarrow CH_2OH^+ + C + 1.0$ eV (0.3) **(113b)**

$\Rightarrow HCO^+ + CH_2 + 3.1$ eV (0.3) **(113c)**

$\Rightarrow CH_2CO^+ + H + 4.3$ eV (0.1) **(113d)**

$k_{(113)\ 300K} = (3.2 \pm 0.6) \times 10^{-9}$ cm^3 s^{-1}

Note that channel **(113b)** is proton transfer but the other three channels involve more complex rearrangement.

Ions derived from neutral precursors with large IPs and low proton affinities, (eg. NH^+ [42]), often react via several channels. These reactions are typically fast, ($k \sim 10^{-9}$ cm^3 s^{-1}), and multiple products lead to a diverse chemistry.

g. Associative Detachment. An example of this type of reaction is the interaction between a hydroxyl anion and a hydrogen atom: [43]

$OH^- + H \Rightarrow H_2O + e^- + \leq 2.5$ eV + $h\nu$? **(114)**

$k_{(114)\ 296K} = (1.4 \pm 0.4) \times 10^{-9}$ cm^3 s^{-1}

The above reaction can be envisaged as occurring via a three-step mechanism, viz:

$OH^- + H \Rightarrow H_2O^{-*}$ **(114a)**

$H_2O^{-*} \Rightarrow H_2O^* + e^- + \leq 2.5$ eV **(114b)**

$H_2O^* \Rightarrow H_2O + h\nu$? **(114c)**

Autodetachment of an electron from the H_2O^{-*} complex occurs in approximately 10^{-14} seconds. [43] The veracity of this mechanism has not been established and, in particular, the emission of a photon from vibrationally excited H_2O,

[process **(114c)**], is speculative.

Only negative ions can participate in this sort of reaction.

The autodetachment process may be visualised as an ion-neutral association, stabilised by electron emission. These reactions are only viable if the electron detachment energy is less than the energy of the chemical bond formed from the association. Associative detachment reactions therefore often involve the conversion of radical reactants into stable molecules.

Analysis of attendant infrared emissions from several associative detachment reactions, (eg. CN^-, F^- and Cl^- with H; also O^- with CO), [44] have shown that the highest energetically accessible vibrational levels are populated.

Rate constants for this category of reaction are typically ~ 10^{-9} cm^3 s^{-1}. [45, 46]

Temperature Dependence of Binary Ion-Neutral Processes

An important influence on the temperature dependence of binary ion-neutral processes is the magnitude of the neutral species' dipole moment. Experimental studies have shown highly significant increases in rate coefficients as the temperature is lowered for reactions between simple ions and highly polar molecules, (eg. $He^+ + NH_3$).[47, 48] If, however, the reacting neutral is non-polar or has a small dipole moment then the temperature dependence is often negligible, providing the reaction is significantly exoergic, with k close to the limiting collisional value. In general, slow reactions show an inverse temperature dependence whereby $k \propto \sim T^{-0.5}$. An explanation for this behaviour is that the intermediate complex has a shorter lifetime at higher temperatures, hence less time is available for reaction. [49]

Ternary Ion-Neutral Processes

In situations where binary channels are endoergic, termolecular association reactions may proceed. An example of such a process is the association between methyl ions and molecular hydrogen, viz: [39]

$$CH_3^+ + H_2 + M \Rightarrow CH_5^+ + M + 2.0\ eV \qquad \textbf{(115)}$$

$$k_{(115)\ 300K\ @\ \sim 0.2\ -\ \sim 0.8\ Torr} = (1.3 \pm 0.3) \times 10^{-28}\ cm^6\ s^{-1}$$

The above reaction proceeds via the following two step mechanism:

$$CH_3^+ + H_2 \Rightarrow CH_5^{+}* \qquad \textbf{(115a)}$$

$$CH_5^{+}* + M \Rightarrow CH_5^+ + M^*\ (\text{energy} \leq 2.0\ eV) \qquad \textbf{(115b)}$$

Often ternary association competes with binary reaction channels as in the following system where the product distribution was determined at a helium pressure of 0.2 Torr: [24, 39]

Bimolecular channels:

$CH_3^+ + NH_3 \Rightarrow H_4CN^+ + H_2 + 2.2\ eV \quad (0.7)$ **(116a)**

$\Rightarrow NH_4^+ + CH_2 + 0.3\ eV \quad (0.1)$ **(116b)**

Termolecular channel:

$CH_3^+ + NH_3 + He \Rightarrow CH_3^+.NH_3 + He^*$ (energy $\leq$ 4.5 eV) (0.2) **(116c)**

$k_{(116)\ 300K\ @\ 0.2\ Torr} = (1.75 \pm 0.2) \times 10^{-9}\ cm^3\ s^{-1}$.

Room temperature rate coefficients, k_3, vary from ~ 10^{-31} $cm^6\ s^{-1}$ to 10^{-22} $cm^6\ s^{-1}$. [50, 51] Rate coefficients for ternary association processes show a marked variation with temperature. A theoretical treatment predicts that $k_3 \propto T^{-(l/2\ +\ \delta)}$. [30] In this expression l is the number of rotational degrees of freedom in the separated reactants and δ allows for temperature variation of the collision efficiency of M. Experimentally k_3 obeys this expression tolerably well if δ is ~ 0.2 - 0.3 when M is helium. [49, 52] The temperature dependence of k_3 also appears to be sensitive to the number of vibrational degrees of freedom in systems where the reactant neutral has closely spaced vibrational levels. [53]

For complex systems, intermediate lifetimes increase and thus in high pressure regimes all intermediates are stabilised and the reaction kinetics proceed independently of the pressure of M. This "saturation" is avoided in low pressure experiments where a reduced collision frequency ensures that standard ternary kinetics apply. For certain systems at low pressure a pressure independent component to k_3 remains which is attributed to radiative stabilisation of the intermediate, eg. [51, 54]

$CH_3^+ + CH_3CN \Rightarrow CH_3^+.CH_3CN + h\nu$ **(117)**

$k_{(117)\ 300K} = (9 \pm 2) \times 10^{-11}\ cm^3\ s^{-1}$

Note that reaction **(117)** is in fact a 5 % channel of the overall reaction of methyl cations with acetonitrile, at room temperature. The other bimolecular product channels are $C_2H_5^+ + HCN$, (0.37), and $HCNH^+ + C_2H_4$, (0.58). The overall rate constant for the reaction of CH_3^+ with CH_3CN, (ie. all three product channels), is 1.8×10^{-9} $cm^3\ s^{-1}$. [51]

Recombination Processes

Recombination reactions are notable because they involve the neutralisation of charged species and the production of neutrals. Only about 100 recombination reactions have been studied [55]; this is a very small sample compared with the ~ 10,000 ion-neutral reactions that have been characterised. [24, 50] Little data on the products of recombination processes is currently available due to the experimental difficulty in detecting neutral species. The key features of recombination reactions are discussed below:

a. Electron-Ion Recombination. These reactions are vital since they are thought to be the final step in the synthesis of many neutral molecules observed in interstellar clouds. As an example consider the following process: [56, 57, 58]

$H_3O^+ + e^- \Rightarrow OH + 2H + 1.3\ eV$ (0.29) / *(0.48)* **(118a)**

$\Rightarrow OH + H_2 + 5.7\ eV$ (0.36) / *(0.18)* **(118b)**

$\Rightarrow H + H_2O + 6.4\ eV$ (0.05) / *(0.33)* **(118c)**

$\Rightarrow O + H + H_2 + 1.4\ eV$ (0.30) / *(0.01)* **(118d)**

$\alpha_{e(118)\ 295K} = (1.0 \pm 0.2) \times 10^{-6}\ cm^3\ s^{-1}$

Note that considerable uncertainty exists in the product distribution for reaction **(118),** most significantly with regard to the proportion of H_2O formed. Adams and co-workers, using laser induced fluorescence in a FA / SIFT instrument, (with Langmuir probe), have reported the values underlined above. [58] Conflicting results, (shown in italics), have been obtained by Anderson et al during experiments involving a heavy ion storage ring. [56] The disparity between the two measurements has yet to be resolved.

Although few electron-ion recombination reactions have been satisfactorily studied in the laboratory they are known to proceed expeditiously, ($\alpha_e \sim 10^{-7}$ $cm^3\ s^{-1}$ for diatomic ions; $\alpha_e > 1 \times 10^{-6}\ cm^3\ s^{-1}$ for polyatomic ions). [59, 60] The recombination of electrons with atomic ions is much slower, ($\alpha_e \sim 10^{-11}$ - 10^{-12} $cm^3\ s^{-1}$), as the product must stabilise itself via photon emission during the period of the electron-ion encounter, (~ 10^{-15} seconds), eg. [61]

$He^+ + e^- \Rightarrow He^* \Rightarrow He + h\nu$ **(119)**

$\alpha_{e(119)\ 300K} < \sim 10^{-11}\ cm^3\ s^{-1}$

Little temperature dependence is observed for fast reactions although those processes that proceed at only a fraction of the collision limit exhibit power law temperature dependencies of ~ -0.7 to -1 within a temperature range of 80 to 600 K. [60]

In general electron-ion recombination is dissociative, breaking up large molecular ions into smaller fragments. For many of these reactions the products are poorly characterised.

Two mechanisms for dissociative ion-electron recombination have been suggested:

(i) The **direct** pathway whereby the neutralised ion moves via a radiationless transition onto a repulsive potential curve from which dissociation to products occurs [62] ; or

(ii) The **indirect** route that involves an initial transfer of the neutralised ion to a Rydberg state prior to a radiationless transition to a repulsive curve. [63]

Theory predicts a rate coefficient temperature dependence of $T^{-0.5}$ and $T^{-1.5}$ for the direct and indirect mechanisms respectively. [64]

Experiment and theory are in general agreement for the ion electron recombination of O_2^+, NO^+, N_2^+ and HCO^+ [65, 66] however the theory is not yet sufficiently developed to provide a satisfactory treatment for larger polyatomic ions. [67, 68]

For ions containing H or O atoms, common product fragments of ion electron recombination include H and OH. [69, 70] Due to the energetic nature of ion electron recombination processes, electronically excited states are sometimes accessed. The vibrational population densities of the neutral fragments have been determined for several systems. [30, 71]

b. Ion-Ion Recombination (Mutual Neutralisation). A comprehensive survey of these reactions has not been undertaken and in particular little product information has been collated. Several processes have been examined in the laboratory however, and compared with electron-ion recombination less fragmentation is apparent. Electron-ion recombination reactions are invariably highly exoergic; ion-ion recombination less so. The variance in degree of fragmentation between these two recombination processes is presumably due to this difference in exoergicity.

Rate coefficients for ion-ion recombination reactions are faster, ($\alpha_i \sim 10^{-8}$ cm^3 s^{-1} [55, 72]), than those obtained for ion-neutral interactions due to the enhanced coulombic attraction between two oppositely charged ions. Only two mutual neutralisation reactions have been studied over a range of temperatures and for these systems a power law temperature dependence of ~ 0.4 has been noted. [72] This value is consistent with Landau-Zener theory which predicts a temperature dependence of $T^{0.5}$. [73] A pressure dependence has been observed in two ion-ion recombination reactions with rate coefficients quadrupling as the pressure was raised from 1 to 8 Torr. [72, 74]

An example of this class of reaction is: [75, 76]

$NO^+ + NO_2^- \Rightarrow NO(A\,^2\Sigma^+) + NO_2$ **(120)**

$\alpha_{i(120)\ 300K} = (6.4 \pm 0.7) \times 10^{-8}$ cm^3 s^{-1}

The mechanism for reaction **(120)** involves electron transfer from the NO_2^- anion to the NO^+ cation.

Electron Attachment Reactions

The dissociative attachment of an electron to carbon tetrachloride is illustrative of this type of process, viz: [57]

$CCl_4 + e^- \Rightarrow Cl^- + CCl_3 + \leq 0.5$ eV **(121)**

$\beta_{(121)\ 300K} = (3.9 \pm 0.6) \times 10^{-7}$ cm^3 s^{-1}

These reactions may be dissociative or non-dissociative. Dissociative electron attachment processes are extremely fast, ($k \sim 10^{-7}$ cm^3 s^{-1} [57, 77]). The attachment of an electron to hexafluorobenzene is an example of a non-dissociative electron attachment process, viz: [57]

$C_6F_6 + e^- + M \Rightarrow C_6F_6^- + M^*$ (energy ≤ 0.5 eV) **(122)**

$\beta_{(122)\ 300K\ @\ 0.6\ Torr} = (1.1 \pm 0.2) \times 10^{-7}$ cm^3 s^{-1}

Non-dissociative processes require collisional stabilisation to occur within the lifetime of the "attached" complex and are therefore more viable in high pressure regimes. Reaction **(122)** is a saturated three-body attachment reaction and $\beta_{(122)}$ the equivalent two-body attachment coefficient. For some ions, under high pressure conditions, dissociative and non-dissociative electron attachment

occur as competing channels, eg. [78]

$C_6F_5I + e^- \Rightarrow C_6F_5^- + I + 1.4\,eV \quad (\geq 0.95)$ **(123a)**

$C_6F_5I + e^- + M \Rightarrow C_6F_5I^- + M^* \quad (\leq 0.05)$ **(123b)**

$\beta_{(123)\ 300K\ @\sim 1\ Torr} = (3.1 \pm 0.8) \times 10^{-8}\ cm^3\ s^{-1}$

The non-dissociative channel, **(123b)**, was not observed in low pressure experiments on this system presumably because the autodetachment lifetime was shorter than the time between collisions. [79] Some non-dissociative electron attachment reactions are very slow with $k \sim 10^{-12}\ cm^3\ s^{-1}$.

For electron attachment to be efficient, low energy, (slow), electrons are required. This type of reaction proceeds for several halides due to the large attachment cross sections of halogen atoms. The upper limit rate coefficient for an electron attachment process is given by the expression: [80]

$$\beta \approx 5x10^{-7}\left(\frac{300}{T}\right)^{\frac{1}{2}} cm^3 s^{-1} \qquad \textbf{(124)}$$

Activation energy barriers of between 0 - 300 meV may result in β being less than this optimal value. [57] In such cases the rate coefficient shows Arrhenius behaviour with temperature variation, ie:

$$\beta(T) \approx \beta_0 \exp\left(\frac{-\Delta E}{k_B T}\right) \qquad \textbf{(125)}$$

In a series of electron attachment experiments to the halocarbon species CF_2BrCF_2Br and CH_2BrCH_2Br, a Br_2^- channel was observed. In these parent molecules the two bromine atoms are attached to separate carbon atoms, hence the intermediate complex must experience substantial distortion and rearrangement. [81]

1.4: Non-Ionic Interstellar Chemical Processes.

Two categories of non-ionic reactions are also thought to facilitate molecular synthesis. Both neutral-neutral chemistry and dust grain catalysis are postulated to occur in interstellar clouds. Important features of these reaction types are discussed below.

Neutral-Neutral Chemistry

Recent experimental studies have demonstrated that several neutral-neutral processes are rapid, even at low temperatures, ($k \sim 10^{-10}$ - $10^{-11}\ cm^3\ s^{-1}$), and

proceed without activation energy barriers. [82-84] These fast neutral-neutral reactions may involve "stable species", atoms, or radicals, and because of the absence of barriers are likely to be of relevance to interstellar chemistry. The interaction between oxygen atoms and hydroxyl radicals illustrates this class of reaction: [85]

$$O + OH \Rightarrow O_2 + H + 0.7\ eV \qquad \textbf{(126)}$$

$$k_{(126)\ 298K} = (3.3 \pm 0.7) \times 10^{-11}\ cm^3\ s^{-1}$$

The detection of reactive neutral species is difficult and hence relatively few neutral-neutral systems have been characterised. Some insight has been provided by theoretical calculations on particularly intractable reactions, (eg. $C_3 + O$). [86]

Model studies have examined the effect of neutral-neutral reactions on the chemistry of interstellar clouds with somewhat equivocal results. [87, 88] Reactions between atomic oxygen and unsaturated carbon clusters are of particular interest as they may impede the synthesis of complex hydrocarbon species. [86] Recent work has also focussed upon the reactivity of carbon atoms with stable hydrocarbons. [89, 90] Other research has examined the role of tunnelling in the interaction between hydrocarbon species and molecular hydrogen. [91]

Neutral-neutral reactions may be of particular importance in the higher temperature shocked regions of interstellar clouds. Their role in interstellar chemistry is uncertain due to a paucity of experimental and theoretical data.

Interstellar Dust Grain Catalysis

The chemisorption and physisorption of gas phase molecules onto interstellar dust grain surfaces is thought to facilitate chemical reactions.

Weakly bound adsorbed species may migrate along the surfaces of dust grains and undergo reactive collisions. [92] This Langmuir-Hinshelwood mechanism [93, 94] is favoured over the alternative Eley-Rideal sequence [95] in which reaction occurs between an adsorbed molecule and an impinging gas phase species. [96] In order to be viable at interstellar temperatures, grain catalytic processes must proceed via low activation energy pathways. [97]

The association of atomic hydrogen to produce molecular hydrogen

probably occurs on the surface of dust grains, viz: [98]

$H + H + Grain \Rightarrow H_2 + Grain + 4.5\ eV$ **(127)**

$k_{(127)\ @\ 50K} = 1.0 \times 10^{-17}\ cm^3\ s^{-1}$ (theoretical value)

Excess energy generated in this process is deflected into the phonon modes of the dust grain. [92] The molecular hydrogen is readily desorbed into the gas phase even at temperatures as low as 10 K.

Radiative association of atomic hydrogen to form molecular hydrogen (reaction **(128)** below) is forbidden because of the vanishingly small dipole moment of H_2. [99]

$H + H \Rightarrow H_2 + h\nu$ **(128)**

Alternative gas phase synthetic routes to molecular hydrogen, (reactions **(129)** and **(130)** detailed below), are slow and hence unimportant: [98]

$H + e^- \Rightarrow H^- + h\nu (Energy < 0.8\ eV)$ **(129a)**

$k_{(129a)\ @\ 50K} = 5.3 \times 10^{-17}\ cm^3\ s^{-1}$ (theoretical value)

followed by; [50, 100]

$H^- + H \Rightarrow H_2 + e^- + 3.8\ eV$ **(129b)**

$k_{(129b)\ @\ 296K} = (1.8\ [+\ 100\ \%;\ -50\ \%]) \times 10^{-9}\ cm^3\ s^{-1}$

and also: [101]

$H^+ + H \Rightarrow H_2^+ + h\nu (Energy < 2.7\ eV)$ **(130a)**

$k_{(130a)\ @\ 200K} = 2.46 \times 10^{-19}\ cm^3\ s^{-1}$ (theoretical value)

followed by; [102]

$H_2^+ + H \Rightarrow H^+ + H_2 + 1.8\ eV$ **(130b)**

$k_{(130b)\ 300K} = (6.4 \pm 1.2) \times 10^{-10}\ cm^3\ s^{-1}$

Other reactions such as the association of a slow moving hydroxyl radical and a rapidly moving hydrogen atom may be catalysed by dust grain surfaces. [103] Evaporation of the heavy species produced is unlikely and hence a build-up of ices around the siliceous or carbonaceous dust grain core occurs. [104]

The grain catalysis of molecules is poorly understood; indeed even the composition and structure of interstellar dust grains remains uncertain.

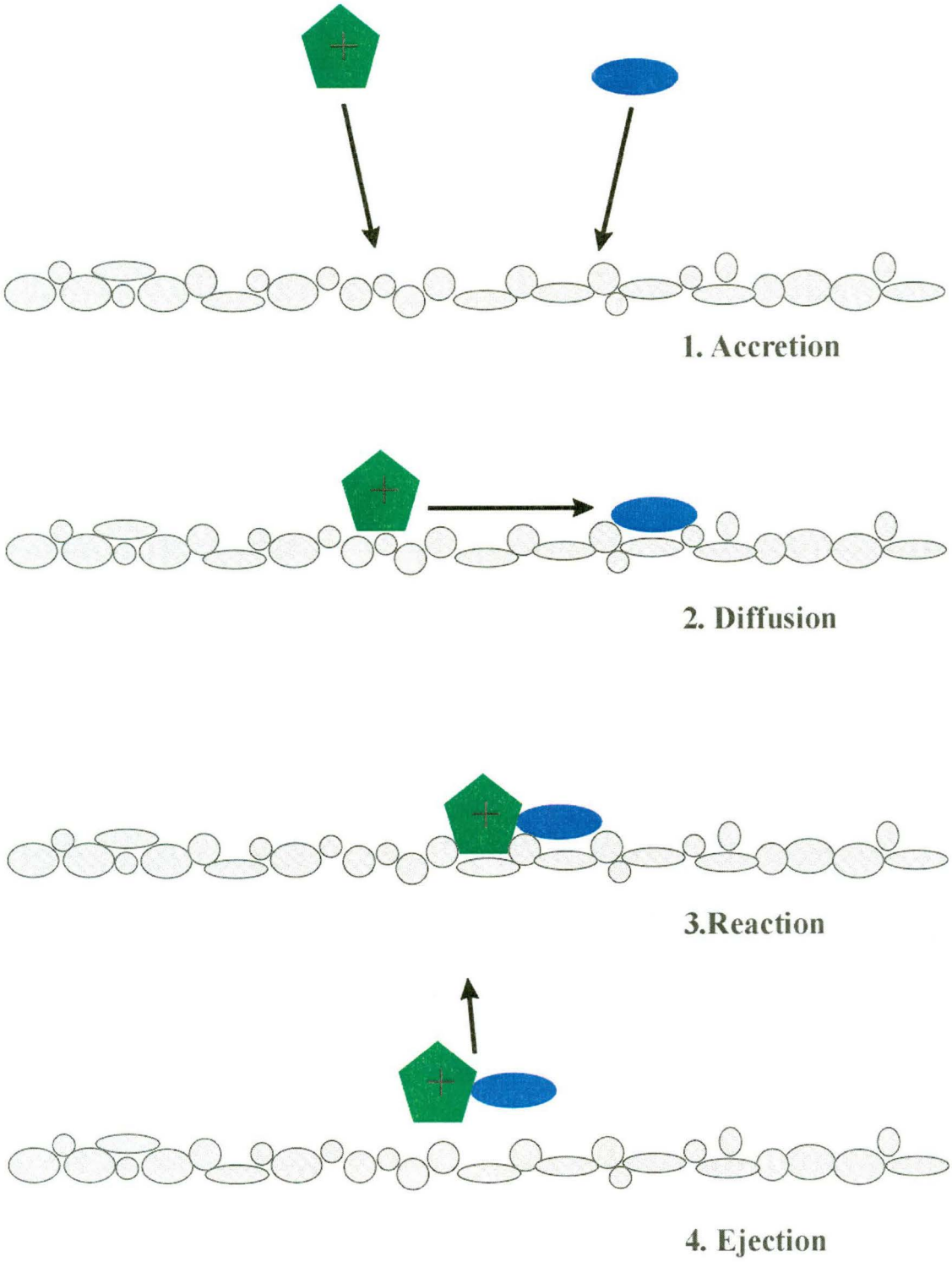

Figure 1.1. Grain-surface chemistry. Gas phase species accrete, diffuse and then react on a grain surface before the product is ejected.

1.5: Theoretical Treatments of Ion-Neutral Interactions.

The theoretical treatment of collisions between ions and neutral species has been of interest for over 90 years. This section is an abridged, non-rigorous synopsis of the theoretical efforts to derive ion-neutral rate constants.

The various theories all assume that ion-neutral interactions arise from long range attractive forces between the two species. The forces cause the ion and neutral to accelerate towards one another to form an orbiting complex. The collision complex generally has sufficient internal energy to overcome any activation energy barriers and allow the reaction to proceed.

Pure Polarisation Theory

Langevin's seminal paper of 1905 [1] was extended by Gioumousis and Stevenson in their 1958 derivation of the general form of the ion-neutral cross-section. [105] In this classical description a point charge (q) of mass m interacts with a point polarisable molecule of mass M and polarizability α. The interaction potential, $V(r)$, for this encounter is given by the following relation:

$$V(r) = -\frac{\alpha q^2}{2r^4} \qquad \textbf{(131)}$$

The relative energy of the system and the impact parameter, b, determine the orbits for ion-induced dipole events. [1, 106] There is a critical value of the impact parameter, b_c, such that for ion trajectories with $b \leq b_c$ capture occurs and for ions with $b > b_c$ the closest point of approach to the molecule is $b_c/\sqrt{2}$. [105] The value of b_c is given by the following expression:

$$b_c = \left(\frac{2\alpha q^2}{E_r}\right)^{\frac{1}{2}} \qquad \textbf{(132)}$$

where E_r is the total relative energy of the ion-neutral system.

The capture cross section ($= \pi b_c^2$) is thus:

$$\sigma_c(v_r) = \pi q\left(\frac{2\alpha}{E_r}\right)^{\frac{1}{2}} \qquad \textbf{(133)}$$

where v_r is the relative velocity of the ion-neutral pair.

Noting that the collision rate is defined as $v_r\sigma_c(v_r)$ and that the reduced mass of the colliding pair is μ (where $1/\mu = 1/m + 1/M$), then the following expression

gives the Langevin collision rate:

$$k_L = 2\pi q\left(\frac{\alpha}{\mu}\right)^{\frac{1}{2}} \qquad \textbf{(134)}$$

The Langevin collison model successfully predicts rate coefficients for some low energy ion-induced dipole systems even when the neutral species possess significant quadrupole moments. [52, 107, 108] Expression **(134)** is independent of energy and shows no temperature dependence. Unfortunately pure polarisation theory underestimates the experimental rate coefficient for ion-permanent dipole interactions by up to 75 %. [109]

Ion-Permanent Dipole Theories

The interaction potential for an encounter between an ion and a neutral species possessing a permanent dipole is: [110]

$$V(r,\theta) = -\frac{\alpha q^2}{2r^4} - \frac{q\mu_D}{r^2}\cos\theta \qquad \textbf{(135)}$$

where μ_D is the dipole moment of the neutral and θ is the angle that the dipole makes with the line of centres of the collision. The ion is still regarded as a point charge and ion-neutral capture is defined in an analogous fashion to the ion-induced dipole interaction.

Several efforts have been made to formulate a rate constant by manipulating $\cos\theta$ in various ways. The "locked dipole" approximation, (setting $\theta = 0$), resulted in a significant overestimation of the rate constant. [111, 112] In 1973 Su and Bowers developed Average Dipole Orientation (ADO) theory which assumed only a partial locking of the dipole to the attractive ion potential. [113, 114] The parameterised form of their theoretical value for k is:

$$k_{ADO} = \frac{2\pi q}{\mu^{\frac{1}{2}}}\left(\alpha^{\frac{1}{2}} + C\mu_D\left(\frac{2}{\pi k_B T}\right)^{\frac{1}{2}}\right) \qquad \textbf{(136)}$$

where k_B is the Boltzmann constant, T is the temperature, C is a dipole locking expression and all other symbols are as previously defined.

The inclusion of angular momentum produced a modified ADO theory entitled Average Dipole Orientation Theory with Conservation of Angular Momentum (or "AADO") by its authors.[115] This theory produced the following

expression for the rate coefficient:

$$k_{AADO} = \frac{2\pi q}{\mu^{\frac{1}{2}}}\left(\alpha^{\frac{1}{2}} + C\mu_D\left(\frac{2}{\pi k_B T}\right)^{\frac{1}{2}} + \frac{Z\mu_D I^{\frac{1}{2}}}{\mu^{\frac{1}{4}}}\right) \quad \textbf{(137)}$$

where I is the moment of inertia of the molecule, Z is a temperature dependent parameter and all other symbols have been already defined. AADO theory usually predicts a larger capture rate coefficient than its ADO predecessor, particularly when the neutral reactant has a large permanent dipole. [109, 115] Both theories predict rate constants that agree broadly with experimental measurements at room temperature. [109, 115, 116]

Trajectory Calculations

In 1980 Chesnavich et al used classical trajectory calculations to derive an upper bound to k for ion capture in a non-central field. [117] They argued that the two species in a reactive ion-neutral collision must initially traverse a long range potential before encountering a short range potential where bond rupture and reformation occur. The experimental rate coefficient is obtained from the following relation:

$$k_{EXP} \approx \omega(T)k_{CAP}(T) \quad \textbf{(138)}$$

where $\omega(T)$ is the thermal reaction probability, (ie $0 \leq \omega(T) \leq 1$), and $k_{CAP}(T)$ is the capture rate constant at temperature T. Consideration of the short range potential allows the evaluation of $\omega(T)$ whilst $k_{CAP}(T)$ is determined by calculating the number of trajectories originating at $r = \infty$, that reach $r = 0$.

The model used is that of a point charge interacting classically with a rigid dipole. The Hamiltonian for this system is:

$$H = \frac{p_r^2}{2\mu} + \frac{L^2}{2\mu r^2} + \frac{J^2}{2I} + V(r,\theta) \quad \textbf{(139)}$$

where p_r is the radial momentum of the colliding species, L is their orbital angular momentum, J and I are the angular momentum and moment of inertia of the rigid dipole respectively and $V(r, \theta)$ is as per expression **(135)** above.

The thermal capture rate coefficient is evaluated by averaging the microcanonical rate coefficient, $[k_{CAP}(E)]$, thus:

$$k_{CAP} = \int_0^\infty P(T;E)k_{CAP}(E)dE \quad \textbf{(140)}$$

where *P(T; E)* is a five dimensional Boltzmann energy distribution.

The microcanonical rate coefficient is in turn obtained from the following expression:

$$k_{CAP}(E) = \frac{F_{CAP}(E)}{\rho(E)} \qquad \textbf{(141)}$$

where $\rho(E)$ is the total density of states per unit volume of the colliding species at infinite separation and $F_{CAP}(E)$ is the capture flux. The capture flux is computed from the following relation:

$$F_{CAP}(E) = \int d\tau \vec{v}.\vec{\nabla} S \chi_r \delta[S]\delta[E-H] \qquad \textbf{(142)}$$

where $\hat{v}$ is the phase space velocity vector, $\vec{v}\vec{\nabla}S\chi_r$, is the differential capture flux and χ_r is the characteristic function labelling the trajectories on the phase space surface *S* as reactive or non-reactive. The equations of motion are solved to determine which trajectories lead to capture.

The variational upper bound for ion dipole capture is:

$$k_{CAP}(T) = \frac{1}{2Ik_BT(2\pi\mu k_BT)^{\frac{3}{2}}} \cdot \int \chi_r d_{\gamma 1} d_{\gamma 2} dL dJ 2P dP \exp\left(\frac{-E}{k_BT}\right) dE \qquad \textbf{(143)}$$

where *P* is the total angular momentum of the system, γ_1 and γ_2 are Euler angles and all other symbols are as previously defined. The trajectories are integrated from the capture radius $r_0 = (\alpha q^2/2E)^{1/4}$ to $r \cong r_0 + 16$ Angstroms. The authors argue that this theory generates rate coefficients which have an error of < 8 %. [117]

Parameterised Trajectory Theory

Two years after the initial trajectory investigation, Su and Chesnavich published an improved parameterised version for ion-dipole reactions at ambient temperatures. [118]

Defining the parameter *X* as:

$$X = \frac{\mu_D}{(2\alpha k_BT)^{\frac{1}{2}}} \qquad \textbf{(144)}$$

and utilising equation **(134)** above the authors suggested that the following

expression for $k_{CAP}(T)$:

$$k_{CAP}(T) = k_L \begin{cases} 0.4767X + 0.62 & ; X \geq 2 \\ \dfrac{(X + 0.509)^2}{10.526} + 0.9754 & ; X \leq 2 \end{cases} \quad \textbf{(145)}$$

The originators of this parameterised version claim an error of < 3 %. [118] Many experimentalists working in the field consider equation **(145)** to be the best formulation of the room temperature collision rate currently available.

Adiabatic Capture Centrifugal Sudden Approximation Theory (ACCSA)

Other workers have considered ion-dipole interactions at low temperature, however at higher temperature these theories give virtually the same value of $k_{CAP}(T)$ as that obtained using equation **(145)** above. [119]

In 1985 Clary published a paper outlining the features of Adiabatic Capture Centrifugal Sudden Approximation, (ACCSA), theory. [120] His calculations suggested that the individual rotational quantum state coefficient, k_J, would rise in response to a fall in the rotational quantum number. At 5 - 50 K, the distribution of rotational states is such that the J = 0 state has the highest population. In this situation the ACCSA model predicts that k_{CAP} will increase by an order of magnitude. [121] Several low temperature experimental studies involving the reaction of ions with strongly polar neutral molecules provided support for the temperature dependence predicted by this theory. [47, 48] Clearly this theory has important implications for ion-neutral processing in interstellar clouds.

Quantum Mechanical Calculations of Rate Coefficients

Quantum mechanical calculations of k_{CAP} are only useful at low temperatures; even then classical trajectory theory predicts low temperature experimental data with tolerable accuracy. [119] Quantum reactive scattering is discussed in considerable detail by McDaniel et al., (1970). [122] The authors suggest that an ion–molecule collision will produce rotational excitation in the molecule. The orbital angular momentum, $\vec{l}$, of the relative motion is not conserved. This model is comparable to the scattering of an ion by a rigid rotor with angular momentum $\vec{J}$. [123]

The total Hamiltonian is:

$$H = H_{rot} - \frac{\hbar^2}{2\mu}\nabla_r^2 + V(r,\theta) \quad \textbf{(146)}$$

where ∇_r^2 is the Laplacian of the centre of mass system and $V(r,\theta)$ is the ion-dipole interaction potential [as per equation **(135)**].

H_{rot} is the Hamiltonian of the rigid rotor (= $P^2/2I$) satisfying the relation:

$$H_{rot}Y_{jm}(\vec{r}) = \frac{\hbar^2}{2I}J(J+1)Y_{jm}(\vec{r}) \qquad \textbf{(147)}$$

where $Y_{jm(}(\vec{r})$ are the spherical harmonics and I is the moment of inertia of the rigid rotor. Total angular momentum ($\vec{L}+\vec{J}$) is conserved. A partial wave analysis gives a scattering cross section dependent on the rotational quantum number, j, thus:

$$\sigma(j) \approx \frac{1}{(2j+1)} \qquad \textbf{(148)}$$

This relation suggests that a reduction in energy, with attendant lowering of a polar molecule's rotational state, results in a larger cross section.

1.6: Experimental Studies of Ion-Neutral Processes.

A number of different instruments and techniques have been developed over the last 40 years to study ion-neutral processes. Experimental measurements really began in earnest in the 1960s when advances in flow tube technology and mass spectrometry enabled the construction of the first Flowing Afterglow instruments. The Flowing Afterglow, (FA), apparatus was tremendously successful but in the 1970s it in turn gave way to a new instrument - the Selected Ion Flow Tube, (SIFT). Since that time, the basic SIFT has been enhanced with the incorporation of a drift tube section and provision for variable temperature operation. Ion Cyclotron Resonance, (ICR), is another technique that was developed in the 1960s to investigate ion-neutral reactions. As with flow techniques, ICR instruments have been extensively upgraded over the ensuing four decades. In the last ten years ion-beam techniques have also been applied to the measurement of ion-neutral reactions.

Ion-Cyclotron Resonance (ICR)

The principle behind Ion Cyclotron Resonance is that charged particles subjected to mutually perpendicular magnetic and electric fields will move in

cycloidal orbits at frequencies (ω_c) dictated by their mass to charge ratios:

$$\omega_c = z.\frac{B}{m} \quad \textbf{(149)}$$

where B = magnetic flux density, z = charge on the particle, m = mass of the particle.

Ions are formed in the centre of a cell by electron impact on a neutral gas. Irradiation of the ions by an excitation radio frequency (rf) electric field at the cyclotron resonance frequency, ω_c, causes absorption of energy from the external field which is detected using a marginal oscillator. [124-126] Alternatively, a capacitance balanced bridge circuit may be used to measure the "image current" created by the motion of ions through the rf field. [125, 127-129] ICR instruments may be operated in two modes, namely "drift mode" and "trapped mode". Drift mode involves continuous ion formation and ongoing movement of the ions through the reaction cell, whereas in the trapped mode, ions are stored for varying periods in the presence of a reactant gas prior to their release and detection. [130] Fourier-transform mass spectrometry, (FTMS), is a modern derivative of ICR and has the features of ultrahigh mass resolution, high mass range, and accurate product mass determination, (in the ppm range). [131, 132]

ICR instruments can operate over a wide pressure range, (10^{-8} - 10^{-3} Torr), and are very suitable for the investigation of ion-molecule reactions. [133, 134] Ion-atom processes are not readily studied using this technique because atomic species are usually generated in a microwave discharge at ~ 0.1 - 0.01 Torr which is incompatible with the operating pressure range of an ICR mass spectrometer. [102, 135]

Flowing Afterglow (FA)

The first flowing afterglow instrument was constructed by Fehsenfeld, Ferguson and Schmeltekopf in the early 1960s. [136] This technique allowed ion-neutral reactions to be studied at thermal energies. Atmospheric chemistry research was growing prolifically in the 1960s and the concurrent emergence of the flowing afterglow technique enabled important data on many ion-neutral reactions that occur in the earth's ionosphere to be obtained.

Figure 1.2 depicts the essential features of the flowing afterglow. The apparatus consists of a flow tube through which a bath gas such as He or H_2 is passed at such a rate that a pressure of ~ 0.1 - 1.0 Torr is maintained. Ionisation

via electron impact or a microwave discharge is created in the pure bath gas, or in the bath gas containing a small admixture of another ion source gas. [137] An afterglow plasma comprising positive ions, metastable atoms and electrons is produced. The ion source gas may be added downstream of the ionisation source thereby generating the required reactant ion species through chemi-ionisation. Collisions with bath gas molecules thermalise the reactant ions within ~ 10 - 15 cm of the ionisation source.

Reactant neutral gases are admitted to the flow tube through one or more axially positioned entry ports. After a reaction distance of typically 40 - 50 cm, a small fraction of the ions are sampled through an ~ 1 mm orifice at the tip of a nose cone assembly. [138] These ions are filtered through a quadrupole mass spectrometer prior to detection by an off-axis particle multiplier / ion-counting system. [137, 139] Differential pumping of the entire detection system is required to maintain an operating pressure of $< \sim 10^{-4}$ Torr. A high throughput roots pump removes the bulk of the bath gas and reaction mixture from the flow tube. Some flowing afterglow instruments have a facility to operate over the temperature range 80 – 900 K. [140]

Rate constants are evaluated by measuring the primary and / or product ion count rate as a function of neutral reactant concentration. Radial and axial diffusion, non-uniform velocity profile and inlet effects are accounted for with corrective coefficients. [137] In simple cases a semilogarithmic plot of reactant ion count rate versus neutral gas flow yields a straight line with slope proportional to the rate coefficient.

Several excellent reviews, (including one by the originators [137]), are available on the flowing afterglow technique. [139, 141]

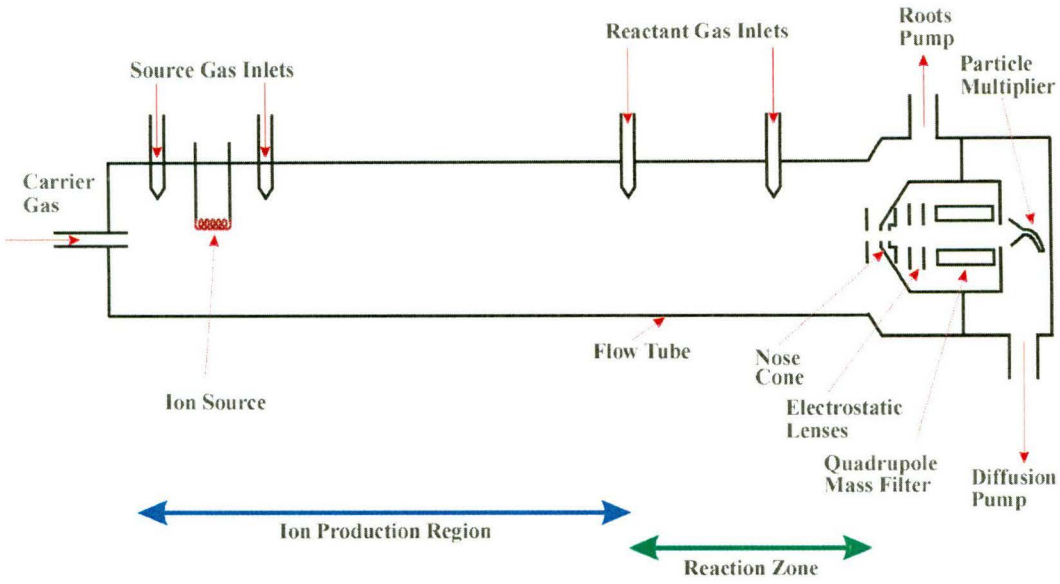

Figure 1.2. Schematic diagram of a flowing afterglow apparatus.

Flow-Drift Tube (FDT)

The flow-drift tube is a logical modification of the flowing afterglow which enables ion-neutral reactions to be studied over a wide energy range, (0.05 – 5 eV). The downstream area of a flow-drift tube consists of a series of segmented stainless steel rings to which suitable potentials are applied, thereby establishing an axial electric field. [138, 139] The ratio of electric field strength to pressure, (E/N), inside the flow tube determines the average ion energy. Reaction data collated over a range of ion energies can provide a detailed mechanistic understanding of ion-neutral reactive collisions. [139]

Flowing Afterglow Langmuir Probe (FALP)

Flowing Afterglow Langmuir Probe, (FALP), instruments have been built to study ion-electron dissociative recombination processes. This apparatus differs from a conventional flowing afterglow only to the extent that it incorporates a moveable Langmuir probe. The Langmuir probe measures the electron density as a function of distance along the flow tube thereby allowing the evaluation of ion-electron recombination coefficients, α_e. [141]

Recently an upgraded FALP incorporating laser induced fluorescence, (LIF), resonance enhanced multi-photon ionisation, (MPI), vacuum ultra-violet, (VUV), and visible absorption capabilities has been commissioned at the

University of Georgia. [142] This instrument has been used to detect the neutral products of electron ion recombination reactions. [58]

Selected Ion Flow Tube (SIFT)

Many of the limitations of the flowing afterglow and flow-drift tube can be overcome by incorporating an upstream quadrupole mass filter to select ions of a particular mass to charge ratio. With this goal in mind, in 1976 Smith and Adams built the prototype Selected Ion Flow Tube, (SIFT). [143]

Figure 1.3 shows a simplified diagram of the SIFT. Ions are created via electron impact on an appropriate source gas in a high pressure / low pressure source remote from the flow tube. Following selection in a quadrupole mass filter, ions of a single mass to charge ratio are injected through a purpose built nozzle, or venturi, into the flow tube proper. As in FA instruments, the injected ions quickly thermalise by colliding with bath gas molecules. Gaseous neutral reagents are added through radial entry ports and the primary and product ions sampled by a downstream quadrupole mass filter after passing through a small orifice. The ions are detected by a particle multiplier coupled to conventional pulse counting electronic equipment. [143, 144] The bulk of the bath gas and entrained reagents are removed from the flow tube using a high capacity roots type blower.

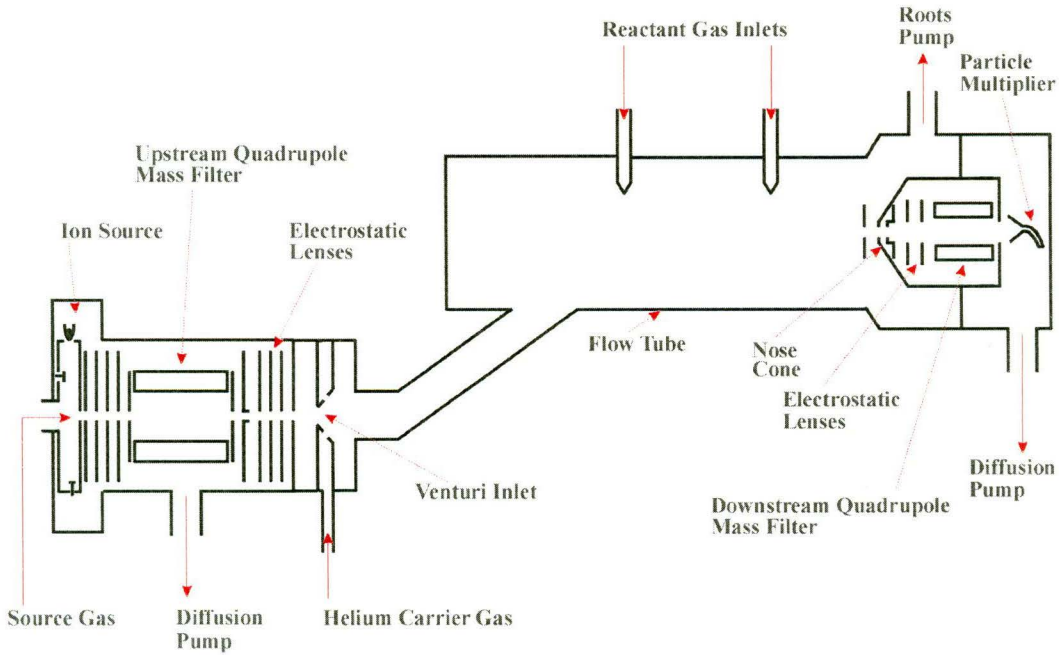

Figure 1.3. Schematic diagram of a selected ion flow tube, (SIFT).

Perhaps the most crucial feature of the SIFT is the venturi type inlet, (of which there are several designs [139, 141, 143, 144]), which facilitates the low energy injection of ions from a quadrupole mass filter operating at ~ 10^{-4} Torr into a bath gas at a relatively high pressure, (~ 0.2 - 1 Torr). Injected ions enter the flow tube with sufficiently low energy to avoid collisionally activated dissociation.

The general configuration of the SIFT allows the investigation of a wide variety of ion-molecule reactions. Enhancements to the basic design include the addition of a variable temperature facility and incorporation of a flow-drift tube. [141, 143, 144] The performance of the SIFT instrument has also been improved by the installation of a flowing afterglow plasma source of cations and anions. [145, 146]

A major strength of the SIFT is the relative ease with which rate coefficients and product ratios for ion-neutral reactions are obtained. The neutral reactant densities, (~ 10^{12} particles cm^{-3}), are substantially in excess of the ion densities, (~ 10^{3} –10^{6} ions cm^{-3}), hence pseudo-first-order kinetics prevail. For many simple reactions a semilogarithmic plot of ion count rate versus neutral flow yields a straight line with slope $\propto k$. [137]

Several comprehensive reviews of the SIFT technique and its applications are available. [139, 141, 144, 147]

Ion-Beam Techniques

Beam instruments may be categorised as either "crossed beam" or "merged beam".

Crossed beam and collision cell instruments allow the initial and final conditions in a collision to be precisely defined. This outcome is achieved by collimating reactants with known speed.

Beam collision cell instruments involve the interaction of an ion beam with a neutral reactant that is contained at very low pressures, (10^{-2} - 10^{-4} Torr), within a collision cell. Under these conditions the probability of multiple collisions is insignificant and the ion beam is attenuated by only a few percent. [148]

The crossed beam apparatus replaces the target gas cell with a neutral molecular beam that usually intersects the ion beam at an angle of 90°. This geometry is preferred for experiments demanding very high energy and angular

resolution. [149] Moreover, the crossed beam instrument allows control over the internal state populations of the neutral reactant as compared with the thermal equilibration of collision cells.

The merged beam technique allows very low collision energies to be studied by merging the almost parallel reactant beams in a common volume. [148] Relative energies as low as 0.002 eV have been attained. [150] The crossed beam and merged beam techniques are discussed and compared in a review. [149]

The measured quantity in a beam experiment is the *cross section,* $[\sigma(v)]$, which may be converted to a rate constant using the relation:

$$k = \int \sigma(v) f(v) dv \qquad \textbf{(150)}$$

where v is the mean relative velocity of the reacting ion-neutral pair and $f(v)$ is the distribution of v. Absolute cross-sections have been obtained for both crossed and merged beam experiments.

FA, FDT or SIFT data, and beam measurements show good agreement for a number of ion-neutral processes.

High Pressure Mass Spectrometry

This pseudo-static technique involves ionisation of the gaseous reagent(s) in a stainless steel reaction chamber, under high pressure conditions, (0.2 - 10 Torr), whilst allowing the leakage of a plasma sample through a pinhole orifice, (~ 60 μm diameter), into a quadrupole mass filter or magnetic sector mass spectrometer. An automatic pressure controller attached to a capacitance manometer, or a variable leak valve, is used to establish and maintain an approximately constant pressure in the reaction vessel. The reaction chamber may be heated or cooled over a typical temperature range of 170 – 680 K. Usually a pulsed electron gun is used to effect ionisation, however photoionisation may also be employed. Ions diffusing out of the reaction chamber are focused into the mass spectrometer using conventional ion optics. Ions traversing the quadrupole mass filter are detected by an electron multiplier and this signal fed through an amplifier and signal averager to a personal computer. The mass spectrometer and particle multiplier are housed in a differentially pumped assembly. This versatile instrument is capable of providing equilibrium and kinetic measurements and has been successfully employed in the investigation of many ion-neutral systems. [151-153]

1.7: Ion-Atom Chemistry.

Atomic species, in particular H, N, O and C, are major constituents of interstellar clouds [13, 17] yet little data is available on their reactivity with common ions. [24, 50, 135] Ion-atom reactions present considerable experimental challenges and this is undoubtedly why so few reactions have been characterised to date. The majority of ion-atom reactions for which data exists have only been studied in a single laboratory. The replication of experiments performed in other laboratories is therefore of considerable value as is the extension of the database by new measurements.

Ion Reactions with Hydrogen Atoms

Of the four atomic species mentioned above, hydrogen is the easiest to generate and monitor, hence a moderately large body of experimental data on ion-H atom reactions is available. [24, 50, 135]

Atomic hydrogen is usually produced by a microwave discharge in dilute H_2 / He mixtures or alternatively in pure molecular hydrogen. The degree of dissociation is high, (being ~ 90 - 95 % [154]), however surface recombination rapidly reduces the percentage dissociation to between 30 - 60 % in the reaction region for most experimental apparatus. [154] Thermal dissociation on the surface of a tungsten filament has also been used to create H atoms. [43] The H atom flux may be monitored using "indirect" chemical methods [43, 154-156] or from direct mass spectrometric analysis of the gas flow in the reaction zone. [157, 158]

Only a few cation-H atom reactions have been the subject of more than one study, (eg. $CO_2^+ + H$ [102, 154, 159, 160] ; $O^+ + H$ [161, 162] ; $CH_5^+ + H$ [102, 160, 163]), and for these systems the data is in general agreement. The reactivity of some small hydrocarbon cations, ($C_mH_n^+$; n = 1, 2; m= 2 - 6 [102, 164]), and three benzenoid hydrocarbon cations, ($C_6H_n^+$; n = 5 - 7 [165]), with H atoms has been reported. Data is also available for the reaction of other readily generated positive ions, (eg. CO^+ [162], HS^+ [166], H_2S^+ [166], H_3S^+ [166]). Some anions have also been found to react with H atoms, (eg. Cl^- [43, 167-171], F^- [100, 171], Br^- [171], I^- [43, 171], O_2^- [43], OH^- [43, 100, 155, 168] and H^- [100, 168, 172]). More recently accounts have been published detailing reactions between H atoms and some quite exotic species such as cluster anions, (eg. $OH^-(H_2O)_2$ [43]), fullerene cations [173, 174] and polycyclic aromatic hydrocarbon cations such as $C_{10}H_8^+$. [175]

Significant gaps exist in the ion-H atom experimental data currently available. In particular the reactivity of medium sized hydrocarbon ions, ($C_mH_n^+$; m= 2 - 6, n =1 - 9), needs to be probed. The paucity of experimental data is a serious impediment to modellers, particularly in view of the cosmological abundance of atomic hydrogen.

Ion Reactions with Nitrogen Atoms

Only a modest number of reactions between ions and atomic nitrogen have been reported in the literature. [24, 50, 135] This may be largely due to the small amount of dissociation, (typically 0.5 – 1.0 % [176, 177]), that is obtained by subjecting molecular nitrogen to a microwave discharge. The low percentage of dissociation is explained by the difficulty in breaking the N_2 triple bond and the high rate of homogenous three-body N atom recombination, (10^{-32} cm^6 $molecule^{-2}$ s^{-1} [176]), in a molecular nitrogen bath gas.

The flow of N atoms is often measured using the titration reaction: [85]

$$N + NO \Rightarrow N_2 + O \qquad \textbf{(151)}$$

$$k_{(151)\,@\,298K} = (3.4 \pm 1.0) \times 10^{-11}\ cm^3\ s^{-1}$$

Reaction **(151)** is also a convenient method for producing atomic oxygen. Alternatively the N atom flux may be determined by reference to a calibration reaction, (eg. $C_2H_2^+ + N$ [177, 178]).

Care must be taken to eliminate excited neutral species, (eg. vibrationally excited N_2), from the reaction zone; this is conveniently done by inserting a glass wool plug into the N_2 / N atom flow downstream of the microwave discharge. [179]

Reactions between many of the small hydrocarbon cations, (eg. CH^+ [177, 178], CH_3^+ [178, 180], CH_5^+ [177, 178], $C_2H_2^+$ [177, 178] and $C_3H_3^+$ [178]), and atomic nitrogen have been reported. Data also exists for the reaction between N atoms and easily generated ions such as CO^+ [161], CO_2^+ [181], O_2^+ [179, 182], H_2O^+ [177] and NO_2^+. [182] There are very few accounts of anion-N atom reactions, although the species O_2^- [169, 183], O^- [169, 183] and OH^- [169] have been reacted with N. The reaction of some polycyclic aromatic cations with N have been reported very recently. [175]

Large gaps exist in the compendium of experimental data currently available for ion-N atom reactions. Additional studies are required to examine the reactivity of various hydrocarbon cations with N. Rate coefficients and product ratios for the reaction of nitrile cations with atomic nitrogen need to be

measured and the reaction between H_3^+ and N is an important unresolved problem. [17, 185, 186]

Reactions Between Oxygen Atoms and Ions.

A relatively small number of ion-O atom reactions have been studied experimentally. [24, 50, 135] Atomic oxygen is usually created via the rapid reaction of N with NO, [reaction **(151)**], [161] although sometimes direct microwave discharge of dilute O_2 / He mixtures has been employed. [186] Rate coefficients and product ratios for the reaction of specific ions with both N and O are obtained by deconvolution of these "NO titrations". [137] Some volume and surface recombination of O atoms is unavoidable; this phenomenon may produce a 20 % reduction in rate constants. [161]

Atomic oxygen has been reacted with a number of small hydrocarbon cations, (eg. CH^+ [177], CH_3^+ [180, 187], CH_5^+ [177, 188], and $C_2H_2^+$ [177]), and a number of other important cations, (eg. N_2^+ [181, 189, 190], N_2H^+ [188], H^+ [161], CO^+ [161], CO_2^+ [181], and NO_2^+ [182]). Data is also available for several anion-O atom reactions, (eg. CO_3^- [183], CO_4^- [191], O_4^- [191], O^- [168, 169, 183], O_2^- [168, 169, 183], OH^- [168, 169], and SF_6^- [170]). A recent paper discusses the reaction between some naphthalene derived polycyclic aromatic hydrocarbon cations and O atoms. [175]

Experimentation on many ion-O atom systems is still needed. In particular, data is required on the reactivity of many hydrocarbon cation species, (eg. $C_6H_6^+$, $C_6H_5^+$, $C_3H_3^+$, $C_4H_2^+$, and $C_4H_3^+$), with atomic oxygen. Furthermore, the reactions of such prevalent ions as HCO^+, HCO_2^+, HCN^+ and $HCNH^+$ with O need to be studied in the laboratory. Rate coefficients and product ratios for many of these unstudied ion-O atom reactions are necessary to improve the veracity of interstellar cloud models.

1.8: Introduction to the Current Research.

The following eight chapters discuss the results of experiments and theoretical calculations performed from March 1993 to May 1997. Where possible I have commented briefly upon the implications of this work for chemistry in the interstellar medium.

Chapter Two outlines the experimental procedures employed and details several modifications to the SIFT instrument. This section includes a general

discussion on pyrex / quartz neutral inlet probes suitable for ion-atom experimentation.

Chapter Three examines experimental and theoretical studies of the association reaction between $C_2H_3^+$ and carbon monoxide. This work is pertinent to the production of propynal in interstellar clouds.

Chapter Four presents data on a large number of ion-H atom reactions. In particular rate coefficients and product distributions are presented for the reaction of several hydrocarbon cations with atomic hydrogen. Some comment is made upon the relevance and importance of these reactions to interstellar synthesis.

Chapter Five reports on the reactions between a substantial number of ions and atomic nitrogen. The effect of these ion-N atom processes on interstellar chemistry is also briefly addressed.

Chapter Six discusses the reaction of atomic nitrogen with the ubiquitous H_3^+ cation. This reaction has important consequences for the synthesis of ammonia in interstellar clouds.

Chapter Seven describes a number of ion-O atom experiments. Again the effects of these reactions upon the chemistry of interstellar clouds is explored concisely.

Chapter Eight gives details of some preliminary (unsuccessful) attempts to explore reactions between various cations and atomic carbon.

Finally in Chapter Nine I summarise this work and offer suggestions for future endeavours.

CHAPTER 2.

EXPERIMENTAL.

2.1: General Description.

The measurements reported in this work were made using a Selected Ion Flow Tube, (SIFT), located at the University of Canterbury. This instrument was constructed between 1982 – 1985 and has been extensively modified and upgraded since its original commissioning.

A photograph of the Canterbury SIFT is shown in Figure 2.1 overleaf. Furthermore, the schematic diagram of a "generic SIFT" in Chapter 1, (Figure 1.3), faithfully depicts this instrument. Knight [192] and Petrie [18] have provided a detailed description of this apparatus, hence the ensuing summary will be restricted to a consideration of the major components plus a description of those modifications added during the course of this research.

Principal Sections

The Canterbury SIFT is essentially a flow tube coupled to differentially pumped mass spectrometers at each end. An off-axis SIFT chamber containing the ion source, quadrupole mass filter and ion optics is attached to the upstream end of the flow tube. The downstream end of the flow tube is connected to an on-axis analyser assembly comprising ion optics, quadrupole mass filter and particle multiplier.

The SIFT Chamber

Ions are generated by electron impact on a suitable precursor gas or vapour in the ion source. A sequence of five electrostatic lenses focus the ions into the upstream quadrupole mass filter which transmits ions of a single mass to charge ratio. The upstream and downstream quadrupole mass filters are identical. Both are Extrel 7-270-9 models, and consist of four, 16 mm diameter, 22 cm long stainless steel rods, mounted on ceramic supports and encased in a stainless steel cylinder, providing an overall field radius of 1.49 cm. The upstream mass

filter is driven by an Extranuclear power supply through a compatible Model 13 high-Q head. A further cluster of six electrostatic lenses direct the ion swarm into a annulus type venturi inlet [144, 192-194] where they are entrained by the bath gas. Differential pumping by a 10 cm oil diffusion pump maintains the SIFT source chamber at an operating pressure of ~ < 10^{-4} Torr. The upstream ion optics were designed using the SIMION program [195, 196] and installed by Petrie during the course of his research. [18] The ion source was upgraded in 1994 to improve performance and permit operation under high or low pressure conditions.

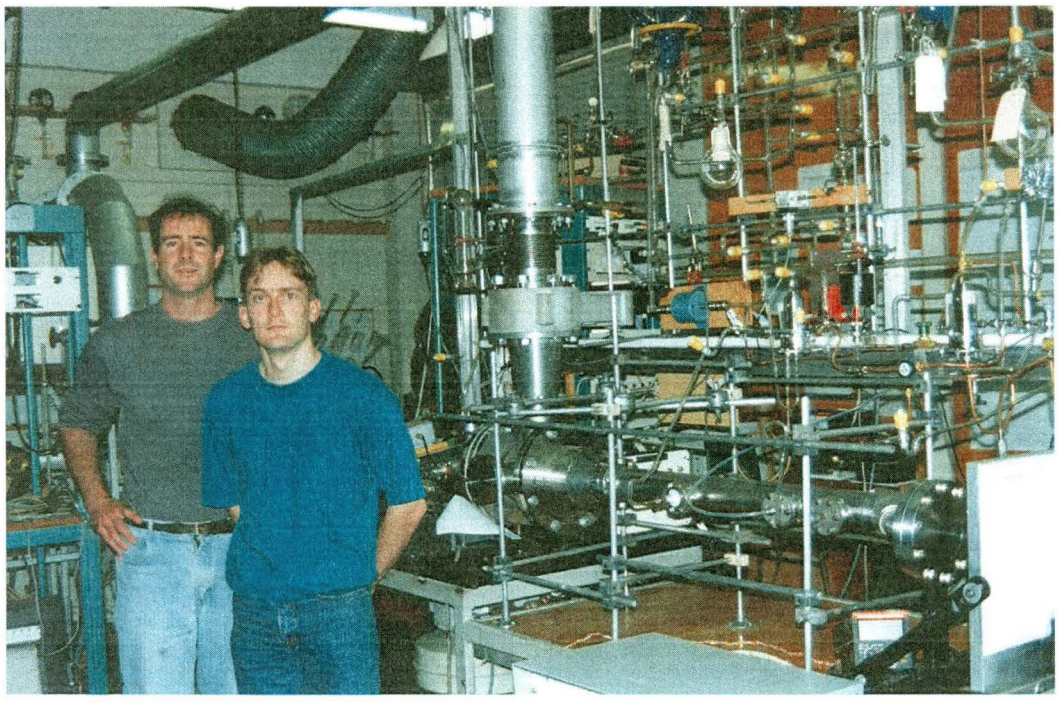

Figure 2.1. Wide angle view of the selected ion flow tube (SIFT) at the University of Canterbury.

The Flow Tube Section

The stainless steel flow tube used in the Canterbury SIFT is ~111 cm in length and has an internal diameter, (i.d.), of 7.32 cm. The facility exists to insert a 67 cm drift tube section, (i.d. 6.03 cm), consisting of fifty, 0.9 cm wide stainless steel rings and a 17.5 cm field free section, allowing the establishment of an axial electrostatic field. The drift tube insert was present in many of the experiments discussed in this thesis. Typically the bath gas flow rate is ~ 119 Torr L s^{-1} at a pressure of 0.30 - 0.35 Torr. This flow rate creates a bath gas

velocity of ~ 8800 cm s^{-1}, (~ 11500 cm s^{-1} with the drift tube inserted), with the ion velocity on the tube axis being ~ 1.5 times faster than the carrier gas "plug velocity". [144] Three reactant gas inlets are located at various positions along the flow tube. For most neutral reagents ring type neutral inlets are optimal, [18, 197] however purpose designed and built probes are necessary to efficiently admit atoms into the reaction zone. The flow tube is pumped by a high capacity roots blower, (Japan Vacuum Engineering Model PMB-020 with a maximum pumping speed of 0.57 $m^3 s^{-1}$ @ 0.1 Torr), backed by a large mechanical backing pump, (Japan Vacuum Engineering Model PKS-030).

The Analyser Assembly

A small fraction of the ion swarm travelling down the flow tube is sampled through a 0.46 mm hole in a molybdenum disc, situated at the apex of a nose cone. Four electrostatic lenses focus these ions into a downstream quadrupole mass filter which is connected to an Extranuclear power supply via a compatible Model 15 or 12 high-Q head. A working pressure of ~ 1 x 10^{-5} Torr is established by differentially pumping the analyser assembly with a 10 cm oil diffusion pump. The downstream mass filter is coupled to a personal computer, (PC), and controlled by purpose written software, ("SIFT for Windows"). Transmitted ions encounter a particle multiplier, the entrance of which is biased to ~ -2700 Volts. The particle multiplier installed in the Canterbury SIFT is a De-Tech Model 203 with a nominal gain of 8.98 x 10^7 at 2200 Volts. Electron pulses from the particle multiplier are fed to an amplifier-discriminator which outputs TTL pulses. Parallel circuits direct this TTL signal to a PC Lab Card, (Advantech PCL-812PG), and an A-D pulse counting circuit incorporated into a ratemeter.

2.2: The Bath Gas Flow System.

The bath gas flow system must fulfil the requirements of purifying the carrier gas prior to admission to the flow tube at constant measurable rates. For most applications helium is the preferred gas, however hydrogen, nitrogen and argon may be used for particular experiments.

Overview of the Bath Gas Flow System on the Canterbury SIFT

A cylinder containing the bath gas is coupled, via a regulator, to 0.635 mm copper pipe. The gas is ducted into a molecular sieve trap, cooled to ~ 77 K by immersion in liquid nitrogen. This purification removes trace impurities including water, oxygen and argon. Particulates, (including macroscopic grains of molecular sieve), are removed by a filter, prior to the gas being admitted to a Tylan FC 261 flowmeter. This particular model has a working range of 0 – 10 standard litres per minute, (of H_2), tolerates a maximum inlet pressure of 150 psig, and functions correctly with a differential pressure of 10 - 40 psid across the valve. The flow rate of the bath gas is regulated by the flowmeter to maintain a constant flow-tube pressure during the course of experimental measurements. The measured flow of carrier gas is admitted to the flow tube via a venturi inlet. [144, 192-194] Following traversal of the flow tube the gas is pumped away through a 15 cm Temescal high vacuum gate valve into a roots pump / backing pump assembly and is eventually exhausted into the atmosphere.

Modifications to the Bath Gas Flow System

Several modifications have substantially upgraded the bath gas flow system.

Firstly two large heating elements have been installed around the molecular sieve trap. This allows the molecular sieve beads to be baked overnight, or for extended periods, and any adsorbed impurities pumped away using a two stage backing pump. The two U-shaped heating elements run the full length, (~ 108 cm), of the molecular sieve trap, draw a maximum of 1 kW, and have a variable temperature mode of operation. They are capable of heating the copper sleeves of the trap to ~ 80 °C.

Secondly a Norgen Mk III F13-000-V2T0 high pressure vacuum filter has been installed in the bath gas reticulation system between the molecular sieve trap and the Tylan flowmeter. This filter accepts inlet pressures up to 10 Bar and is capable of removing particulate material of 25 μm size or above, that could otherwise block the venturi inlet into the flow tube. Degradation of molecular sieve beads over time is the most likely source of particulate material in the bath gas delivery line.

Automatic monitoring of the bath gas flow rate has been provided by directing a voltage output from the Tylan flowmeter to the PC Lab card. The

Tylan flowmeter display unit generates a 0 - 5 Volt signal that is directly proportional to the carrier gas flow rate. This voltage signal is the input to an appropriate channel of the PC Lab Card.

Similarly the flow tube pressure is now recorded automatically by feeding a 0 - 5 Volt signal from the Baratron power supply to a suitable channel of the PC Lab Card.

The ambient temperature in the laboratory, and hence the temperature of the bath gas, is now sensed by a LM 335 temperature sensitive diode and the output from this device is automatically provided to a channel on the PC Lab Card.

2.3: Ion Source.

During the course of his Ph.D. research Petrie designed and built a new ion source and associated ion optics. [18] Whilst this source generated most ions tolerably well, moderately high lens voltages were often required to inject workable quantities of some species. The operation of the ion source with these high voltages, particularly on the repeller, created collisionally induced dissociation, (CID), of hydrocarbon ions such as CH_3^+. This phenomenon is well understood having been attributed to bond fracture in ions that are injected into the bath gas with high energies. [139, 144]

Ion Source Upgrade

In 1994 the ion source was modified according to advice received from Professor D. Smith and Dr P. Spanel. For most ionic species the upgraded ion source gives enhanced ion signals compared with that obtained from its predecessor and the problem with CID has been largely overcome.

Essentially the ion source upgrade consists of four changes. Firstly the body of the ion source, or cage, has been floated. This has necessitated the insertion of a thin sheet of insulating teflon between the ion source / filament assembly and the supporting cradle. The diameter of the aperture through which electrons enter the ion source has been reduced from 3.0 mm to 1.0 mm. This smaller aperture has made accurate positioning of the filament above the hole an exacting task and critical to the efficient production of ions. Similarly the diameter in the exit plate of the ion source has been reduced from 2.5 mm to 1.0 mm. The downsizing of these two orifices has modified the ion source from a

low pressure source to a high pressure source. Finally the repeller plate has been repositioned forward, taking up a position closer to the electron entrance aperture.

For most applications, the ion source is operated as a high pressure source but the facility exists to insert an exit plate having a larger central orifice of 2.5 mm. This low pressure configuration seems to produce more fragmentation in the ion source and has been used to enhance the generation of certain species, (eg. HCO^+ from dimethoxymethane).

A schematic diagram of the modified ion source is shown in Figure 2.2 overleaf.

2.4: Admission of Neutral Species.

Measured flow rates of neutral reagents are added from a pyrex flow line into the flow tube through any of three inlets. The glass line is maintained at a pressure of ~ 10^{-3} Torr by a single-stage oil glass diffusion pump backed by a two-stage mechanical pump, (Alcatel model 370-C55). The flow rate of the neutral species is monitored either by pressure reduction out of a calibrated volume, or directly using a flowmeter. Neutral reagents used in this research were gases, vapours derived from volatile liquids, and atomic species such as H, N, and O. Special techniques are employed to generate atoms and efficiently admit them into the flow-tube at known flow rates.

Measurement of Neutral Flow Rate by Pressure Reduction from a Calibrated Volume

Neutral flow rates may by determined by measuring the pressure reduction as a gas or vapour flows from a calibrated volume into the flow tube over a discrete time interval. This method was used by both Knight [192] and Petrie. [18] The gaseous reagent is expanded from one of three calibrated volumes, (small ~ 0.18 L, medium ~ 0.77 L and large ~ 5.7 L). A Varian variable leak valve incorporating a helium flush is used to control the flow rate. The pressure drop in the chosen volume is monitored by a differential transducer, (Validyne model DP15-20, 7 Torr diaphragm). The voltage signal from the transducer is the input

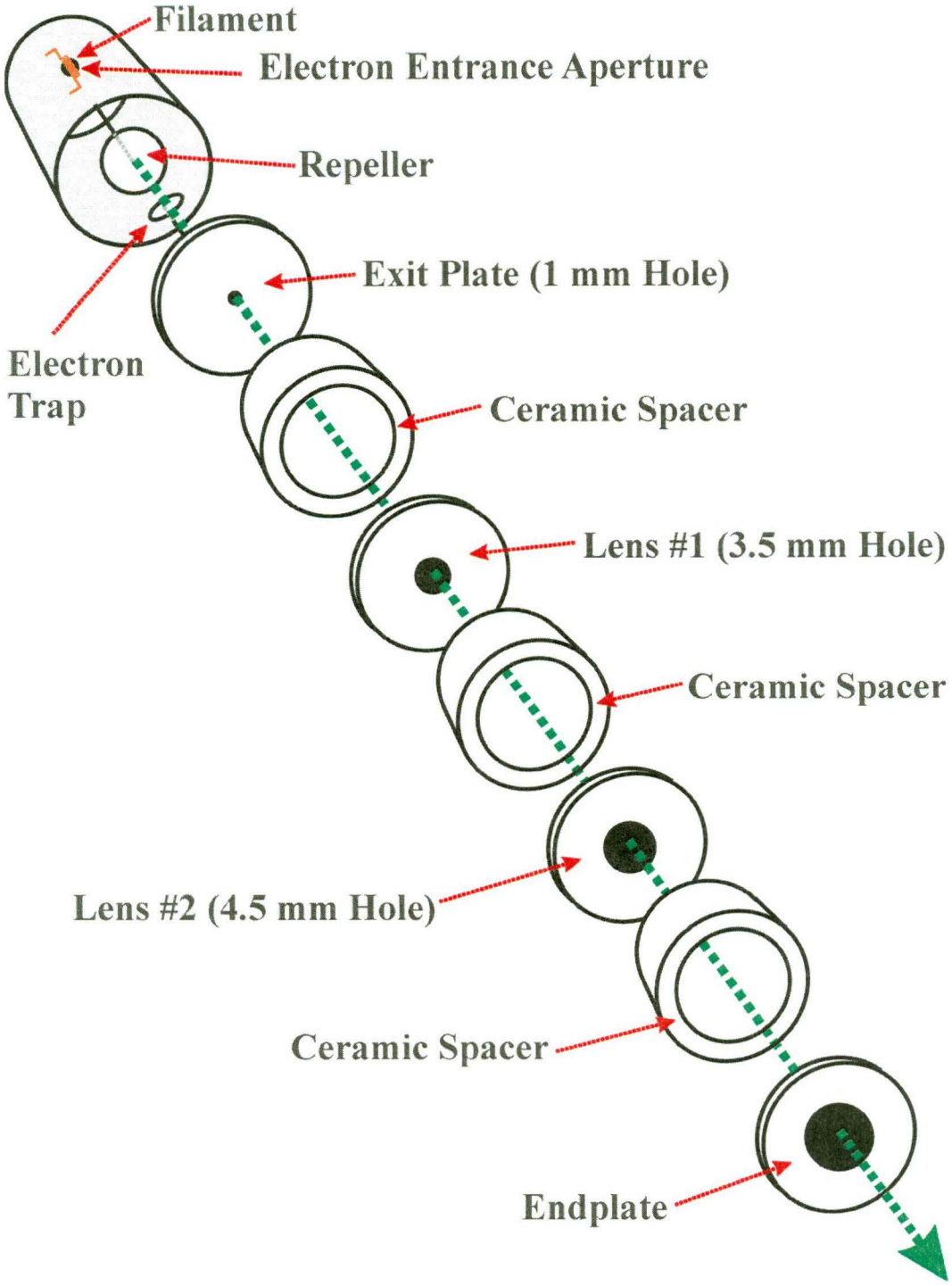

Figure 2.2. Exploded diagram showing the upgraded high pressure ion source.

to an appropriate channel of the PC Lab Card. The Validyne transducer is periodically calibrated to ensure that an output of 0.7 Volts corresponds to a pressure differential of 7 Torr.

Measurement of Neutral Flow Rate using a Flowmeter

In 1994 a MKS 1259C-00010SK Mass Flow Meter was installed on the SIFT apparatus. This model is powered by a ± 15 Volt DC power supply, accepts a maximum inlet pressure of 150 psig and has a full scale range of 10 standard cubic centimetres per minute, (sccm), of N_2. The command and output signals are both 0 – 5 Volts DC. Standard 0.635 mm Swagelock fittings are used to connect the flowmeter to the neutral delivery line. The manufacturer claims an accuracy of ± 0.8 % of the full scale range, (this equates to ± 0.08 sccm), for this instrument. This flowmeter is suitable for monitoring the flow of most gases and some vapours. Manufacturer supplied gas correction factors, (GCF's), must be used when the neutral is other than air, nitrogen or oxygen. GCF's may also be calculated for any substance provided the density and specific heats are known.

Manual or automatic control, (via the PC), of the flowmeter is possible.

When operating under manual control a variable potentiometer directs an input voltage to the flowmeter thereby establishing the desired flow rate. The output signal, (which is directly proportional to flow rate), is fed into a nominated channel of the PC Lab Card. Switching options also exist to drive the control valve fully open or fully closed.

Automatic control of the flowmeter is achieved by programming purpose-written software, ("SIFT for Windows"). One module of this program is interfaced to the flowmeter and allows the user to nominate the number of neutral flows to be measured within a particular flow range. The PC then automatically varies the input voltage, and hence flow rate within the desired flow range, over a series of discrete time windows, (typically 10 seconds). Flow rate dependent output voltages are fed back to a dedicated channel of the PC Lab Card. This feedback feature allows flow rates to be changed rapidly and hence measurements can be made expeditiously without sacrificing precision.

Generation of Atoms

Atomic species are generated by creating a microwave discharge in a precursor gas. The discharge is established within a quartz section of a purpose designed probe containing a known flow rate of a parent molecular gas, (eg. N_2 or a dilute mixture of H_2 in He).

A Microtron 200 Microwave Power Generator Mk III powers an Evenson, Broida, Fehsenfeld microwave discharge cavity [198] which envelops a small section, (~ 2.1 cm), of the quartz tubing. Figure 2.3 depicts this cavity and the associated cabling. Depending on the specific application, an incident power of between 50 and 90 Watts is applied to the discharge cavity at a frequency of 2450 MHz. The cavity is tuned by two adjustable metal probes enabling ≤ 2 Watts of reflected power to be dissipated in most experimental situations. Considerable heat is generated and therefore the cavity and encapsulated quartz section of tube are cooled using a flow of air.

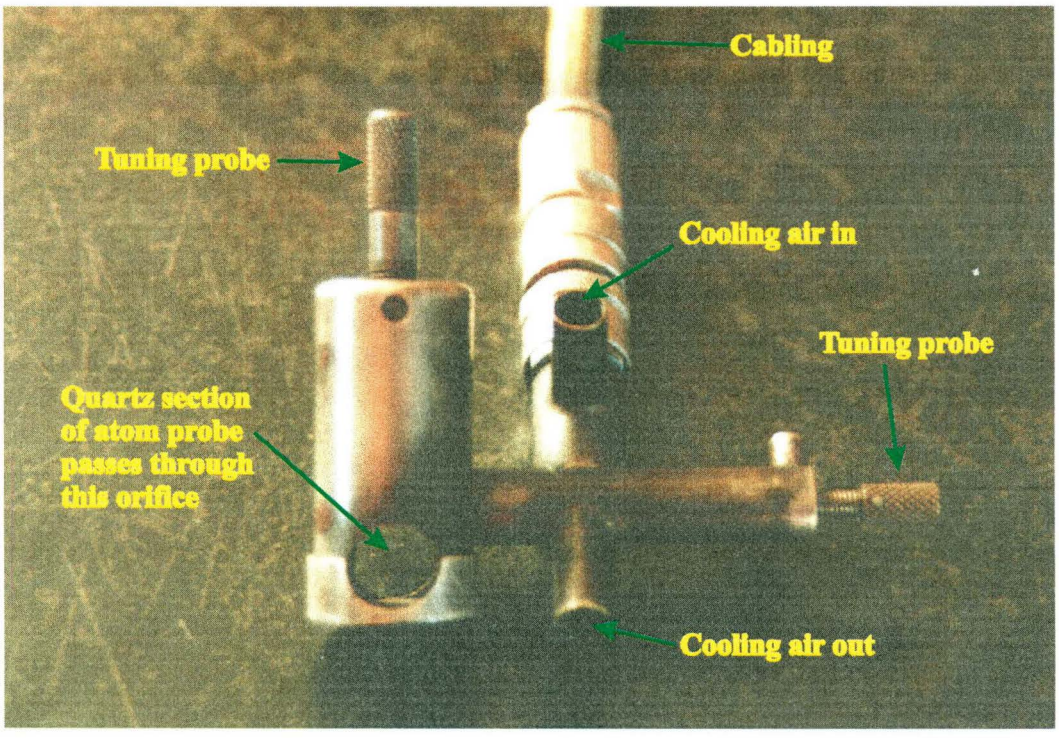

Figure 2.3. The Evenson, Broida, Fehsenfeld microwave discharge cavity used to generate atomic species.

The pyrex / quartz atom probes vary subtly in design, depending upon which atomic species is to be generated. In general the probes are L-shaped with a light horn incorporated at the apex of the "L". The light horn prevents energetic photons created in the microwave discharge, from entering the flow tube where photoionisation could cause unwanted ions. The generic atom probe consists of an ~ 20 cm length of hollow quartz section with the remainder of the probe being constructed of pyrex. The microwave discharge cavity is positioned around the quartz section, and may be moved closer to the flow tube entrance or further away as desired. The section of the probe protruding into the flow tube is sheathed in stainless steel sheet, which is earthed to the flow tube to prevent a charge build up on the glass probe with attendant loss of ion signal. A small stainless steel cap covers the tip of the probe and partially extends over the stainless steel sheath. Typically 10 mm i.d., 13 mm o.d., pyrex and quartz tubing are used to construct the atom probes that have been used in this research. A schematic diagram of a generic atom probe is shown in Figure 2.4 overleaf. Detailed descriptions of the atom probes that have been designed and built to generate H, N, O and C atoms are given in forthcoming chapters of this work.

The interior of the atom probe (downstream of the discharge region) is coated with a halocarbon wax / chloroform mixture to mitigate the recombination of atoms on glass surfaces. This coating is prepared by adding ~ 10 mls of halocarbon wax to 1 litre of chloroform. After ~ 2 hrs a homogenous mixture is obtained and the atom probe is immersed in the solution for at least 30 minutes. The probe is then removed from the mixture, air-dried, and installed into the SIFT apparatus.

The determination of atomic fluxes requires dedicated techniques and is the major source of inaccuracy in ion-atom measurements. Again the specific method employed depends on the atomic species being monitored, however in general, chemical methods are utilised. For H atoms a mathematical deconvolution of the reaction between CO_2^+ and a mixture of molecular and atomic hydrogen has become a standard method of determining H atom flow rates. [154, 173, 174] For N and O atoms it is usual to make use of the so called "NO titration" which conveniently enables the simultaneous evaluation of N and O fluxes. [177, 179, 189] Alternatively N atom flow rates may be readily determined by

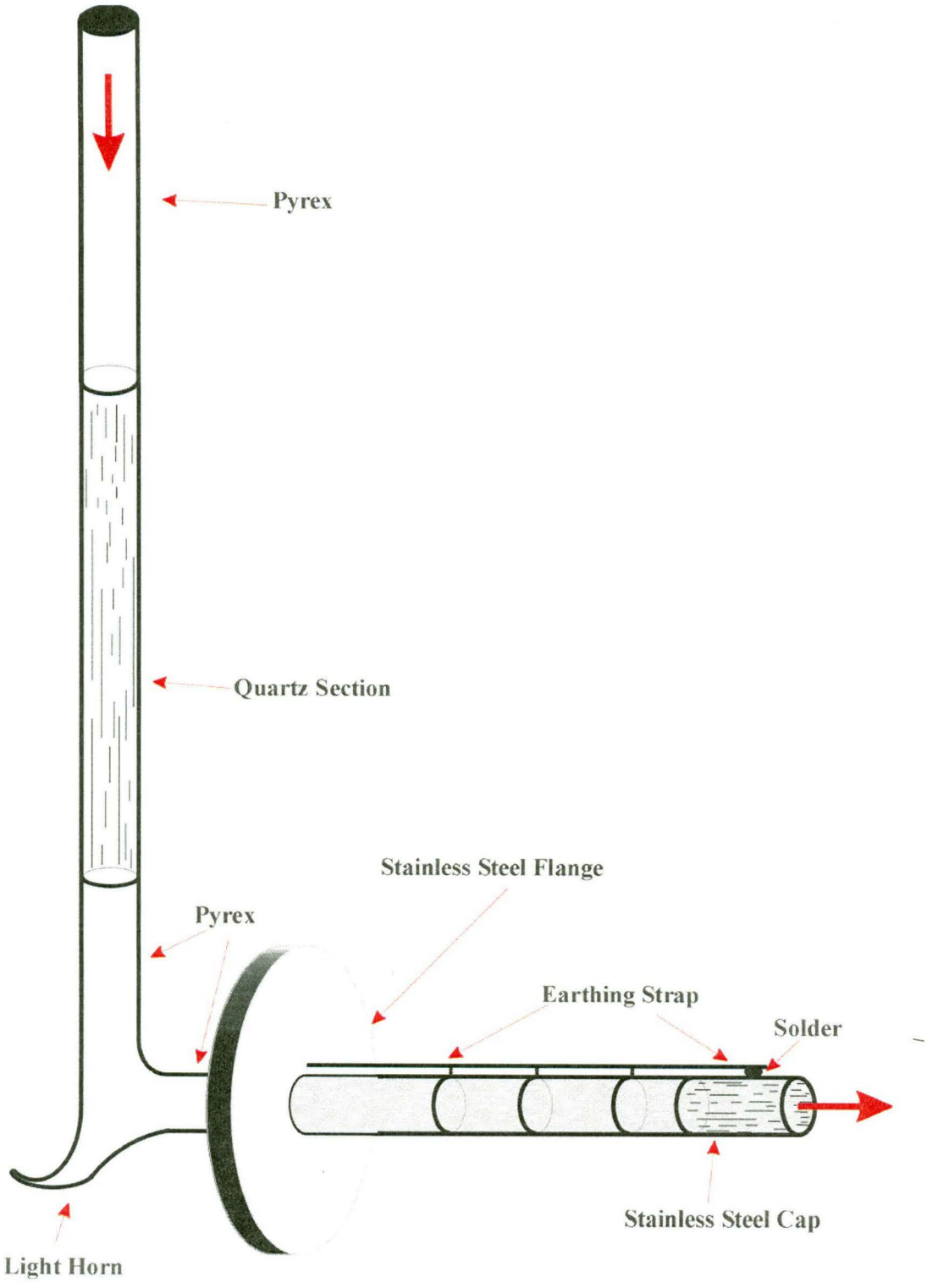

Figure 2.4. Schematic diagram showing the salient features of a generic atom probe.

referencing the "raw rate coefficient" obtained for a calibration reaction, (eg. $C_2H_2^+ + N$), to the well established "absolute value" of this rate constant. The particular details of how atomic H, N and O flow rates are measured are described in subsequent chapters.

Figure 2.5 shows a microwave discharge in nitrogen gas, producing a small but adequate flux of atomic nitrogen. The discharge cavity and atom probe are clearly visible.

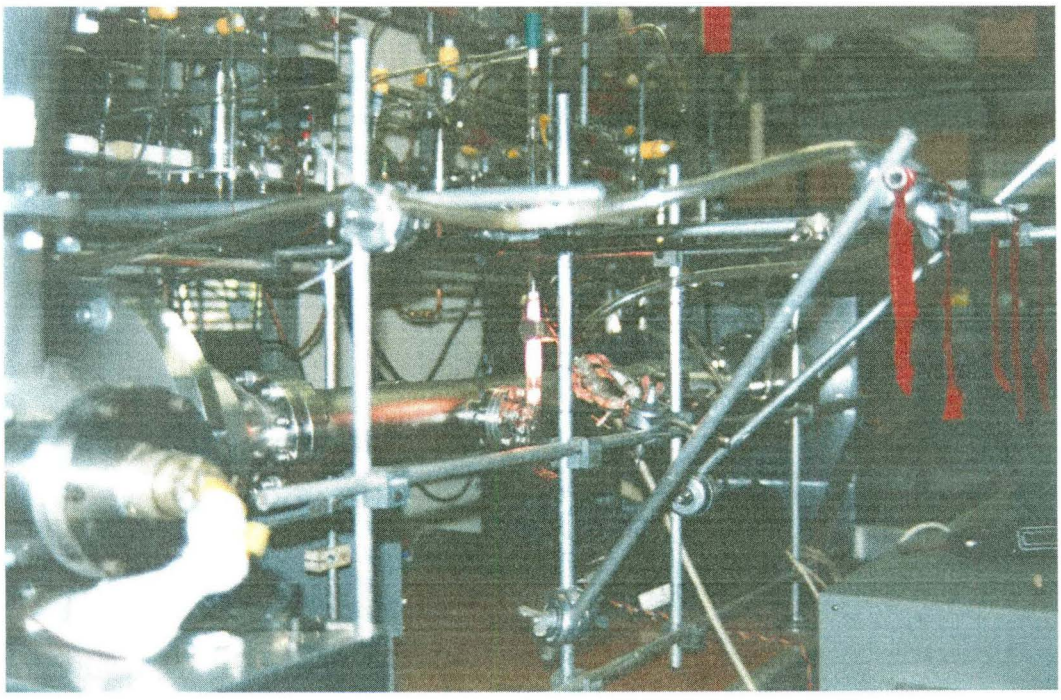

Figure 2.5. A view of the microwave discharge head and nitrogen atom probe in situ on the SIFT instrument. The orange glow originating from the microwave discharge of N_2 may be clearly seen.

2.5: Data Acquisition and Analysis.

Some early data was collected using a program written by Morrison in QuickBasic code entitled "SIFT2D". [199] This prototype program was not particularly sophisticated but represented a significant advance over the manual recording techniques used by Knight [192] and Petrie. [18] Essentially this program recorded a series of flow rates and ion counts. The software was able to cope with sequentially recording both primary and product ions, however a number of important parameters such as pressure and temperature were entered manually. There was no facility for PC control of the downstream, (analyser), quadrupole

mass filter and mass spectra could only be viewed on an oscilloscope. This early program did not provide product distributions for ion-molecule reactions but rate coefficients were calculated and displayed. Product ratios were obtained by entering the raw ion counts data (corrected for any mass discrimination) into another QuickBasic program written by Wilson. [130] Most of the data discussed in the next chapter were collected and analysed using this early suite of programs, however many of the reactions were repeated following the 1994 software upgrade.

SIFT for Windows

In 1994 a macroscopic leap forward occurred when the program "SIFT for Windows" was installed and proven on the Canterbury SIFT. The code was written by Dr P. Spanel who developed the software under the guidance of Professor D. Smith. This program was purpose written to control a modern SIFT instrument, record experimental data and perform analysis. The software runs under a Windows operating system and is written in Borland Pascal. It is no exaggeration to state that this program has totally revolutionised the way SIFT data is collected and analysed and furthermore it has considerably enhanced the utility of the SIFT technique.

The original code was customised by Dr Spanel during installation and initial testing to take account of minor differences between the Canterbury SIFT and the Innsbruck SIFT which the program was originally written for. A series of relatively small, cosmetic changes have subsequently been made locally by Fairley to further improve the overall package. In 1996 an upgrade of the original SIFT software was received from Spanel and Smith. This enhanced version has been installed and has operated successfully for the last six months.

SIFT for Windows has a number of advanced features, arguably the most important of which is the facility for remote control of the downstream quadrupole mass filter. This feature allows any accessible mass range to be swept, the resulting spectrum being displayed on the computer monitor and / or printed out if required. Ion peaks are readily identified and appropriately annotated with their m/z ratio. Accurate mass assignment is achieved by regular calibration of the downstream quadrupole mass filter. The calibration procedure involves injecting Ar^+ ions and adjusting the calibration potentiometer to ensure that at resolution 8.0, the high mass edge of the m/z = 40 peak occurs at

40 amu. The 1996 upgrade also allows for an instantaneous readout of peak height ratios. This feature was introduced for trace gas analysis but may be also used to give an initial approximate guide to product distributions. Spectra may be saved to disk and retrieved for inspection at any time. They may also be copied to a Windows clipboard and pasted into a variety of documents, (eg. Word document or CorelDraw graphic). Options are available to traverse the desired mass range in varying lengths of time, recording differing number of data points per mass unit. Spectra obtained may be smoothed and the ion peaks displayed on a linear or logarithmic scale. Figure 2.6 shows a typical mass spectrum collected using SIFT for Windows.

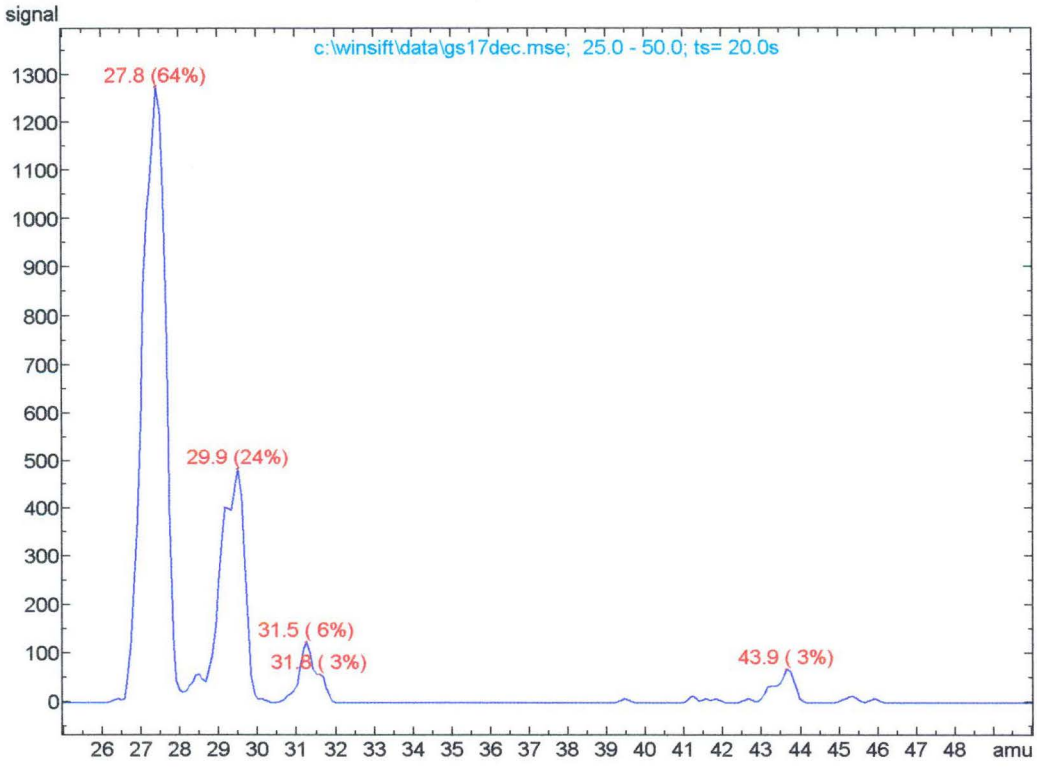

Figure 2.6. A typical mass spectrum obtained using SIFT for Windows. This spectrum was obtained by reacting N_2^+ with a mixture of N, O, NO and O_2 during an "NO titration".

The features described above allow the experimentalist to see what is occurring in any given ion-neutral reaction. Primary ion peaks are seen to diminish when reactive neutral reagents are added and product peaks appear. Quantitative data collection is commenced following the exact location of these primary and product ion masses using the mass spectrum module detailed above. The positions of all peaks of interest are entered into the SIFT for Windows

program along with an indication as to their status, ie either primary ion, product ion or other, (spectator), ion. The program is then told whether the neutral reagent will be added via the flowmeter or by monitoring the pressure drop out of a calibrated volume. If the neutral is to be added using the flowmeter then the GCF is entered and a decision made as to whether the flowmeter will be commanded manually or automatically from the PC. If automatic control of neutral flow is required then the number of data points to be collected is entered along with the minimum and maximum flow rates. Manual control of the flowmeter simply requires a keystroke once the desired flow has been established on the flowmeter. The other option of adding the neutral manually through the variable leak valve and monitoring the pressure drop out of a calibrated volume simply requires the calibrated volume to be entered.

Following this initialisation phase the data is collected. If the neutral is being added automatically by flowmeter under PC control, a single keystoke initiates data collection. The entire data set is then collected as the analyser sequentially visits each programmed mass for each discrete neutral flow. The PC automatically commands a different neutral flow from the flowmeter once all programmed masses have been sampled. Both manual methods of neutral addition involve the interrupted collection of an ensemble of data points. Once the desired neutral flow has been manually attained a single keystroke initiates data collection and the mass spectrometer is cycled through each of the programmed masses in turn. A different neutral flow is then set manually and the process of data acquisition repeated until sufficient information has been obtained.

Following the data collection phase the file is saved. Data analysis occurs concomitantly with data acquisition. Rate coefficients and product distributions are calculated and displayed as a data set is recorded. The SIFT for Windows program produces a table of raw data, a semilogarithmic plot of ion counts versus neutral flow rate, and a graph showing the product ratio as a function of neutral flow. In addition the program performs a least squares fit of Ln [ion count] versus neutral flow rate and displays the calculated values of the rate coefficients for one or more reactive primary ions. Approximate fractional abundances of product ions are also calculated and shown in real time.

Data may be downloaded to a printer, pasted into another Windows application, (eg. Word or CorelDraw), or retrieved for further analysis at a later date. A typical "raw" data set for the reaction of $C_6H_6^+$ + NO is tabulated in Table 2.1. Figure 2.7 shows a graph of Ln [Ion Count] versus neutral flow rate. Figure 2.8 is a product distribution graph which is a plot of the fraction of each product ion as a function of neutral flow.

GS20JUNA.SDE #0 $C_6H_6^+$ + NO

Flow	$C_6H_6^+$	NO^+	$C_6H_6^+.NO$
0.00000	1900	0	7
0.00000	1917	5	16
0.00864	1400	147	325
0.00783	1427	123	289
0.00544	1620	96	234
0.00340	1646	68	155
0.01470	1083	199	500
0.00000	2062	0	4

L = 44.7 cm, p = 0.360 Torr, f_c = 119.1 Torr L s^{-1}, GCF = 1.00, Tg = 299, v_g = 11580 cm s^{-1}, Vol = 0.181 L, R_{tube} = 3.015 cm, 20.06.1997, 20:16

$C_6H_6^+$ m = 78.51: k = 1.6 x10^{-10} cm^3 s^{-1} IO = 1972.9 c/s
NO^+ m = 29.70: 31.2 %
$C_6H_6^+.NO$ m = 108.9: 68.8 %

Table 2.1. A table showing the raw data obtained for the reaction of $C_6H_6^+$ + NO.

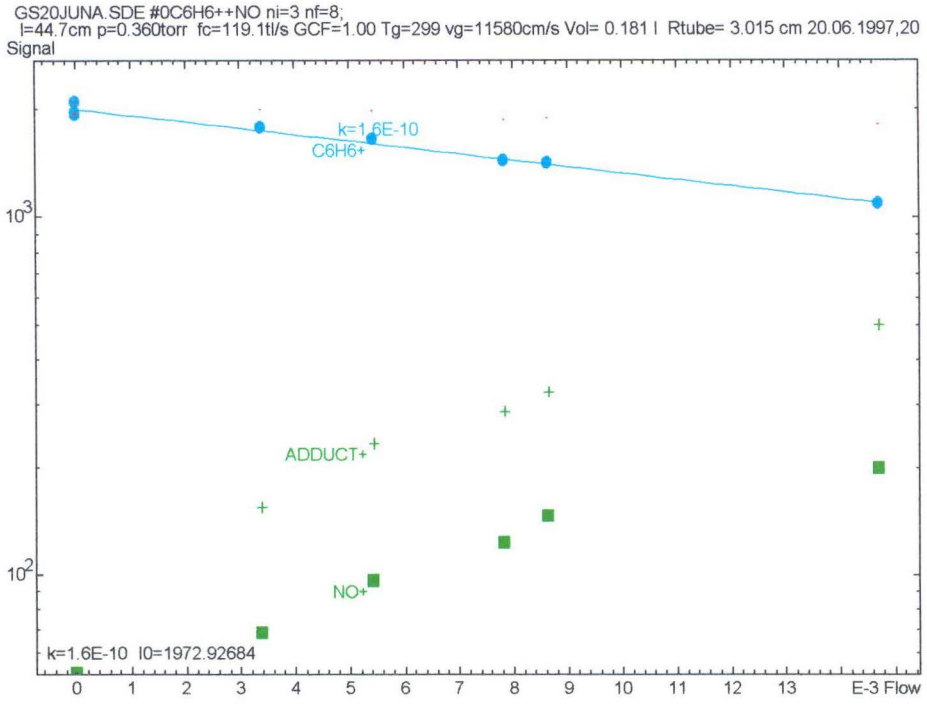

Figure 2.7. A semilogarithmic plot of Ln [Ion Count] versus neutral flow rate, for the reaction of $C_6H_6^+$ + NO. The linear decay of the $C_6H_6^+$ ion counts (●) and commensurate rise of the product ion counts ($C_6H_6^+$.NO [+] and NO^+ [■]) is clearly seen as the flow of NO is increased.

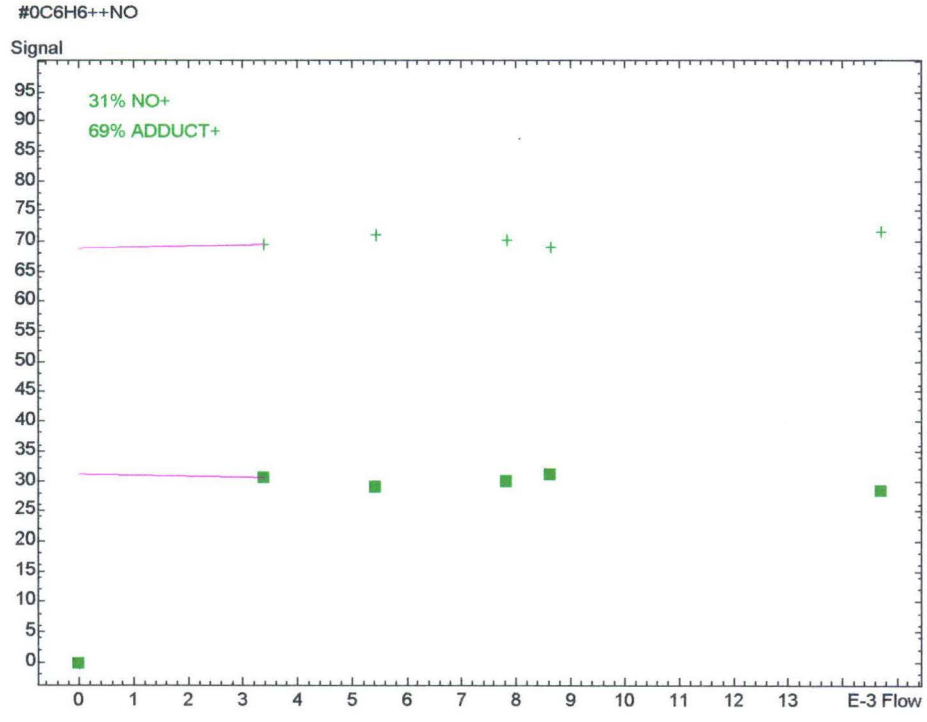

Figure 2.8. A product distribution graph for the reaction of $C_6H_6^+$ + NO. In this reaction approximately 69 % of the reactant ions undergo 3-body association to form the adduct, $C_6H_6^+$.NO (+). The remaining 31 % react via charge transfer, generating NO^+ + C_6H_6 (■).

Evaluation of Rate Coefficients

This section provides a concise discussion on the theoretical and experimental aspects of determining rate constants for ion-neutral reactions.

(i). Theory. The rate law for a bimolecular ion-molecule reaction $A^+ + N \Rightarrow$ Products is:

$$Rate = -\frac{d[A^+]}{dt} = k[A^+][N] \qquad \textbf{(201)}$$

where $[A^+]$ and $[N]$ are the concentrations of the reactants after time, t, and k is the second-order rate coefficient.

In flow-tube experiments $[A^+]$ is monitored not as a function of time but rather as a function of $[N]$, and after a fixed distance z. Elapsed time is proportional to the distance travelled by A^+, assuming ion velocity, v, is independent of position within the flow tube. Noting that v = dz/dt, we obtain the following new expression for the rate law:

$$Rate = -\frac{d[A^+]_z}{dz} = \frac{k}{v}[A^+]_z[N]_z \qquad \textbf{(202)}$$

In equation **(202)**, $[A^+]_z$ and $[N]_z$ are distance-dependent concentrations. In practice, ion-neutral reactions are studied under psuedo-first-order conditions with $[N]_z$ present in large excess. Under such circumstances $[N]_z \approx [N]$.

Rearranging expression **(202)** and integrating between appropriate limits we obtain:

$$-\int_0^z \frac{d[A^+]_z}{[A^+]_z} = \int_0^z \frac{k[N]}{v} dz \qquad \textbf{(203)}$$

which evaluates to:

$$Ln\left(\frac{[A^+]_z}{[A^+]_0}\right) = (Ln[A^+]_z - Ln[A^+]_0) = -\frac{k[N]z}{v} \qquad \textbf{(204)}$$

Equation **(204)** indicates that providing z and v are constant, a plot of $Ln[A^+]_z$ versus $[N]$ should yield a straight line of slope directly proportional to $-k$.

Rearranging expression **(204)** to solve for k we obtain:

$$k = Ln\left(\frac{[A^+]_0}{[A^+]_z}\right)\frac{v}{[N]z} \qquad \textbf{(205)}$$

(ii). Practical Measurement of Rate Coefficients. Determining a rate coefficient using the SIFT instrument involves measuring a series of ion counts as the flow of a reactant neutral is varied.

In expression **(205)**, $[A^+]_0$ is taken to be the ion count with $[N] = 0$. The ion velocity v is assumed to be 1.50 times the bath gas velocity for all ions at thermal energies. This ratio of v_{Ion} / $v_{Bath\ Gas}$, is in rough accordance with the value of 1.45 determined by Smith and Adams. [144] Moreover, recent preliminary experiments made by pulsing specific rings in a drift tube insert have indicated that v_{Ion} / $v_{Bath\ Gas}$ is approximately 1.5 for thermalised ions in the Canterbury SIFT. The distance between the neutral reactant inlet and the molybdenum disc mounted on the nose cone gives an approximate value of z. In practice a small finite distance is required for homogeneous mixing of the buffer gas and neutral reactant, hence z must be altered slightly to allow for this effect. This correction is known as an "end correction", ε, and is determined by repeatedly performing a calibration reaction (eg. $Ar^+ + O_2$) which has a well established rate coefficient. [24, 197] The end correction, ε, is dependent on probe geometry, being typically ± 1- 4 cm for the different inlet probes used in this research.

Taking all of the above into account, rate coefficients are evaluated on the Canterbury SIFT using the following formula:

$$k = Ln\left(\frac{[A^+]_0}{[A^+]_z}\right)\frac{1.5.v_{BathGas}}{[N](z+\varepsilon)} \qquad \textbf{(206)}$$

Experimentally the flow rate of the neutral N, Q_N, (in Torr L s^{-1}), is monitored, hence this flow rate must be converted to a concentration, (in molecules cm^{-3}), using the following relation:

$$[N] = \frac{Q_N.L.P.(273.15K)}{Q_{BathGas}.T} \qquad \textbf{(207)}$$

where Q_N is the flow rate of the neutral reactant, L is Loschmidt's number, P is the flow tube pressure, (in Torr), $Q_{BathGas}$ is the flow rate of the bath gas, (in Torr L s^{-1}), and T is temperature, (in degrees Kelvin).

The bath gas velocity is calculated by knowing the pressure in the flow tube and the bath gas flow rate, (in Torr L s^{-1}), viz:

$$v = \frac{Q_{BathGas}}{P.C} \qquad (208)$$

where C is the cross-sectional area of the flow tube, (in cm^2), and all other symbols have been previously defined.

For most reactions the uncertainty associated with the measurement of rate coefficients using the SIFT technique is between 15 - 30 %. Major sources of error include the uncertainty in the slope of $\frac{dLn[A^+]}{dQ_N}$ (usually less than 10 %), and errors in the measurement of $Q_{BathGas}$, upon which the rate constant depends to the second order, (again $< \sim 10$ %).

Mass Discrimination

A deleterious characteristic of mass spectrometric systems is the variation in response as the m/z ratio is changed. This phenomenon is known as "mass discrimination" and the quadrupole mass filter suffers from this problem. Depending on the resolution setting, discrimination by an order of magnitude, over 200 mass units, is possible. [130]

Mass discrimination is the largest cause of error in product distribution measurements. Transmission through the quadrupole depends upon the position and momenta of ions as they enter the quadrupole, hence the analyser ion optics settings also affect mass discrimination. In practice, allowance for mass discrimination is made by calibrating the response of the analyser quadrupole for a specific configuration of quadrupole resolution and downstream lens voltages.

Two procedures have been employed to calibrate the mass response of the Canterbury SIFT.

The first method was conceived by Smith and Adams and involves measuring the current incident on the molybdenum disc whilst simultaneously monitoring the ion count rate. [200] A plot of the ratio of ion count / ion current over a range of masses gives a calibration curve, valid for a specific set of analyser lens settings and quadrupole resolution. Figure 2.9 shows a typical mass discrimination calibration curve obtained using this procedure. A Keithley 417 high speed picoammeter or (latterly) a Keithley 602 solid state electrometer is used to determine the ion current incident on the molybdenum disc. The magnitude of this ion current is very small, ($\sim 1 - 5 \times 10^{-12}$ Amps), and the

presence of significant leakage currents and experimental noise reduces the precision of this method.

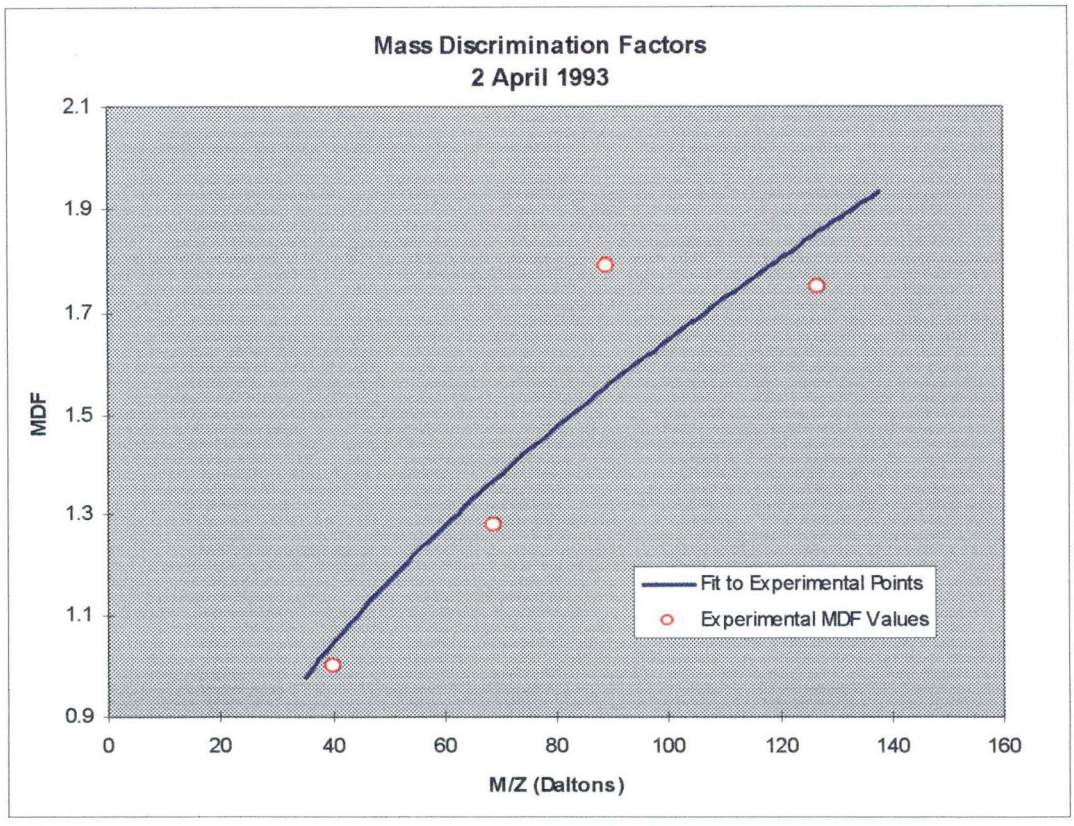

Figure 2.9. A typical mass discrimination curve obtained for the Canterbury SIFT using the method described by Smith and Adams. [200] **Parameters were as follows: Resolution 8.0; Nose Cone @ -2.2 Volts; Molybdenum Disc @ -0.24 Volts; Detection Lens #1 @ -7.0 Volts; Detection Lens #2 @ -19.0 Volts and Detection Lens #3 @ -276.0 Volts.**

The other procedure invoked to determine mass discrimination was initially used by Bohme and co-workers in 1973.[201] Reactant and product ion counts are measured for a particular ion-neutral reaction and the mass discrimination factor determined from the excess or deficit of product ions formed, relative to the number of reactant ions removed. More formally, for the generic ion-neutral reaction: $A^+ + B \Rightarrow E^+ + F$

then;

$$A^+ + mE^+ = A^+_0 \qquad (209)$$

where m is the mass discrimination factor, A^+ and E^+ are the count rates of the primary and product ions respectively, and A^+_0 is the count rate of A^+ with no

neutral, B, flowing. This procedure has limited applicability, being only suitable for those reactions generating a single, unique product ion, E^+, and where no subsequent reactions of E^+ occur. Examples of mass discrimination factors, (MDF's), determined in this way are given in Table 2.2 overleaf.

A final word about mass discrimination. When reactant and product ion masses are relatively close, (ie. $\sim < 30$ Daltons), and provided a downstream quadrupole resolution setting of $\sim \leq 8.2$ is used, the MDF's are tolerably close to 1.0. This finding holds particularly when all of the measured ions have m/z ratios $\sim \leq 90$ Daltons. For a small number of ion-neutral reactions therefore, mass discrimination between multiple product channels is significant but for many systems the amount of discrimination is acceptably small.

Following a careful consideration of the above discussion, the product distribution results presented in this work are considered to be accurate to $\pm$ 20 %.

2.6: Reagents and Physical Conditions.

Reagents specifically used in a particular experimental section are described in the appropriate chapter of this work. Instrument or Zero Grade helium, (stated purity 99.9 % and 99.995 % respectively), was the bath gas for all measurements unless expressly stated otherwise. This gas was obtained commercially from BOC Gases and purified by passage through a molecular sieve trap, (cooled to liquid nitrogen temperatures), and a 25μm vacuum filter.

All experiments were conducted with a flow tube pressure between 0.30 – 0.35 Torr and at a temperature of 300 ± 5 K. A cold cathode gauge monitored the pressure within the ion source chamber, which was typically $< 10^{-4}$ Torr. The pressure within the analyser assembly was similarly observed using an ion gauge and was invariably $< 10^{-5}$ Torr.

Reaction	Settings	MDFs
$H_3O^+ + HCN \Rightarrow HCNH^+ + H_2O$	Resolution = 8.0 Molybdenum Disc = -5.0 Volts Detector Lens #1 = -14.4 Volts Detector Lens #2 = -123.0 Volts Detector Lens #3 = -80.9 Volts Quad Case = -23.5 Volts Nose Cone = +10.8 Volts Bath Gas = Helium	H_3O^+ (m/z = 19) = 1.0 $HCNH^+$ (m/z=28) = 0.993
$H_3O^+ + HCN \Rightarrow HCNH^+ + H_2O$	All settings as above except Bath Gas = Hydrogen	H_3O^+ (m/z = 19) = 1.0 $HCNH^+$ (m/z = 28) = 0.961
$Ar^+ + SF_6 \Rightarrow SF_5^+ + F + Ar$	Resolution = 8.0 Molybdenum Disc = -5.0 Volts Detector Lens #1 = -11.7 Volts Detector Lens #2 = -122.8 Volts Detector Lens #3 = -19.3 Volts Quad Case = -11.0 Volts Nose Cone = +17.6 Volts Bath Gas = Helium	Ar+ (m/z = 40) = 1.0 SF_5^+ (m/z = 127) = 1.37

Table 2.2. Mass discrimination factors determined on the Canterbury SIFT instrument using the method prescribed by Bohme et al. [201]

CHAPTER 3.

THE ASSOCIATION REACTION $C_2H_3^+$ + CO AND INTERSTELLAR PROPYNAL.

3.1: Introduction.

Propynal, HC≡C-CHO, is one of the molecules possessing a carbon chain skeleton in a growing inventory of such molecules that have been identified in interstellar clouds. Propynal was first detected in the cold interstellar cloud TMC-1 from its rotational line emission between 18 and 19 GHz. [202] A search was also made for an isomer of propynal, propadienone, $H_2C=C=C=O$, both in TMC-1 and in Sgr B2 molecular clouds, but in each cloud it was below the limit of detection. [202]

Sequences of ion-molecule reactions have provided a cogent synthetic route for the generation of most molecular species observed thus far in the interstellar medium. [17] Among the processes suggested for the synthesis of propynal is the ion-molecule association reaction: [203]

$$C_2H_3^+ + CO \Rightarrow C_3H_3O^+ + h\nu(\text{energy} < 0.5\ \text{eV}^a) \qquad \textbf{(301)}$$

The analogous three body process in a helium bath gas has been investigated and a rate coefficient of 1.6×10^{-27} cm^6 s^{-1} at 300 K determined. [204] Reaction **(301)** has also been postulated as a synthetic route to tricarbon oxide, C_3O, which has been similarly observed in the interstellar medium.

Alternatively, reactions between hydrocarbon cations and atomic oxygen might initiate the synthesis of propynal in interstellar clouds, eg. [205]

$$C_3H_5^+ + O \Rightarrow C_3H_3O^+ + H_2 + 2.8\ \text{eV}^b \qquad \textbf{(302)}$$

---

[a] Thermochemistry based on the $HC{\equiv}CCHOH^+$ cation.

[b] Thermochemistry based on the $CH_3C=CH_2^+$ and $HC{\equiv}CCHOH^+$ cations.

HC≡C-CHO may then be produced from the $C_3H_3O^+$ cation via dissociative ion-electron recombination, viz:

$$C_3H_3O^+ + e^- \Rightarrow HC{\equiv}C\text{-}CHO + H \qquad \textbf{(303)}$$

Dissociative ion-electron recombination processes are assumed to be fast, with minimal attendant molecular rearrangement. [206]

Each of these propositions, [reactions **(301)** and **(302)**], is eminently reasonable on the grounds that the precursor ion in each case, $C_2H_3^+$ or $C_3H_5^+$, is unreactive with H_2. What is not known, however, is the isomeric form of the $C_3H_3O^+$ ion produced in reactions **(301)** and **(302)**.

In 1993 Petrie et al. published two papers which presented data obtained from the reaction of $C_3H_3O^+$ cations with various neutrals. In this work $C_3H_3O^+$ ions were generated by electron impact on the acrylic anhydride dimer. [404, 405]

In this work, an experimental SIFT study was conducted to examine the feasibility of reaction **(301)** producing protonated propynal. A theoretical examination of the $C_3H_3O^+$ potential surface was also undertaken. The combined approach, experimental and theoretical, leads to some interesting conclusions. In the experiments described in this chapter, the $C_3H_3O^+$ ion was formed by three body collisional stabilization of the $(C_3H_3O^+)^*$ intermediate, whereas in interstellar clouds the ion is produced by radiative stabilization of the complex, [reaction **(301)**]. It is conceivable (although unlikely) that the two processes may generate different products.

3.2: Experimental Study.

A series of experiments were conducted to establish whether the $C_3H_3O^+$ association ion generated in reaction **(301)** has the same reactivity as protonated propynal. This involved reacting both ions with a number of neutral reagents, in each case measuring rate coefficients and determining product distributions. A congruence in reactivity would suggest that the association between $C_2H_3^+$ and carbon monoxide constitutes the primary step in the synthesis of propynal in the interstellar medium.

Reagents and Experimental Conditions

The $C_3H_3O^+$ association ion from reaction **(301)** was produced in the flow tube by injecting $C_2H_3^+$ and adding a moderate flow of CO at the first neutral inlet. $C_2H_3^+$ was predominantly generated by electron impact on vinyl bromide,

(CH_2=CHBr), which was prepared according to the method of Kharasch and co-workers. [207] In a number of early experiments $C_2H_3^+$ was produced by electron impact on ethyl bromide, C_2H_5Br. Carbon monoxide, CP grade, (99.5 % pure), was obtained from Matheson Gas Products and was further purified by passage through a dry ice/acetone cooled molecular sieve trap.

Propynal, HC≡C-CHO, was prepared by a standard technique from 2-propyn-1-ol. [208] This synthesis involved adding a mixture of CrO_3 and H_2SO_4, (Jones' reagent), to 2-propyn-1-ol under vacuum conditions, (pressure ~ < 60 Torr). The propynal evolved by this reaction was allowed to condense in a series of traps cooled to -78 ^{o}C using a dry ice / acetone slurry. Proton NMR spectroscopy was used to confirm the purity of the synthesised compound.

In the main, protonated propynal was injected into the flow tube directly from the ion source region. Several experiments were also carried out by injecting HCO^+ and adding HC≡C-CHO at the first inlet port, thereby facilitating proton transfer within the flow tube. No difference in behaviour was found in the $C_3H_3O^+$ ion generated from HC≡C-CHO via these two different routes.

Ethylamine, $C_2H_5NH_2$, CP grade, (98 % pure), and pyrrole, C_4H_5N, CP grade, were obtained from Merck Schuchardt. Methylamine, CH_3NH_2, CP grade, (98 % pure), was procured from Matheson Gas Products. Ammonia, NH_3, CP grade, (99 % pure), was supplied by Christchurch Gases Ltd. Diethylketone, $(C_2H_5)_2CO$, CP grade, (97 % pure), was supplied by Aldrich. n-Dibutyl ether, n-$(C_4H_9)_2O$, laboratory reagent grade, was supplied by BDH. Cyclohexanone, $C_6H_{10}O$, laboratory reagent grade, and benzene, C_6H_6, AR grade, were both obtained from Ajax Chemicals. Iodoethane, C_2H_5I, CP grade, was supplied by Riedel-De Haën A.G. All neutral reagents were further purified by freeze-pump-thaw cycles.

Experimental Results

The results of a series of comparative reactions of the isomeric ions, $C_2H_3^+$.CO, (ie. the association product of $C_2H_3^+$ and CO), and protonated propynal, with nine neutrals, are summarised in Table 3.1. All tabulated rate coefficient values are considered accurate to ± 15 %.

Discussion of the Experimental Results

There is little doubt from the comparative reactivity of the two $C_3H_3O^+$ ions,

that the product of reaction **(301)** is not protonated propynal. The data listed in Table 3.1 show that the proton transfer behaviour of the two $C_3H_3O^+$ ions is divergent. Both ions transfer a proton at close to the collision rate to $C_2H_5NH_2$, (PA = 908 kJ mol^{-1}), and CH_3NH_2, (PA = 896 kJ mol^{-1}), but only protonated propynal transferred a proton to pyrrole and ammonia. In the case of ammonia, $C_2H_3^+$.CO is relatively unreactive, [$k = (3.0 \pm 0.5) \times 10^{-11}$ cm^3 s^{-1}], whereas $HC{\equiv}C\text{-}CHOH^+$ undergoes proton transfer at close to the collision rate, [$k = (1.6 \pm 0.2) \times 10^{-9}$ cm^3 s^{-1}].

Reactant	Product Distribution		k_{coll}[c]	k_{obs}	PA Neutral (kJ mol^{-1})[d]
	Proton Transfer	Adduct			
$C_2H_5NH_2$	0.85	0.15	1.8	1.7	908
	0.85	*0.15*		*1.8*	
CH_3NH_2	0.75	0.25	1.8	1.5	896
	0.90	*0.10*		*2.0*	
C_4H_5N (Pyrrole)	0	1.00	2.0	2.0	868
	0.80	*0.20*		*2.2*	
NH_3	0	1.00	2.3	0.03	854
	1.00	*0*		*1.6*	
$(n\text{-}C_4H_9)_2O$	0	≤ 0.25[e]	1.9	1.6	852
	1.00	*0*		*2.0*	
$(C_2H_5)_2CO$	0	1.00	2.8	1.3	843
	1.00	*0*		*2.5*	
$C_6H_{10}O$ (cyclohexanone)	0	1.0	2.7	2.9	843
	1.00	*0*		*3.2*	
C_6H_6	*0.20*	*0.80*	1.3	*1.0*	759
C_2H_5I	*0*	*1.00*	1.9	*0.1*	~ 736

Table 3.1. Reaction rate coefficients and product ratios for the two $C_3H_3O^+$ isomeric ions, $C_2H_3^+$.CO and $HC{\equiv}C\text{-}CHOH^+$, (italicised values), with the specified neutral reactant. All rate coefficients are given in units of 10^{-9} cm^3 s^{-1}.

[c] Calculated according to the parameterised trajectory theory of Su and Chesnavich. [118]

[d] The neutral proton affinity, (PA), values were obtained from Reference 31.

[e] Other products include $C_4H_9\text{-}O\text{-}C_4H_8^+$, (major peak), and $C_4H_9O^+$.

No proton transfer was observed from the $C_2H_3^+$.CO species to any neutral with a proton affinity less than that of CH_3NH_2, (PA = 896 kJ mol^{-1}). The observation of proton transfer with CH_3NH_2 but not with C_4H_5N, (pyrrole), brackets the proton affinity of C_3H_2O formed after proton transfer from $C_2H_3^+$.CO as 896 kJ mol^{-1} > PA (C_3H_2O) > 868 kJ mol^{-1}.

The proton affinity of propynal may be similarly estimated. Rapid proton transfer was observed from protonated propynal, $HC{\equiv}C\text{-}CHOH^+$, to C_6H_6, (PA = 759 kJ mol^{-1}), but not to C_2H_5I, (PA ~ 736 kJ mol^{-1}). [31, 209] This finding brackets the proton affinity of propynal as 759 kJ mol^{-1} > PA ($HC{\equiv}C\text{-}CHO$) > 736 kJ mol^{-1}.

3.3: Theoretical Calculations.

There have been several previous ab-initio studies of the $C_3H_3O^+$ species, but only that of Bouchoux et al. carried out calculations beyond the Hartree-Fock level of theory. [210] In 1985 Bouchoux et al. published the results of calculations on eleven different structures. They found the lowest energy species to be C2-protonated propadienone, **(VI[f])**, followed by O-protonated cyclopropenone, **(VII[f])**, O-protonated propynal, **(VIII[f], IX[f])**, and O-protonated propadienone, **(X[f])**. Their highest level calculations were at the CIPSI/4-31G*//HF/3-21G level of theory. In 1980 Holmes and co-workers used collisional activation (CA) mass spectrometry to determine heat of formation values for five $C_3H_3O^+$ ions. [211] Their experimental work was coupled with HF/DZ calculations. Hopkinson and Lien have reported HF/6-31G* calculations. [212]

A number of ab-initio studies have examined the unprotonated species, propadienone, **(I[g])**, propynal, **(II[g])**, and the cyclic isomer cyclopropenone, **(III[g])**. At the Hartree-Fock level of theory propadienone is predicted to have C_{2v} symmetry, [213] but the inclusion of electron correlation generates a bent configuration [214] in agreement with the experimental microwave structure. [215] At the Hartree-Fock level of theory the lowest a' frequency is predicted to be very small. Brown and Dittman attributed the kinked nature of propadienone to the influence of a doubly excited σ electron configuration. [214] Propadienone and

---

[f] The Roman Numeral labels refer to the $C_3H_3O^+$ ions depicted in Figure 3.2.

[g] The Roman Numeral labels refer to the C_3H_2O species depicted in Figure 3.1.

propynal are calculated to be very close in energy. At the Hartree-Fock level of theory propynal is slightly lower in energy than propadienone. Cyclopropenone is higher in energy than the other two isomers.

Computational Details

All calculations were performed using the Gaussian 90 and Gaussian 92 programs. [216, 217] The calculations conform to the prescription detailed in the original description of the G2 procedure. [218] The G2 procedure was selected because of the established reliability of the calculations. Curtiss et al. give absolute deviations from experimental values of 3.85 kJ mol^{-1} for atomisation energies and 4.4 kJ mol^{-1} for proton affinities of first row species. [218]

Results

The MP2/6-31G* optimised geometries of the three stable C_3H_2O neutrals and two other C_3H_2O species are shown in Fig. 3.1, and those of the $C_3H_3O^+$ species are depicted in Fig. 3.2. The G2 energies, the energies relative to $C_2H_3^+ + CO$, and calculated enthalpies of formation at 298 K for all $C_3H_3O^+$ species and possible precursors are tabulated in Table 3.2. The enthalpies of formation were calculated using the values of - 110.5 and + 1112.5 kJ mol^{-1} as the enthalpies of formation for CO and $C_2H_3^+$ respectively. [31] Values calculated using the enthalpies of formation of C_2H_2 and COH^+ are more positive by 4.4 kJ mol^{-1}. Calculated proton affinities for the C_3H_2O species, **(I-III[h])**, to form the $C_3H_3O^+$ ions, **(VI-XIII[i])**, are given in Table 3.3. Calculated and experimental values of the rotational constants and dipole moments for the C_3H_2O species, **(I-III[h])**, are tabulated in Tables 3.4 and 3.5 respectively. Calculated values of rotational constants and dipole moments for protonated propadienone, **(VI[i])**, protonated cyclopropenone, **(VII[i])**, and protonated propynal, **(VIII[i])**, are listed in Table 3.6.

Discussion of Results

(i). C_3H_2O Isomers. Propynal, **(II[h])**, is 12.8 kJ mol^{-1} lower in energy than propadienone, **(I[h])**, at the HF/6-31G* level of theory but only 0.4 kJ mol^{-1} lower at the MP2/6-31G* level which includes several correlation terms. Using an enlarged 6-311G** basis set lowers the energy of propadienone to 2.8 kJ mol^{-1} below that of propynal. Increasing the level of theory to MP4SDTQ places

---

[h] The Roman Numeral labels refer to the C_3H_2O species depicted in Figure 3.1.

[i] The Roman Numeral labels refer to the $C_3H_3O^+$ ions depicted in Figure 3.2.

propadienone 14.1 kJ mol^{-1} below propynal. Finally at the G2 level of theory propadienone is calculated to be 7.0 kJ mol^{-1} below propynal, with the Δ(QCI) correction favouring propynal. This relative ordering differs from that reported by Komornicki et al. [213] A higher value for the enthalpy of formation of propynal, (ΔH_f^o = 131.6 kJ mol^{-1}), is obtained than the 94 kJ mol^{-1} value assumed by Holmes et al. [211]

Cyclopropenone, (**III**[j]), is calculated to be 35.1 kJ mol^{-1} higher in energy than propadienone, which is a larger separation between the two species than the 13.4 kJ mol^{-1} calculated by Komornicki et al. [213]

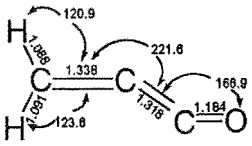

I

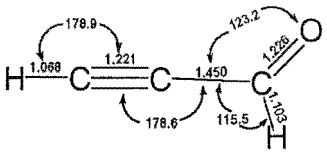

II

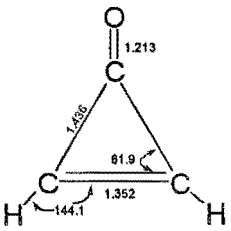

III

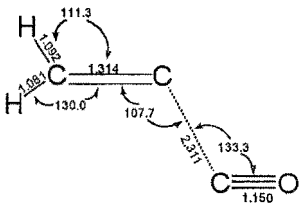

IV

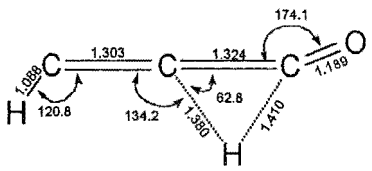

V

Figure 3.1. Optimised structures of C_3H_2O species at the MP2/6-31G* level of theory.

---

j The Roman Numeral labels refer to the C_3H_2O species depicted in Figure 3.1.

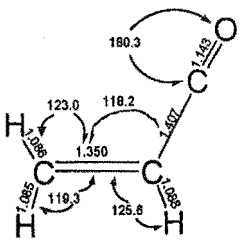

VI

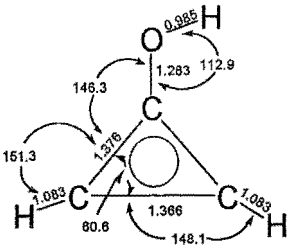

VII

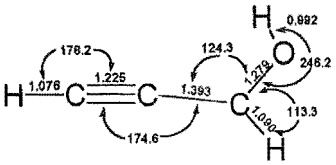

VIII

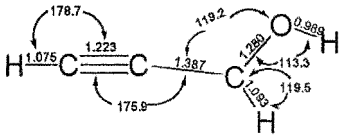

IX

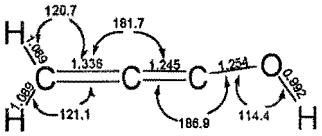

X

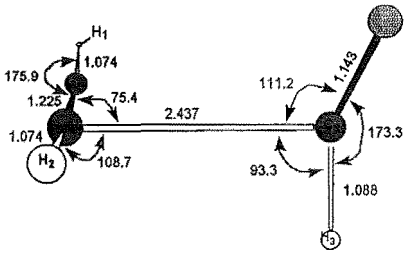

XI

$\omega(H_2C_2C_3H_3) = 89.9°$

$\omega(C_1C_2C_3O) = 95.8°$

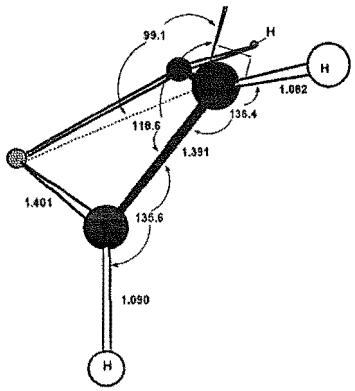

XII

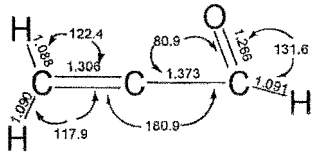

XIII

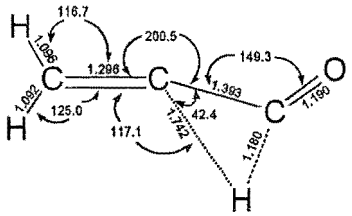

XIV

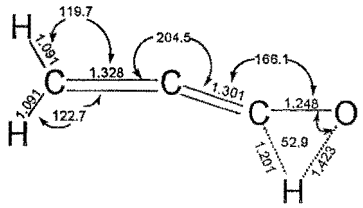

XV

Figure 3.2. Optimised structures of $C_3H_3O^+$ species at the MP2/6-31G* level of theory.

Structure	E(G2)	ΔE(G2) (kJ mol^{-1})[k]	ΔH_f^o (kJ mol^{-1})	
			This Work	Other Work
$C_2H_3^+ + CO$	- 190.60807	0.0	1002.0	
Propadienone, (I)	- 190.35709	+ 659.0	137.0	
Propynal, (II)	- 190.35443	+ 665.9	131.6	
Cyclopropenone, (III)	- 190.34372	+ 694.1	163.6	
(IV), Transition State [(I) ⇒ C_2H_2 + CO]	- 190.29177	+ 830.4	302.8	
(V), Transition State [(II) ⇒ C_2H_2 + CO]	- 190.25259	+ 933.3	404.5	
$C_2H_2 + CO$	- 190.36323	+ 642.8	116.5	
$C_2H + COH$	- 190.10401	+ 1323.4	798.7	
(VI)	- 190.69611	- 231.1	766.1	749[l, m]
(VII)	- 190.65804	- 131.2	865.1	858[l], 900[m]
(VIII)	- 190.64114	- 86.8	911.0	
(IX)	- 190.64025	- 84.4	913.2	833[l], 814[m]
(X)	- 190.62399	- 41.8	956.8	882[l], 857[m]
(XI)	- 190.60706	+ 2.7	1002.0	995[m]
(XII)	- 190.60258	+ 14.4	1011.0	986[m]
(XIII)	- 190.60108	+ 18.3	1017.8	982[m]
(XIV), Transition State [(VI) ⇒ (XIII)]	- 190.58767	+ 53.6	1051.1	1061[m]
(XV), Transition State [(X) ⇒ (XIII)]	- 190.53586	+ 189.6	1189.1	
$C_2H_2 + COH^+$	- 190.52784	+ 210.7	1213.7	
$C_2H_2 + HCO^+$	- 190.58683	+ 55.8	1055.9	
$C_2H_2 + HCOH^+ - H$	- 190.61248	- 11.6	986.1	
$C_2H_2 + H_2COH^+ - H_2$	- 190.62712	- 50.0	945.2	
$C_3H_2^+ + OH$	- 190.44467	+ 429.0	1429.9	
$C_3H^+ + H_2O$	- 190.47262	+ 355.6	1359.2	

Table 3.2. G2 and relative energies for $C_3H_3O^+$ species and possible precursors.

[k] With respect to $C_2H_3^+ + CO$.
[l] Reference 211.
[m] MNDO calculations of Reference 210.

Structure	Proton Affinity					
	(I)		(II)		(III)	
	kJ mol^{-1}	EV	kJ mol^{-1}	eV	kJ mol^{-1}	eV
(VI)	895.5	9.28				
(VII)					828.5	8.59
(VIII)			756.1	7.84		
(IX)			753.8	7.81		
(X)	704.8	7.30				
(XI)			665.0	6.89		
(XII)	650.6[n]	6.74[n]				
(XIII)	643.8	6.67	649.2	6.73		

Table 3.3. Calculated proton affinities for the C_3H_2O species, (I-III), to form the $C_3H_3O^+$ ions, (VI-XIII).

Structure	Rotational Constants, (GHz)		
	Calculated HF/6-31G*	Calculated MP2/6-31G*	Experimental Values
Propadienone, (I)	A = 299.6 B = 4.26 C = 4.20	A = 126.2 B = 4.414 C = 4.264	A = 149.83[o] B = 4.387 C = 4.258
Propynal, (II)	A = 69.7 B = 4.89 C = 4.57	A = 65.137 B = 4.786 C = 4.459	A = 68.04[p] B = 4.826 C = 4.500
Cyclopropenone, (III)	A = 32.9 B = 8.03 C = 6.45	A = 31.90 B = 7.739 C = 6.228	A = 32.05[q] B = 7.825 C = 6.281

Table 3.4. Calculated and experimental rotational constants for the C_3H_2O species, (I-III).

---

[n] Ion **(XII)** cannot be formed directly, without rearrangement, from **(I) – (VI)**.
[o] Reference 215.
[p] Reference 219.
[q] Reference 220.

Structure	Dipole Moments, (Debye)	
	Calculated HF/6-311+G (3df, 2p)	Experimental Values
Propadienone, (I)	3.00	2.297[r]
Propynal, (II)	3.35	2.46[s]
Cyclopropenone, (III)	4.69	4.39[t]

Table 3.5. Calculated and experimental dipole moments for the C_3H_2O species, (I-III).

Structure	Rotational Constants, (GHz)		Dipole Moment, (Debye), HF/6-311+G (3df, 2p)
	Calculated HF/6-31G*	Calculated MP2/6-31G*	
Protonated Propadienone, (VI)	A = 46.45 B = 5.03 C = 4.54	A = 45.17 B = 4.933 C = 4.447	3.11
Protonated Cyclopropenone, (VII)	A = 30.43 B = 7.62 C = 6.09	A = 29.53 B = 7.418 C = 5.929	2.58
Protonated Propynal, (VIII)	A = 56.54 B = 4.82 C = 4.44	A = 56.14 B = 4.679 C = 4.319	1.44

Table 3.6. Calculated rotational constants and dipole moments for the $C_3H_3O^+$ species, (VI-VIII).

Good agreement is obtained between the calculated and experimental values of the rotational constants for all C_3H_3O species at the MP2/6-31G* level. For propadienone the large change in the "A constant" as the level of theory is increased from HF/6-31G* to MP2/6-31G* is due to the change of symmetry.

The calculated values of the dipole moments for propadienone and propynal are in poor agreement with the experimental values, however the calculated dipole moment for cyclopropenone is tolerably close to the reported experimental value. Theoretical calculations have traditionally struggled to evaluate the value

[r] Reference 215.
[s] Reference 219.
[t] Reference 220.

of dipole moments with any degree of accuracy, indeed for many years the calculation of the dipole moment of CO was an intractable problem. The imprecision in the calculation of the dipole moments for propadienone and propynal is indicative of this long standing difficulty.

(ii). $C_3H_3O^+$ Isomers. The comparative energies of various $C_3H_3O^+$ species (relative to $C_2H_3^+ + CO$) are shown in Fig. 3.3. C2-protonated propadienone, **(VI)**, is the lowest energy $C_3H_3O^+$ isomer. Direct association between $C_2H_3^+$ and CO may generate this ion, with a C-H bond broken and a C-C bond formed. A large contribution (29 kJ mol^{-1}) from the zero-point vibrational energy difference reduces the calculated value of the proton affinity.

The next lowest energy isomer is O-protonated cyclopropenone, **(VII)**. The energy difference between isomers **(VI)** and **(VII)** of 99.9 kJ mol^{-1} is in better agreement with Holmes et al.'s estimate of 109 kJ mol^{-1} than with their calculated value of 151 kJ mol^{-1}. [211] Bouchoux et al. calculate that the difference in energy between **(VI)** and **(VII)** is 117 kJ mol^{-1} at the CI/4-31G*//HF/3-21G level of theory. [210] This difference is accentuated by increasing the level of theory but reduced by increasing the size of the basis set.

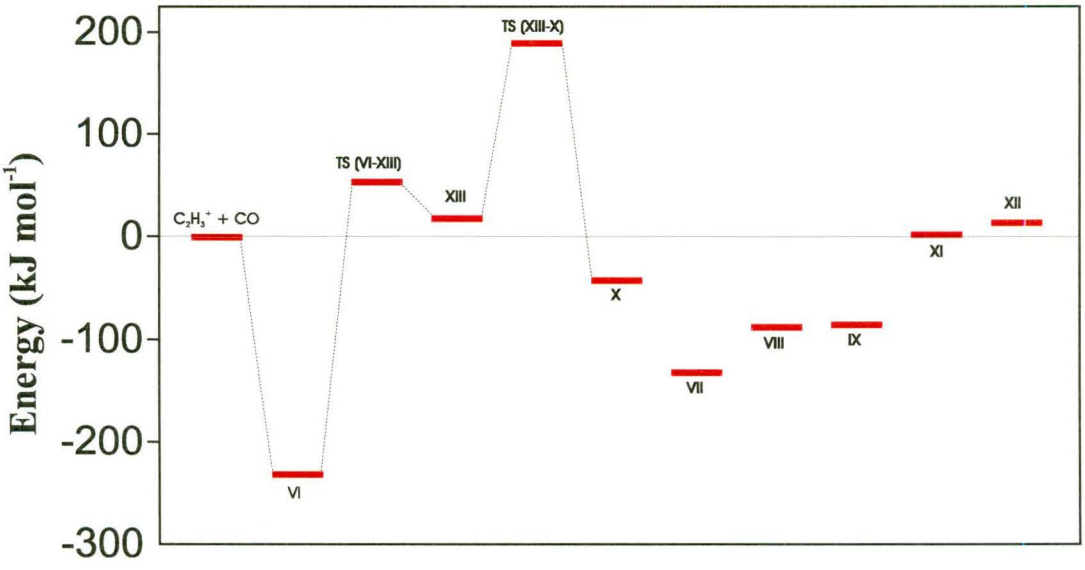

Figure 3.3. Relative energies of $C_3H_3O^+$ species.

For O-protonated propynal there is the possibility of cis or trans isomerism around the C-O bond. The trans isomer, **(VIII)**, is the lowest energy form of protonated propynal and is 2.2 kJ mol^{-1} more stable than the cis isomer, **(IX)**. Holmes et al. reported significantly lower values for ΔH_f^o **(VIII)** and ΔH_f^o **(IX)** than the results obtained from this work, due primarily to their use of a high proton affinity value for propynal, (795 kJ mol^{-1}). [211] The MNDO calculations of Bouchoux et al. suggested a 65 kJ mol^{-1} energy difference between isomers **(VI)** and **(IX)**, compared with 171 kJ mol^{-1} at the CI/4-31G*//HF/3-21G level of theory, [210] which is closer to the G2 **(VI)** - **(IX)** energy split of 146.7 kJ mol^{-1}.

Isomer **(X)** is O-protonated propadienone. The G2 energy difference between isomers **(VI)** and **(X)** is 189.3 kJ mol^{-1}, compared with the Holmes et al. estimate of 133 kJ mol^{-1} [211] and the 108 kJ mol^{-1}, (MNDO), and 218 kJ mol^{-1}, (CI/4-31G*), calculations of Bouchoux et al. [210]

Isomer **(XI)** is C2-protonated propynal which has approximately the same energy as the reactants $C_2H_3^+$ + CO. At the G2 level, protonation at the C2 position is favoured over C3 protonation, in disagreement with the calculations of Bouchoux et al. [210] The C1 $\Rightarrow$ C2 bond is particularly long, which means that this ion is essentially an association complex of C_2H_2 and HCO^+.

Isomer **(XII)** involves a 4 membered C_3O ring. The reaction to form it from $C_2H_3^+$ and carbon monoxide is calculated to be just endothermic, (by + 14.4 kJ mol^{-1}).

Isomer **(XIII)** can be considered to be either C1-protonated propadienone or C3-protonated propynal. The reaction to form **(XIII)** from $C_2H_3^+$ + CO is also calculated to be endothermic by + 18.3 kJ mol^{-1}.

For propadienone the relative proton affinities at 298 K at O, C1 and C2 are 190.7, 251.7 and 0.0 kJ mol^{-1} respectively, compared with the Bouchoux et al. HF/4-31G*//HF/3-21G values of 213, 285 and 0 kJ mol^{-1}. [210] Similarly the relative room temperature proton affinities for propynal at O, C2 and C3 are 0.0, 91.1 and 106.9 kJ mol^{-1} respectively compared with 0, 126 and 109 obtained by Bouchoux and colleagues. [210]

Several other cyclic $C_3H_3O^+$ structures were investigated, but none had energies within 100 kJ mol^{-1} of the $C_2H_3^+$ + CO reagents. An attempted optimisation of C2-protonated cyclopropadienone led to structure **(VI)**.

The lowest energy protonated forms of propadienone, cyclopropenone, and propynal, are the ions **(VI)**, **(VII)**, and **(VIII)** respectively. An examination of the MP2/6-31G* optimised geometries reveals that protonation of propadienone causes the CCC angle to change from 138.4° to 118.2°. Additionally the C1 ⇒ C2 bond lengthens from 1.318 Å to 1.407 Å, as the double bond reduces to a single bond. The C2 ⇒ C3 bond length also changes from 1.338 Å to 1.350 Å. For cyclopropenone, on protonation the CO bond is stretched from 1.213 Å to 1.283 Å, and the C1 ⇒ C2 bond constricts from 1.436 Å to 1.376 Å. On protonation the C1 ⇒ O bond length in propynal increases marginally, from 1.226 Å to 1.279 Å, and the C1 ⇒ C2 bond length contracts from 1.450 Å to 1.393 Å, as it acquires some double bond character.

(iii). Products of the reaction of $C_2H_3^+$ + CO. Thermodynamic constraints suggest that structures **(VI)** to **(X)** could be produced from the association of $C_2H_3^+$ + CO.

Without major rearrangement, ions **(VI)**, **(VII)**, and **(X)** would not yield propynal in a dissociative ion-electron recombination reaction. For ion **(VI)** the loss of a hydrogen atom from C2 generates propadienone while the loss of a hydrogen atom from C3 would produce a pentavalent carbon atom at this site in a major resonance structure. For isomer **(VII)** hydrogen atom detachment from the O atom would give cyclopropenone, **(III)**, while loss of atomic hydrogen from C2 would give a cyclopropadiene ring or, if ring opening occurred, a pentavalent carbon atom at C2. H atom loss from the O atom in ion **(X)** forms either propadienone or the neutral formed by atomic hydrogen detachment from C2 in ion **(VII)**.

Only the two $HC{\equiv}C\text{-}CHOH^+$ isomers, **(VIII)** and **(IX)**, along with structures **(XI)** and **(XIII)**, may form propynal via minimal rearrangement dissociative ion-electron recombination processes. Figure 3.3 indicates that the $[C_2H_3^+ \text{- - - CO}]$ condensation ion, **(VI)**, is located at the global minimum of the $C_3H_3O^+$ potential surface. A mechanism by which ion (**VI**) can rearrange to form isomers **(VIII)**, **(IX)**, **(XI)** or **(XIII)** is required to generate propynal, **(II)**, from the reagents $C_2H_3^+$ + CO. Any rearrangement from **(VI)** to **(XI)** would involve a transition state higher in energy than $C_2H_3^+$ + CO which is untenable at the temperature of interstellar clouds. The rearrangement of **(VI)** to form **(XIII)** involves the shift

of an H atom from C2 to C1 and proceeds via a transition state, **(XIV)**, located 53.6 kJ mol^{-1} above the energy of $C_2H_3^+$ and carbon monoxide. Again such a process is not possible in the interstellar medium. Furthermore, at the G2 level of theory the formation of ion **(XIII)** from $C_2H_3^+ + CO$ is endothermic. Under conditions quite different from those prevailing in interstellar clouds, O-protonated propadienone, **(X)**, might result from the further rearrangement of ion **(XIII)**. The transition state for this transformation, **(XV)**, is even higher above the energy of the $C_2H_3^+ + CO$ baseline than the transition state **(XIV)**.

(iv). Alternative Synthetic Routes to $C_3H_3O^+$ Ions. $C_2H_3^+$ and CO seem to be the obvious precursors of propynal and propadienone in the interstellar medium. In their standard model, Herbst and Leung [221] calculate the abundance of $C_2H_3^+$ and CO relative to H_2 to be 6.7×10^{-12} and 1.5×10^{-4} respectively. The calculated relative abundances of C_2H_2 and HCO^+ are 1.5×10^{-8} and 9.5×10^{-9} respectively, giving, assuming similar reaction rates, an order of magnitude smaller production rate of propynal or propadienone.

The generation of ion **(XIII)** from C_2H_2 and HCO^+ is exothermic, and if ion **(VI)** is the initial association product then isomerisation to structure **(XIII)** is just possible at interstellar temperatures. At room temperature however, a collision rate proton transfer reaction is the sole channel observed. [222]

Another possibility is the reaction of acetylene with the $HCOH^+$ cation to form either **(VIII)** or **(IX)**, with attendant loss of atomic hydrogen. Alternatively, protonated formaldehyde, H_2COH^+, could react with acetylene, forming the ions **(VIII)** or **(IX)**, and H_2.

The reaction between the hydroxide radical, OH, and $C_3H_2^+$ is thermodynamically favourable and could directly form ions **(VII)**, **(VIII)** or **(IX)**. Unfortunately the calculated relative abundances of $C_3H_2^+$ and OH are 8.4×10^{-13} and 2.4×10^{-7}, resulting in a rate of reaction four orders of magnitude slower than $C_2H_3^+ + CO$.

For $C_3H^+ + H_2O$ similar circumstances exist, where the calculated relative abundances are 7.0×10^{-15} and 1.3×10^{-6} for C_3H^+ and H_2O respectively, giving a rate five orders of magnitude slower than $C_2H_3^+ + CO$. Additionally the room temperature ion products of this reaction have been reported as HCO^+ (0.55), $C_2H_3^+$ (0.40) and $CHCCO^+$ (0.05). [223]

(v). Dissociative Ion-Electron Recombination of $C_3H_3O^+$. The calculations outlined suggest that C2-protonated propadienone, **(VI)**, is formed by the reaction of $C_2H_3^+ + CO$. Why then is propynal rather than propadienone observed in interstellar clouds? A possible reason for the apparent absence of propadienone is that sufficient energy is released in the dissociative ion-electron recombination reaction to permit the unimolecular decomposition of propadienone, to acetylene and carbon monoxide. The G2 exothermicity of the ion-electron recombination process, [**(VI)** + $e^- \Rightarrow C_2H_2 + CO + H$], is 438.8 kJ mol^{-1}. The decomposition of propadienone to HCCH + CO is 16.1 kJ mol^{-1} exothermic. The transition state for the unimolecular dissociation of propadienone is 171.4 kJ mol^{-1} above propadienone, which means that sufficient energy is released during recombination to allow the dissociation to proceed. Komornicki et al. estimated this transition state energy as 134.7 kJ mol^{-1}. [213]

The energy available from recombination reactions is invariably large, and the above argument for propadienone could be reiterated for propynal. For example, although dissociation into C_2H and COH is endothermic with a calculated dissociation energy of 657.5 kJ mol^{-1}, other dissociative channels are accessible. Dissociation into $C_2H_2 + CO$ is feasible providing sufficient energy is released to permit a 1,2 hydrogen atom transfer from C1 to C2. The transition state for this H-transfer is calculated to be 267.4 kJ mol^{-1} above propynal, which falls inside the available energy constraints of the dissociative ion-electron recombination reaction. The decomposition of propynal to $C_2H_2 + CO$ is 23.1 kJ mol^{-1} exothermic.

3.4: Comparison of Experiment and Theory.

The experimental measurements bracket the proton affinity, (PA), of C_3H_2O formed after proton transfer from $C_2H_3^+$.CO as 896 kJ mol^{-1} > PA (C_3H_2O) > 868 kJ mol^{-1}. Comparing this value with the calculated proton affinities summarised in Table 3.3 allows the identification of $C_2H_3^+$.CO ion as C2-protonated propadienone, $H_2C{=}CHCO^+$, **(VI)**, which is the global minimum on the $C_3H_3O^+$ potential surface. Further, the calculated value for PA ($H_2C{=}C{=}C{=}O$), with the proton attaching at the C2 position, is 895.5 kJ mol^{-1} which is in good agreement with the results of our bracketing experiments.

The experimental data is also consistent with the findings of the theoretical study which predicted that C2-protonated propadienone could be formed directly via the association of $C_2H_3^+$ and CO. Although the proton affinity of propadienone at O is significantly lower than at the C2 position, the deep potential well encountered when entering the $C_3H_3O^+$ surface through the $C_2H_3^+$ + CO entrance, favours C2 protonation. Moreover, the transition state between the C2 and O-protonated forms of propadienone is inaccessible given the energy available from the $C_2H_3^+$ and CO reactants.

A comparison of the experimental data obtained in the current study with that reported by Petrie et al. [404, 405] suggests that the $C_3H_3O^+$ cation generated from the acrylic anhydride dimer is also C2-protonated propadienone. In particular Petrie and colleagues obtained a rate coefficient of 2.1 x 10^{-11} cm^3 s^{-1} for the reaction between $C_3H_3O^+$ and NH_3. [405] This value is in reasonable agreement with the value obtained in the present study for the $C_2H_3^+$.CO + NH_3 reaction. Furthermore, a cursory examination of the structure of the acrylic anhydride dimer indicates that C2-protonated propadienone may be readily formed during electron impact on the neutral precursor.

The calculated proton affinity for propynal, (HC≡C-CHO), assuming protonation at the O site, is 756 kJ mol^{-1}; this value is in excellent agreement with the experimental proton affinity of 759 – 736 kJ mol^{-1}.

3.5: Conclusions.

The $C_3H_3O^+$ ion formed from the association of $C_2H_3^+$ and CO is C2-protonated propadienone, [structure **(VI)**], and not protonated propynal, (structures [**(VIII)** or **(IX)**]). This outcome makes the proposed mechanism for the interstellar synthesis of propynal from the radiative association of $C_2H_3^+$ and CO followed by dissociative recombination, [reactions **(301)** and **(303)**], unlikely. If propynal is generated during dissociative ion-electron recombination then so also should propadienone be formed, yet the latter has not been detected. [202] Although the products of dissociative recombination are unknown, it is quite unlikely that preferential isomerization would occur considering the fragmentation products of dissociative recombination reported from smaller

ions. [142] Instead, $H_2C{=}C{=}C{=}O$, and not HC≡C-CHO, is the more probable outcome of recombination.

In view of the projected rate of reaction **(301)** under interstellar cloud conditions, [203] the non-observation of propadienone presents as much a predicament as does the detection of propynal. The experiments reported above do not bar the production of C_3O in reaction **(3)** as proposed by Herbst, Smith and Adams. [204] The elimination of three H atoms from the C_3O skeleton during the recombination process is conceivable. The apparent absence of $H_2C{=}C{=}C{=}O$ in TMC-1 may be evidence for fragmentation of the C2-protonated propadienone ion, **(VI)**, during recombination. Possible fragmentation channnels might include $C_2H_2 + H + CO$, as justified above in the theoretical discussion, or perhaps C_2H_3 and CO.

What then is the mechanism by which propynal and not propadienone is formed in interstellar clouds? The discriminative synthesis of HC≡C-CHO over $H_2C{=}C{=}C{=}O$ requires a pathway specific in its selection of $HC{\equiv}C\text{-}CHOH^+$, **[(VIII)** or **(IX)]**, and not $H_2C{=}CHCO^+$, **(VI)**, if an ion-molecule mechanism is the source. This specificity requires entry to the $C_3H_3O^+$ protential surface in the vicinity of $HC{\equiv}C\text{-}CHOH^+$, **[(VIII)** or **(IX)]**, and remote from $H_2C{=}CHCO^+$, **(VI)**. The theoretical study was unable to identify a transition state between C2-protonated propadienone, **(VI)**, and O-protonated propynal, **[(VIII)** or **(IX)]**. An appropriate entry route onto the $C_3H_3O^+$ potential surface which could access protonated propynal and not protonated propadienone, might be reaction **(302)** as proposed by Bettens and Brown: [205]

$$C_3H_5^+ + O \Rightarrow C_3H_3O^+ + H_2 + 2.8^{u}\ eV \qquad \textbf{(302)}$$

Alternatively, a reaction between water and the $C_3H_2^+$ ion could conceivably generate a $C_3H_3O^+$ species with the structure of ions **(VIII)** or **(IX)**, viz: [224]

$$C_3H_2^+ + H_2O \Rightarrow C_3H_3O^+ + H + 0.3^{v}\ eV \qquad \textbf{(304)}$$

An experimental investigation of reactions **(302)** and **(304)** might therefore be valuable. Other ion-molecule synthetic schemes considered as part of the theoretical study are impracticable due to the low interstellar abundance of the reactants.

---

[u] Thermochemistry based on the $CH_3C{=}CH_2^+$ and $HC{\equiv}CCHOH^+$ cations.
[v] Thermochemistry based on the $HC{\equiv}CCH^+$ and $HC{\equiv}CCHOH^+$ cations.

It is evident that polyatomic ions exist in many different isomeric forms. As illustrated in this work, detailed ab initio calculations may allow the identification of a particular isomeric species formed during radiative association. Unfortunately isolation of a particular isomer only advances the research up to the terminal step of dissociative ion-electron recombination. For most systems the products of this final process are uncertain.

Reluctantly we conclude that the route to the formation of propynal in interstellar clouds via ion-molecule reactions is uncertain.

3.6: Epilogue.

The theoretical section of this chapter was published in June 1995 [225] whilst the experimental results were reported in November 1995. [226] Since that time several pieces of research pertaining to this work have appeared in the scientific literature.

In December 1995 Petrie suggested that propynal might be synthesised in interstellar clouds by the gas phase radical/neutral reaction between C_2H and formaldehyde, H_2CO. [227] In this paper Petrie reported the results of a series of ab initio calculations of the C_3H_3O potential energy surface. He found a number of C_3H_3O intermediates which could be formed by the reaction of the reagents C_2H and H_2CO. He argued that two of these C_3H_3O structures had configurations which, with minimal rearrangement, might yield propynal upon dissociation, (loss of atomic hydrogen). Additionally he proposed that the interstellar abundances of C_2H and CH_2O were sufficient to account for the observed propynal abundance and urged an experimental study of the C_2H + H_2CO reaction.

In October 1996 Ekern and colleagues reported the results of an ab initio study of the C_3H_2O potential surface. [228] They also outlined a mechanism for the observed evolution of propynal, C_3O and 3-hydroxypropadienylidene, (abbreviated to "t-HPD", which has the structure: C=C=CHOH), products following photolysis of a $C_3.H_2O$ cluster embedded in an Ar matrix at 12 K. Their calculations suggest that t-HPD is the initial product formed after photolysis of the $C_3.H_2O$ cluster. They propose that additional photolysis will produce propynal via sequential H atom migrations along the CCCO sketeton.

The propynal is photodepleted by sustained photolysis of the $C_3.H_2O$ complex resulting in the generation of acetylene and carbon monoxide. This work strongly suggests that propynal could be produced by the photolysis of $C_3.H_2O$ complexes in the icy mantles of interstellar dust grains. Having been formed the problem is extracting this molecule into the gas phase in an environment where the temperature is 10 - 100 K. Workers involved in grain chemistry usually resort to shocks permeating throughout the interstellar medium, raising the local temperature to ~ 1000 K at this juncture. This does not solve the problem however, as pyrolysis at these elevated temperatures is likely.

In May 1997 they published another paper which refined and extended their initial model. [229] In this second publication they proposed the existence of two photoconversion pathways for the $C_3.H_2O$ complex depending upon the wavelength of the incident radiation. One pathway leads to t-HPD and thence to propynal while the other channel involves H-atom loss to an HC_3O intermediate. This intermediate may then either lose another hydrogen atom to form C_3O or capture a hydrogen atom producing propynal. The wavelength of the incident radiation apparently influences the selection of reaction pathway.

Each of the above proposals has merit, although acceptance of the $C_3.H_2O$ photolysis route to propynal must await a cogent explanation as to how condensates escape the icy mantles of interstellar dust grains. The synthesis of propynal via the radical - neutral $C_2H + H_2CO$ reaction would presumably be verified or discounted by an experimental measurement. In short, additional research is required to satisfactorily resolve the question of the synthetic pathway to propynal in the interstellar medium.

CHAPTER 4.

EXPERIMENTAL STUDIES OF SOME CATIONS WITH ATOMIC AND MOLECULAR HYDROGEN

4.1: Introduction.

Molecular and atomic hydrogen are the most ubiquitous and abundant species in the universe. The immense clouds of gas and dust that populate the interstellar medium are composed chiefly of H_2 and H atoms, along with smaller quantities of molecules and ions. [230, 231] One of these ions is H_3^+ which was recently detected in the interstellar medium for the first time. [22] This species is considered to be the precursor ion in many synthetic schemes, or models, which simulate the chemistry occurring within interstellar clouds. These models use experimental data as input and provide reasonable estimates of the observed abundances for many interstellar species. [88, 185] Many laboratory investigations of ions reacting with molecular hydrogen, pertinent to interstellar cloud chemistry, have been made, however the same is not true for ion-H atom processes. Atomic hydrogen is not an easy reactant to monitor experimentally and this is the primary reason why reported ion reactions with H_2 outnumber those with H by about a factor of twenty. [24, 50] Also, while atomic hydrogen is readily generated it then undergoes rapid recombination, thereby reducing the H atom number density available for reaction in the flow tube.

Whilst ion-H_2, H reactions are relevant to interstellar chemistry, there is a more fundamental aspect. Reactions of cations with H atoms and H_2 provide ion stability data and information on the mode of hydrogen addition to ionic species.

Atomic hydrogen is conveniently made by passing a mixture of helium and hydrogen through a microwave cavity, however the measurement of the atomic

flux in the reaction zone is not trivial. Most of the problems encountered during experimental studies of ion-H atom reactions are associated with the determination of H atom number densities. [155, 159] Various groups have expended considerable efforts in surmounting these difficulties, and some ion-H atom reactions have now been characterised, mostly utilising flow tube techniques.

Early ion-H atom measurements adapted conventional methods that had been developed to study neutral-H atom reactions. Fehsenfeld and Ferguson initially calibrated the H atom flow by conducting a titration reaction with NO_2. [155, 159] In these first experiments they also used a theoretical rate coefficient for the associative detachment reaction between F^- anions and atomic hydrogen to determine the H atom flux, viz: [50, 100]

$$F^- + H \Rightarrow HF + e^- + 2.5\ eV \qquad \textbf{(401)}$$

$$k_{(401)\ 296K} = (1.6 + 100\ \%, - 50\ \%) \times 10^{-9}\ cm^3\ s^{-1}$$

In later work, the theoretical rate constant for the analogous reaction between Cl^- and H atoms was similarly employed, ie: [43, 45, 50, 100]

$$Cl^- + H \Rightarrow HCl + e^- + 0.9\ eV \qquad \textbf{(402)}$$

$$k_{(402)\ 296K} = (9.6 \pm 1.9) \times 10^{-10}\ cm^3\ s^{-1}$$

Another methodology utilised by these workers was to monitor the heat liberated by the recombining H atoms on a platinum surface. [43]

Certain ions react with both H_2 and H atoms and since a microwave discharge source generates a mixture of H_2 and H atoms, two simultaneous reactions may occur. Provided a different product ion is formed in each reaction, it is possible to determine the H atom flow rate by comparing the reactant ion loss and product formation in the presence and absence of atomic hydrogen (discharge on / discharge off). In 1984 this procedure was first used to determine the H / H_2 ratio in a flow tube by observing the different products of the reactions of CO_2^+ with H atoms and H_2. [154] Three years later Smith and Adams used both reaction **(402)** and the reaction of Ar^+ ions with molecular hydrogen to establish the H / H_2 ratio in the flow tube of a SIFT. [171] Chloride and sulphur hexafluoride anions have also been utilised to determine the H / H_2 and D / D_2 ratios in a SIFT experiment in which the exchange of H and D atoms was investigated in some ion-neutral reactions of interstellar import. [156]

In 1993 Sablier and Rolando published a comprehensive review of the laboratory chemistry of ion-atom reactions. [135] This review article discusses techniques for the generation of atomic hydrogen, the measurement of the H atom flux, and surveys the ion-H atom reactions for which experimental data is available in the chemical literature.

The procedure chosen to calibrate the H atom flow rate in this study was that involving the $CO_2^+ + H_2$, H reactions (producing HCO_2^+ and HCO^+ respectively), viz: [24, 154]

$CO_2^+ + H_2 \Rightarrow HCO_2^+ + H + 1.3\ eV$ **(403)**

$k_{(403)\ 300K} = (6.2 \pm 2.2) \times 10^{-10}\ cm^3\ s^{-1}$

$CO_2^+ + H \Rightarrow HCO^+ + O + 0.8\ eV^a\ (\sim 0.17)$ **(404a)**

$\Rightarrow H^+ + CO_2 + 0.2\ eV\ (\sim 0.83)$ **(404b)**

$k_{(404)\ 300K} = (3.3 \pm 2.0) \times 10^{-10}\ cm^3\ s^{-1}$

Additionally, the $CO^+ + H_2$, H reactions, [producing (HCO^+, HOC^+) and H^+ respectively], were similarly used, viz: [24, 162]

$CO^+ + H_2 \Rightarrow HCO^+ + H + 2.1\ eV\ (0.52)$ **(405a)**

$\Rightarrow HOC^+ + H + 0.6\ eV\ (0.48)$ **(405b)**

$k_{(405)\ 300K} = (1.4 \pm 0.2) \times 10^{-9}\ cm^3\ s^{-1}$

$CO^+ + H \Rightarrow H^+ + CO + 0.4\ eV$ **(406)**

$k_{(406)\ 300K} = (7.5 \pm 2.3) \times 10^{-10}\ cm^3\ s^{-1}$

These reactions have been used successfully in several laboratories to monitor atomic hydrogen fluxes. [154, 162, 165] Furthermore, this methodology was a convenient choice for the present study as the SIFT apparatus located at the University of Canterbury is configured for cations.

In this study the reactions of a number of cations with H atoms were examined. As part of the study the reactions of the same ions with H_2 were also measured. In particular, this investigation has addressed the reactivity of a series of hydrocarbon ions, $C_mH_n^+$ (m = 2 - 6; n = 0 - 9), with atomic and molecular hydrogen. The ions were primarily chosen on the basis of their importance to gas phase molecular synthesis in interstellar clouds. Principally, although not exclusively, this research has concentrated on reactions that have not been previously studied. In several cases, work performed in other

---

[a] Thermochemistry based on the HCO^+ cation, (not HOC^+).

laboratories was repeated to verify the accuracy of the experimental method and data analysis techniques.

4.2: Experimental.

Hydrogen atoms were produced in a microwave discharge through either an ~ 10 % mixture of hydrogen in helium or, less commonly, through pure, (100 %), hydrogen. The microwave discharge was contained within a Pyrex side tube, with an ~ 20 cm quartz discharge section, connected to the main flow tube. That part of the 13 mm OD, 10 mm ID Pyrex tube that was inserted into the bath gas and exposed to the ion swarm was sheathed in stainless steel on the exterior. Additionally, the interior of the probe, downstream of the discharge region, was coated with a halocarbon wax / chloroform mixture in order to reduce atom / atom surface recombination. A light horn attenuated the photon flux produced in the discharge, thereby reducing the number of photons reaching the reaction zone of the flow tube. The microwave cavity was located approximately 28.5 cm from the flow tube axis. The distance from the discharge region to the elbow was approximately 11.2 cm with the remaining distance to the flow tube axis being ~ 17.3 cm. Approximately 7 cm of the probe protruded into the flow tube. A photograph of the hydrogen atom probe is shown in Figure 4.1 below.

Small fluxes of minor species were formed in the discharge concomitantly with H atoms, (eg. H^+, H_2^+, H_3^+, metastable atoms such as He 2 ^3S, and electrons). Surface neutralisation and ion-electron recombination processes reduced the flux of charged species to an insignificant level, relative to the reacting atomic and molecular hydrogen. The removal of helium 2 ^3S metastable atoms was not so easily effected. Even with an ~ 28.5 cm separation between the microwave discharge and the flow tube axis, a low concentration of He 2 ^3S metastables entered the flow tube, at high flows of the H_2 / He mixture, creating Penning ionisation of any neutral reagent present. Such interference from

He 2 ^3S Penning ionisation was avoided by replacing the ~ 10 % H_2 / He mixture with pure (100 %) hydrogen. This procedure was adopted for determining the reactivity of the acyclic $C_6H_4^+$ and $C_6H_5^+$ cations with atomic and molecular hydrogen.

Other researchers have recognised that the fractional dissociation of H_2 to H atoms in a microwave discharge fluctuates in an erratic manner. [159] This fraction was repeatedly monitored throughout the course of these experiments using the reference CO_2^+ / H_2, H and CO^+ / H_2, H reactions which provided an absolute measure of the H atom flux within the flow tube. A series of some twenty or so measurements of these reference reactions, over several weeks, indicated a variation of $\leq$ 8 % in the fraction of the H_2 dissociated. This data is depicted in Figure 4.2. Using the ~ 10 % H_2 / He mixture a typical degree of dissociation of hydrogen in the flow tube was 20 - 40 %. Over the range of flows used, the degree of dissociation remained essentially constant with variation in H_2 / He flow.

It is interesting to compare the degree of dissociation obtained using the $CO_2^+ + H_2$ / H and $CO^+ + H_2$ / H reactions with that found using several other reactions, including the $CN^+ + H_2$ / H and $C_2N_2^+ + H_2$ / H reactions which give different products when reacting with H_2 and H atoms, (see Tables 4.1 and 4.2 below). All systems studied yielded the same H atom densities, (within experimental uncertainty), thus indicating that possible contamination from $H_2(v)$ in the discharge was not a significant source of error. If $H_2(v)$ was present, then dissimilarity in the apparent degree of dissociation of molecular hydrogen would presumably be observed for the various systems. No such variation was apparent, hence this substantiates the argument that H_2 (v) was not present in sizeable concentrations during these experiments.

Similar reasoning to the above discussion suggests that vibrational excitation was absent in the CO_2^+ and CO^+ monitor ions. Additionally, all the reactant ions experience multiple collisions with the He bath gas atoms before they react with the H_2 and H atoms in the reaction zone and this, whilst not guaranteeing the quenching of excess vibrational energy, must certainly tend to do so.

For several reactions, deuterium was substituted for hydrogen in the He / H_2 mixture to aid product determination because of the difficulty of detecting H^+ ions.

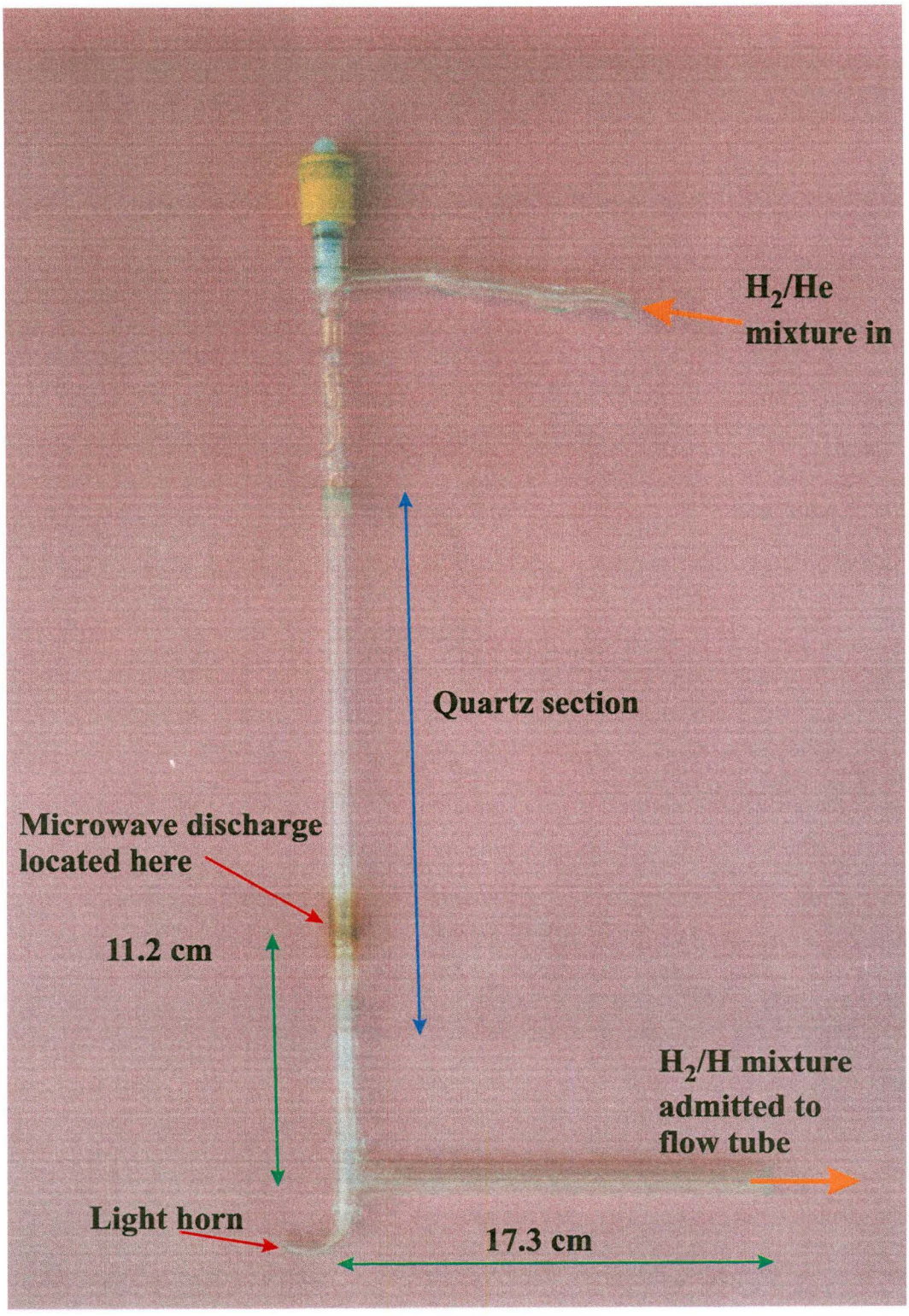

Figure 4.1. Photograph of the hydrogen atom probe used in these experiments.

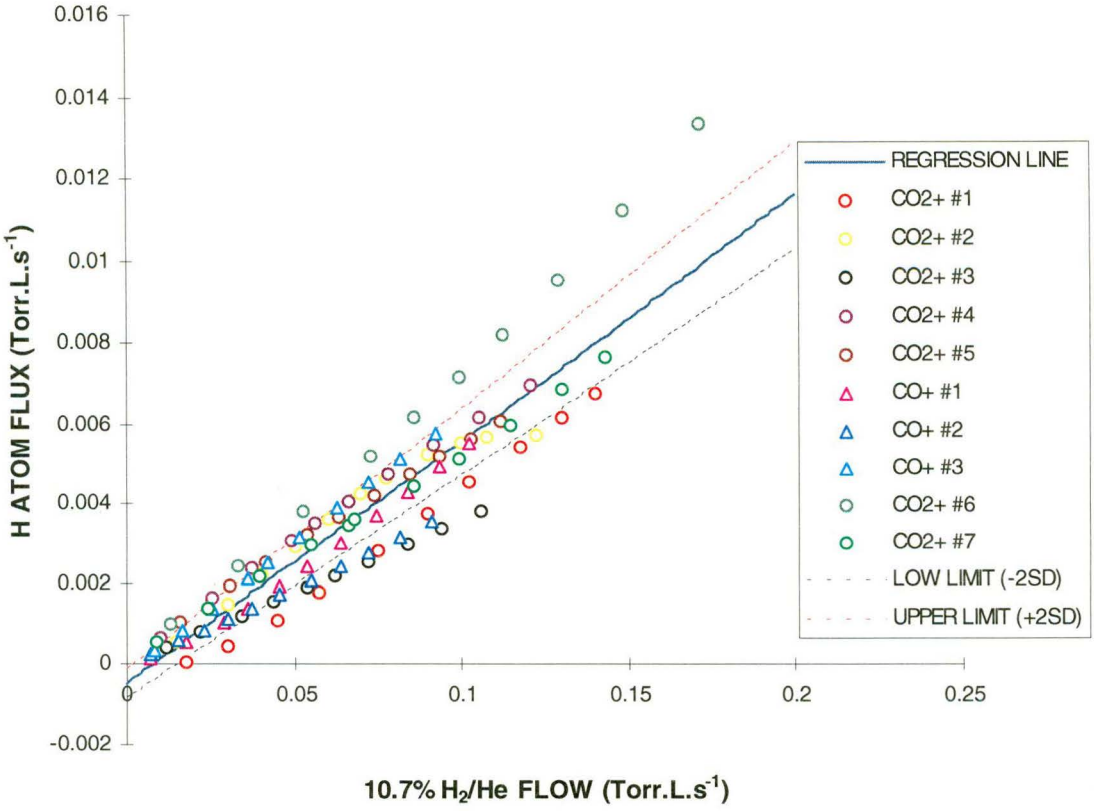

Figure 4.2. The variability in H atom flux with flow of 10.7 % H_2 / He mixture through the microwave discharge cavity. Note that the H atom fluxes were determined from the $CO_2^+ + H_2$ / H (#) and $CO^+ + H_2$ / H (•) reactions.

Reagents and Experimental Conditions

Hydrogen, (zero grade, > 99.995 % pure), and helium, (instrument grade, > 99.99 % pure), were both supplied by BOC gases. Deuterium was supplied by Alphagaz and has a nominal purity of > 99.7 %. All of these gases were further purified by passage through a molecular sieve trap, cooled to liquid nitrogen temperatures.

Hydrogen / helium mixtures were prepared by separately admitting measured pressures of these gases into glass bulbs of known, (calibrated), volume and then allowing the contents to mix via a connecting glass manifold for approximately twelve hours. The smaller of the two bulbs was ~ 1.2 litres in volume and was filled with H_2, while He was admitted to the larger bulb which had a volume of ~ 11.4 litres. Following the twelve hour mixing period the contents were expanded into an evacuated five litre glass bulb and left to stand for ~ five minutes to complete the homogenisation of the mixture. Deuterium / helium mixtures were prepared using the same procedure.

Carbon Monoxide, (CP grade, 99.5 % pure), was procured from Matheson gas products. Acetylene, (instrument grade, > 98 % pure), was supplied by BOC gases. Ethylene, (CP grade, > 99.5 % pure), was procured from New Zealand Industrial Gases, (NZIG). These gaseous reagents were further purified by passage through a dry ice / acetone cooled molecular sieve trap.

Carbon dioxide, (industrial grade, > 99.8 % pure), was supplied by NZIG. Sulphur dioxide, (CP grade, > 99.5 % pure), was obtained from BDH Chemicals Ltd. Propadiene, (allene ≡ C_3H_4), was supplied by Alphagaz and has a nominal purity of > 97 %. These gases were further purified by passage through a salt / ice / water cooled molecular sieve trap.

2-Butene, ($CH_3CH=CHCH_3$), (CP grade, > 98 % pure), and 1-3 butadiene, ($CH_2=CHCH=CH_2$), (CP grade, > 99 % pure), were both supplied by Tokyo Chemical Industry Co. Ltd, (TCI). Benzene, (AR grade, > 99.94 % pure), was obtained from Ajax Chemicals. Carbon disulphide, (analytical reagent, > 99.997 % pure), was supplied by Riedel-De Haën A.G. 1-Bromopropane ($CH_2BrCH_2CH_3$), (CP grade, > 96 % pure), was obtained from Hopkin and Williams. 2-Bromopropane, ($CH_3CHBrCH_3$), laboratory reagent, was supplied by BDH. These liquid reagents were further purified by several freeze-pump-thaw cycles.

Nitrogen dioxide was prepared by admitting an excess of oxygen into a glass bulb containing nitric oxide. The NO_2 product was trapped out using a dry ice / acetone slurry, (~ - 78 ^{o}C), and the remaining unreacted oxygen pumped away by a backing pump. Additional purification was achieved by several freeze-pump-thaw cycles.

Cyanogen was synthesised according to the method of Janz. [232]

Propyne was prepared according to the method of Brandsma. [233]

Experimental Uncertainty

The uncertainty in the rate coefficients for the H atom reactions detailed below is estimated as ± 30 %. This is a larger uncertainty than is generally reported for stable neutral reactants (± 15 %), due primarily to the difficulty in accurately establishing the H atom number density in the main flow tube.

4.3: Results.

A summary of all the results obtained in this work are presented in Tables 4.1 to 4.4. Tables 4.1 and 4.2 detail the results obtained for the reaction of several non-hydrocarbon cations with H_2 and H atoms respectively. The results for the reaction of various hydrocarbon cations with H_2 and H atoms are summarised in Tables 4.3 and 4.4 respectively. Previous measurements, where they exist, are catalogued in column 4 of each Table.

4.4: Discussion of Results.

(i). $CO_2^+ + H_2$ / H. The reaction between the carbon dioxide cation and atomic hydrogen, [reaction **(404)**], was one of the earliest ion-H atom reactions to be investigated. [159] In this system the determination of a rate coefficient is complicated by the concomitant fast reaction of CO_2^+ with the H_2 which is also present in the flow tube, [reaction **(403)**].

It is rather surprising that the previously reported values of the rate constant for reaction **(403)** should exhibit such a considerable spread, ranging from 4.0×10^{-10} to 1.4×10^{-9} $cm^3\ s^{-1}$. [24, 102, 154, 234-236, 240-242] During the course of this research $k_{(404)}$ was measured more than twenty times over a period of several months. The mean of these experiments gives a rate constant for $CO_2^+ + H_2$ of $(8.7 \pm 1.3) \times 10^{-10}$ $cm^3\ s^{-1}$ which is in good agreement with Tosi and associates. [154] Electron impact on carbon dioxide gas directly yielded the CO_2^+ primary (reactant) ion at high count rates.

In 1971 Fehsenfeld and Ferguson made the first measurement of the rate coefficient for the overall reaction between CO_2^+ and H, [reaction **(404)**], obtaining a value of $(6 \pm 3) \times 10^{-10}$ $cm^3\ s^{-1}$. [159] They did not measure a product branching ratio, although indirect evidence supported an HCO^+ / H^+ ratio of 5 / 1.

Both HCO^+ and H^+ are energetically allowed products thus:

$$CO_2^+(^2\Pi_g) + H(^2S) \Rightarrow HCO^+(^1A) + O(^3P) + 0.8\ eV^b \quad (\sim 0.17) \quad \textbf{(404a)}$$

$$\Rightarrow H^+(^1S) + CO_2\,(1\Sigma_g^+) + 0.2\ eV \quad (\sim 0.83) \quad \textbf{(404b)}$$

[b] Thermochemistry based on the HCO^+ cation, (not HOC^+).

Reactant Ion	Products and Branching Ratio	k_{obs}[a]	k_{prev}[b]	ΔH^o (kJ mol^{-1})[c]
CO^+	$HOC^+ + H$ 0.5 $HCO^+ + H$ 0.5	15	20[d], 11.9[e], 14[f] 13.9[g], 18[h], 13[i] 15[j]	- 61.3 - 198.1
CO_2^+	$HCO_2^+ + H$ 1.0	8.7	14[d], 10.1[e], 8[f], 4[k] 7.2[l], 5.8[m], 9.5[n] 4.7[o], 9.0[p]	- 127.5
SO_2^+	$HSO_2^+ + H$ 1.0	0.05	0.17[o]	- 74.9
NO_2^+	No Reaction	< 0.001		
CS_2^+	No Reaction	< 0.0005		
CN^+	$HCN^+ + H$ 0.5 $HNC^+ + H$ 0.5	16	12.4[o], 10.0[q], 11[r]	- 128.8 - 170.7
$C_2N_2^+$	$HC_2N_2^+ + H$ 1.0	8.8	9.6[s]	- 219.6

Table 4.1. Reactions of the given non-hydrocarbon reactant ion with H_2.

[a] Observed rate coefficient in units of 10^{-10} cm^3 s^{-1}. The Langevin capture rate coefficient for all reactions in this Table is 1.5 x 10^{-9} cm^3 s^{-1}. [b] Rate coefficients determined in other laboratories in units of 10^{-10} cm^3 s^{-1}. [c] The listed exothermicities are taken from Reference 31.
[d] Reference 234. [e] Reference 235. [f] Reference 236. [g] Reference 237. [h] Reference 238.
[i] Reference 162. [j] Reference 239. [k] Reference 240. [l] Reference 241. [m] Reference 102.
[n] Reference 242. [o] Reference 24. [p] Reference 154. [q] Reference 243. [r] Reference 244.
[s] Reference 245.

Reactant Ion	Products and Branching Ratio	k_{obs}[a]	k_{prev}[b]	ΔH^o (kJ mol^{-1})[c]
CO^+	$H^+ + CO$ 1.0	4.0	7.5[d]	- 40.1
CO_2^+	$HCO^+ + O$ > 0.95 $H^+ + CO_2$ < 0.05	4.7	6[e], 1.1[f], 2.9[g]	- 78.6 - 17.0
SO_2^+	$SO^+ + OH$ 1.0	4.2		- 69.4
NO_2^+	No Reaction	< 0.1		
CS_2^+	$HCS^+ + S$ 1.0	2.8		- 12.1
CN^+	$H^+ + CN$ 1.0	6.4		- 77.4
$C_2N_2^+$	$HNC^+ + CN$ 0.8 $C_2H^+ + N_2$ 0.2	6.2	< 0.1, 1.0	- 11.5[h] - 120.1

Table 4.2. Reactions of the given non-hydrocarbon reactant ion with H atoms.

[a] Observed rate coefficient in units of 10^{-10} cm^3 s^{-1}. The Langevin capture rate coefficient for all reactions in this Table is 1.9 x 10^{-9} cm^3 s^{-1}. [b] Rate coefficients determined in other laboratories

in units of 10^{-10} cm^3 s^{-1}. [c] The listed exothermicities are taken from Reference 31.

[d] Reference 162. [e] Reference 159. [f] Reference 102. [g] Reference 154. [h] See text.

Reactant Ion	Products and Branching Ratio	k_{obs} [a]	k_{prev} [b]	ΔH^o (kJ mol^{-1})[c]
C_2^+	$C_2H^+ + H$ 1.0	11	11[d], 14[e], 12[f]	- 88
C_2H^+	$C_2H_2^+ + H$ 1.0	11	7.8[d], 17[e]	- 149
$C_2H_3^+$	No Reaction	< 0.05	< 0.01[g], < 0.001[h]	
$HCCCH_2^+$	No Reaction	< 0.05	< 0.05[I]	
c-$C_3H_3^+$	No Reaction	< 0.05	< 0.05[I]	
$H_2CCCH_2^+$	No Reaction	< 0.05	< 0.001[j]	
$HCCCH_3^+$	No Reaction	< 0.005	< 0.001[j]	
$C_3H_5^+$	No Reaction	< 0.005	No Reaction[k]	
$C_3H_7^+$	No Reaction	< 0.05	No Reaction[k]	
C_4H^+	$C_4H_2^+ + H$ 1.0	1.8	< 0.001[k], 1.5[l], 1.8[f]	~ - 137
$C_4H_2^+$	No Reaction	< 0.04		
$C_4H_3^+$	No Reaction	< 0.02		
$C_4H_4^+$	No Reaction	< 0.03		
$C_4H_5^+$	No Reaction	< 0.03		
$C_4H_6^+$	No Reaction	< 0.04		
$C_4H_8^+$	No Reaction	< 0.005		
$C_4H_9^+$	No Reaction	< 0.005		
ac-$C_6H_4^+$	No Reaction	< 0.005		
c-$C_6H_4^+$	No Reaction	< 0.03		
ac-$C_6H_5^+$	No Reaction	< 0.01	< 0.01[n]	
c-$C_6H_5^+$	$C_6H_7^+$ 1.0	< 0.38[o]	0.15[p], 0.5[l,n]	- 273
c-$C_6H_6^+$	No Reaction	< 0.05	< 0.01[n]	

Table 4.3. Reactions of the given $C_mH_n^+$ reactant ion with H_2.

[a] Observed rate coefficient in units of 10^{-10} cm^3 s^{-1}. The Langevin capture rate coefficient for all reactions in this Table is 1.5 x 10^{-9} cm^3 s^{-1}. [b] Rate coefficients determined in other laboratories in units of 10^{-10} cm^3 s^{-1}. [c] The listed exothermicities are taken from Reference 31.

[d] Reference 237. [e] Reference 246. [f] Reference 247. [g] Reference 248. [h] Reference 249. No bimolecular reaction was observed, but a limit to termolecular association of $k_3 \sim < 1 \times 10^{-30}$ cm^6 s^{-1} at 80 K was reported. [i] Reference 250. [j] Reference 249. Results are measured at 80 K. Isomeric form of $C_3H_4^+$ not specified. No bimolecular reaction was observed, but a limit to termolecular association of $k_3 < 1 \times 10^{-30}$ cm^6 s^{-1} was reported. [k] Reference 249. A limit to termolecular association of $k_3 < 1 \times 10^{-30}$ cm^6 s^{-1} at 80 K was reported. [l] Reference 251.

[m] Exothermicity from References 31 and 252. [n] Reference 165. [o] Pseudo-bimolecular reaction. The rate constant shown is for a flow tube pressure of 0.30 Torr. The termolecular rate for the three-body association process is estimated as $k_3 \geq 3.9 \times 10^{-27}$ cm^6 s^{-1}. [p] Reference 253.

Reactant Ion	Products and Branching Ratio	k_{obs} [a]	k_{prev} [b]	ΔH^o (kJ mol^{-1})[c]
C_2^+	No Reaction	< 1.0		
C_2H^+	No Reaction	< 1.0		
$C_2H_3^+$	$C_2H_2^+ + H_2$ 1.0	0.68	< 0.1[d], 1.0[e]	- 5.8[f]
$HCCCH_2^+$	No Reaction	< 0.03		
c-$C_3H_3^+$	No Reaction	< 0.03		
$H_2CCCH_2^+$	$C_3H_3^+ + H_2$ 1.0	1.7		- 164[g]
$HCCCH_3^+$	$C_3H_3^+ + H_2$ 1.0	3.0		- 224[g]
$C_3H_5^+$	$C_3H_6^+$ 1.0	1.6[h,i]		- 206[j]
$C_3H_7^+$	$C_3H_6^+ + H_2$ 1.0	0.32		- 59[k]
C_4H^+	$C_4H_2^+$ 1.0	~ 5.8[h,l]		~ - 574[m]
$C_4H_2^+$	$C_4H_3^+$ 1.0	2.6[h,n]		~ - 420
$C_4H_3^+$	$C_4H_4^+$ 1.0	~ 0.5[h,o]		~ - 206[g]
$C_4H_5^+$	No Reaction	< 0.4		
$C_4H_6^+$	$C_2H_3^+ + C_2H_4$ ~ 0.15 $C_2H_5^+ + C_2H_2$ ~ 0.65 $C_4H_5^+ + H_2$ ~ 0.20	1.9		- 38[p] - 73[p] - 174[q]
$C_4H_8^+$	$C_4H_7^+ + H_2$ 1.0	1.1		- 193[r]
$C_4H_9^+$	No Reaction	< 0.2		
ac-$C_6H_4^+$	No Reaction	< 0.05		
c-$C_6H_4^+$	$C_6H_5^+$ 1.0	0.33[h,s]		- 400[t]
ac-$C_6H_5^+$	No Reaction	< 0.05	< 0.05[u]	
c-$C_6H_5^+$	No Reaction	< 0.1	< 0.1[u]	
c-$C_6H_6^+$	$C_6H_5^+ + H_2$ ~ 0.35 $C_6H_7^+$ ~ 0.65	2.1[w]	2.5[u]	- 67[v] - 340[x]

Table 4.4. Reactions of the given $C_mH_n^+$ reactant ion with H atoms.

[a] Observed rate coefficient in units of 10^{-10} cm^3 s^{-1}. The Langevin capture rate for all reactions in this Table is 1.9 x 10^{-9} cm^3 s^{-1}. [b] Rate coefficients determined in other laboratories in units of 10^{-10} cm^3 s^{-1}. [c] The listed exothermicities are taken from Reference 31. [d] Reference 102. [e] Reference 164. [f] See text. [g] Thermochemistry for acyclic isomers. [h] Pseudo-bimolecular reaction. The rate coefficient shown is for a flow tube pressure of 0.30 Torr. [i] The termolecular rate for the three body association process is estimated as $k_3 \geq 1.6 \times 10^{-26}$ cm^6 s^{-1}. [j] Thermochemistry for lowest energy acyclic isomers. [k] This value corresponds to the iso $C_3H_7^+$ structure converted to the acyclic $C_3H_6^+$ species. [l] The termolecular rate for the three-body association process is estimated as $k_3 \sim \geq 6 \times 10^{-26}$ cm^6 s^{-1}. [m] References 31 and 252. [n] The termolecular rate for the three-body association process is estimated as $k_3 \geq 2.7 \times 10^{-26}$ cm^6 s^{-1}. [o] The termolecular rate for the three-body association process is estimated as $k_3 \geq 5.1 \times 10^{-27}$

$cm^6\ s^{-1}$. [p] Thermochemistry based on (E)-1,3-butadiene ion. [q] Thermochemistry as for p and $CH_2{=}CCH{=}CH_2^+$. [r] Thermochemistry based on (E)-2-$C_4H_8^+$ and $CH_3CCHCH_3^+$. [s] The termolecular rate for the three-body association process is estimated as $k_3 \geq 3.4 \times 10^{-27}\ cm^6\ s^{-1}$. [t] Thermochemistry based on benzyne ion and phenyl radical ion. [u] Reference 165. [v] Thermochemistry based on benzene ion and phenyl radical ion. [w] The termolecular rate for the three-body association channel between c-$C_6H_6^+$ + H is estimated as $k_3 \geq 1.4 \times 10^{-26}\ cm^6\ s^{-1}$. [x] Thermochemistry based on benzene ion and protonated benzene ion.

Tosi and colleagues [154] differentiated between reactions **(403)** and **(404)**, which proceed simultaneously, by comparing the relative ion signals of CO_2^+ and the product ion of the reaction with H_2, HCO_2^+, with the microwave discharge on and off. The rate coefficient for reaction **(403)** is well known and furthermore, it is readily determined with the discharge off. This data analysis methodology facilitates the evaluation of the absolute H atom number density in the reaction zone of the flow tube. [154] Tosi et al. reported a rate coefficient value of $(2.9 \pm 0.9) \times 10^{-10}\ cm^3\ s^{-1}$ for the reaction between CO_2^+ and atomic hydrogen. [154]

The research discussed here has necessitated measuring the rate coefficient for reaction **(404)** in excess of twenty times, over an extended period, (several months). Using the data analysis prescription of Tosi and co-workers [154] the mean of these separate experimental determinations is $k_{(404)} = (4.7 \pm 1.4) \times 10^{-10}\ cm^3\ s^{-1}$. This value is not inconsistent with both of the prior measurements, considering the collective large uncertainties in these three experimental studies. [154, 159]

Both CHO^+ isomeric structures, (HOC^+ and HCO^+), are energetically accessible in reaction **(404a)**. In 1987 Freeman et al. demonstrated that HOC^+ reacts rapidly with nitrous oxide, (N_2O), [$k = (1.2 \pm 0.2) \times 10^{-9}\ cm^3\ s^{-1}$], whereas HCO^+ is less reactive, [$k = (3.3 \pm 0.5) \times 10^{-12}\ cm^3\ s^{-1}$]. [239] This differing reactivity with N_2O provided a viable strategy for elucidating the structure of the CHO^+ product ion generated from the reaction of $CO_2^+ + H$. The CHO^+ product of reaction **(404a)** is found to be entirely HCO^+.

The H^+ / HCO^+ branching ratio for reaction **(404)** was also evaluated by reacting CO_2^+ with a 10 % deuterium / helium mixture. With the microwave discharge on, no D^+ product was observed even though channel **(404b)** is exothermic by 17 kJ mol^{-1}. This outcome allows a limit of < 5 % to be placed

on the branching ratio for the D^+ channel, **(404b)**. By inference this result permits a similar limit to be reported for the formation of the H^+ product from the $CO_2^+ + H$ reaction.

The Langevin rate coefficient for reaction **(404)** is $k_L = 1.9 \times 10^{-9}$ cm^3 s^{-1}. When spin conservation is considered, the spin-weighted fraction of channel **(404a)** has an upper limit of 3/4 k_L, ie. 1.4×10^{-9} cm^3 s^{-1}, whereas the unobserved pathway **(404b)** has an upper limit of 1/4 k_L, ie. 4.8×10^{-10} cm^3 s^{-1}. These upper limits clearly exceed the measured values, and therefore other, undetermined factors are reducing the rate of reaction below the collision rate.

(ii). $CO^+ + H_2$ / H. The rate coefficient for the well-studied reaction between CO^+ and molecular hydrogen has been evaluated by Anicich as $k = (1.4 \pm 0.2) \times 10^{-9}$ cm^3 s^{-1}. [24] A 1987 study by Freeman and associates determined that this reaction produces the HCO^+ and HOC^+ isomers in approximately equal proportions, [reactions **(405a)** and **(405b)**]. [239] This reaction was reinvestigated and a rate coefficient of $k = (1.5 \pm 0.2) \times 10^{-9}$ cm^3 s^{-1} determined which agrees favourably with the evaluated figure. The CO^+ cation was produced by electron impact on carbon monoxide gas.

One previous measurement of the reaction between CO^+ and H, [reaction **(406)**], has been undertaken in which the products were reported as $H^+ + CO$. [162] This reaction was re-examined by studying the analogous process with D atoms. The observation of D^+ allowed the confirmation, (by analogy), of H^+ as the sole product ion of reaction **(406)**.

Federer et al. [162] observed that only singlet products of reaction **(406)** are energetically accessible, viz:

$$CO^+(^2\Sigma) + H(^2S) \Rightarrow H^+(^1S) + CO(^1\Sigma) + 0.4\ eV \qquad \textbf{(406)}$$

If spin is conserved in this process then $k \leq 1/4\ k_L$, (ie. $k \leq 4.8 \times 10^{-10}$ cm^3 s^{-1}), which is the statistical weight ratio of singlet-to-total products. The rate constant reported by Federer et al. [162] of $k_{(406)} = (7.5 \pm 2.3) \times 10^{-10}$ cm^3 s^{-1} is larger than the spin weighted collision rate and the authors argued for some spin conversion during the collision.

The simultaneous reactions **(405)** and **(406)** were utilised to provide absolute H atom number densities in the flow tube in a comparable manner to that described for the $CO_2^+ + H_2$ / H reactions. Atomic hydrogen fluxes derived

from the analysis of this system were used to obtain the rate coefficient for reaction **(406)**. In this way a value of $k_{(406)} = (4.0 \pm 1.2) \times 10^{-10}$ cm^3 s^{-1} for the reaction between CO^+ and H atoms is obtained. Interestingly, this experimental rate coefficient is < 1/4 k_L and hence supports spin conservation. Within the bounds of the aggregate experimental uncertainty, this new measurement is consistent with the earlier reported value of $k_{(406)}$ by Federer and co-workers. [162]

(iii). $SO_2^+ + H_2$/H. The reaction between SO_2^+ and H_2 has been investigated once previously using the ion cyclotron resonance, (ICR), technique and was observed to proceed via hydrogen atom abstraction, viz: [24]

$SO_2^+ + H_2 \Rightarrow HSO_2^+ + H + 0.8$ eV **(407)**

$k_{(407)\ 300K} = (1.7 \pm 0.7) \times 10^{-11}$ cm^3 s^{-1}

A re-examination verified that this reaction proceeds, but very slowly, the rate coefficient, $k_{(407)}$ being ~ $(5.0 \pm 0.8) \times 10^{-12}$ cm^3 s^{-1}. The product ion is confirmed as HSO_2^+. Electron impact on sulphur dioxide readily formed the SO_2^+ cations used in these experimental investigations.

In contrast, a relatively fast reaction occurs between SO_2^+ and H atoms, the sole product ion being SO^+, ie.

$SO_2^+(^2A_1) + H(^2S) \Rightarrow SO^+(^2\Pi) + OH(^2\Pi) + 0.7$ eV **(408)**

$k_{(408)\ 300K} = (4.2 \pm 1.3) \times 10^{-10}$ cm^3 s^{-1}

Spin is conserved in reaction **(408),** however the observed rate coefficient is only ~ 20 % of the Langevin collision rate, ($k_L = 1.9 \times 10^{-9}$ cm^3 s^{-1}). The fact that the observed rate coefficient is less than 1/4 k_L, (the statistical weight of the spin allowed singlet reaction pathway), suggests that this reaction proceeds via a singlet potential surface. Several spin-allowed ion-atom reactions have been reported that display similar characteristics. [162, 254]

(iv). $NO_2^+ + H_2$ / H. The nitrogen dioxide cations used in these experiments were produced by electron impact on nitrogen dioxide gas.

The present work shows that NO_2^+ is unreactive with both H_2, ($k < 1 \times 10^{-12}$ cm^3 s^{-1}), and H atoms, ($k < 1 \times 10^{-11}$ cm^3 s^{-1}), at thermal energies. This result is mildly surprising as exothermic channels are available for both reactions, viz:

$NO_2^+ + H_2 \not\rightarrow NO^+ + H_2O + 2.4$ eV **(408)**

$NO_2^+(^1\Sigma) + H(^2S) \not\rightarrow NO^+(^1\Sigma) + OH(^2\Pi) + 1.8$ eV **(409)**

Note that in the unobserved exothermic reaction between NO_2^+ and atomic hydrogen, [process **(409)**], spin is conserved, however there is a change in orbital angular momentum, (from $\Lambda = 0$ to $\Lambda = 1$). The unreactivity therefore suggests the existence of a substantial barrier on the $(NO_2H^+)^*$ surface, or, alternatively, that the selection rule for orbital angular momentum conservation is more binding than might be anticipated. Interestingly, the analogous atom-neutral reaction of H atoms with NO_2, (forming OH + NO), is fast [255] as is also the reaction between the NO_2^- anion and atomic hydrogen. [155]

(v). $CS_2^+ + H_2$ / H. The reactivity of the carbon disulphide cation with either molecular or atomic hydrogen has not been characterised by any previous experimental studies. In the present work, CS_2^+ is found to be unreactive with H_2, ($k < 5 \times 10^{-13}$ cm^3 s^{-1}), but undergoes a moderately fast reaction with H atoms producing HCS^+ and a sulphur atom, viz:

$CS_2^+(^1\Sigma) + H(^2S) \Rightarrow HCS^+(^1A) + S(^3P) + 0.1$ eV **(410)**

$k_{(410)\ 300K} = (2.8 \pm 0.8) \times 10^{-10}$ cm^3 s^{-1}:

The CS_2^+ cation was formed directly by electron impact on carbon disulphide.

Spin is not conserved for ground state products and reaction **(410)** is insufficiently exothermic, ($\Delta H^\circ = -12$ kJ mol^{-1}), to generate metastable $S(^1D)$ atoms.

(vi). $CN^+ + H_2$ / H. Three previous investigations have determined that the cyanide cation reacts with H_2 at a rate approaching the Langevin collision rate, ($k_L = 1.5 \times 10^{-9}$ cm^3 s^{-1}), via a hydrogen atom abstraction process. [24, 243, 244] Furthermore, the 1991 study by Petrie et al. demonstrated that the $CN^+ + H_2$ reaction forms two product ions, namely the isomers HCN^+ and HNC^+. These isomeric species are formed in equal proportion. [244] Both primary ion products then undergo secondary reaction with H_2 to produce the terminal ion in this system, $HCNH^+$. The rate coefficient obtained for this reaction from the current research is $(1.6 \pm 0.2) \times 10^{-9}$ cm^3 s^{-1}, which is in tolerable agreement with the previous measurements.

In the present study electron impact upon cyanogen gas produced a sizeable signal of CN^+ ions. The method of analysis, as pioneered by Tosi and colleagues, [154] was once again used in this system to obtain the H / H_2 ratio and thence to obtain the rate coefficient for the reaction of CN^+ with H atoms. Due

to the secondary reactions of HNC^+ and HCN^+ with H_2 it was necessary to monitor both HCN^+ / HNC^+ and their product ion $HCNH^+$. Identification of the reaction ion products was achieved by using a 10 % deuterium / helium mixture to generate D atoms. The sole ion product produced in the reaction between CN^+ and D, (analogous to the CN^+ + H reaction), is D^+, this being the only exothermic channel, ie.

$CN^+(^1\Sigma) + H(^2S) \Rightarrow H^+(^1S) + CN(^2\Sigma^+) + 0.5$ eV **(411)**

$k_{(411)\ 300K} = (6.4 \pm 1.9) \times 10^{-10}$ cm^3 s^{-1}

The exothermicity emanates from the difference in ionisation potentials, viz IP(CN) - IP(H) = 47.4 kJ mol^{-1} ≡ 0.5 eV. This reaction is very fast for an ion-atom process and spin is conserved.

It has been previously suggested that D^+ can be formed in the reaction between HCN^+ + D. [102] This reaction was reinvestigated and no D^+ product was detected.

(vii). $C_2N_2^+$ + H_2 / H. No earlier studies have been reported for the reaction of $C_2N_2^+$ with H atoms.

In this work a large signal of $C_2N_2^+$ was directly generated by electron impact on cyanogen. The cyanogen cation reacts at little more than half the collision rate with H_2, via H atom abstraction, producing $HC_2N_2^+$ + H, ie.

$C_2N_2^+ + H_2 \Rightarrow HC_2N_2^+ + H + 2.3$ eV **(412)**

$k_{(412)\ 300K} = (8.8 \pm 1.3) \times 10^{-10}$ cm^3 s^{-1}

These findings are in good agreement with an earlier measurement. [245]

Two product channels are evident in the rapid reaction of $C_2N_2^+$ with hydrogen atoms, viz:

$C_2N_2^+(^2\Sigma) + H(^2S) \Rightarrow HNC^+(^2\Sigma) + CN(^2\Sigma^+) + 0.1$ eV (0.8) **(413a)**

$\Rightarrow C_2H^+(^1\Sigma) + N_2(^1\Sigma_g^+) + 1.2$ eV (0.2) **(413b)**

$k_{(413)\ 300K} = (6.2 \pm 1.9) \times 10^{-10}$ cm^3 s^{-1}

Reaction **(413a)** conserves spin provided the multiplicities of all ground state reactants and products are doublets. The thermodynamic data compiled by Lias et al. [31] suggests that reaction **(413a)** is endothermic by 27 kJ mol^{-1}, however, more recent data suggests that this channel is in fact exothermic by 12 kJ mol^{-1}. [256, 257] The absence of a charge transfer reaction between HNC^+ and O_2

provides evidence which substantiates the exothermicity of channel **(413a)**. This outcome constrains the heat of formation of HNC^+ as ΔH_f^o (HNC^+) $\leq$ 1373 kJ mol^{-1}. [256] Moreover, Ferguson recently calculated $\Delta H_f^o(HNC^+)$ = 1368 kJ mol^{-1} from an Arrhenius plot of the slightly endothermic reaction between HNC^+ and carbon monoxide. [257] Energy constraints dictate that only the lower energy CHN^+ isomer, HNC^+, is accessible to thermal energy reactants in reaction **(413a)**. Further, in this process, end attack by H followed by C-C bond cleavage leads directly to HNC^+ rather than HCN^+.

The 20 % C_2H^+ channel presumably results from the colliding H atom encountering the $C_2N_2^+$ ion near the midpoint of the species rather than at the terminus. The H atom might conceivably bridge the C-C bond in a 5-atom transition state structure prior to the elimination of nitrogen and the formation of C_2H^+. The above argument is conjecture and a detailed understanding of the mechanism of reaction **(413b)** must await an ab-initio study.

(viii). C_2^+ and $C_2H^+ + H_2$ / H. Both of these ions were generated by electron impact on a mixture of ~10 % C_2H_2 in He. In each case the evaluation of the rate coefficient with H was impeded by a rapid hydrogen atom abstraction reaction with H_2, ie.

$C_2^+ + H_2 \Rightarrow C_2H^+ + H + 0.9$ eV **(414)**

$k_{(414)\ 300K} = (1.1 \pm 0.2) \times 10^{-9}$ cm^3 s^{-1}

$C_2H^+ + H_2 \Rightarrow C_2H_2^+ + H + 1.5$ eV **(415)**

$k_{(415)\ 300K} = (1.1 \pm 0.2) \times 10^{-9}$ cm^3 s^{-1}

The rate coefficients obtained from the current work compare favourably with the evaluated rate constants tabulated for these reactions by Anicich, [$(1.24 \pm 15\ \%) \times 10^{-9}$ cm^3 s^{-1} for $C_2^+ + H$, and $(1.24 \pm 50\ \%) \times 10^{-9}$ cm^3 s^{-1} for $C_2H^+ + H$]. [405] With the microwave discharge on, the observed rate coefficients for reactions **(414)** and **(415)** decreased to values commensurate with that expected from diluting the H_2 with a non-reacting gas at the equivalent proportion to the H atoms. Furthermore, no additional product ions were discerned with the microwave discharge on. The conclusion of this experimental study is that neither C_2^+ nor C_2H^+ reacts with H at measurable rates. This outcome is in accordance with the fact that no exothermic binary channels are available for either reaction.

(ix). $C_2H_3^+ + H_2$ / H. Two earlier room temperature studies of the reaction between $C_2H_3^+$ and atomic hydrogen have been undertaken. The first of these investigations was conducted in 1979 by Karpas and co-workers, using the ICR technique, and no reaction was observed. [102] Later, in 1989, Hansel and colleagues reported the contrary finding of a moderately fast reaction occurring via an H atom transfer pathway, viz: [164]

$C_2H_3^+(^1A) + H(^2S) \Rightarrow C_2H_2^+(^2\Sigma) + H_2(^1\Sigma_g^+) + 0.03\ eV$ **(416)**

$k_{(416)\ 300K} = (1.0 \pm 0.2) \times 10^{-10}\ cm^3\ s^{-1}$

Note that spin is conserved in the above process, **(416)**. Smith and colleagues have applied the latter result to the evaluation of the energetics of the reaction between $C_2H_2^+ + H_2$, [258] this reaction being a critical step in the synthesis of hydrocarbons in interstellar clouds. [17]

Reaction **(416)** was re-examined as part of the current study and the product channel confirmed as $C_2H_2^+ + H_2$. The $C_2H_3^+$ ion was generated by a sequential process from $C_2H_5^+$, which is the major ion formed when ethylbromide, (C_2H_5Br), is subjected to electron impact. $C_2H_5^+$ was mass selected and injected into the flow tube with sufficient energy to induce fragmentation to $C_2H_3^+$ via collision-induced dissociation with the helium bath gas during the injection process.

A rate coefficient of $k_{(416)} = (6.8 \pm 2.0) \times 10^{-11}\ cm^3\ s^{-1}$ is found. This value is the mean of five separate experimental determinations. Note that value for $k_{(416)}$ obtained by Hansel et al. [164] and that derived as a result of the present work are not drastically different, (in view of the uncertainty in the determination of H atom densities); indeed these measurements agree within experimental error.

Smith and co-workers have measured the rate constant for the "forward" direction of the equilibrium between $C_2H_2^+ + H_2$ and $C_2H_3^+ + H$, viz: [258]

$C_2H_2^+ + H_2 \rightleftharpoons C_2H_3^+ + H$ **(417)**

$k_{f\,(417)\ 300K} = 2.6 \times 10^{-12}\ cm^3\ s^{-1}$.

When this result is combined with the present rate coefficient for, (the "reverse"), reaction **(416)**, it affords an equilibrium constant for reaction **(417)** of $K = 3.8 \times 10^{-2}$. Employing the relation $\Delta G^\circ = - RT\ Ln(K)$, the Gibbs free energy change for the $C_2H_2^+ + H_2$ reaction, **(417$_f$)**[c], is calculated to be 8.16 kJ mol^{-1} at

[c] The identifier "**(417$_f$)**" denotes the forward reaction of the **(417)** equilibrium process.

300 K. Total partition functions have been used to calculate a value for the standard entropy change, ΔS°, of - 7.9 J K^{-1} mol^{-1} for reaction **(417$_f$)**[c]. [258] Noting that $\Delta G = \Delta H - T\Delta S$ allows the enthalpy of reaction **(417$_f$)**[c] to be established as $\Delta H^{\circ} = +$ 5.8 kJ mol^{-1}. This endothermicity precludes the $C_2H_2^+ + H_2$ reaction from proceeding at a significant rate in cold interstellar clouds, which is in accordance with earlier conclusions. [17, 258]

The $C_2H_3^+$ ion is observed to be unreactive with molecular hydrogen, ($k < 5 \times 10^{-12}$ cm^3 s^{-1}), which is in agreement with two earlier studies.

(x). $C_3H_3^+ + H_2$ / H. Two low energy $C_3H_3^+$ isomers exist, namely the cyclopropenylium ion, c-$C_3H_3^+$, and the acyclic propargyl ion, $HCCCH_2^+$.

Mixtures of these ions, (typically 60 % acyclic, 40 % cyclic), were readily produced from ensuing reactions after initial electron impact on ethylene, C_2H_4. The primary ion, $C_2H_4^+$, undergoes further reaction with C_2H_4 in a high pressure ion source to form $C_3H_5^+$. The $C_3H_5^+$ ion subsequently fragments after mass selection into the two isomeric forms of $C_3H_3^+$ during the injection process. In 1994 McEwan et al. outlined methods based on differing reactivities for differentiating between the two isomers of $C_3H_3^+$. [250] In all cases $HCCCH_2^+$ was found to be more reactive than c-$C_3H_3^+$.

In the current work neither ion is observed to react with H_2, ($k < 5 \times 10^{-12}$ cm^3 s^{-1}). Similarly, no reaction is apparent with H atoms despite each isomeric ion ostensibly having an exothermic binary reaction channel available [31] leading to their respective cyclic and acyclic $C_3H_2^+$ isomers (+ H_2). These experimental findings are in accord with comprehensive ab-initio calculations of the $C_3H_2^+$ and $C_3H_3^+$ surfaces [259, 260] which indicate that both H atom transfer reactions are endothermic. The ab-initio studies calculate that the endothermicity of the ac-$C_3H_3^+$ / H atom transfer reaction is slight, being merely 8 kJ mol^{-1}. [259]

(xi). $H_2CCCH_2^+$ and $HCCCH_3^+ + H_2$ / H. The $HCCCH_3^+$ and $H_2CCCH_2^+$ ions were formed via electron impact on their parent precursors, propyne and allene, respectively.

No reaction is observed between molecular hydrogen and either $C_3H_4^+$ ion,

---

[c] The identifier "**(417$_f$)**" denotes the forward reaction of the **(417)** equilibrium process.

($k < 5 \times 10^{-12}$ cm^3 s^{-1} for $H_2CCCH_2^+$, and $k < 5 \times 10^{-13}$ cm^3 s^{-1} for $HCCCH_3^+$). Both $C_3H_4^+$ species undergo efficient H atom transfer when reacting with H atoms, viz:

$H_2CCCH_2^+(^1A_1'') + H(^2S) \Rightarrow$ ac-$C_3H_3^+(^1A) + H_2(^1\Sigma_g^+) + 1.7$ eV **(418)**

$k_{(418)\ 300K} = (1.7 \pm 0.5) \times 10^{-10}$ cm^3 s^{-1}

and;

$HCCCH_3^+(^2A') + H(^2S) \Rightarrow$ ac-$C_3H_3^+(^1A) + H_2(^1\Sigma_g^+) + 2.3$ eV **(419)**

$k_{(419)\ 300K} = (3.0 \pm 0.9) \times 10^{-10}$ cm^3 s^{-1}

The $C_3H_3^+$ products of reactions **(418)** and **(419)** are represented as ac-$C_3H_3^+$, (acyclic $C_3H_3^+$), on the premise that the precursor ions are acyclic, although this was not verified experimentally. Moreover, the isomeric structures of the $C_3H_4^+$ ions in reactions **(418)** and **(419)** were not identified by experiment, rather structures are assumed that conform most closely to the precursor neutral molecule. Indeed, the comparatively high uncertainty associated with rate coefficients obtained for cation-H atom reactions means that it is impossible to rule out the possibility that the two $C_3H_4^+$ cations have the same structure.

It is of interest to note that spin is not conserved in the reaction of the allene cation with H atoms **(418)**, yet it is conserved in the analogous, (faster), reaction **(419)** of the propyne cation with this atomic species. Furthermore, the observed rate coefficient for process **(419)** is < 1/4 k_L, which is the statistical weight of the spin allowed singlet reaction pathway. The violation of spin conservation may retard the rate at which process **(418)** is able to proceed.

(xii). $C_3H_5^+ + H_2$ / H. Electron impact on ethylene was utilised to generate the $C_3H_5^+$ ion. As discussed in **(x)** above, $C_3H_5^+$ is the major product ion formed during the reaction between $C_2H_4^+$ and C_2H_4. Following mass selection, $C_3H_5^+$ was injected into the flow tube, using sufficiently low energies to avoid fragmentation into $C_3H_3^+$.

The $C_3H_5^+$ ion is unreactive with H_2, ($k < 5 \times 10^{-13}$ cm^3 s^{-1}), however an observable reaction occurs with H atoms via an association process, ie.

$C_3H_5^+(^1A) + H(^2S) \Rightarrow C_3H_6^+(^2A) + 2.1$ eV[d] **(420)**

$k_{(420)\ 300K} = (1.6 \pm 0.5) \times 10^{-10}$ cm^3 s^{-1}

[d] Thermochemistry based on the $CH_2CH{=}CH_2^+$ and $CH_3CH{=}CH_2^+$ cations.

Spin is conserved in reaction **(420)**. Note that $k_{(420)}$ is reported for the pseudo-bimolecular reaction between $C_3H_5^+$ and H atoms at a helium bath gas pressure of 0.3 Torr. The termolecular rate coefficient for the three-body association process between $C_3H_5^+$, H atoms, and He is calculated to be $k_3 \geq 1.6 \times 10^{-26}$ cm^6 s^{-1}.

A curved semilogarithmic decay of $Ln(C_3H_5^+)$ count versus H atom flow may indicate the presence of at least two $C_3H_5^+$ isomers. Assuming this to be the case, $k_{(420)}$ represents the rate coefficient for the reaction of the more reactive isomer with H atoms, (ie. the steepest part of the double exponential decay at low H atom flows). No reaction is observed for the less reactive isomer(s).

An alternative possible explanation for the observed curvature in the plot of $Ln(C_3H_5^+)$ versus H atom flux is that the $C_3H_6^+$ product from reaction **(420)** is back reacting with H_2 and / or H atoms, resulting in the establishment of an equilibrium between $C_3H_5^+$ and $C_3H_6^+$.

Additional research is required to establish the precise reason for the curvature, however the core findings that $C_3H_5^+$ associates with H atoms to form $C_3H_6^+$ with a rate coefficient of $(1.6 \pm 0.5) \times 10^{-10}$ cm^3 s^{-1} are correct. An experimental study of the three $C_3H_5^+$ isomers is needed; also it would be useful to characterise the reactivity of $C_3H_6^+$ with both H_2 and H.

(xiii). $C_3H_7^+ + H_2$ / H. This ion was produced by electron impact on either 1-bromopropane or 2-bromopropane, C_3H_7Br and $CH_3CHBrCH_3$, respectively. The behaviour of the $C_3H_7^+$ ions arising from either precursor was, (within experimental error), equivalent when reacted with H_2 and H.

No reaction is evident between $C_3H_7^+$ and molecular hydrogen. This outcome is consistent with the absence of a bimolecular exothermic channel. Both $C_3H_7^+$ species do however react slowly with H atoms via an H atom transfer process in which spin is conserved, viz:

$$C_3H_7^+(^1A) + H(^2S) \Rightarrow C_3H_6^+(^2A) + H_2(^1\Sigma_g^+) + 1.5\ eV^e \quad \textbf{(421)}$$

$$k_{(421)\ 300K} = (3.2 \pm 1.0) \times 10^{-11}\ cm^3\ s^{-1}$$

The observation that the H atom transfer reaction seems to be independent of ion structure is an intriguing result. If the $C_3H_7^+$ ions generated from 1- and

---

[e] Thermochemistry based on the n-$C_3H_7^+$ and $CH_3CH{=}CH_2^+$cations. The exoergicity based on the iso-$C_3H_7^+$ and $CH_3CH{=}CH_2^+$ cations is 0.6 eV. [31]

2-bromopropane retain the structural integrity of their precursor, then the slow rate coefficient measured for the reaction of each ion with atomic hydrogen may indicate a comparable kinetic barrier. Alternatively, the $C_3H_7^+$ ions derived from the two precursors may have the same structure. Energies and geometries of the $C_3H_6^+$, $C_3H_7^+$ and $C_3H_8^+$ ions have been characterised using quantum chemistry ab-initio methods. [261-263] An investigation of the [$C_3H_7^+$ ..... H] transition state(s) has not been reported; such a study would be helpful in elucidating the mechanistic details of reaction **(421)**.

(xiv). C_4H^+, $C_4H_2^+$, $C_4H_3^+$ + H_2 / H. All three ions were generated by processes following electron impact on C_2H_2 in a high pressure ion source.

$C_4H_2^+$ and $C_4H_3^+$ are the product ions formed via the fast secondary reaction of $C_2H_2^+$ on C_2H_2; similarly C_4H^+ is the product ion of the fast reaction between C_2^+ and C_2H_2.

The present study confirms that $\mathbf{C_4H^+}$ undergoes an H atom abstraction reaction with H_2 at approximately 10 % of the collision rate, ie.

$$C_4H^+ + H_2 \Rightarrow C_4H_2^+ + H + 1.4\ eV^f \qquad \textbf{(422)}$$

$$k_{(422)\ 300K} = (1.8 \pm 0.3) \times 10^{-10}\ cm^3\ s^{-1}$$

This value for $k_{(422)}$ is in excellent agreement with the evaluated value for this rate constant as tabulated by Anicich. [24] The C_4H^+ ion also exhibits a rather efficient association reaction with H atoms, viz:

$$C_4H^+(^3A'') + H(^2S) \Rightarrow C_4H_2^+(^2\Pi_g) + 6.0\ eV^f \qquad \textbf{(423)}$$

$$k_{(423)\ 300K} \sim (5.8 \pm 2.9) \times 10^{-10}\ cm^3\ s^{-1}$$

Note that reaction **(423)** conserves spin, and the observed rate coefficient is marginally less than 2/6 k_L, which is the statistical weight of the spin allowed doublet reaction pathway. The value reported here for $k_{(423)}$ is for the pseudo-bimolecular reaction between C_4H^+ and atomic hydrogen at a bath gas pressure of 0.3 Torr. The corresponding termolecular rate constant for the three-body process is estimated as $k_3 > \sim 6 \times 10^{-26}\ cm^6\ s^{-1}$.

Note that C_4H^+ produces the same product ion with H_2, (H atom abstraction), as with H, (association). It is therefore impossible to differentiate between the simultaneous reactions of C_4H^+ with atomic and molecular

---

[f] Thermochemistry based on the theoretical ΔH_f^o (C_4H^+) = 1779 kJ mol^{-1}as estimated by Reference 252.

hydrogen, (which are both present with the microwave discharge on), on the basis of product ions. To separate the C_4H^+ loss via H_2 from the H atom loss, the observed aggregate decay was computer-modelled using the rate coefficient for reaction **(422)**, (determined with the microwave discharge off), as input. This set of circumstances and method of analysis engenders a higher uncertainty, (± 50 %), in the rate coefficient for reaction **(423)**.

The observation of reaction **(422)** allows an estimation of the standard heat of formation for C_4H^+ as ΔH_f^o $(C_4H^+) \geq 1640$ kJ mol^{-1}. This value is in reasonable agreement with the best theoretical calculation for the heat of formation of C_4H^+, ie. ΔH_f^o $(C_4H^+) = 1779$ kJ mol^{-1}.[252]

$C_4H_2^+$ and **$C_4H_3^+$** are unreactive with H_2, ($k < 4 \times 10^{-12}$ cm^3 s^{-1}, and $k < 2 \times 10^{-12}$ cm^3 s^{-1} respectively), but in both cases associate with H atoms, viz:

$C_4H_2^+(^2\Pi_g) + H(^2S) \Rightarrow C_4H_3^+(^1A_1) + 4.4$ eV **(424)**

$k_{(424)\ 300K} = (2.6 \pm 0.8) \times 10^{-10}$ cm^3 s^{-1}

and;

$C_4H_3^+(^1A_1) + H(^2S) \Rightarrow C_4H_4^+(^2B_2) + 2.1$ eV[g] **(425)**

$k_{(425)\ 300K} = (5.0 \pm 2.5) \times 10^{-11}$ cm^3 s^{-1}

Again $k_{(424)}$ and $k_{(425)}$ are pseudo-bimolecular rate coefficients for a flow tube pressure of 0.3 Torr. The corresponding termolecular rate coefficients for the three-body association processes are $k_3 \geq 2.7 \times 10^{-26}$ cm^6 s^{-1} ($C_4H_2^+ + H + He$) and $k_3 \geq 5.1 \times 10^{-27}$ cm^6 s^{-1} ($C_4H_3^+ + H + He$).

Spin is conserved in reaction **(424)** with $k_{(424)}$ being less than 1/4 k_L, which is the statistical weight of the spin allowed singlet reaction pathway. Spin is also conserved in the reaction between $C_4H_3^+$ and H atoms, **(425)**.

Note that it is not possible to inject $C_4H_3^+$ in the complete absence of a small attendant $C_4H_2^+$ ion signal. Accordingly, the larger uncertainty in the rate coefficient for reaction **(425)** is due to a small contribution to the $C_4H_3^+$ signal from the simultaneous reaction **(424)**.

The association rate coefficients decrease as the number of H atoms is increased in the series $C_4H_n^+$ (n = 1 - 3). This trend is possibly a consequence of the increasing shallow well depth of the $(C_4H_{n+1}^+)^*$ collision complex as n increases. A progressive decrease in well depth results in a commensurate

[g] Thermochemistry for either $C_4H_4^+$ acyclic cation ($CH_2{=}C{=}C{=}CH_2^+$ or $CH_2{=}CHC{\equiv}CH^+$).

shortening of the complex lifetime, thus permitting less time for complex stabilisation. Assuming the lowest energy structures for the acyclic ions $C_4H_n^+$ (n = 1 - 4), the well depths are [31, 252] : reaction **(423)**, (≥ 574 kJ mol^{-1}); reaction **(425)**, (~ 420 kJ mol^{-1}); and reaction **(426)**, (~ 205 kJ mol^{-1}).

(xv). $C_4H_5^+$, $C_4H_6^+$ + H_2 / H. Both ions were formed by electron impact on 1,3 butadiene, (CH_2=CHCH=CH_2), and injected into the flow tube after mass selection, together with smaller amounts of $C_4H_7^+$.

Neither $C_4H_5^+$ nor $C_4H_6^+$ undergo reaction with H_2, ($k < 3 \times 10^{-12}$ cm^3 s^{-1}, and $k < 4 \times 10^{-12}$ cm^3 s^{-1} respectively). The $C_4H_5^+$ ion is produced in the fast reaction of $C_4H_6^+$ + H, however $C_4H_5^+$ itself does not appear to react with atomic hydrogen. Accordingly, an upper limit for the reaction of $C_4H_5^+$ with H is assessed as $k < 4 \times 10^{-11}$ cm^3 s^{-1}. The rapid reaction of $C_4H_6^+$ with H atoms yields three product channels including a 20 % H atom transfer pathway, viz:

$C_4H_6^+(^2B_g)$ + $H(^2S)$ ⇒ $C_2H_3^+(^1A)$ + $C_2H_4(^1A_g)$ + 0.4 eV (~ 0.15) **(426a)**

⇒ $C_2H_5^+(^1A_1)$ + $C_2H_2(^1\Sigma_g^+)$ + 0.8 eV (~ 0.65) **(426b)**

⇒ $C_4H_5^+(^1A)$ + $H_2(^1\Sigma_g^+)$ + 1.8 eV[h] (~ 0.20) **(426c)**

$k_{(426)\ 300K}$ = $(1.9 \pm 0.6) \times 10^{-10}$ cm^3 s^{-1}

All of the above reactions conserve spin, and all have rate coefficients that are $< 1/4 k_L \times f$[Channel][i], (ie. the Langevin collision rate factored by the statistical weight of the spin allowed singlet reaction pathway, and multiplied by the appropriate fraction of each channel).

Reaction **(426)** is significantly different from all other $C_mH_n^+$ / H reactions studied thus far; the multiple dissociative reaction pathways indicate that a different reaction mechanism is in operation. Insertion of an H atom into $C_4H_6^+$ to produce the $(C_4H_7^+)$* intermediate, promotes rapid fragmentation of the collision complex before stabilisation can occur. The ~ 360 kJ mol^{-1} of available excitation energy above the $C_4H_7^+$ well is sufficient to induce dissociation at the C2 position of a C4-protonated 1,3-butadiene type ion, $CH_3CHCH{=}CH_2^+$, giving rise to the ~ 15 % $C_2H_3^+$ + C_2H_4 fragmentation channel. The mechanistic details leading to the major product channel are less obvious. Conceivably, the ~ 65 % $C_2H_5^+$ + C_2H_2 pathway might eventuate if fragmentation at the C2 site of

---

h Thermochemistry for E - CH_2=CHCH=CH_2^+ and CH_2=CCH=CH_2^+ cations.

i f[Channel]denotes the "fraction" of each product channel **(426a)** – **(426c)**.

the $CH_3CHCH{=}CH_2^+$ ion is accompanied two concerted 1-2 hydrogen atom shifts from C1 to C2 and from C2 to C3 on the $CH_3CHCH{=}CH_2^+$ ion. This particular suggestion is hardly a minimal rearrangement route. Alternatively, a cyclic 4-membered transition state may allow transfer of an H atom from C1 to C4 of C3-protonated 1-3 butadiene, ($CH_2CH_2CH{=}CH_2^+$). A further and somewhat novel suggestion arises from the observation that proton transfer from $C_2H_3^+$ to C_2H_4, [formed in channel **(426a)**], produces $C_2H_5^+ + C_2H_2$, [24] ie. the products of channel **(426b)**. The clear implication is that channel **(426b)** might arise through proton transfer between the products formed in pathway **(426a)** whilst the loosely bound species are still confined within the collision complex. As with so much of this research ab-initio calculations would be valuable in clarifying the precise nature of the reaction mechanism for channel **(426b)**.

(xvi). $C_4H_8^+$, $C_4H_9^+$ + H_2 / H. Electron impact on 2-butene was used to produce both of these ions. Neither ion reacts with H_2, ($k < 5 \times 10^{-13}$ cm^3 s^{-1} for both $C_4H_8^+$ and $C_4H_9^+$). $C_4H_9^+$ is also unreactive with atomic hydrogen, ($k < 2 \times 10^{-11}$ cm^3 s^{-1}), but $C_4H_8^+$ exhibits H atom transfer with this reagent, viz:

$C_4H_8^+(^2A) + H(^2S) \Rightarrow C_4H_7^+(^1A) + H_2(^1\Sigma_g^+) + 2.0\ eV$[j] **(427)**

$k_{(427)\ 300K} = (1.1 \pm 0.3) \times 10^{-10}$ cm^3 s^{-1}

Spin is conserved in reaction **(427)**, with $k_{(427)}$ being < 1/4 k_L, (the statistical weight of the spin allowed singlet reaction channel).

(xvii). $C_6H_4^+$, $C_6H_5^+$, $C_6H_6^+$ + H_2/ H. These $C_6H_n^+$ ions were formed either directly by electron impact on benzene, (c-$C_6H_4^+$, c-$C_6H_5^+$, c-$C_6H_6^+$) or following electron impact on acetylene in a high pressure source, (ac-$C_6H_4^+$, ac-$C_6H_5^+$). With the second method, $C_4H_2^+$ and $C_4H_3^+$ were produced from C_2H_2, as described in **(xiv)** previously, and injected into the flow tube. C_2H_2 was subsequently admitted to the flow tube at the first inlet port, forming $C_6H_4^+$ and $C_6H_5^+$ as the primary products of the reactions of $C_4H_2^+$ and $C_4H_3^+$, respectively, with acetylene. [264]

Two stable isomeric structures are known to exist for $C_6H_4^+$ and $C_6H_5^+$ when prepared from $C_2H_2^+$ in the above manner. These two species are believed to be the cyclic and acyclic isomers which may be conveniently distinguished by their different reactivities. Originally the more reactive isomer of $C_6H_5^+$ was

---

j Thermochemistry for E - 2-$C_4H_8^+$ and $CH_3CCHCH_3^+$ cations.

ascribed to acyclic $C_6H_5^+$ [265, 266] but a subsequent investigation showed that the lower energy phenylium ion is more reactive than the acylic isomer. [253] Accordingly, the $C_6H_5^+$ isomer that undergoes three-body association with molecular hydrogen, is attributed to c-$C_6H_5^+$ in accordance with the findings of Petrie and associates. [165] Likewise, the benzene derived $C_6H_4^+$ ion was observed to have a higher reactivity with C_2H_2 than did the $C_6H_4^+$ isomer generated via the reaction between $C_4H_2^+$ and C_2H_2. [265] Analogous reasoning to that employed in the assignment of the $C_6H_5^+$ isomers suggests that the more reactive benzene derived $C_6H_4^+$ species be assigned to c-$C_6H_4^+$.

Neither isomer of $C_6H_4^+$ appears to react with H_2, ($k < 5 \times 10^{-13}$ cm^3 s^{-1} for ac-$C_6H_4^+$, and $k < 3 \times 10^{-12}$ cm^3 s^{-1} for c-$C_6H_4^+$). Only the cyclic isomer, c-$C_6H_4^+$, participates in an association reaction, (almost certainly 3-body), with H atoms, in which spin is conserved, viz:

c-$C_6H_4^+(^2A_u)$ + $H(^2S)$ $\Rightarrow$ c-$C_6H_5^+(^1A_1)^k$ + 4.2 eV[l] **(428)**

$k_{(428)\ 300K}$ = $(3.3 \pm 1.0) \times 10^{-11}$ cm^3 s^{-1}

The observed rate coefficient for process **(428)** is substantially less than 1/4 k_L, which is the statistical weight of the spin allowed singlet pathway.

Acyclic $C_6H_5^+$ is unreactive with both H_2 and H atoms, ($k < 1 \times 10^{-12}$ cm^3 s^{-1}, and $k < 5 \times 10^{-12}$ cm^3 s^{-1} respectively). Cyclic-$C_6H_5^+$ does not react with H atoms, ($k < 1 \times 10^{-11}$ cm^3 s^{-1}), but a reaction with H_2 is apparent, ie.

c-$C_6H_5^+$ + H_2 $\Rightarrow$ c-$C_6H_7^+$ + 2.8 eV[m] **(429)**

$k_{(429)\ 300K}$ = $(3.8 \pm 0.6) \times 10^{-11}$ cm^3 s^{-1}

The rate coefficient for reaction **(429)** obtained from the present research agrees favourably with the result reported by Petrie. [165] Once more the reaction between c-$C_6H_5^+$ and H_2 is surely a three-body process, resulting from the collisional stabilisation of the (c-$C_6H_7^+$)* collision complex by the helium bath gas. The rate coefficient detailed above is for the pseudo-bimolecular reaction at a flow tube pressure of 0.3 Torr. The termolecular rate coefficient for the analogous three-body association reaction is estimated as $k_3 > 3.9 \times 10^{-27}$ cm^6 s^{-1}.

Cyclic-$C_6H_6^+$ does not react with H_2, ($k < 5 \times 10^{-12}$ cm^3 s^{-1}), but undergoes a

---

k The $^3B_1$ first excited electronic state of c-$C_6H_5^+$ is only ~ 20 kJ mol^{-1} higher in energy than the $^1A_1$ ground state of c-$C_6H_5^+$. [267] Conceivably, reaction **(428)** is sufficiently exothermic to access the first electronic excited state of c-$C_6H_5^+$.

l Thermochemistry for benzyne and phenyl radical cations.

m Thermochemistry for phenyl radical and protonated benzene cations.

relatively fast two-channel reaction with H atoms. The major product channel is association but a significant amount of H atom transfer is also noted, viz:

$$c\text{-}C_6H_6^+(^2E_{1g}) + H(^2S) \Rightarrow c\text{-}C_6H_5^+(^1A_1)^k + H_2(^1\Sigma_g^+) + 0.7\ eV^n\ (0.35)\ \textbf{(430a)}$$

$$\Rightarrow c\text{-}C_6H_7^+(^1A_1) + 3.5\ eV^o\ (0.65)\ \textbf{(430b)}$$

$$k_{(430)\ 300K} = (2.1 \pm 0.6) \times 10^{-10}\ cm^3\ s^{-1}$$

Note that spin is conserved in both of the above reaction pathways, **(430a)** and **(430b)**, with the observed rate coefficients for these channels being $< 1/4\ k_L$ .0.35, and $< 1/4\ k_L$. 0.65, respectively, [these values correspond to the statistical weight of the spin allowed singlet reaction pathway multiplied by the fraction of each channel].

This data is in good accord with the results of Petrie and associates, with the exception that they did not report the 35 % H atom transfer channel. [165] Petrie et al. contended that the efficiency of association of H_2 with the $c\text{-}C_6H_5^+$ ion stems from H_2 bond insertion into the vacant sp^2 orbital on the ipso carbon of the phenylium ion. [165] In the $c\text{-}C_6H_6^+$ ion this orbital is occupied and there is no observable association of $c\text{-}C_6H_6^+$ with molecular hydrogen. They also suggested that the non-reaction between $c\text{-}C_6H_5^+$ and atomic hydrogen, and in particular the absence of association between these two species, might be explained by the formation of an excited electronic state of $(c\text{-}C_6H_6^+)^*$. This excited state reduces the well depth of the $(c\text{-}C_6H_6^+)^*$ collision complex to ≤ 130 kJ mol^{-1}, thus reducing the complex lifetime. [165] It is interesting to observe that both $c\text{-}C_6H_4^+$ and $c\text{-}C_6H_6^+$ demonstrate the same reactivity: neither react with H_2, yet both associate with H atoms. The potential surface of $C_6H_4^+$ is not well characterised and a more comprehensive comparison must await the completion of this task.

4.5: Implications of this Study to Extraterrestrial Chemistry.

The two neutral reactants of this work, namely molecular and atomic hydrogen, are extremely abundant species in the universe. Much of the chemistry summarised in Tables 4.1 through 4.4, and discussed in Section 4.4 above, is of relevance to extraterrestrial chemistry.

---

n Thermochemistry for benzene and phenyl radical cations.

o Thermochemistry for benzene and protonated benzene cations.

Implications of the Reactions of Non-Hydrocarbon Cations with H_2 and H Atoms to Extraterrestrial Chemistry

The reactions of CO^+ and CO_2^+ with molecular hydrogen have been characterised in many earlier studies. Both CHO^+ isomeric product ions formed in the reaction of $CO^+ + H_2$, viz HOC^+ and HCO^+, have been unequivocally identified in the interstellar medium, with HOC^+ being confirmed as recently as 1995. [268] It is of peripheral interest to note that the isoformyl cation, HOC^+, reacts rapidly with H_2 at room temperature [269] and hence the interstellar observation of this species was not immediately explicable. In 1996, Herbst and Woon resolved this dilemma using theoretical arguments that suggested the rate coefficient for the $HOC^+ + H_2$ reaction reduces to $< 1 \times 10^{-10}$ cm^3 s^{-1} at temperatures below 100 K. [270]

Of the remaining reactant ions in Table 4.1, CN^+ and $C_2N_2^+$ have rapid reactions with H_2 and thus these species should have low fractional abundances in dense interstellar clouds. Conversely, NO_2^+, SO_2^+ and CS_2^+ may reach appreciable number densities because of their unreactivity with H_2.

The non-hydrocarbon ion-H atom reactions detailed in Table 4.2 are especially pertinent to the chemistry of those regions of the interstellar medium where the fractional abundance of atomic hydrogen is high. Both CO^+ and CO_2^+ react rapidly with atomic hydrogen so these species will be somewhat depleted in the so-called "H I" regions of the interstellar medium. Despite the confirmed presence of SO_2, SO, and SO^+, the SO_2^+ ion has not yet been detected in interstellar clouds, [17] possibly because of its (albeit slow) reactivity with H_2. [24] Notably, the fast reaction between SO_2^+ and H produces SO^+ and a hydroxide radical, both of which have been observed in the interstellar medium. [17] A sequence of molecules and ions containing a C-S bond have been observed in interstellar clouds, (eg. CS, HCS^+, OCS, H_2CS and C_3S). [17] The presence of CS_2 is also quite likely but this molecule has not been detected in the interstellar medium [17] due to the absence of a permanent dipole moment. The efficient reaction between CS_2^+ and H yields HCS^+ as the product ion which is an observed interstellar ion. [17] The detection of HCS^+ in the interstellar medium is consistent with the fact that this species does not react with H_2. [24] The reactions of CN^+ and $C_2N_2^+$ with H atoms are relevant to the ion chemistry of Titan's nitrogenous atmosphere [271] in addition to the chemistry of interstellar clouds.

Implications of the Reactions of Hydrocarbon Cations with H_2 and H Atoms to Extraterrestrial Chemistry

Ion-neutral reactions involving hydrocarbon cations are the backbone for the syntheses of many interstellar organic molecules. A substantial number of hydrocarbon species are not detectable in the interstellar medium, (due primarily to their lack of a permanent dipole moment), and evaluation of their abundances relies solely on ion chemical models.

The new data obtained in this study extends the trend evident in existing data compilations which indicates that only cations with a very low degree of hydrogenation react with H_2 via H atom abstraction processes, forming $C_mH_{n+1}^+ + H$, (eg. $C_4H^+ + H_2 \Rightarrow C_4H_2^+ + H$). More saturated hydrocarbon cations tend to be unreactive with molecular hydrogen, hence a level of hydrogenation is quickly reached whereby no further addition of H_2 is possible. This inertness of highly saturated hydrocarbon cations in the presence of H_2 creates many "bottlenecks" in the hydrocarbon chemistry network.

In small areas of the interstellar medium where significant concentrations of atomic hydrogen exist, (ie. the so-called "H I" regions), hydrocarbon cation-H atom reactions can circumvent the "choke points" in the hydrocarbon synthetic network. Note that if the reaction of a given hydrocarbon cation with H_2 is fast then reaction with H atoms cannot compete, except perhaps in localised H I regions of diffuse clouds. Only in these discrete areas may the number density of H atoms approach that of H_2.

Sufficient systems have now been investigated (in this study and others) to generalise that $C_mH_n^+$ reactions with atomic hydrogen proceed by two major channels, namely association, (to give $C_mH_{n+1}^+$), and / or H atom transfer, (producing $C_mH_{n-1}^+ + H_2$), if exothermic. Both of these pathways are common, eg. association is apparent in the reaction of $C_4H_2^+ + H$ to form $C_4H_3^+$, and H atom transfer from the $C_mH_n^+$ species is seen in the reaction of $C_3H_4^+ + H_2$ to form $C_3H_3^+ + H_2$. Furthermore, H atom association reactions appear to proceed for sequences of unsaturated hydrocarbon cations, eg. the $C_4H_n^+$ cations, (where n = 1 - 3), associate with H atoms. Hydrocarbon cations that have reached their level of saturation in the presence of molecular hydrogen may proceed to a higher degree of saturation in the presence of atomic hydrogen. Hence in this

manner the termination steps for hydrocarbon cations with molecular hydrogen may be bypassed. As noted above, this has great significance for interstellar chemistry as many interstellar clouds are somewhat clumpy, with the H atom to H_2 ratio being quite variable throughout these objects. Taking this discussion a step further, observations of the number densities of a series of hydrocarbon species with varying degrees of saturation could conceivably act as a coarse monitor of the H_2 to H atom ratio in any given region of space. Indeed the CH radical has already been employed as a monitor for H_2. [272]

An additional point concerning the inertness of several hydrocarbon cations is worth stating. Of the hydrocarbon cations examined in this study, the cations $C_3H_3^+$, $C_4H_5^+$, $C_4H_9^+$, ac-$C_6H_4^+$ and ac-$C_6H_5^+$ seem to be species of particular stability in that they are unreactive with both H_2 and H atoms. This finding suggests that at least some of these species may be amongst the "terminal" ions present in interstellar clouds.

4.6: Concluding Remarks.

Remarkably, all the ion-H atom processes measured in this study have rate coefficients significantly less than the Langevin capture rate. In a number of reactions the smaller rate coefficients observed are a consequence of the spin statistics. The same may be true of other reactions, (eg. $SO_2^+ + H$), but the potential surfaces of such reactions need to be better defined before any explicit conclusions can be made.

The reaction of seven non-hydrocarbon cations with H_2 and H atoms was examined during this experimental study. Most of these cations react with H_2 at a large fraction of the Langevin collision rate; the product in all cases is the hydrogenated primary, (reactant), ion. Data for only two of the cation-H atom reactions tabulated in Table 4.2 has been reported previously. [24] These processes proceed via atom exchange, (with attendant fragmentation in several cases eg. $C_2N_2^+ + H$ and $SO_2^+ + H$), and charge transfer when allowed by the thermochemistry, (eg. $CO^+ + H$ and $CN^+ + H$). In the relatively small number of systems examined, charge transfer is only observed for those reactions in which it is the sole thermodynamically accessible channel. None of the non-

hydrocarbon cation-H atom reactions investigated proceeded at rates in excess of $k_L/3$ and several appeared to be affected by the spin states of the product species.

Sufficient reactions of $C_mH_n^+$ with H_2 and H atoms have now been investigated in the laboratory for some interesting trends to emerge. A comparison of the present results with those already reported [24, 237, 247] indicates that highly unsaturated cations ($C_mH_n^+$, m = 1 - 4, n = 0 - 1) participate primarily in H atom abstraction reactions with molecular hydrogen. As m approaches 4, the rate coefficient reduces to $\leq$ 10 % of the Langevin capture rate. More saturated hydrocarbon cations ($n \geq 2$) are unreactive with H_2, which is chiefly a consequence of the absence of exoergic channels available for H atom abstraction. The only alternative reaction pathway to H atom abstraction, is association - when H_2 inserts into the hydrocarbon cation. These association reactions are rare however, as Tables 4.1 and 4.3 show, occurring only for c-$C_6H_5^+$. The chemical literature reveals that association also occurs between C_3H^+ and H_2, [273, 274] but this system was not re-examined as part of the present study.

Association of a hydrocarbon cation with *molecular hydrogen* usually generates a product ion that is more stable by at least 100 kJ mol^{-1}. Why then is association not observed for a greater number of $C_mH_n^+$ cations? In 1993 Maluendes and associates published the results of a detailed ab-initio theoretical study of the association reaction between C_3H^+ and H_2. [260] The conclusion of that research was that the $C_3H^+ + H_2$ association process proceeds because the collision complex can access the deep potential well of ac-$HCCCH_2^+$. [260] For an adduct ion to be observed in a flow tube experiment, collisions with bath gas molecules must act to stabilise the association complex before it dissociates. The transitory lifetime of the complex is extended by access to deep wells on the potential surface thereby allowing collisional stabilisation to occur. In the flow tube the mean time between collisions is typically ~ 70 ns. It is apparent then that for most ions, the ($C_mH_n^+$ ---- H_2)* complex does not persist long enough for stabilisation to take place. When association does proceed, (eg. $C_3H^+ + H_2$, c-$C_6H_5^+ + H_2$), the products are new covalently bound $C_mH_{n+2}^+$ cations.

$C_mH_n^+$ cations exhibit somewhat different reactivity with *atomic hydrogen* than is observed in the corresponding intermittent H atom abstraction or

condensation reactions of these hydrocarbon cations with H_2. Two types of $C_mH_n^+ + H$ reactions are prevalent, namely H atom transfer and association. When an exothermic channel is available for H atom transfer, it usually proceeds. The outcome of H atom transfer is a reduction in hydrogenation of the ion, whereas H atom abstraction, which occurs in several $C_mH_n^+ + H_2$ systems, results in an increase in hydrogenation. Highly unsaturated ions, such as C_2^+ and C_2H^+, do not react with H atoms but larger unsaturated ions, such as C_4H^+ and $C_4H_2^+$, that are intermediate in size, participate in association reactions. The higher number of atoms in larger ions enlarges the number of modes amongst which the energy of the collision complex can be dissipated. This greater complex stability is manifested as an enhanced predilection for $C_mH_n^+$ cations to associate with H atoms, as compared with H_2. It seems that reactive encounters between $C_mH_n^+$ cations and H atoms form collision complexes that can access the region of the $(C_mH_{n+1}^+)^*$ potential surface above the deepest wells. The mechanistic details of such processes may involve hydrogen atoms tunnelling through barriers.

The structures of the $C_mH_n^+$ cations used in this research were not always identified from experiment. In several instances it was loosely assumed that the configuration of the ion generated via electron impact on the neutral precursor, was the isomer most closely resembling the precursor structure. In practice, this "minimal rearrangement" assumption is occasionally violated. As noted in Section 4.4 above, sometimes cyclic ions can be formed from acyclic precursors, (eg. c-$C_3H_3^+$ from C_2H_4), and acyclic ions from cyclic precursors, (eg. ac-$C_6H_5^+$ from benzene). There has been some debate about the structures of many of these cations and distonic configurations of some $C_mH_n^+$ cations, producing radical cations, have been proposed for several radical hydrocarbon cations. [275, 276]

Many of the reactions detailed above between various cations and atomic and molecular hydrogen are relevant to extraterrestrial chemistry. The data presented in this study, when incorporated into standard models, may result in significant changes to the number densities of many observed interstellar species. This particular endeavour is being pursued at the time of preparation of this manuscript and assuredly the results will be of interest to all workers in the field.

CHAPTER 5.

REACTIONS OF SOME CATIONS WITH ATOMIC AND MOLECULAR NITROGEN.

5.1: Introduction.

Much of the data required to model interstellar ion chemistry have been provided by laboratory investigations. Interstellar cloud ion-chemical models are based upon a complex network of interdependent reactions. [13, 16] Whilst all contemporary models include ion-atom processes in their reaction networks, relatively few data are available on these types of reactions. [24, 50, 135] Several laboratory studies of ion-atom reactions have demonstrated that such processes may often be quite rapid. [177, 178] This observation further reinforces the significance of this class of reaction, and the consequential need for the inclusion of ion-atom processes in interstellar ion-chemical models.

Ion-atom reactions may be particularly important in the diffuse interstellar clouds where the atom-to-molecule ratio is comparatively high. [177] Diffuse interstellar clouds harbour a number of reactive atomic species, with hydrogen, nitrogen, oxygen and carbon atoms being present in the highest abundances. [277] In 1980, Viggiano and colleagues suggested that the reaction of atoms with chain-initiating cations, such as CH^+, could be competitive with the reaction of such cations with H_2. [177] In the case of dense clouds, Iglesias has speculated that regions juxtaposed to the numerous embedded luminous infra-red sources, (stellar or protostellar), might contain significant concentrations of reactive atomic species. [278] Viggiano et al. subsequently suggested that these atoms could possibly react with chain terminating hydrocarbon cations, such as CH_5^+, which are somewhat unreactive towards molecular hydrogen. [177] Finally, these workers noted that more complex ions might also react with atomic species at

rates which could conceivably rival radiative association processes between H_2 and larger polyatomic ionic species. The authors added the caveat that the viability and importance of such large polyatomic ion-atom reactions would depend on the rapidity of these processes and the number densities of the atomic species concerned. [177]

This chapter focuses upon the reaction of various cations with atomic nitrogen. Lee et al., in their new standard model, tabulate the number density of atomic nitrogen in dense clouds as 1.9×10^{-5} atoms cm^{-3} at 10 K, and 6.6×10^{-6} atoms cm^{-3} at 50 K, relative to H_2 (= 1.0). [16] Atomic nitrogen is thus relatively plentiful in interstellar molecular clouds and therefore is likely to be implicated in much of the chemistry occurring in these objects.

In particular, reactions between cations and N atoms may be relevant to the synthesis of nitriles in interstellar molecular clouds of which several have been detected to date, eg. HCN, $H_2C{=}CHCN$, and $H(C{\equiv}C)_nCN$, where n = 1 - 5. [13, 17] Many other interstellar molecules also contain nitrogen atoms, eg. NO, NH_2CHO and HNCO, and atomic nitrogen may participate in the synthetic pathways to some of these species. It is of considerable interest to determine whether C-N bonds are formed via the reaction of hydrocarbon cations with atomic nitrogen. Additionally, atomic nitrogen is a constituent of the earth's upper atmosphere and the chemistry of this region is strongly influenced by ion-N atom processes. [182] Reactions between charged species and atomic nitrogen are also pertinent to the chemistry occurring in the upper ionised regions of nitrogenous extraterrestrial atmospheres of which only one has been identified thus far: Titan, the largest "moon" of Saturn. On a slightly more controversial and speculative note it may be that atomic nitrogen is also implicated in the formation of amino acids that some commentators believe exist in the interstellar medium but, aside from the tentative observation of glycine, [406] have yet to be confirmed.

Over the preceding thirty or so years, several research groups have obtained experimental data pertaining to the reactions between various ions and atomic nitrogen. [177-180, 182] In the main these studies have utilised flow tube techniques, in particular the flowing afterglow and SIFT. [135] The atomic nitrogen used in these studies has invariably been generated by subjecting molecular nitrogen to a microwave discharge. The amount of dissociation obtained is small, ranging from 0.5 % up to 3 - 4 %, depending upon the precise specifications of the

equipment used to generate the discharge, the geometry and design of the neutral inlet probe, and its distance from the reaction zone of the flow tube. [135] Most research groups have used the $N + NO \Rightarrow N_2 + O$ "titration reaction" to quantitatively measure the N atom flow rate. [135]

In the early years of experimentation with N atoms there was concern over the possible presence of excited neutral species in the reaction zone of the flow tube, in particular N_2 ($v > 0$) and metastable N atoms (^2D and ^2P). [135] To overcome this problem Goldan and co-workers inserted a glass wool plug into the neutral probe, immediately downstream of the microwave discharge, which removed excited neutral species, in particular N_2 ($v > 0$). [180] In addition, it was soon realised that most vibrationally excited N_2 molecules are relaxed quickly by collisions with other molecules or glass surfaces. [179] The $A\ ^3\Sigma_u^+$ long-lived state of N_2 has been detected in the microwave discharge region but fortunately this state is efficiently quenched by ground state N ^4S atoms, ($k = 3.1 \times 10^{-11}$ $cm^3\ s^{-1}$). [279] Presumably for this reason, ($A\ ^3\Sigma_u^+$) N_2 is not observed downstream of the microwave discharge. [279] A body of experimental evidence suggests that the low-lying metastable excited N atoms that may be produced in the microwave discharge do not find their way into the reaction zone of the flow tube to "contaminate" the results. [177] This evidence indicates that only about 1 % of all N atoms are expected to be metastable [280] and, furthermore, both metastable species, (N ^2D and N ^2P), are efficiently relaxed by collisions with glass surfaces. [281] Experimental apparatuses that employ a glass wool plug immediately downstream of the microwave discharge will therefore deplete the metastable atom densities to trace values.

There remains an obvious need for the gathering of reliable experimental data on previously unstudied ion-atom reactions of astrophysical import. Additionally, it is desirable to corroborate the data that has already been reported by many skilled workers who have performed experiments in this field. The present work makes a contribution in this regard by reporting the study of several "new" reactions between various cations and atomic nitrogen. Furthermore, a number of reactions for which data exists in the chemical literature have been re-examined, primarily to establish the veracity of the experimental techniques and data analysis methods employed in the present study.

Data for the reaction of a number of cations with molecular nitrogen is also presented here as it was necessary to establish the reactivity of a given ion with N_2, (if any), in order to differentiate this process from the simultaneous reaction with N atoms. These ion-N_2 reactions are relevant to the chemistry of extraterrestrial atmospheres with a high nitrogen content, eg. Titan's atmosphere. [282, 283]

5.2: Experimental.

For almost every experiment surveyed in the present study the nitrogen atoms were generated in a microwave discharge of pure (100 %) nitrogen. A small subset of data, pertaining only to the measurement of the reaction between H_3^+ and atomic nitrogen, was obtained using 4.98 %, ~ 10 % and ~ 50 % mixtures of N_2 in He. The 4.98 % N_2 / He mixture was a prepared mixture procured from Alphagaz. All other mixtures were prepared using the procedure described in Chapter 4, Section 4.2, of this thesis.

Three different nitrogen atom probes were used at different times to conduct all of the experiments described in this section of work.

Primary N Atom Probe

A probe of virtually identical design to the hydrogen atom probe, which was discussed at length in the preceding chapter, was used to obtain the majority of the data tabulated in Section 5.3. This "primary" N atom probe differed from the H atom probe only to the extent that a small glass wool plug was inserted into the interior of the probe, downstream of the microwave discharge, and immediately above the elbow of the probe. The glass wool plug rested, under the influence of gravity, on four tiny internal Pyrex ledges, or "dimples". The dimples protruded into the interior of the Pyrex tubing by ~ 1.5 mm, thereby constricting the internal diameter (i.d.) of the probe down to about 7 mm over a minimal ~ 2 mm of probe length. In all other respects this nitrogen atom probe, (including dimensions), was a facsimile of the hydrogen atom probe. A labelled photograph of the hydrogen atom probe is depicted in Figure 4.1.

Secondary N Atom Probe

This primary probe was later modified by shortening the length from the elbow to the flow tube axis from ~ 17.3 cm to ~ 10.5 cm. This length reduction

was undertaken to minimise the length of Pyrex tubing available for surface atom-atom recombination, and accordingly maximise the number density of N atoms entering the reaction zone of the flow tube. Particularly for the measurement of the $H_3^+ + N$ reaction it was critical to ensure that the N atom flux was as high as practicable. Figure 2.5 in Chapter 2 of this thesis shows a photograph of this "secondary", or shortened probe in operation.

Determination of Relative Rate Coefficients

These two probes were used to obtain "relative" rate coefficients for the reactions between various cations and N atoms. The procedure that was adopted was to firstly determine that the cation of interest, A^+, was unreactive with molecular nitrogen, ie. microwave discharge off. In the overwhelming majority of cases this was true. The microwave discharge was then "initiated" and the "raw" rate coefficient measured for the reaction between A^+ and the neutral mixture of N_2 and N atoms. The product distribution for the reaction was also determined at this stage. The "raw" value of the rate coefficient is the observed value, uncorrected for the true or "absolute" value of the N atom flux. As soon as practicable afterwards, (almost always on the same day), the raw rate coefficient for the selected reference reaction between $C_2H_2^+$ and N was measured. This particular reaction was selected as a calibration reaction because it is one of the few processes involving atomic nitrogen that has been studied in two different research laboratories. [177, 178] Furthermore, both research groups reported the same rate coefficient for this reaction, namely 2.5 x 10^{-10} cm^3 s^{-1}. [177, 178] A preliminary value for the "absolute" rate coefficient for any given cation-N atom reaction was thus obtained by applying the following relation:

$$Absolute\ k\{A^+\} \approx \frac{Raw\ k\{A^+\}}{Raw\ k\{C_2H_2^+\}}\ .\ 2.5\ x\ 10^{-10}\ cm^3 s^{-1} \qquad \textbf{(501)}$$

In expression **(501)** *Raw* $k\{A^+\}$ and *Raw* $k\{C_2H_2^+\}$ are the measured raw rate coefficients for the reaction of N atoms with A^+, and $C_2H_2^+$ respectively; *Absolute* $k\{A^+\}$ is the preliminary value of the absolute rate coefficient for the cation-N atom reaction being studied; and 2.5 x 10^{-10} cm^3 s^{-1} is the literature value of the rate constant for the $C_2H_2^+ + N$ reaction. [177, 178]

Tertiary N Atom Probe

Finally, a third probe was designed and constructed to perform a measurement of the absolute rate constant for the reference reaction between $C_2H_2^+ + N$. A photograph of this "tertiary" probe is shown in Figure 5.1.

The upstream section of the tertiary probe, (above the elbow), was of similar design to both the primary and secondary N atom probes described above. A set of four dimples, located ~ 14 mm above the elbow of the probe, created a minor constriction, (or concentric ledge). This constriction allowed the placement of a small plug of glass wool immediately downstream of the microwave discharge region. The microwave discharge was typically located ~ 77 mm upstream of the probe's elbow.

Immediately downstream of the elbow, a secondary reactant inlet allowed nitric oxide to be admitted into the neutral flow stream. This NO inlet had several dispersed minute holes, (< ~ 1 mm in diameter), faced upstream into the N_2 / N atom flow, and was connected to the flowmeter assembly via standard 8 mm o.d., 5 mm i.d. Pyrex tubing.

Downstream of the NO inlet the probe coiled into a compact helical section consisting of three loops. These coils were constructed from 13 mm o.d., 10 mm i.d. Pyrex tubing. At the downstream terminus of the helical section, the probe broadened into a substantially thicker section of Pyrex tubing, (75 mm o.d., 71 mm i.d.), which was designed to be a neutral reactant mixing volume. This larger diameter section of Pyrex tubing was approximately 105 mm in length. These dimensions were chosen following a calculation of the approximate reaction volume needed to ensure that the NO + N, neutral-neutral reaction would be essentially complete prior to the NO and N atom reagents reaching the outlet into the main flow tube. [85] This calculation assumed the "worst case" situation for the physical parameters present inside the N atom probe, ie. maximum N_2 flow rate (~ 2 Torr L s^{-1}), and minimum pressure, (~ 0.35 Torr). The cumulative effect of the "backwards" facing NO inlet, the spiral section of Pyrex tubing, and the wider reactant mixing volume ensured that considerable surplus volume, and hence time, was available for the N + NO titration reaction to proceed to completion in the side arm, before the reagents entered the flow tube proper.

At the end of the 105 mm long, larger diameter reactant mixing volume, the probe again constricted down to 13 mm o.d., 10 mm i.d. Pyrex tubing which passed through a stainless steel flange before terminating on the axis of the flow tube.

Preparation of the N atom Probes

The microwave discharge was established near the bottom section of an ~ 22 cm quartz discharge section which was common to all N atom probes. A small piece of glass wool, which had been soaked in phosphoric acid, was inserted into all of the N atom probes immediately downstream of the microwave discharge region and prior to the probe's elbow. This measure was taken to remove excited metastable neutral species, [eg. N_2 ($v > 0$), N ^{2}D, and N ^{2}P], from the neutral flow. [179] The exterior of the ~ 7 cm section of the 13 mm o.d., 10 mm i.d. Pyrex tube that protruded into the flow tube, and hence was exposed to the ion swarm, was sheathed in stainless steel. Furthermore, the interior surfaces of all three N atom probes, downstream of the discharge region, were coated with a halocarbon wax / chloroform mixture in order to reduce atom / atom surface recombination. A light horn trapped out most of the photon flux produced in the discharge, thereby reducing the number of photons reaching the reaction zone of the flow tube. [177]

Methodology for the Determination of Absolute Rate Coefficients

A large body of relative rate coefficient data was collected during this study, all of which could only be converted to absolute values provided total confidence was established in the precision of the literature rate coefficient value for the calibration reaction, $C_2H_2^+$ + N atoms. [177, 178] Notwithstanding the obvious expertise of the researchers who had performed the two previous measurements, it was deemed necessary to conduct a local independent experiment to verify the published value of this rate coefficient. A "NO titration" was performed to obtain this measurement. This procedure is well established, having been comprehensively described by various authors including Goldan et al. [179] and Viggiano et al., [177] and is summarised below.

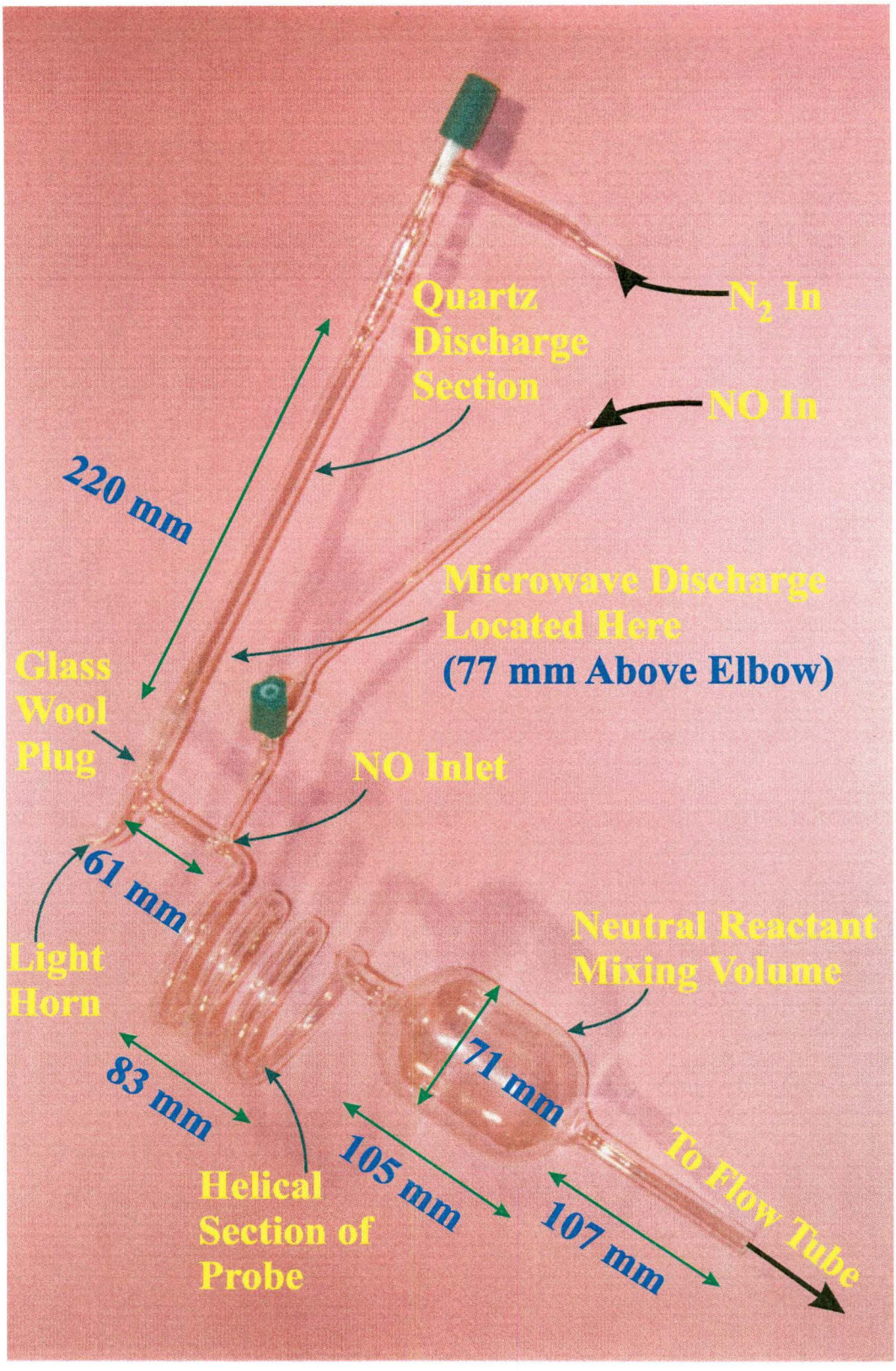

Figure 5.1. Labelled photograph of the "tertiary" N atom probe.

The Generic NO Titration Procedure

Essentially the NO titration method relies upon the reaction between atomic nitrogen and nitric oxide, viz: [85]

$$N + NO \Rightarrow N_2 + O \qquad \textbf{(502)}$$

$k_{(502)\,298K} = (3.4 \pm 1.0) \times 10^{-11}\ cm^3\ s^{-1}$

In practice, NO is added to the neutral stream of N_2 / N atoms and the signal of some monitor ion species recorded at a series of measured NO flow rates. The stoichiometry of equation **(502)** indicates that for a given initial flux of N atoms, as the NO flow rate is progressively increased, the flux of atomic nitrogen will systematically reduce until at the endpoint it is zero. Note that for every nitrogen atom consumed, an oxygen atom is formed. Precisely at the endpoint there is zero flow of N atoms, a maximum flow of O atoms and zero flow of nitric oxide. As the endpoint is exceeded, the flow of NO starts to increase whilst the fluxes of N atoms and O atoms remain constant at their endpoint values, (zero flow and a maximum flow rate respectively). If the log of the ion signal is plotted against NO flow rate the endpoint of the titration is often readily visible as an intersection of two lines. The above reasoning is contingent upon sufficient reaction distance being available for the complete reaction of the atomic nitrogen and NO reagents before the neutral flow mixture is admitted into the flow tube proper. The paper by Viggiano and colleagues [505] depicts three excellent graphical examples, (for the reactant ions CH_5^+, H_2O^+, and CH^+), obtained using this NO titration procedure.

Determination of the Absolute Rate Coefficient for the $C_2H_2^+$ + N Reaction

A specific strategy was developed for the task of determining the absolute rate coefficient for the reference $C_2H_2^+$ + N reaction. The initial step was to measure a series of raw rate coefficients for the reaction of $C_2H_2^+$ + N, ie. plots of $Ln[C_2H_2^+]$ versus N_2 flow out of a calibrated volume.

Immediately thereafter, ground state O_2^+ cations were generated by injecting Ar^+ ions into the flow tube and adding molecular oxygen at the first neutral inlet. [179] The O_2^+ cations were used to "monitor" the endpoint of the N + NO reaction. A known ~ constant flow of N_2, (measured by pressure reduction out of a calibrated volume), was subjected to a microwave discharge, thus forming a small flux of N atoms within the (mainly) undissociated flow of molecular

nitrogen. Measured flows of nitric oxide, (NO), were then progressively added under flowmeter control to the N_2 / N neutral flow until a sudden decrease in the O_2^+ ion signal was observed. This flow signified the endpoint of the NO titration where flux of [N atoms] = flow [NO]. Figure 5.2 below shows a typical set of experimental data obtained by performing a NO titration using O_2^+ as the monitor ion. This sequence of steps was repeated for a series of N_2 flow rates, (and hence N atom fluxes). The N_2 flow rates were chosen to cover the range over which the $C_2H_2^+ + N$ reaction had been measured. This NO titration procedure was repeated during several runs undertaken in the course of a given day.

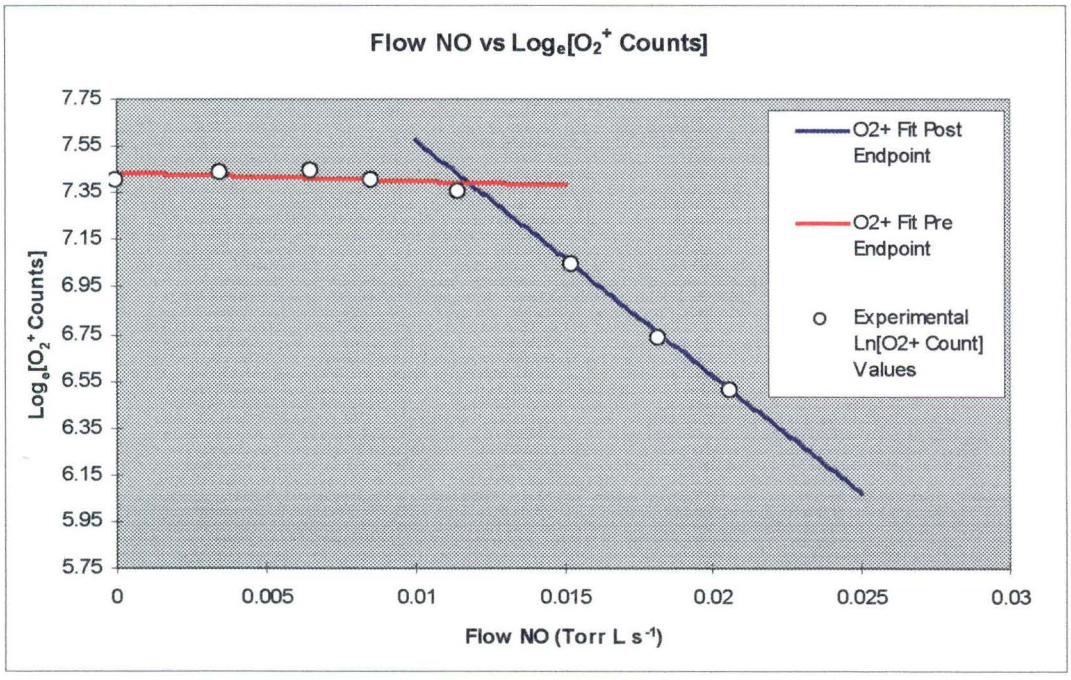

Figure 5.2. A typical set of experimental data obtained from a NO titration using O_2^+ as the monitor ion. The endpoint of the titration is clearly visible as the intersection of the red and blue lines.

The data derived from these experiments was then graphed with N_2 flow rate being plotted against the endpoint flow rate of the NO titration. The line of best fit obtained allowed the N atom flux to be read off for any given N_2 flow rate. Figure 5.3 is a graph of N_2 flow versus N atom flux. The data presented on this graph is typical and was obtained in a sequence of experiments performed over the course of a single day. The N_2 flow rates measured in the $C_2H_2^+ + N$ runs were then replaced by the N atom fluxes read off the calibration graph and

absolute rate coefficients obtained. This mode of operation is a variant of the method first described by Goldan and associates. [179]

The entire sequence of experiments described above, including the $C_2H_2^+$ + N atom runs and the NO titrations, was repeated over the period of several days. The mean rate coefficient obtained for the $C_2H_2^+$ + N reaction from this block of experiments is (2.4 ± 0.7) x 10^{-10} cm^3 s^{-1}. Given the experimental difficulties involved, this value is in excellent agreement with both prior measurements [177, 178] and gives confidence to the accuracy of the experimental techniques and data analysis methods.

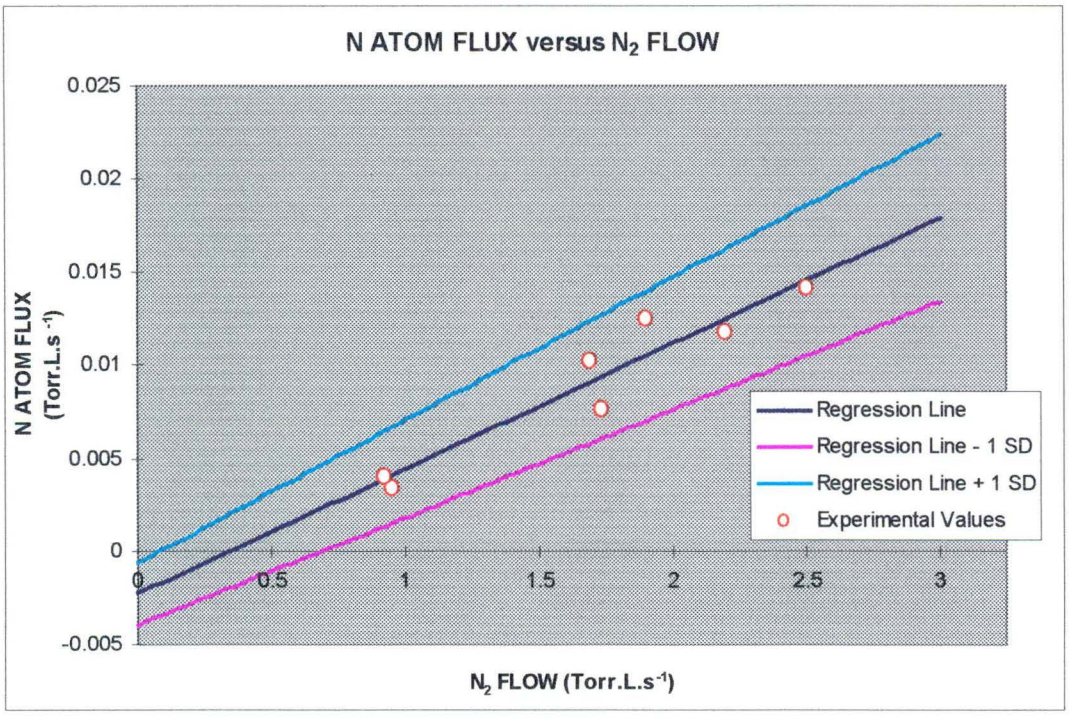

Figure 5.3. A plot of N atom flux versus N_2 flow, obtained from a series of NO titrations such as that shown in Figure 5.2. All data points were obtained from a sequence of experiments carried out on a single day.

A rate coefficient for the reaction of O_2^+ + N was obtained in an identical manner to that described above for the reference reaction, $C_2H_2^+$ + N. Again, acceptable agreement is apparent between the value obtained from the present work, [k = (1.0 ± 0.3) x 10^{-10} cm^3 s^{-1}], and the later of the prior measurements, both of which involved the participation of Fehsenfeld, [ie. k = (1.8 ± 0.9) x 10^{-10} cm^3 s^{-1}, (1965/66) [179, 284] ; and k = (1.2 ± 0.5) x 10^{-10} cm^3 s^{-1}, (1977) [182]].

A series of NO titrations identical in nature to the generic procedure described by Viggiano et al. [177] were also performed to establish the rate

coefficient for the calibration reaction $C_2H_2^+ + N$. This involved injecting $C_2H_2^+$ cations, establishing the microwave discharge, and measuring the ion signal in the absence of any neutral flowing. A steady flow of N_2 was then established and the depleted ion signal remeasured. The ion signal was then recorded at a series of NO flows, which allowed an endpoint to be observed as the intersection between a shallow decay followed by a steeper, post-endpoint slope. A typical set of experimental data obtained using this NO titration procedure is depicted in Figure 5.4. Within experimental error this series of experiments gave the same rate coefficient value for the reaction of $C_2H_2^+ + N$ as did the earlier set of measurements. This value is $(2.0 \pm 0.6) \times 10^{-10}$ cm^3 s^{-1}. These experiments were performed several months after the earlier determination of the absolute rate coefficient for the reference reaction, $C_2H_2^+ + N$ atoms. That the same result was obtained using two variants of the NO titration method, combined with the fact that the results obtained from the present study agree almost exactly with established literature values, [177, 178] indicates a better than tolerable level of precision in the cation-N atom data collected during this investigation.

Final Conversion of Relative Rate Coefficients into Absolute Rate Coefficients

Final absolute values of the rate coefficients for the reactions of various cations with N atoms were obtained by modifying expression **(501)** as follows:

$$Absolute\ k\{A^+\} = \frac{Raw\ k\{A^+\}}{Raw\ k\{C_2H_2^+\}} \cdot 2.4 \times 10^{-10} cm^3 s^{-1} \qquad \textbf{(503)}$$

In expression **(503)** the only alteration to relation **(501)** is the minimal change in the rate coefficient value for the reaction of $C_2H_2^+ + N$.

Determination of Rate Coefficients for Various Cations via the NO Titration Method

The NO titration technique was also used to obtain absolute rate coefficients for the reaction of several cations, (in addition to $C_2H_2^+$), with atomic nitrogen. These cations included CH_3^+, $C_2H_3^+$, $C_2H_4^+$, $C_2H_5^+$, $C_6H_6^+$, $HCNH^+$, $H_2C_3N^+$, H_3O^+, HCO^+ and HCO_2^+. Usually this was done as an aside to characterising the reactivity of these cations with atomic oxygen. The reactions of various cations with atomic oxygen are discussed at length in Chapter 7 of this thesis.

Agreement, within experimental error, was obtained in all cases where rate coefficient data was determined via the two different methods, namely the measurement of rate constants relative to the $C_2H_2^+$ + N calibration reaction, and the NO titration technique. This complementarity between results obtained using two quite different methodologies further increases confidence in the veracity of the data presented here. Rate coefficient data for a small minority of cations, [(c) and (ac)-$C_6H_5^+$, and H_2O^+], was obtained solely from the NO titration technique.

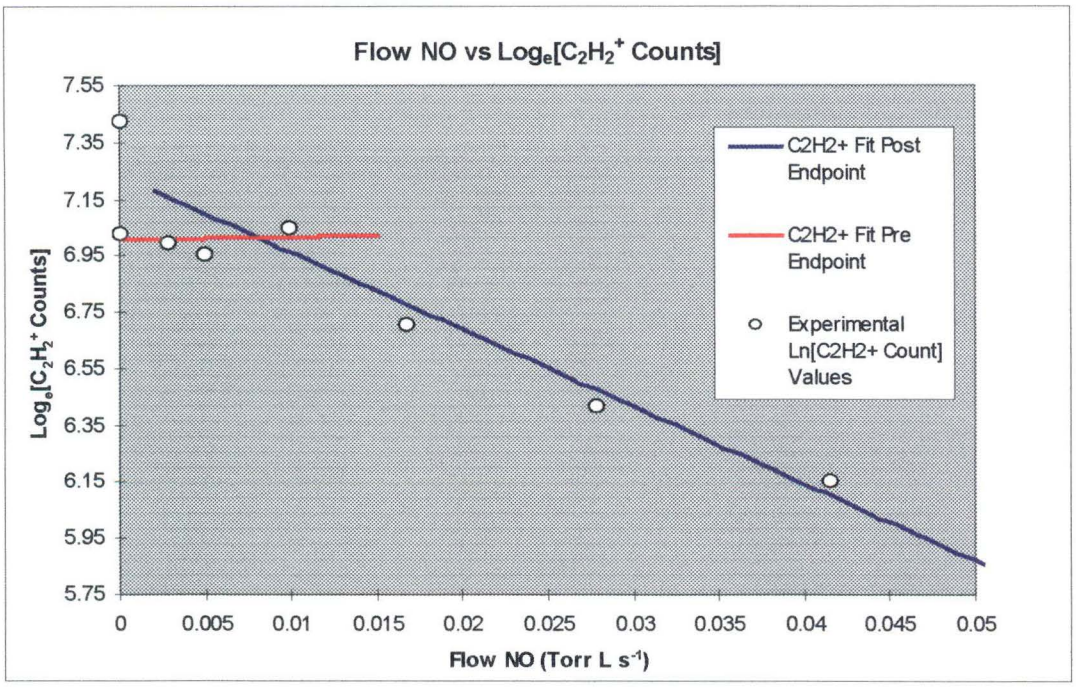

Figure 5.4. Data obtained for the reaction of $C_2H_2^+$ with N atoms, O atoms and NO. The endpoint of the NO titration is clearly visible as the intersection of the red and blue lines. The uppermost left data point at zero NO flow is the $C_2H_2^+$ signal with no N_2 flowing, ie. zero flux of N atoms.

Determination of the Rate Coefficient for the H_3^+ + N Reaction

A specific methodology was developed to study this very important reaction, the details of which are outlined in the next chapter of this thesis.

Reagents and Experimental Conditions

Nitrogen, (> 99.998 % pure), and hydrogen, (> 99.995 % pure), both zero grade quality, were obtained from BOC Gases. Helium, (instrument grade, > 99.99 % pure), which was used in several ~ 10 % and ~ 50 % N_2 / He mixtures, was procured from BOC Gases. These gases were further purified by passage through a molecular sieve trap, cooled to liquid nitrogen temperatures.

As previously mentioned, a commercially prepared mixture of 4.98 % N_2 in Helium, ("certified" standard, analytical accuracy within ± 3 % of the nominal value of the components present), was supplied by Alphagaz. Oxygen, (ultra-high purity grade, > 99.98 %), was supplied by Matheson Gases. Acetylene, (instrument grade, > 98 % pure), was supplied by BOC gases. Ethylene, (CP grade, > 99.5 % pure), was procured from NZIG. Carbon Monoxide, (CP grade, 99.5 % pure), was procured from Matheson Gas Products. These gaseous reagents were further purified by passage through a dry ice / acetone cooled molecular sieve trap.

Carbon dioxide, (industrial grade, > 99.8 % pure), was supplied by New Zealand Industrial Gases (NZIG). Methyl bromide, (CP grade, > 99.5 % pure), was obtained from Aldrich. These gases were further purified by passage through a salt / ice / water cooled molecular sieve trap.

Deionised water, H_2O, was obtained from the local departmental source. Dimethoxymethane, $(CH_3O)_2CH_2$, (CP grade, > 99 % pure), was supplied by Aldrich. Benzene, (AR grade, > 99.94 % pure), was obtained from Ajax Chemicals. Bromobenzene, C_6H_5Br, and Bromoethane, C_2H_5Br, (both CP grade), were supplied by May and Baker Ltd. These liquid reagents were further purified by several freeze-pump-thaw cycles.

Propyne was prepared according to the method of Brandsma. [233]

Cyanogen, C_2N_2, was prepared according to the method of Janz. [232]

Hydrocyanic acid, HCN, was synthesised in vacuo by the addition of KCN, (Fluka, 98 - 99 % cyanide), to 100 % orthophosphoric acid. [285]

Cyanoacetylene, HC_3N, was prepared by ammonolysis of methyl propiolate followed by dehydraration. The sample was trapped under vacuum and further purified by trap-to-trap distillation. [286]

Experimental Uncertainty

The uncertainty in the rate coefficients for the N atom reactions detailed below is estimated as ± 30 %. This is a larger uncertainty than is generally reported for stable neutral reactants (± 15 %), due primarily to the difficulty in accurately establishing the N atom number density in the main flow tube.

5.3: Results.

A summary of all the results obtained in this work are presented in Tables 5.1 to 5.4. Tables 5.1 and 5.2 detail the results obtained for the reaction of several hydrocarbon cations with N_2 and N atoms respectively. The results for the reaction of various non-hydrocarbon cations with N atoms and N_2 are summarised in Tables 5.3 and 5.4 respectively. Previous measurements, where they exist, are catalogued in column 4 of each Table.

Reactant Ion	Products and Branching Ratio	k_{obs} [a]	k_{prev} [b]	k_{coll} [c]	ΔH^o (kJ mol^{-1})[d]
CH_3^+	$CH_3^+.N_2$	0.005[e]	0.006[f]	9.85	- 189.6[g]
C_2H^+	$C_2H^+.N_2$ 1.0	0.029[h]		8.47	- 535.5[i]
$C_2H_2^+$	No Reaction	< 0.005		8.38	
$C_2H_3^+$	No Reaction	< 0.005		8.30	
$C_2H_4^+$	No Reaction	< 0.005		8.23	
$C_2H_5^+$	No Reaction	< 0.005		8.15	
C_3^+	No Reaction	< 0.005		7.76	
C_3H^+	No Reaction	< 0.005	< 0.001[j]	7.71	
$C_3H_2^+$	No Reaction	< 0.005		7.67	
(ac)-$C_3H_3^+$	No Reaction	< 0.005		7.62	
(c)-$C_3H_3^+$	No Reaction	< 0.005		7.62	
$C_3H_5^+$	No Reaction	< 0.005		7.55	
$C_4H_2^+$	No Reaction	< 0.005		7.26	
$C_4H_3^+$	No Reaction	< 0.005		7.24	
$C_6H_2^+$	No Reaction	< 0.005		6.83	
$C_6H_3^+$	No Reaction	< 0.005		6.82	
(c)-$C_6H_5^+$	(c)-$C_6H_5^+.N_2$ 1.0	0.091[k]		6.79	- 198.0[l]
(ac)-$C_6H_5^+$	No Reaction	< 0.005		6.79	
(c)-$C_6H_6^+$	No Reaction	< 0.005		6.78	

Table 5.1. Reactions of the given $C_mH_n^+$ reactant ion with N_2.

[a] Observed rate coefficient in units of 10^{-10} cm^3 s^{-1}. [b] Rate coefficients determined in other laboratories, in units of 10^{-10} cm^3 s^{-1}. [c] Langevin collision rate in units of 10^{-10} cm^3 s^{-1}. k_{coll} values were calculated according to the parameterised theory of Su and Chesnavich. [118] [d] The listed exothermicities are taken from Lias et al. [31] [e] Pseudo-bimolecular reaction. The rate constant shown is for a flow tube pressure of 0.36 Torr. The termolecular rate for the three-body association process is estimated as $k_3 \geq 4.3 \times 10^{-29}$ cm^6 s^{-1}. [f] No bimolecular reaction was observed, but termolecular rate coefficients of $k_3 = 5.3 \times 10^{-29}$ cm^6 s^{-1} at 300 K [39] and

$k_3 = 5.5 \times 10^{-29}$ cm^6 s^{-1} at 287 K [287] were reported. [i] Thermochemistry for the $CH_3N_2^+$ cation, (not H_2NCNH^+). [h] Pseudo-bimolecular reaction. The rate constant shown is for a flow tube pressure between 0.32 - 0.36 Torr. The termolecular rate for the three-body association process is estimated as $k_3 \geq 2.6 \times 10^{-28}$ cm^6 s^{-1}. [i] Thermochemistry for the $NCCNH^+$ cation. [j] References 223 and 288. [k] Pseudo-bimolecular reaction. The rate constant shown is for a flow tube pressure of 0.35 Torr. The termolecular rate for the three-body association process is estimated as $k_3 \geq 8.0 \times 10^{-28}$ cm^6 s^{-1}. [l] Thermochemistry for the $C_6H_5N_2^+$ cation which was obtained from the proton affinity of 3-pyridinecarbonitrile. [289]

Reactant Ion	Products and Branching Ratio		k_{obs} [a]	k_{prev} [b]	k_{coll} [c]	ΔH^o (kJ mol^{-1}) [d]
CH_3^+	$H_2CN^+ + H$ $HCN^+ + H_2$	0.65 0.35	0.94	0.67[e]	9.09	- 239.3[f] - 118.4[g]
$C_2H_2^+$	$HC_2N^+ + H$ $HCNH^+ + C$ $C_2N^+ + H_2$ $CH^+ + HCN$	0.60 0.25 0.10 0.05	2.4	2.5[h]	8.11	- 51.5 - 138.5[i] - 85.4[j] - 43.1[k]
$C_2H_3^+$	$HCCN^+ + H_2$ $H_2CCN^+ + H$	> 0.90 < 0.10	0.22	2.2[l]	8.06	- 54.0 - 153.9
$C_2H_4^+$	$CH_2CNH^+ + H$	1.0	3.0		8.01	- 316.6[m]
$C_2H_5^+$	No Reaction		< 0.23		7.96	
C_3^+	$C_2^+ + CN$ C_3N^+	0.5 0.5	5.7[n]		7.71	- 41.8
C_3H^+	HC_3N^+	1.0	1.7[o]		7.68	
$C_3H_2^+$	$C_2H_2^+ + CN$ $HCNH^+ + C_2$	0.85 0.15	0.44		7.65	- 90.4[p] - 76.1[q]
(ac)-$C_3H_3^+$	$HC_3N^+ + H_2$	1.0	0.58	1.3[l]	7.62	-179.9
(c)-$C_3H_3^+$	No Reaction		< 0.25		7.62	
$C_3H_5^+$	No Reaction		< 0.25	1.25[l]	7.57	
$C_4H_2^+$	$C_3H^+ + HCN$ $C_4HN^+ + H$ $HCNH^+ + C_3$	0.90 0.05 0.05	1.9		7.40	-166.2[k] - 113.0[i]
$C_4H_3^+$	No Reaction		< 0.25		7.38	
$C_6H_2^+$	$C_5H^+ + HCN$	1.0	1.9		7.13	
(c)-$C_6H_5^+$	$C_5H_4^+ + HCN$	1.0	0.37		7.11	- 146.5[s]
(ac)-$C_6H_5^+$	No Reaction		< 0.5		7.11	
$C_6H_6^+$	$C_5H_5^+ + HCN$ $C_3H_3^+ + C_3H_3N$	> 0.95 < 0.05	1.4		7.10	- 259.0[t] - 189.2[u]

Table 5.2. Reactions of the given $C_mH_n^+$ reactant ion with N atoms.

[a] Observed rate coefficient in units of 10^{-10} cm^3 s^{-1}. [b] Rate coefficients determined in other laboratories, in units of 10^{-10} cm^3 s^{-1}. [c] Langevin collision rate in units of 10^{-10} cm^3 s^{-1}. k_{coll}

values were calculated according to the parameterised theory of Su and Chesnavich. [118] [d] The listed exothermicities are taken from Lias et al. [31] [e] References 177 and 180. [f] Themochemistry for the H_2CN^+ cation, (not $HCNH^+$). [g] Themochemistry for the HCN^+ cation, (not HNC^+). [h] References 177 and 178. [i] Themochemistry for the $HCNH^+$ cation, (not H_2CN^+). [j] Themochemistry for the CCN^+ cation, (not CNC^+). [k] Themochemistry for HCN, (not HNC). [l] Reference 178. [m] Themochemistry for the CH_2CNH^+ cation. [n] The reaction between $C_3^+ + N$ to form C_3N^+ is presumably a pseudo-bimolecular reaction. The rate constant shown is for flow tube pressures between 0.330 - 0.355 Torr. The termolecular rate for the three-body association process is estimated as $k_3 \geq 2.6 \times 10^{-26}$ cm^6 s^{-1}. [o] Pseudo-bimolecular reaction. The rate constant shown is for a flow tube pressure of 0.35 Torr. The termolecular rate for the three-body association process is estimated as $k_3 \geq 1.5 \times 10^{-26}$ cm^6 s^{-1}. [p] Thermochemistry for the $HC{\equiv}CCH^+$ cation. [q] Thermochemistry for the $HC{\equiv}CCH^+$ and $HCNH^+$ cations. [r] Reference 178. The $C_3H_3^+$ and $C_3H_5^+$ cations were produced from C_3H_7Br. [s] Thermochemistry for the $H_2C{=}C{=}C{=}C{=}CH_2^+$ cation and HCN, (not HNC). [t] Thermochemistry for the cyclopentadienyl cation and HCN, (not HNC). [u] Themochemistry for the cyclopropenyl cation and CH_2CHCN.

Reactant Ion	Products and Branching Ratio		k_{obs} [a]	k_{prev} [b]	k_{coll} [c]	ΔH^o (kJ mol^{-1}) [d]
CN^+	$N_2^+ + C$	1.0	6.1		8.11	- 47.3
HCN^+	$CH^+ + N_2$	1.0	2.2		8.06	- 297.9[e]
$HCNH^+$	No Reaction		< 0.25		8.01	
HC_3N^+	$C_2N^+ + HCN$ $C_3H^+ + N_2$	0.6 0.4	2.4		7.38	- 95.1[f] - 351.5
$H_2C_3N^+$	No Reaction		< 0.25		7.37	
H_3^+	$NH_2^+ + H$	1.0	4.5	6.5[g]	15.57	- 97.9
H_2O^+	$NOH^+ + H$ $NO^+ + H_2$	0.8 0.2	1.4	1.9[h]	8.72	- 82.0[i] - 463.1
H_3O^+	No Reaction		< 0.25		8.62	
N_2^+	N_3^+	1.0	0.14[j]	< 0.1[k]	8.01	
CO^+	$NO^+ + C$	1.0	0.82	< 0.2[l]	8.01	- 13.1
HCO^+	No Reaction		< 0.25		7.96	
O_2^+	$NO^+ + O$	1.0	1.0	1.8[m] 1.2[n]	7.84	- 404.0
CO_2^+	$CO^+ + NO$	1.0	3.5	< 0.1[o]	7.51	- 75.4
HCO_2^+	No Reaction		< 0.28		7.49	

Table 5.3. Reactions of the given reactant ion with N atoms.

[a] Observed rate coefficient in units of 10^{-10} cm^3 s^{-1}. [b] Rate coefficients determined in other laboratories, in units of 10^{-10} cm^3 s^{-1}. [c] Langevin collision rate in units of 10^{-10} cm^3 s^{-1}. k_{coll} values were calculated according to the parameterised theory of Su and Chesnavich. [118] [d] The listed exothermicities are taken from Lias et al. [31] [e] Themochemistry for the HCN^+ cation, (not HNC^+). [f] Themochemistry for C_2N^+, (not CNC^+), and HCN, (not HNC). [g] References 24 and

184. Note that the veracity of this measurement has been called into question. [184] See Chapter 6 of this thesis for a full discussion of this prior investigation. [h] Reference 177. [i] Thermochemistry for the NOH^+ cation, (not HNO^+). [j] See text. [k] Reference 290. [l] Reference 161. [m] References 179 and 284. [n] Reference 182. [o] Reference 181 and 291.

Reactant Ion	Products and Branching Ratio	k_{obs} [a]	k_{prev} [b]	k_{coll} [c]	ΔH^o (kJ mol^{-1}) [d]
CN^+	$CN^+.N_2$	0.006[e]	< 0.1[f] < 0.043[g]	8.38	
HCN^+	No Reaction	< 0.005	< 0.1[h]	8.30	
$HCNH^+$	No Reaction	< 0.005		8.23	
HC_3N^+	No Reaction	< 0.005		7.24	
$H_2C_3N^+$	No Reaction	< 0.005		7.21	
H_3^+	$N_2H^+ + H_2$ 1.0	16.3		18.7	- 71.2
H_2O^+	No Reaction	< 0.005	< 0.1[i] ~ 0.001[j,k]	9.30	
H_3O^+	No Reaction	< 0.005		9.15	
N_2^+	$N_2^+.N_2$ 1.0	0.004[l]	~ 0.0006[j,m] ~ 0.002[j,n] ~ 0.019[j,o] ~ 0.45[j,p] ~ 0.001[j,q]	8.23	
CO^+	$CO^+.N_2$ 1.0	0.005[r]	~ 0.002[j,s]	8.23	+ 17.4[t]
HCO^+	No Reaction	< 0.005	< 0.0004[u] 6.7[v]	8.16	
O_2^+	No Reaction	< 0.006	< 0.00001[w] ~ 0.002[j,x] ~ 0.00009[i,y] < 2 x 10^{-18}[z]	7.96	
Ar^+	$N_2^+ + Ar$ 1.0	0.12	~ 0.1[A] 0.44[B], 0.1[C] 0.11[D], 0.22[E] 0.045[F] 0.04 – 0.1[G] 0.06[H] 0.025[I], 0.15[J] 0.049[K] 0.037[L] 0.66[M] 0.13[N] 0.02 – 0.15[O]	7.58	- 17.3
CO_2^+	No Reaction	< 0.005		7.44	
HCO_2^+	No Reaction	< 0.005	< 1.0[P] < 0.0002[Q]	7.41	

Table 5.4. Reactions of the given reactant ion with N_2.

[a] Observed rate coefficient in units of 10^{-10} cm^3 s^{-1}. [b] Rate coefficients determined in other laboratories, in units of 10^{-10} cm^3 s^{-1}. [c] Langevin collision rate in units of 10^{-10} cm^3 s^{-1}. k_{coll} values were calculated according to the parameterised theory of Su and Chesnavich. [118] [d] The listed exothermicities are taken from Lias et al. [31] [e] Pseudo-bimolecular reaction. The rate constant shown is for a flow tube pressure of 0.35 Torr. The termolecular rate for the three-body association process is estimated as $k_3 \geq 5.4 \times 10^{-29}$ cm^6 s^{-1}. [f] Reference 292. [g] Reference 243. [h] Reference 293. [i] Reference 294. [j] No bimolecular reaction was observed. [k] A termolecular rate coefficient of $k_3 = 9 \times 10^{-30}$ cm^6 s^{-1} was reported. [295] [l] Pseudo-bimolecular reaction. The rate constant shown is for a flow tube pressure of 0.35 Torr. The termolecular rate for the three-body association process is estimated as $k_3 \geq 3.5 \times 10^{-29}$ cm^6 s^{-1}. [m] A termolecular rate coefficient of $k_3 = (5.3 \pm 0.3) \times 10^{-30}$ cm^6 s^{-1} was reported. [296] [n] The following termolecular rate coefficients have been reported: $k_3 = (1.9 \pm 0.6) \times 10^{-29}$ cm^6 s^{-1} at 280 K, [297] $k_3 = (1.8 \pm 0.4) \times 10^{-29}$ cm^6 s^{-1} at 287 K, [191] $k_3 = 1.39 \times 10^{-29}$ cm^6 s^{-1} within the temperature range 100 K < T < 300 K, [298] and $k_3 = 1.8 \times 10^{-29}$ cm^6 s^{-1} within the temperature 100 K < T < 520 K. [299] [o] A termolecular rate coefficient of $k_3 = (1.7 \pm 0.4) \times 10^{-28}$ cm^6 s^{-1} at 0.03 eV kinetic energy was reported. [300] [p] A termolecular rate coefficient of $k_3 = 4.0 \times 10^{-27}$ cm^6 s^{-1} at 20 K was reported. [301] [q] A termolecular rate coefficient of $k_3 = 8.9 \times 10^{-30}$ cm^6 s^{-1} at 300 K was reported. [302] [r] Pseudo- bimolecular reaction. The rate constant shown is for a flow tube pressure of ~ 0.45 Torr. The termolecular rate for the three-body association process is estimated as $k_3 \geq 3.4 \times 10^{-29}$ cm^6 s^{-1}. [s] A termolecular rate coefficient of $k_3 = (2.1 \pm 0.4) \times 10^{-29}$ cm^6 s^{-1} at 298 K was reported. [303] [t] Thermochemistry for $ONCN^+$ cation. [u] Reference 238. [v] Reference 304. [w] References 305 and 306. [x] A termolecular rate coefficient of $k_3 = (1.9 \pm 0.6) \times 10^{-29}$ cm^6 s^{-1} at 80 K was reported. [307] [y] A termolecular rate coefficient of $k_3 = (8 \pm 6) \times 10^{-31}$ cm^6 s^{-1} at 296 K was reported. [308] [z] Reference 309. [A] Reference 310 @ 293 K and 0.04 eV centre of mass kinetic energy. [B] References 311 and 312. [C] References 313-315. Reference 314 reported a rate coefficient of 1.0×10^{-11} cm^3 s^{-1} for 80 K < T < 300 K. [D] Reference 316. [E] Reference 317 and 318. [F] Reference 319. [G] The measured rate coefficient at 280 K was 4×10^{-12} cm^3 s^{-1} at high Ar flows, increasing to 1×10^{-11} cm^3 s^{-1} at low Ar flows. [320] [H] Reference 321. [I] Reference 322. [J] Reference 323. [K] Reference 324. [L] Reference 325. [M] Reference 326. [N] Reference 327. [O] The lowest value of 2×10^{-12} cm^3 s^{-1} was noted with a 1 % N_2 in Ar mixture, whilst the highest value of 1.5×10^{-11} cm^3 s^{-1} was observed with a 0.1 % N_2 in Ar mixture @ 0.45 Torr. [328] [P] Reference 329. [Q] Reference 330.

5.4: Discussion of Results.

(i). $CH_3^+ + N_2$ / N. The CH_3^+ cations that participated in these experiments were generated from methyl bromide, CH_3Br. Molecular nitrogen and CH_3^+ react via a very slow association reaction, [$k = (5.0 \pm 0.8) \times 10^{-13}$

$cm^3\ s^{-1}$]. This result is in agreement with two previous investigations of the $CH_3^+ + N_2$ reaction. [39, 287] In contrast, methyl cations undergo a moderately fast reaction with atomic nitrogen, viz:

$CH_3^+(^1A) + N(^4S) \Rightarrow H_2CN^+(^1A) + H(^2S) + 2.5\ eV^a\ (0.65)$ **(504a)**

$\Rightarrow HCN^+(^2\Sigma) + H_2(^1\Sigma_g^+) + 1.2\ eV^b\ (0.35)$ **(504b)**

$k_{(504)\ 300K} = (9.4 \pm 2.8) \times 10^{-11}\ cm^3\ s^{-1}$

Both previous studies of this reaction, **(504)**, found a rate coefficient of $6.7 \times 10^{-11}\ cm^3\ s^{-1}$ with varying uncertainties, (± 50 % for the earlier measurement [180] and ± 20 % for the later result [178]). The value of $k_{(504)}$ obtained from the present study is within the experimental error of both literature values. [178, 180] The two product channels noted above were observed in these prior experimental investigations, although neither study reported a product branching ratio. [178, 180]

Note that in the channel **(504a)** the m/z = 28 ion may also be $HCNH^+$, as both $CHNH^+$ isomers are thermodynamically accessible, (ΔH^o for $CH_3^+ + N \Rightarrow HCNH^+ + H$ is - 402.5 kJ mol^{-1}). [31] Similarly, HNC^+ is thermodynamically accessible in channel **(504b)**, [ΔH^o for $CH_3^+ + N \Rightarrow HNC^+ + H_2$ is - 160.3 kJ mol^{-1}]. The isomeric identity of the ionic products was not determined from experiment, however the channels **(504a)** and **(504b)** detailed above involve the least rearrangement. Channel **(504a)** merely involves an exchange of H for N.

Spin is not conserved in either product channel although the exothermicity of pathway **(504a)** is sufficient to allow the possibility of access to an excited triplet state of the H_2CN^+ ion.

(ii). $C_2H_n^+$ (n = 1 to 5) + N_2 / N. The **C_2H^+** cation was formed by electron impact on a 10 % mixture of acetylene in helium. This cation undergoes a slow association with molecular nitrogen, [$k = (2.9 \pm 0.4) \times 10^{-12}\ cm^3\ s^{-1}$]. The reaction of $C_2H^+ + N$ atoms was not re-examined as part of the present study. [177, 178]

The **$C_2H_2^+$** cation, which was formed directly by electron impact on acetylene, is unreactive with N_2, ($k < 5 \times 10^{-13}\ cm^3\ s^{-1}$). As previously observed [177, 178] this species did react at a moderate rate with atomic nitrogen, viz

---

[a] Themochemistry for the H_2CN^+ cation, (not $HCNH^+$).

[b] Themochemistry for the HCN^+ cation, (not HNC^+).

$C_2H_2^+(^2\Sigma)$ + $N(^4S)$ ⇒ $HCCN^+(^2A)$ + $H(^2S)$ + 0.5 eV (0.60) **(505a)**

⇒ $HCNH^+(^1\Sigma_g)$ + $C(^3P)$ + 1.4 eV[c] (0.25) **(505b)**

⇒ $C_2N^+(^1\Sigma)$ + $H_2(^1\Sigma_g^+)$ + 0.9 eV[d] (0.10) **(505c)**

⇒ $CH^+(^1\Sigma)$ + $HCN(^1\Sigma^+)$ + 0.4 eV[e] (0.05) **(505d)**

$k_{(505)\ 300K}$ = (2.4 ± 0.7) x 10^{-10} cm^3 s^{-1}

As already remarked upon in Section 5.2 above, the rate constant obtained for the overall reaction **(505)** is in excellent agreement with the value obtained by both sets of workers who have previously studied this reaction. [177, 178]

Channel **(505b)** was not reported by either of the previous research groups that examined this reaction. [177, 178] This non-observation may have been because changes in m/z = 28 ions are somewhat difficult to observe when reactions with atomic nitrogen are being performed. This difficulty is due to the creation of small quantities of N_2^+ ions in the microwave discharge, which also have a mass to charge ratio of 28. Note that the H_2CN^+ isomer cannot be formed in reaction **(505b)** as its formation is endothermic by + 24.7 kJ mol^{-1}. The fact that $HCNH^+$ is produced, (rather than H_2CN^+), implies that channel **(505b)** proceeds via a mechanism which involves major rearrangement.

In accordance with the work of Viggiano et al. [177] and Federer et al. [178] the dominant product channel was observed to be **(505a)** which proceeded via H-N exchange and in which spin was conserved. The rate constant for this channel alone, is ~ 1.4 x 10^{-10} cm^3 s^{-1}, which is < (3/8 k_L x 0.60), [ie. k_L multiplied by the statistical weight of the spin allowed triplet reaction pathway and the "fraction" of channel **(505a)**]. The newly observed product channel **(505b)** also conserves spin, whilst both minor product channels **(505c)** and **(505d)** involve the violation of spin conservation. Channel **(505b)** has a rate constant of ~ 6.0 x 10^{-11} cm^3 s^{-1} which is < (3/8 k_L x 0.25).

Thermochemistry dictates that the m/z = 38 cation in channel **(505c)** could also be CNC^+, (ΔH^o for $C_2H_2^+ + N \Rightarrow CNC^+ + H_2$ is - 181.6 kJ mol^{-1}). [31] Conversely, the neutral in channel **(505d)** can only be HCN due to thermochemical considerations, (ΔH^o for $C_2H_2^+ + N \Rightarrow CH^+ + HNC$ is + 22.6 kJ mol^{-1}). [31]

---

[c] Themochemistry for the $HCNH^+$ cation, (not H_2CN^+).

[d] Themochemistry for the CCN^+ cation, (not CNC^+).

[e] Themochemistry for HCN, (not HNC).

$C_2H_3^+$ ions were produced from the collisional dissociation of the $C_2H_5^+$ ions generated when C_2H_5Br vapour was subjected to electron impact. The $C_2H_3^+$ species is unreactive with molecular nitrogen, ($k < 5 \times 10^{-13}$ cm^3 s^{-1}), however a slow two-channel reaction with atomic nitrogen does occur:

$C_2H_3^+(^1A) + N(^4S) \Rightarrow HC_2N^+(^2A) + H_2(^1\Sigma_g^+) + 0.6$ eV (> 0.90) **(506a)**

$\Rightarrow H_2C_2N^+(^1A_1) + H(^2S) + 1.6$ eV (< 0.10) **(506b)**

$k_{(506)\ 300K} = (2.2 \pm 0.7) \times 10^{-11}$ cm^3 s^{-1}

Reaction **(506a)** appears to violate spin conservation, (unless the ground state of $HCCN^+$ is a quartet), as does the minor channel, **(506b)**.

Inexplicably, despite this measurement being repeated several times on four different days, the rate constant observed in the present study is an order of magnitude slower than that reported by Federer et al. [178] Furthermore, these workers apparently did not observe the minor product channel, **(506b)**, reported above. [178] Given the slow overall rate of reaction **(506)**, it is not surprising that the minor product channel, **(506b)**, was not observed in the earlier study.

There were two differences in experimental methodology between the two studies. Firstly, Federer and co-workers formed the $C_2H_3^+$ cation from ethane, C_2H_6, [178] whereas in the present study this species was formed from ethyl bromide, C_2H_5Br. Secondly, the work of Federer et al. was carried out in a flow drift tube at "*near* thermal energies (≈ 0.1 - 0.2 eV)". [178] The minor dissimilarity between ion precursor molecules is unlikely to be the cause of the disagreement between current and prior results, as only one stable $C_2H_3^+$ isomer is known. The small amount of kinetic energy imparted to all ionic species in the Federer investigation [178] may have possibly perturbed their results and produced an artifically high rate coefficient. This statement is only rigorously true if a barrier to reaction exists for the $C_2H_3^+ + N$ process, as seems plausible.

The **$C_2H_4^+$** cations used in the current work were formed directly by electron impact on ethylene. This species is unreactive with N_2, ($k < 5 \times 10^{-13}$ cm^3 s^{-1}), however $C_2H_4^+$ does participate in a moderately fast reaction with atomic nitrogen, viz:

$C_2H_4^+(^2A) + N(^4S) \Rightarrow CH_2{=}C{=}NH^+(^2B_1) + H(^2S) + 3.3$ eV[f] **(507)**

$k_{(507)\ 300K} = (3.0 \pm 0.9) \times 10^{-10}$ cm^3 s^{-1}

---

[f] Themochemistry for the $CH_2{=}C{=}NH^+$ cation.

Again this reaction proceeds via an H-N exchange pathway in which spin is conserved. Note that $k_{(507)} \approx 3/8\ k_L$, which is the Langevin collision rate multiplied by the statistical weight of the spin allowed triplet reaction pathway.

$C_2H_5^+$ was formed directly by electron impact on ethyl bromide, C_2H_5Br, and injected with sufficiently low energy to avoid collisional break-up to $C_2H_3^+$. No reaction occurs between $C_2H_5^+$ and either molecular or atomic nitrogen, ($k < 5 \times 10^{-13}$ cm^3 s^{-1} and $k < 2.3 \times 10^{-11}$ cm^3 s^{-1}, respectively).

(iii). $C_3H_n^+$ (n = 1 to 3 and n = 5) + N_2 / N. C_3^+, C_3H^+, $C_3H_2^+$, and $C_3H_3^+$ were generated via electron impact on propyne, HC≡C-CH_3.

C_3^+ does not react with N_2, ($k < 5 \times 10^{-13}$ cm^3 s^{-1}), however a fast reaction, with two product channels, occurs between this species and atomic nitrogen, ie.

$$C_3^+(^2B_2) + N(^4S) \Rightarrow C_2^+(^2\Pi) + CN(^2\Sigma^+) + 0.4\ eV \quad (0.5)\mathbf{(508a)}$$

$$\Rightarrow C_3N^+(^3\Sigma) \quad (0.5)\mathbf{(508b)}$$

$$k_{(508)\ 300K} = (5.7 \pm 1.7) \times 10^{-10}\ cm^3\ s^{-1}$$

No thermochemical data is available for the C_3N^+ species, therefore the ergicity of channel **(508b)** cannot be evaluated. Note that channel **(508a)** occurs via C atom transfer, whilst channel **(508b)** is presumably a three-body association process, (the termolecular rate constant for which is estimated as $k_3 \geq 2.6 \times 10^{-26}$ cm^6 s^{-1}).

Spin is conserved in both product channels and the observed rate for each pathway is more than double (3/8 k_L x 0.5), [ie. k_L multiplied by the statistical weight of the spin allowed triplet reaction pathway and the "fraction" of each channel, **(508a)** and **(508b)**]. This phenomenon has been previously observed in a number of reactions, [eg. $H_2O^+(^2B) + NO_2(^2A) \Rightarrow H_2O(^1A) + NO_2^+(^1\Sigma)$], and commented upon by Federer et al. [178]

There is no reaction between **C_3H^+** and N_2, ($k < 5 \times 10^{-13}$ cm^3 s^{-1}), but a moderately fast association reaction is apparent with N atoms:

$$C_3H^+(^1\Sigma_g) + N(^4S) \Rightarrow HC_3N^+(^2\Pi) \quad \mathbf{(509)}$$

$$k_{(509)\ 300K} = (1.7 \pm 0.5) \times 10^{-10}\ cm^3\ s^{-1}$$

Experimental thermochemical data is also not available for the C_3H^+ ion, hence the ergicity of the above reaction, **(509)**, cannot be determined. Spin is not conserved in the reaction between C_3H^+ and N atoms.

The rate coefficient reported above is for the pseudo-bimolecular reaction at a flow tube pressure of 0.35 Torr. The termolecular rate coefficient for reaction **(509)** is assessed as $k_3 \geq 1.5 \times 10^{-26}$ cm^3 s^{-1}.

The $\mathbf{C_3H_2^+}$ cation is unreactive with molecular nitrogen, ($k < 5 \times 10^{-13}$ cm^3 s^{-1}), but undergoes a slow reaction with atomic nitrogen via two product channels, viz:

$C_3H_2^+(^2A') + N(^4S) \Rightarrow C_2H_2^+(^2\Sigma) + CN(^2\Sigma^+) + 0.9\ eV^g\ (0.85)$ **(510a)**

$\Rightarrow HCNH^+(^1\Sigma_g) + C_2(^3\Pi_u) + 0.8\ eV^h\ (0.15)$ **(510b)**

$k_{(510)\ 300K} = (4.4 \pm 1.3) \times 10^{-11}$ cm^3 s^{-1}

Spin is conserved in both of the above processes and the rate of each channel is $< (3/8\ k_L \times f[\text{Channel}]^i)$, (this being the Langevin rate coefficient factored by the statistical weight of the spin allowed triplet reaction pathway, and multiplied by the "fraction" of each channel).

The $C_3H_2^+$ ion was formed from a linear precursor (propyne) and therefore for the thermochemical calculations it has been assumed that the $C_3H_2^+$ cation is the linear isomer $HC{\equiv}CCH^+$, rather than the lower energy cyclic structure c-$C_3H_2^+$. This supposition was not confirmed by experiment.

The major product channel, **(510a)**, is accessed via simple carbon atom loss from the reactant cation, whereas channel **(510b)** presumably involves more extensive rearrangement. Note that the formation of the (alternative) H_2CN^+ cation in channel **(510b)** is endothermic, [ΔH_f° for (l)-$C_3H_2^+ + N \Rightarrow H_2CN^+ + C_2$ = + 87.1 kJ mol^{-1}; or ΔH_f° for (c)-$C_3H_2^+ + N \Rightarrow H_2CN^+ + C_2$ = + 292.1 kJ mol^{-1}], [31] and hence is not possible.

The $\mathbf{C_3H_3^+}$ species were generated from two different neutral precursors in two separate experiments.

In several initial experiments propyne was subjected to electron impact and the resultant (c,ac)-$C_3H_3^+$ species reacted with N_2 and N atoms. The (c,ac)-$C_3H_3^+$ cations formed in this manner do not react with N_2, ($k < 5 \times 10^{-13}$ cm^3 s^{-1}), but react with N atoms, albeit slowly, [$k = (2.2 \pm 0.6) \times 10^{-11}$ cm^3 s^{-1}].

In a sequence of later experiments (c)-$C_3H_3^+$ was produced by injecting the $C_2H_4^+$ cation, (formed via electron impact on ethylene), into the flow tube and

---

g Thermochemistry for the $HC{\equiv}CCH^+$ cation.

h Thermochemistry for the $HC{\equiv}CCH^+$ and $HCNH^+$ cations.

i f[Channel] denotes the "fraction" of each doublet product channel, **(510a)** and **(510b)**.

adding acetylene at the first neutral inlet port. The thermochemistry of this second method of $C_3H_3^+$ formation is such that only the cyclic isomer is thermodynamically accessible, (production of the acyclic isomer is endothermic by + 31.5 kJ mol^{-1}). [31] No reaction is observed between (c)-$C_3H_3^+$ and either N_2 or N atoms, ($k < 5 \times 10^{-13}$ cm^3 s^{-1}, and $k < 2.5 \times 10^{-11}$ cm^3 s^{-1}, respectively).

The proportion of (ac)-$C_3H_3^+$ produced from electron impact on propyne was determined by reacting the (c,ac)-$C_3H_3^+$ mixture with acetylene. This experiment showed a (c)-$C_3H_3^+$: (ac)-$C_3H_3^+$ ratio of ~ 60 % : 40 %.

The outcome of these two experiments is that (c)-$C_3H_3^+$ is unreactive with N_2 or atomic nitrogen, whereas (ac)-$C_3H_3^+$ reacts slowly with atomic nitrogen but is unreactive with N_2, viz:

$$(ac)\text{-}C_3H_3^+(^1A) + N(^4S) \Rightarrow HC_3N^+(^2\Pi) + H_2(^1\Sigma_g^+) + 1.9\ eV \qquad \textbf{(511)}$$

$$k_{(511)\ 300K} = (5.8 \pm 1.7) \times 10^{-11}\ cm^3\ s^{-1}$$

Spin is not conserved in reaction **(511)**.

The results of the present study are not in agreement with Federer et al. who reported a moderately fast rate of 1.3×10^{-10} cm^3 s^{-1} and a product channel of $H_2C_3N^+ + H$ for reaction **(511)**. [178] In their study, Federer and co-workers produced the $C_3H_3^+$ cation from propyl bromide, C_3H_7Br, [178] which is a different precursor again to either of the ion source gases used in the current work. The use of different neutral precursors may have some effect on the proportion in which the $C_3H_3^+$ isomers are formed, although the present study indicates that neither $C_3H_3^+$ species is particularly reactive with N atoms and no $H_2C_3N^+$ product ion was detected. Also, the work of Federer and associates was performed in a flow-drift tube at "*near* thermal energies (≈ 0.1 - 0.2 eV)", [178] so once again this may partially account for the discrepancies between their results and the current findings.

$C_3H_5^+$ cations were produced as a result of secondary reactions following electron impact on ethylene in a high pressure ion source. The $C_3H_5^+$ ion is the major product of the reaction between the primary ion, $C_2H_4^+$, and neutral C_2H_4. [24] No reaction is observed between the $C_3H_5^+$ cation and either N_2 or N atoms, ($k < 5 \times 10^{-13}$ cm^3 s^{-1}, and $k < 2.5 \times 10^{-11}$ cm^3 s^{-1}, respectively). This result is at variance with the outcome of the experiment conducted by Federer and colleagues who observed a moderately fast reaction, ($k = 1.25 \times 10^{-10}$

$cm^3\ s^{-1}$), with two product channels. [178] Again the fact that these workers used C_3H_7Br as a neutral precursor for $C_3H_5^+$, and operated slightly above thermal energies [178] may explain the disagreement between their results and the non-reaction found in the present study.

(iv). $C_4H_n^+$ (n = 2 and 3) + N_2 / N. Both $C_4H_2^+$ and $C_4H_3^+$ were formed by electron impact on acetylene in a high pressure ion source. Neither $C_4H_n^+$ cation is reactive with N_2, ($k < 5 \times 10^{-13}$ $cm^3\ s^{-1}$ for both species). $C_4H_3^+$ is also unreactive with atomic nitrogen, ($k < 2.5 \times 10^{-11}$ $cm^3\ s^{-1}$), however a moderately fast reaction is observed between $C_4H_2^+$ and N atoms, viz:

$$C_4H_2^+(^2\Pi_g) + N(^4S) \Rightarrow C_3H^+(^1\Sigma_g) + HCN(^1\Sigma^+) + 1.7eV^j \quad (0.90) \quad \textbf{(512a)}$$

$$\Rightarrow HCNH^+(^1\Sigma_g) + C_3(^1\Sigma_g^+) + 1.2eV^k \quad (0.05) \quad \textbf{(512b)}$$

$$\Rightarrow C_4HN^+ + H(^2S) \quad (0.05) \quad \textbf{(512c)}$$

$$k_{(512)\,300K} = (1.9 \pm 0.6) \times 10^{-10}\ cm^3\ s^{-1}$$

The major product channel involves transfer of a CH unit from cation to atom. Note that no thermochemical data is available for the C_4HN^+ cation, hence the ergicity of this channel cannot be evaluated. On the basis of thermochemical arguments, either HCN or HNC may be formed in reaction **(512a)**, [ΔH^o for $C_4H_2^+ + N \Rightarrow C_3H^+ + HNC$ is - 100.5 kJ mol^{-1}]. [31] Conversely, H_2CN^+ is not a thermodynamically accessible cationic product in channel **(512b)**, [ΔH^o for $C_4H_2^+ + N \Rightarrow H_2CN^+ + C_3$ is + 50.2 kJ mol^{-1}]. [31]

Channels **(512a)** and **(512b)** both involve the non-conservation of spin. The ground electronic state of C_4HN^+ is not known, although it is likely to be a doublet. Consequently, the minor channel, **(512c)**, is probably spin allowed with an observed rate coefficient < 3/8 k_L , (ie. k_L multiplied by the statistical weight of the spin allowed triplet reaction pathway).

(v). $C_6H_n^+$ (n = 2 - 3 and n = 5 - 6) + N_2 / N. Both the $C_6H_2^+$ and $C_6H_3^+$ cations were made from electron impact on C_2H_2 in a high pressure ion source. Neither of these cations reacts with N_2, ($k < 5 \times 10^{-13}$ $cm^3\ s^{-1}$), however $C_6H_2^+$ reacts with atomic nitrogen via a single product channel, in which spin is not conserved, ie.

$$C_6H_2^+(^2\Pi_u) + N(^4S) \Rightarrow C_5H^+(^1\Sigma^+) + HCN(^1\Sigma^+) \quad \textbf{(513)}$$

---

j Themochemistry for HCN, (not HNC).

k Themochemistry for the $HCNH^+$ cation, (not H_2CN^+).

$k_{(513)\ 300K}$ = $(1.9 \pm 0.6) \times 10^{-10}$ $cm^3\ s^{-1}$

No thermochemical data is available for the C_5H^+ cation hence the ergicity of reaction **(513)** cannot be determined. The reaction between $C_6H_3^+$ and atomic nitrogen was not characterised as part of the present study.

A mixture of acyclic and cyclic $\mathbf{C_6H_5^+}$ cations was produced via electron impact on bromobenzene, C_6H_5Br. The cationic mixture formed from this precursor is ~ 70 % cyclic isomer : ~ 30 % acyclic isomer. A double exponential decay is observed when this mixture of $C_6H_5^+$ ions reacts with molecular nitrogen. The (ac)-$C_6H_5^+$ cation is unreactive with N_2, ($k < 5 \times 10^{-13}$ $cm^3\ s^{-1}$), whereas (c)-$C_6H_5^+$ reacted slowly, [$k = (9.1 \pm 2.7) \times 10^{-12}$ $cm^3\ s^{-1}$], giving the adduct, $C_6H_5^+.N_2$, as the sole product. Similarly, (ac)-$C_6H_5^+$ does not react with atomic nitrogen, ($k < 5 \times 10^{-11}$ $cm^3\ s^{-1}$), however (c)-$C_6H_5^+$ reacts slowly with N atoms via a single product channel, viz:

(c)-$C_6H_5^+(^1A_1)$ + $N(^4S)$ ⇒ $C_5H_4^+$ + $HCN(^1\Sigma^+)$ + 1.5 eV[l] **(514)**

$k_{(514)\ 300K}$ = $(3.7 \pm 1.1) \times 10^{-11}$ $cm^3\ s^{-1}$

Again the reaction seems to proceed via transfer of a CH fragment from the cation to the N atom. Note that three stable $C_5H_4^+$ isomers are known, namely $CH{\equiv}CCH_2C{\equiv}CH^+$, $CH_2{=}C{=}C{=}C{=}CH_2^+$, and $CH_3C{\equiv}CC{\equiv}CH^+$, along with two forms of the "CHN" neutral, ie. HCN and HNC. [31] All combinations of product cations and CHN neutrals are thermodynamically accessible except for $CH{\equiv}CCH_2C{\equiv}CH^+$ + HNC, which is endothermic by + 15.4 kJ mol^{-1}. [31]

The ground electronic states of the $C_5H_4^+$ cations have not been calculated but they are likely to be doublets, hence spin is probably not conserved in process **(514)**.

Cyclic $\mathbf{C_6H_6^+}$ cations were formed by electron impact on benzene vapour. This ion is unreactive with molecular nitrogen, ($k < 5 \times 10^{-13}$ $cm^3\ s^{-1}$), however a moderately fast reaction, with two product channels, was observed with N atoms, ie.

(c)-$C_6H_6^+(^2E_{1g})$ + $N(^4S)$ ⇒ $C_5H_5^+(^3A'_2)$ + $HCN(^1\Sigma^+)$ + 2.7 eV[m] (> 0.95)**(515a)**

⇒ $C_3H_3^+(^1A)$ + $CH_2CHCN(^1A')$ + 2.0 eV[n] (< 0.05)**(515b)**

$k_{(515)\ 300K}$ = $(1.4 \pm 0.4) \times 10^{-10}$ $cm^3\ s^{-1}$

---

l Thermochemistry for the $H_2C{=}C{=}C{=}C{=}CH_2^+$ cation and HCN, (not HNC).

m Thermochemistry for the cyclopentadienyl cation and HCN, (not HNC).

n Themochemistry for the cyclopropenyl cation and CH_2CHCN.

Once more the major product channel **(515a)** proceeds by CH transfer from the $C_6H_6^+$ cation to the N atom. Again a number of possible $C_5H_5^+$ isomers are thermodynamically accessible in channel **(515a)**, namely the cyclopentadienyl radical cation, the $HC{\equiv}CCHCH{\equiv}CH_2^+$ cation, and the vinylcyclopropenyl radical cation. [31] Furthermore, the neutral molecule produced by process **(515a)** may be HNC and / or HCN. All six possible $C_5H_5^+$ cation - CNH combinations are allowed thermochemically. [31] The minor product channel **(515b)** involves fragmentation of the collision complex. The thermochemistry dictates that both the cyclopropenyl radical cation, (c)-$C_3H_3^+$, and the acyclic $C_3H_3^+$ isomer, $CH_2C{=}CH^+$, are accessible in process **(515b)**. [31]

The minor channel, **(515b)**, is spin disallowed, however the major channel, **(515a)**, does conserve spin and proceeds with an observed rate coefficient that is $< 3/8\ k_L$, this being Langevin rate coefficient factored by the statistical weight of the spin allowed triplet reaction pathway.

(vi). Nitrile Cations + N_2 / N. Cyanide cations, $\mathbf{CN^+}$, were formed from cyanogen, C_2N_2. This cation participates in a slow termolecular association reaction with N_2, ($k_3 \geq 5.4 \times 10^{-29}$ cm^6 s^{-1}). The pseudo-bimolecular rate coefficient obtained from the present work, ($k = 6 \times 10^{-13}$ cm^3 s^{-1}), is in accord with two previous studies of this reaction, [243, 292] although the $CN^+.N_2$ adduct was not reported in the previous SIFT study. [243] In contrast, this species undergoes a very rapid spin allowed reaction with N atoms, viz:

$$CN^+(^3\Pi) + N(^4S) \Rightarrow N_2^+(^2\Sigma_g^+) + C(^3P) + 0.5\ eV \quad \textbf{(516)}$$

$$k_{(516)\ 300K} = (6.1 \pm 1.8) \times 10^{-10}\ cm^3\ s^{-1}$$

Note that the observed rate coefficient is significantly greater than $1/2\ k_L$, (ie. the Langevin collision rate weighted by the statistical weight of the spin allowed quartet channel). Reaction **(516)** proceeds by N^+ transfer from the cation to the neutral N atom.

The "CNH^+", (ie. a mixture of HCN^+ and HNC^+ [407]), and $HCNH^+$ cations were formed by electron impact on hydrogen cyanide, HCN. The $\mathbf{HCN^+}$ / $\mathbf{HNC^+}$ species are unreactive with N_2, ($k < 5 \times 10^{-13}$ cm^3 s^{-1}, compared with a literature value [293] of $k < 1 \times 10^{-11}$ cm^3 s^{-1}), however one or both of these cations react with atomic nitrogen moderately rapidly, ie.

$HCN^+(^2\Sigma) + N(^4S) \Rightarrow CH^+(^1\Sigma^+) + N_2(^1\Sigma_g^+) + 3.1\ eV$ **(517)**

$k_{(517)\ 300K} = (2.2 \pm 0.7) \times 10^{-10}\ cm^3\ s^{-1}$

Note that the reactions of both isomeric species HCN^+ and HNC^+ with N are exothermic, although the observed product channel in reaction **(517)** indicates that HCN^+ is the more likely reactant ion.

It is apparent that reaction **(517)**, which proceeds via N atom transfer from cation to neutral, does not conserve spin.

$HCNH^+$ is unreactive with both molecular and atomic nitrogen, ($k < 5 \times 10^{-13}\ cm^3\ s^{-1}$ and $k < 2.5 \times 10^{-11}\ cm^3\ s^{-1}$, respectively).

Electron impact on cyanoacetylene, HC_3N, was used to generate both **HC_3N^+** and **$H_2C_3N^+$**. Neither of these species react with N_2, ($k < 5 \times 10^{-13}\ cm^3\ s^{-1}$ for both cations), and $H_2C_3N^+$ is unreactive with N atoms, ($k < 2.5 \times 10^{-11}\ cm^3\ s^{-1}$). A moderately rapid reaction is however observed between HC_3N^+ and atomic nitrogen, with two product channels, viz:

$HC_3N^+(^2\Pi) + N(^4S) \Rightarrow C_2N^+(^1\Sigma) + HCN(^1\Sigma^+) + 1.0\ eV^{\circ}$ (0.6)**(518a)**

$\Rightarrow C_3H^+(^1\Sigma_g) + N_2(^1\Sigma_g^+) + 3.6\ eV$ (0.4)**(518b)**

$k_{(518)\ 300K} = (2.4 \pm 0.7) \times 10^{-10}\ cm^3\ s^{-1}$

Both product channels violate spin conservation. All four combinations involving the C_2N^+ or CNC^+ cations and the HCN or HNC neutrals are thermodynamically accessible in reaction **(518a)**. [31] The major channel, **(518a)**, once again proceeds via CH transfer from cation to the reactant N atom, whereas in reaction **(518b)** an N atom is transferred from cation to neutral.

(vii). $H_3^+ + N_2$ / N. In the context of interstellar chemistry this reaction is arguably the most important process studied in this entire work. Consequently the entire succeeding chapter, **(6)**, is devoted to a discussion of this reaction.

(viii). H_2O^+ and $H_3O^+ + N_2$ / N. Both H_2O^+ and H_3O^+ were generated by electron impact on water vapour. No reaction is observed between H_2O^+ and N_2, ($k < 5 \times 10^{-13}\ cm^3\ s^{-1}$). This outcome is in broad agreement with two previous studies of this reaction. [294, 295] One of the previous studies by McCrumb and Warneck reported a very slow termolecular association reaction between H_2O^+ and N_2 but this was not observed in the current study. [295] The water cation underwent a reasonably rapid two-channel reaction with atomic nitrogen, ie.

° Themochemistry for C_2N^+, (not CNC^+), and HCN, (not HNC).

$H_2O^+(^2B)$ + $N(^4S)$ $\Rightarrow$ $NOH^+(^2A')$ + $H(^2S)$ + 0.9 eV[p] (0.8)**(519a)**

$\Rightarrow$ $NO^+(^1\Sigma)$ + $H_2(^1\Sigma_g^+)$ + 4.8 eV (0.2)**(519b)**

$k_{(519)\ 300K}$ = $(1.4 \pm 0.4) \times 10^{-10}$ cm^3 s^{-1}

In channel **(519a)** both the NOH^+ and HNO^+ cations are thermodynamically accessible, [ΔH^o for $H_2O^+ + N \Rightarrow HNO^+ + H$ is - 157.3 kJ mol^{-1}]. [31] The predominant pathway, **(519a)**, proceeds via OH^+ transfer from cation to neutral while O^+ transfer occurs in the minor channel, **(519b)**. Channel **(519a)** is spin allowed, however the minor channel, **(519b),** violates the principle of spin conservation. The observed rate coefficient for channel **(519a)** is ~ 1.1×10^{-10} cm^3 s^{-1}, which is < 3/8 k_L, (the Langevin collision rate weighted by the statistical weight of the spin allowed triplet pathway).

The results of the current study are in general agreement with a previous investigation of this reaction by Viggiano and associates. [177] These researchers reported a slightly higher rate coefficient of $(2 \pm 1) \times 10^{-10}$ cm^3 s^{-1}, [177] which is within experimental error of the rate coefficient value obtained from the current work. Additionally, they noted both product channels observed in the present investigation of reaction **(519)**, although no product distribution was reported. [177]

H_3O^+ is unreactive with both N_2 and N atoms, ($k < 5 \times 10^{-13}$ cm^3 s^{-1} and $k < 2.5 \times 10^{-11}$ cm^3 s^{-1}, respectively).

(ix). N_2^+ + N_2 / N. Electron impact on nitrogen gas was used to form the N_2^+ cations used in this study. The N_2^+ cation is observed to undergo a slow termolecular association reaction with N_2, ($k = 4 \times 10^{-13}$ cm^3 s^{-1}). This finding is in coarse agreement with a number of previous studies. Note that data for this particular reaction has been reported on 24 previous occasions, [50] but only those values which have been obtained for the specific reaction
$N_2^+ + N_2 + He \Rightarrow N_3^+ + He$ are listed in column four of Table 5.4. [191, 296-302]

A slow association reaction is also observed between N_2^+ and atomic nitrogen, viz:

$N_2^+(^2\Sigma_g^+)$ + $N(^4S)$ $\Rightarrow$ $N_3^+(^3\Sigma)$ **(520)**

$k_{(520)\ 300K}$ = $(1.4 \pm 0.4) \times 10^{-11}$ cm^3 s^{-1}

No experimental thermochemical data is available on the N_3^+ species, hence the ergicity of the reaction **(520)** could not be evaluated. Reaction **(520)** is

---

[p] Thermochemistry for the NOH^+ cation, (not HNO^+).

unusual in that it is only the third process encountered in this study where the cation reacts with atomic nitrogen via termolecular association, ($k_3 \geq 1.2 \times 10^{-27}$ cm^3 s^{-1}). Spin is conserved in this process, with $k_{(520)}$ being well less than 3/8 k_L, which is the Langevin collision rate weighted by the statistical weight of the spin allowed triplet channel.

The findings of the current study do not agree with a much earlier, (1968), investigation of the $N_2^+ + N$ reaction by Ferguson. [290] This worker reported that the reaction proceeded via charge transfer with a rate $< 1 \times 10^{-11}$ cm^3 s^{-1}. [290] An N^+ product is not observed for reaction **(520)** in the current study, however the presence of secondary chemistry may mean that the work of Ferguson is not in total discord with the present results. A comparison of the upper limit for the rate coefficient of reaction **(520)** obtained by Ferguson, [290] with the value obtained from the present measurement indicates tolerable agreement. The chemical literature [50] also records that the N^+ cation undergoes a three-body reaction with N_2 to form the adduct, N_3^+, ($k_3 \sim (2.8 \pm 1.8) \times 10^{-29}$ cm^6 s^{-1}).[q] Under the prevailing experimental conditions, (ie. a large flow of N_2 in the flow tube), it is difficult to be unequivocal about whether the observed N_3^+ ion is the direct association product of reaction **(520)**, or the result of secondary chemistry, ($N^+ + N_2 + M \Rightarrow N_3^+$).

(x). $CO^+ + N_2$ / N. The CO^+ cation was formed via electron impact on carbon monoxide. A slow termolecular association reaction was observed between CO^+ and N_2, (the observed pseudo-bimolecular rate coefficient obtained was $k = (5.0 \pm 0.8) \times 10^{-13}$ cm^3 s^{-1}). The value obtained for the rate coefficient is in rough agreement with the sole prior measurement of this reaction. [303]

In disagreement with an earlier 1972 measurement by Fehsenfeld and Ferguson, [161] a reaction is observed between the carbon monoxide cation and atomic nitrogen, viz:

$CO^+(^2\Sigma^+) + N(^4S) \Rightarrow NO^+(^1\Sigma) + C(^3P) + 0.1$ eV **(521)**

$k_{(521)\ 300K} = (8.2 \pm 2.5) \times 10^{-11}$ cm^3 s^{-1}

This reaction proceeds via O^+ transfer from the cation to the N atom. Spin is conserved in reaction **(521)**, with the observed rate being substantially less

---

[q] This value shown for the termolecular rate coefficient for the reaction of $N^+ + N_2 + M \Rightarrow N_3^+$ is the mean of five literature values. [143, 296, 297, 331, 332] The error shown is one standard deviation.

than 3/8 k_L which is the Langevin collision rate weighted by the statistical weight of the spin allowed triplet channel. This reaction was revisited several times on different days, with the above result being reproduced on each occasion.

(xi). HCO^+ and HCO_2^+ + N_2 / N. The HCO^+ cations were formed by electron impact on either dimethoxymethane vapour, $H_2C(OCH_3)_2$, or a mixture of ~ 10 % CO in H_2. No difference in reactivity was observed for HCO^+ cations generated via the two different neutral precursors. HCO^+ is unreactive with both N_2 and N atoms, ($k < 5 \times 10^{-13}$ cm^3 s^{-1}, and $k < 2.5 \times 10^{-11}$ cm^3 s^{-1}, respectively). The reaction of HCO^+ with N_2 has been studied twice previously and conflicting results obtained. [238, 304] The present study agrees with the SIFT experiments carried out by Adams, Smith and Grief [238] but disagrees with the tandem ICR measurements of Wagner-Redeker et al. [304]

HCO_2^+ was produced by electron impact on a mixture of ~ 10 % CO_2 in H_2. The HCO_2^+ cation is unreactive with N_2, ($k < 5 \times 10^{-13}$ cm^3 s^{-1}), and this finding is in accord with two previous examinations of this reaction. [329, 330] HCO_2^+ is also observed to be unreactive with atomic nitrogen, ($k < 2.8 \times 10^{-11}$ cm^3 s^{-1}).

(xii). O_2^+ + N_2 / N. The oxygen cation was formed by injecting Ar^+ ions and subsequently adding O_2 at the first neutral inlet. O_2^+ is unreactive with N_2, ($k < 6 \times 10^{-13}$ cm^3 s^{-1}), however this species does react with N atoms, ie.

$$O_2^+(^2\Pi_g) + N(^4S) \Rightarrow NO^+(^1\Sigma) + O(^3P) + 4.2 \text{ eV} \quad \textbf{(522)}$$

$$k_{(522)\ 300K} = (1.0 \pm 0.3) \times 10^{-10} \text{ cm}^3 \text{ s}^{-1}$$

The value obtained for $k_{(522)}$ is within experimental error of the two previous measurements of the O_2^+ + N reaction. [179, 182, 284] The reaction proceeds by O^+ transfer from the cation to the N atom. Reaction **(522)** conserves spin and the observed rate coefficient is < 3/8 k_L, this being the Langevin collision rate weighted by the statistical weight of the spin allowed triplet channel.

The reaction of O_2^+ with N_2 has been examined on four previous occasions and broad consistency is apparent in the data obtained. In 1965 Ferguson and colleagues made the initial observation of a non-reaction between O_2^+ and N_2, ($k < 1 \times 10^{-15}$ cm^3 s^{-1}). [305, 306] Following this early experiment the reaction was re-examined in 1970 by Adams et al. [307] who observed a slow termolecular association process at 80 K with $k = (1.9 \pm 0.6) \times 10^{-29}$ cm^3 s^{-1}, and then again in 1972 by Howard and co-workers [308] who noted an association reaction with

$k_3 = (8 \pm 4) \times 10^{-31}$ cm^6 s^{-1} at 296 K. Finally, in 1981, Matsuoka et al. [309] reported an upper limit for this rate coefficient of $k < 2 \times 10^{-18}$ cm^3 s^{-1} using a stationary pulsed afterglow technique. This latter observation is somewhat inconsistent with the earlier measurement of Howard et al.

During this sequence of experiments the reaction of $Ar^+ + N_2$ was also examined. The reaction proceeded via charge transfer, with a rate coefficient of $(1.2 \pm 0.2) \times 10^{-11}$ cm^3 s^{-1}. This result is in excellent agreement with the evaluated value of the rate coefficient for the reaction, of $k = (1.1 \pm 0.2) \times 10^{-11}$ cm^3 s^{-1} as published by Anicich. [24]

(xiii). $CO_2^+ + N_2$ / N. Electron impact on carbon dioxide gas was used to produce the CO_2^+ cation. CO_2^+ is unreactive with N_2, ($k < 5 \times 10^{-13}$ cm^3 s^{-1}), however it does undergo a moderately fast reaction with atomic nitrogen, viz:

$$CO_2^+(^2\Pi_g) + N(^4S) \Rightarrow CO^+(^2\Sigma^+) + NO(^2\Pi) + 0.8 \text{ eV} \quad \textbf{(523)}$$

$$k_{(523)\,300K} = (3.5 \pm 1.1) \times 10^{-10} \text{ cm}^3 \text{ s}^{-1}$$

This result is markedly different with a previous examination of reaction **(523)** by Fehsenfeld and colleagues, [181, 291] (who reported a non-reaction for $CO_2^+ + N$ atoms with $k < 1 \times 10^{-11}$ cm^3 s^{-1}), hence the measurement was repeated several times on different days to ensure the experiment had been interpreted correctly. The outcome detailed in equation **(523)** above was observed on every occasion.

This reaction, **(523)**, proceeds via O atom transfer from the cation to the N atom, conserves spin, and, interestingly, has a rate coefficient which exceeds 3/8 k_L, (ie. the Langevin collision rate multiplied by the statistical weight of the spin allowed triplet channel).

5.5: Implications of this Study to Extraterrestrial Chemistry.

Molecular and atomic nitrogen are quite abundant species throughout the universe. Within interstellar clouds both N_2 and N atoms exist in relatively high number densities. Lee and associates using their standard model have calculated that at 10 K, the fractional abundance of N = $f[N] = 1.9 \times 10^{-5}$, and $f[N_2] = 1.2 \times 10^{-5}$, whilst at 50 K, $f[N] = 6.6 \times 10^{-6}$, and $f[N_2] = 1.8 \times 10^{-5}$. All of these values are relative to $H_2 = 1$. [16] Much of the chemistry detailed in Tables 5.1

through 5.4, and discussed in Section 5.4 above, is pertinent to extraterrestrial chemistry.

Implications of the Reactions of Hydrocarbon Cations with N_2 and N Atoms to Extraterrestrial Chemistry

Molecular nitrogen is rather inert in that it is observed to be quite unreactive with most species, including hydrocarbon cations. [24, 50] Where a reaction does occur between N_2 and a hydrocarbon cation it is normally a very slow three-body association reaction. [24, 50] Such reactions are unimportant in the low density conditions typically found in the interstellar medium. Fast termolecular reactions are, however, an indicator as to the viability of analogous radiative stabilisation processes in interstellar clouds. [18, 192]

The other regime where the reaction between hydrocarbon species, (including ions), and N_2 may be important is in the ionosphere of planets with a significant nitrogen content in their atmosphere. Many of the reactions characterised in the current study are relevant to the nitrogenous atmosphere of the second largest satellite in the solar system, Titan, (the largest moon of Saturn). [282, 283] Further, the detection of significant quantities of hydrocarbons in Titan's atmosphere makes many of the reactions particularly relevant. The inertness of nitrogen in this atmosphere may act as a stabilising influence in a similar manner to the situation on Earth.

In contrast, many hydrocarbon cations undergo relatively rapid reactions with atomic nitrogen. [24, 50] Significant concentrations of this atomic species are likely to be present throughout the full extent of diffuse interstellar clouds. [277] With regard to dense interstellar clouds, it is probable that clumps of atomic nitrogen, in excess of the average number density, are located in "shielded" sub-regions of these objects. [278] Reactions between hydrocarbon cations and N atoms may therefore be relatively important within diffuse interstellar clouds and somewhat less significant in the dense interstellar clouds.

A perusal of the data in Table 5.1 indicates that the smaller hydrocarbon cations, ($C_mH_n^+$; $m \leq 3$), tend to react with atomic nitrogen via N atom insertion into the carbon skeleton of the hydrocarbon. This type of reaction may also be viewed as an N-H exchange process, wherein a C-N bond is formed. The

outcome of such reactions is normally a nitrile cation and either H_2 or H as the neutral fragment. This has important implications for interstellar chemistry, as it indicates a possible synthetic route to many of the smaller nitrile molecules that have been detected in interstellar clouds, eg. $HCNH^+$, HCCN, CH_3CN. Nitriles may also be formed by the association of hydrocarbon cations with N atoms but this type of process was only observed for two cases in the present study, namely C_3^+ and C_3H^+.

Interestingly, the findings of the current study do not support the involvement of either the $C_3H_2^+ + N$ or (c)-$C_3H_3^+ + N$ reactions in the synthesis of interstellar HC_3N as suggested by Knight et al. [333] The present results do however indicate that the radiative association of C_3^+ or C_3H^+ and atomic nitrogen, or, alternatively, the bimolecular reaction of (ac)-$C_3H_3^+$ with N may be implicated as a primary step in a synthetic route to cyanoacetylene in the interstellar medium.

In contrast, the larger hydrocarbon cations ($C_mH_n^+$; $m \geq 4$) often react with N atoms via a process of CH transfer from cation to the N atom. This process results in the formation of HCN, which is a very stable species, and an observed interstellar species. [13, 17] The implications of this finding are that the larger cyanopolyynes are probably not formed *directly* by the reaction of large polyatomic hydrocarbon cations with atomic nitrogen. Rather, they are more likely produced by the sequential reaction of small nitriles with small or medium sized hydrocarbon cations. In this way the largest cyanopolyynes are built up from smaller members of the family. [17]

Implications of the Reactions of Non-Hydrocarbon Cations with N_2 and N Atoms to Extraterrestrial Chemistry

As with the hydrocarbon cations most other ions are also unreactive with molecular nitrogen. [24, 50] The only major exception to this is the H_3^+ cation which reacts at the collision rate with N_2 via proton transfer. [24] The product, N_2H^+, is an observed interstellar molecule. [13, 17] The H_3^+ cation also reacts at the collision rate with many other species that populate the interstellar medium. [24]

Several of the nitrile cations examined in this study react with atomic nitrogen, although there is no obvious pattern in the reactivity of these species. Nitrogen atom transfer from cation to neutral is observed in two cases,

(HCN^+ + N and HC_3N^+ + N); this mechanism results in the formation of a stable N_2 molecule and a small hydrocarbon cation. The implications of this trend for interstellar chemistry are that nitrile ions, once formed, may fragment if they undergo subsequent encounters with N atoms.

Of the remaining species examined in this study, three react with N atoms via O^+ transfer from ion to neutral. These cations are H_2O^+, CO^+, and O_2^+, the product ion being NO^+ in all three cases. The neutral NO species is an observed interstellar molecule [13, 17] but the NO^+ cation has not yet been detected in this environment, although it is presumably present due to its unreactivity with H_2. [24]

5.6: Concluding Remarks.

As with the cation-H atom process discussed in the preceding chapter, most cation-N atom reactions proceed at a rate that is substantially less than the Langevin collision rate. In several cases this may be due to the effect of spin statistics, although it appears that the conservation of spin is not a particularly important parameter in these reactions. Federer et al. discussed this phenomenon of "wholesale violation of spin conservation" for cation-N atom reactions at some length in their 1986 paper. [178] They suggested that in these reactions the collision complexes experience multiple curve crossings between states of different multiplicity. [178] This curve crossing mechanism allows for the outcome of a change in overall spin without an attendant reduction in reaction efficiency.

For a small number of cation-N atom reactions, (eg. C_3^+ + N and CN^+ + N), the observed rate coefficient for a particular pathway is in excess of the Langevin rate coefficient appropriately factored by the "fraction" of the particular channel and the statistical weight of the route by which the reaction apparently proceeds. In their 1986 paper, Federer and associates commented that this experimental observation might be explained by collision complexes of high multiplicity crossing onto surfaces with lower multiplicity and exciting the transition state on this low multiplicity surface to products. [178]

Irrespective of the precise mechanistic details of cation-N atom processes, the data presented in the current study reinforces the suggestion that spin conservation is an unimportant parameter in these reactions. [178]

Sufficient reactions between hydrocarbon cations and atomic nitrogen have now been studied to make some generalisations. As already remarked upon in Section 5.5, lower mass hydrocarbon cations, ($C_mH_n^+$; $m \leq 3$), tend to react with N atoms by the formation of C-N bonds and the accompanying elimination of H or H_2. In contrast, higher mass hydrocarbon species react with N atoms to form HCN and a lower mass hydrocarbon cation fragment. The other trend that is evident is that hydrocarbon cations with an even number of hydrogen atoms, (eg. C_3^+, $C_2H_2^+$, $C_2H_4^+$, $C_6H_2^+$, and $C_6H_6^+$), tend to undergo faster reactions with N atoms than those with an odd number of hydrogen atoms. The only exceptions to this observation are the highly unsaturated hydrocarbon cations such as CH^+, and C_3H^+, which also undergo rapid reactions with N atoms. Highly unsaturated hydrocarbon ions are very energetic [31] and it is perhaps not surprising that they are reactive with many neutral species, including atomic nitrogen. Hydrocarbon cations with even numbers of H atoms are invariably doublets, whereas those with odd numbers of hydrogen atoms are usually singlets. Doublet cations may react with atomic nitrogen via either a quintet or triplet transition state, whilst the singlet cations can only react with this neutral via a quartet state. The provision of a manifold of states, (ie. quintet or triplet), to the collision complex may conceivably facilitate particular reactions and quicken their kinetics. The above comments are highly preliminary. A thorough characterisation of the potential surfaces of the collision complexes, in concert with entry and egress routes onto these transition states from reactants and to products respectively, is needed before any definitive conclusions may be drawn.

The trend that most species, including hydrocarbon cations, are unreactive with molecular nitrogen [24, 50] is reinforced by the data collected in the current study. With molecular nitrogen present as the neutral reactant the only pathway for reaction is a slow termolecular association, ($H_3^+ + N_2$ is the obvious exception to this statement).

The study has enabled the characterisation of the reactivity of five nitrile cations with atomic nitrogen. These are the first nitrile cation-N atom reactions to be investigated in laboratory experiments. Interestingly, several nitrile cations appear to react rapidly with atomic nitrogen. There is no clear

mechanistic pattern, (as indicated by the product channels), via which these reactions occur, although in two cases, (HCN^+, and HC_3N^+), the reaction proceeds via N atom transfer from cation to neutral, thereby forming N_2.

The reaction of several O atom containing cations with atomic nitrogen produces NO^+, or NO; these species may have particular stability.

As noted in the preceding chapter, the structures of the hydrocarbon cations used in these experiments were not always unequivocally identified. In a minority of cases it was assumed that the configuration of the cation was the structure that most closely approximated the atomic arrangement in the neutral precursor. This rationale is not infallible, as cyclic neutral molecules sometimes give rise to acyclic ions and vice versa.

A considerable volume of new data, pertaining to the reaction of various cations with atomic and molecular nitrogen, has been presented in this chapter. Of the 31 cation-N atom reactions investigated in this study, only 11 have been previously examined. In a few cases discrepancies have occurred between data published in the chemical literature and the results obtained from the present study. Many of the cation-N atom reactions studied are relevant to chemical processes occurring in interstellar clouds or planetary atmospheres. Data has also been gathered for the (non) reaction of 34 cations with molecular nitrogen. Only 11 of these 34 reactions have been previously reported in the literature. Much of this data is relevant to the chemistry of nitrogenous extraterrestrial atmospheres, eg. Titan. [282, 283] The inclusion of the results gained from the current study in interstellar ion-chemical models may well effect significant changes in the number densities of many observed interstellar species.

CHAPTER 6.

THE REACTION $H_3^+ + N$ AND INTERSTELLAR AMMONIA.

6.1: Introduction.

Ammonia was the first polyatomic molecule to be detected in the interstellar medium. It was identified in 1968 towards Sgr B2 from its microwave emission spectrum. [334] NH_3 has subsequently been observed in several objects including the Orion molecular cloud, TMC-1, L134N and is a widespread constituent of interstellar clouds. [230, 335] In their paper announcing the first observation, Cheung et al. remarked "Since NH_3 is a fairly complex molecule, it is most likely formed by adsorbed N and H atoms on interstellar grain surfaces rather than by successive binary collisions". [334]

The $N^+ + H_2$ Route to Interstellar Ammonia

The suggestion of Cheung and co-workers [334] that interstellar ammonia was probably formed via heterogenous chemistry on the surfaces of interstellar dust grains was favoured for several years after the initial astronomical observation. This "grain chemistry" route did not gain universal acceptance however, as the proposal lacked a convincing mechanism for the post-synthesis volatilisation of the NH_3 molecules into the gas phase. This problem still remains to this day and is one of the major unresolved issues facing researchers who are interested in the production of interstellar molecules on the surfaces of interstellar dust grains.

A plausible gas phase mechanism to explain the presence of NH_3 in the interstellar medium was not forthcoming until 1973, when Herbst and Klemperer published their seminal paper on gas phase ion-molecule synthesis. [14] They suggested that the synthetic route to interstellar ammonia might originate with

the reaction of N^+ and molecular hydrogen and thence proceed via the following sequence, (hereafter HK): [14, 24]

$N^+ + H_2 \Rightarrow NH^+ + H - 0.2$ eV **(601)**

$k_{(601)\ 300K} = (5.0 \pm 1.0) \times 10^{-10}$ cm^3 s^{-1}

$NH^+ + H_2 \Rightarrow NH_2^+ + H + 2.0$ eV **(602)**

$k_{(602)\ 300K} = (1.0 \pm 0.3) \times 10^{-9}$ cm^3 s^{-1}

$NH_2^+ + H_2 \Rightarrow NH_3^+ + H + 1.2$ eV **(603)**

$k_{(603)\ 300K} = (2.0 \pm 1.0) \times 10^{-10}$ cm^3 s^{-1}

$NH_3^+ + H_2 \Rightarrow NH_4^+ + H + 0.9$ eV **(604)**

$k_{(604)\ 300K} = (4.4 \pm 0.9) \times 10^{-13}$ cm^3 s^{-1}

and finally the ion-electron recombination process: [57, 69]

$NH_4^+ + e^- \Rightarrow NH_3 + H + 4.8$ eV **(605)**

$\alpha_{e(605)\ 300K} = (1.4 \pm 0.2) \times 10^{-6}$ cm^3 s^{-1}

In the HK reaction sequence there are three areas of difficulty.

Firstly, Marquette et al. [336] have established that reaction **(601)** is endothermic by about 1734 J mol^{-1}, although in their compendium of thermodynamic data Lias et al. [31] tabulate its endothermicity as 20,900 J mol^{-1}. Notwithstanding this discrepancy, reaction **(601)** is undoubtedly endothermic. This determination casts doubt as to the efficacy of the primary step of the HK mechanism. A number of researchers have considered whether an ~ 1734 J mol^{-1} barrier is sufficient to retard this reaction at the low temperatures of interstellar clouds. In 1984 Adams et al. proposed that N^+ produced in the dissociative charge transfer reaction between helium ions and N_2 may have up to 0.14 eV of kinetic excitation, viz: [24, 337]

$He^+ + N_2 \Rightarrow N^+ + N + He + 0.3$ eV **(606)**

$k_{(606)\ 300K} = (4.8 \pm 0.6) \times 10^{-10}$ cm^3 s^{-1}

Using this idea, Yee and colleagues [338] derived the gas phase equilibrium energy distributions of N^+ ions with temperatures between 10 - 70 K, and subsequently calculated effective reaction rate coefficients for reaction **(601)** over this temperature range. Their derived value for $k_{(601)}$ was 1.3 x 10^{-12} cm^3 s^{-1} at 10 K, rising to 3.1 x 10^{-10} cm^3 s^{-1} at 70 K. [338]

Galloway and Herbst published a paper in 1989, which discussed the effect of the spin orbit state of N^+ on reaction **(601).** [339] In 1991 Boulot examined how

the interstellar ratio of ortho to para H_2 would impact on the same reaction. [340] The current view is that the $N^+ + H_2$ reaction is sufficiently rapid in the interstellar medium to sustain an acceptable rate of formation of NH_3 at temperatures down to 10 K. Under interstellar conditions the rate coefficient for this process remains somewhat indeterminate, with values of 10^{-18} cm^3 s^{-1} to 10^{-13} cm^3 s^{-1} proposed. [13, 339] Recent models assume that the rate constant for reaction **(601)** is given by the rough approximation: $k = 1 \times 10^{-9} \exp(-85/T)$ cm^3 s^{-1}. [13, 16]

The second problem with the HK synthetic scheme is reaction **(604)** which is slow at room temperature and has a small activation barrier. The rate coefficient for the $NH_3^+ + H_2$ process decreases as the temperature is lowered, reaching a minimum at about 80 K. At even lower temperatures the rate constant for this reaction increases again due to tunnelling through the activation barrier. [341] Considering the high relative abundance of molecular hydrogen, and the increase in rate coefficient at temperatures below 80 K, reaction **(604)** remains sufficiently fast to not impede the formation of NH_3.

The third area of uncertainty concerns the products of the dissociative recombination reaction **(605)**. This reaction has been investigated in the laboratory and a fractional H atom contribution to the product distribution of ~ 1 reported. [69] This indicates that the $NH_3^+ + H$ product channel is significant, however atomic hydrogen would also be formed if the $NH + H_2 + H$ or $NH_2 + 2H$ pathways were accessed during dissociative recombination. The measurement of a complete branching ratio is required to resolve this ambiguity. Both $NH_3 + H$ and $NH_2 + H_2$ have been suggested as the major product channels, although the experimental data of Adams and co-workers implies that the $NH_2 + H_2$ channel is probably minor. [69]

It has generally been assumed that H atom loss during dissociative recombination is a reasonably efficient process [342] however a recent experimental investigation of the dissociative recombination of H_3O^+ indicates that the $H_2O + H$ channel accounts for just 5 % of the product channels. [58] Conflicting data has been presented by Anderson et al. in experiments carried out using a heavy ion storage ring in which they measure a 33 % channel to $H_2O + H$. [56] This disparity between the two measurements has yet to be resolved.

Notwithstanding these three areas of difficulty, the HK synthesis has been preferred by most modellers as the mechanism for NH_3 synthesis.

Production of NH_3 via $H_3^+ + N$

In 1974 Dalgarno put forward an alternative synthesis initiated by the reaction between H_3^+ and atomic nitrogen, that bypassed the initial two steps [reactions **(601)** and **(602)**] in the HK scheme, viz: [343]

$$H_3^+ + N \Rightarrow NH_2^+ + H + 1.0\ eV \qquad \textbf{(607)}$$

This mechanism has largely been discounted in favour of reactions **(601)** and **(602)** for several reasons. Huntress questioned the viability of reaction **(607)** on the basis that H_3^+ invariably reacts via proton transfer, not H_2^+ transfer. [344] Many modellers (eg. Bourlot [340] ; Graedel et al. [345] ; Millar et al. [346]) have ignored reaction **(607)** in their models.

Part of the dilemma in deciding whether or not to include reaction **(607)** was because no satisfactory laboratory measurements were available. In 1986 Huntress and colleagues made a preliminary study of reaction **(607)** using an ICR instrument and reported a rate coefficient of 6.5×10^{-10} $cm^3\ s^{-1}$. [24, 184] They also claimed the production of approximately equal quantities of NH^+ and NH_2^+. [24, 184] The generation of NH^+ from ground state H_3^+ and atomic nitrogen is 98.7 $kJ\ mol^{-1}$ endothermic, which indicates that either the nitrogen source must have contained metastable species or that some of the H_3^+ ions must have been vibrationally excited. In this ICR experiment the observed NH_2^+ product could have been formed directly via reaction **(607)**, or indirectly via reaction **(602)**.

There are several reasons why the $H_3^+ + N$ reaction has not been revisited in the laboratory. Most ion-N atom reactions have been studied using flow tube techniques whereby atomic nitrogen is generated by passing N_2 through a microwave discharge in a side entry port to the flow tube. [135] Less than 1 % dissociation of N_2 into N atoms is typical for this process, hence only a small flux of atomic N, in a large excess of molecular nitrogen, enters the flow tube. [177, 179] This dilute mixture of N atoms in a nitrogen buffer usually presents few difficulties as most cations are unreactive with molecular nitrogen. [24] Unfortunately this generalisation fails in the case of H_3^+ which undergoes a collision rate proton transfer reaction to N_2, viz: [24]

$H_3^+ + N_2 \Rightarrow N_2H^+ + H_2 + 0.7\ eV$ **(608)**

$k_{(608)\ 300K} = (1.9 \pm 0.2) \times 10^{-9}\ cm^3\ s^{-1}$

The presence of this rapid reaction channel between H_3^+ and N_2 is likely to impede the observation of the $H_3^+ + N$ reaction, particularly when ~ 99 % of the neutral flow is undissociated nitrogen.

Mindful of the lack of an adequate experimental measurement, in 1987 Herbst and co-workers carried out ab-initio calculations of the NH_3^+ potential surface in which they searched for barrier-free pathways linking reactants and products. [184] The reactants, N (^4S) and H_3^+ ($^1A_1'$), collide on an NH_3^+ potential surface with quartet multiplicity. This intermediate is an excited state of the $(NH_3^+)^*$ complex which correlates with the ground state products NH_2^+ ($^3B_1$) and H (^2S). Several different entrance and exit channel geometries were examined as the authors attempted to assess the contribution (if any) of the $H_3^+ + N$ reaction to interstellar ammonia production. This theoretical study found that reaction **(607)** possesses a significant activation barrier, rendering it unimportant under interstellar cloud conditions. Herbst, DeFrees and McLean concluded that the $H_3^+ + N$ pathway was not effective in ammonia synthesis. [184] As a result of their work, NH_3 generated via the interaction between H_3^+ and N atoms has largely been discredited, (eg. Pineau des Forets et al. [347]).

Production of NH_3 on Interstellar Dust Grains

To further complicate matters, astronomers have detected high abundances of ammonia in the hot core of Orion. This observation has been construed as evidence of NH_3 release from interstellar dust grains during heating. [348] The astronomical data appears to indicate that different mechanisms may be operating in discrete subregions of interstellar clouds. Figure 6.1 gives a summary of the possible synthetic routes to ammonia in the interstellar medium.

Reasons for Performing an Experimental Study of the $H_3^+ + N$ Reaction

Several factors have lent impetus to undertake an experimental measurement of the $H_3^+ + N$ reaction. The theoretical contribution of Herbst and colleagues, along with several other articles, argued that an experimental study of reaction **(607)** was vital. [17, 184, 343] Additionally, in 1996 the H_3^+ species was observed in the interstellar medium for the first time [22] at approximately the densities expected from the models. [13, 16] Finally the project contained

numerous experimental challenges that needed to be overcome in order to characterise an important ion-neutral reaction.

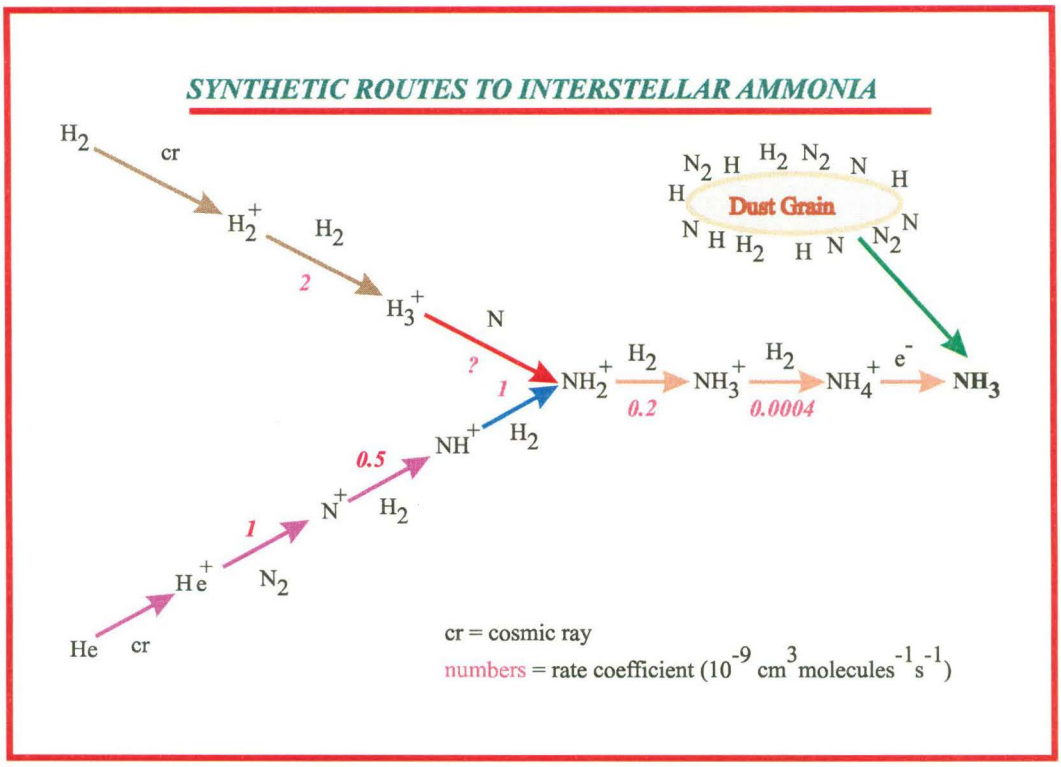

Figure 6.1. A summary of the possible synthetic routes to ammonia in the interstellar medium.

6.2: Experimental.

The H_3^+ ion was generated from Kr^+ ($^2P_{3/2}$ and $^2P_{1/2}$) which was injected into a hydrogen bath gas, (zero grade, > 99.995 % pure, supplied by BOC Gases), or, alternatively, a helium carrier gas in which H_2 was added at the first inlet port of the flow tube. The krypton ion source gas, (research grade quality, nominal purity > 99.995 %), was supplied by Alphagaz. H_3^+ was then produced in the flow tube from Kr^+ according to the following reaction sequence: [24, 349]

$$Kr^+ + H_2 \Rightarrow KrH^+ + H + 0.3\ eV \qquad \textbf{(609)}$$

$$k_{(609)\,300K} = (2.1 \pm 0.6) \times 10^{-10}\ cm^3\ s^{-1}$$

$$KrH^+ + H_2 \Rightarrow H_3^+ + Kr - 0.02\ eV \qquad \textbf{(610)}$$

$$k_{(609)\,300K} = (3.3 \pm 0.8) \times 10^{-10}\ cm^3\ s^{-1}$$

Kr^+ was chosen as the precursor for H_3^+ (rather than H_2^+ or Ar^+) as it offered the best source of H_3^+ in its lowest vibrational state. [349] The ergicities of the above reactions indicate that little surplus energy is available to excite the H_3^+

species, indeed reaction **(610)** is slightly endothermic. This endoergicity results in the establishment of an equilibrium between KrH^+ and H_3^+. In the flow tube, the H_2 number density is ~ $10^6 - 10^9$ times larger then either the Kr^+ or KrH^+ densities, hence the H_3^+/KrH^+ ratio is overwhelmingly in favour of H_3^+. The H_3^+ ions are formed chiefly in the $v = 0$ vibrational level with perhaps a minor quantity of H_3^+ ($v = 1$) because of possible vibrational excitation in the KrH^+ ions. [349]

N atoms were produced in a quartz side tube by a microwave discharge of N_2, (or, alternatively, a mixture of N_2 in He). Zero grade N_2, (> 99.998 % pure), was supplied by BOC Gases. The "secondary N atom probe", as detailed in the previous chapter of this thesis, was used for this section of work. The distance from probe's elbow to the point of entry into the main flow tube was made as short as possible, being ~ 10.5 cm. This particular probe design was favoured because it shortened the distance from the microwave discharge cavity to the reaction zone, thereby maximising the flux of N atoms available for reaction. Figure 2.5 in Chapter 2 of this thesis shows this probe in operation. Vibrationally excited N_2 molecules were eliminated from the discharged gas flow by a glass wool plug located in the side tube immediately downstream from the discharge but prior to the light horn. [179] This configuration also minimised the metastable atom [$N(^2D)$ and $N(^2P)$] number densities in the neutral gas stream entering the flow tube with only about 1 % of all N atoms expected to be metastable. [280] Moreover, both $N(^2D)$ and $N(^2P)$ are known to be efficiently deactivated by wall collisions [281] and therefore the presence of the glass wool plug resulted in additional attrition of the metastable atom densities.

The extent of dissociation of N_2 into $N(^4S)$ atoms was conveniently monitored utilising the reaction between $C_2H_2^+ + N$ which has a well established value for the rate coefficient, viz: [177, 178]

$C_2H_2^+$	+	N	⇒	CH^+	+	HCN	+	0.4 eV	(0.05)	**(611a)**
			⇒	C_2N^+	+	H_2	+	>0.9 eV	(0.35)	**(611b)**
			⇒	HC_2N^+	+	H	+	0.5 eV	(0.60)	**(611c)**

$k_{(611)\,300K} = (2.5 \pm 0.5) \times 10^{-10}$ cm^3 s^{-1}.

Note that during the course of the ion-N atom research, (Chapter 5), an additional product channel ($HCNH^+ + C$) was observed for reaction **(611)**. To determine

the degree of N_2 dissociation on any given day the "raw" (or apparent) rate coefficient for reaction **(611)** was measured and this value compared with the absolute rate constant, $k_{(611)}$.

An absolute value of the rate coefficient for reaction **(611)** was obtained by performing an "NO titration". The atomic nitrogen density in the flow tube was determined by titrating the N atoms with nitric oxide as described by Viggiano et al., [177] and has been comprehensively detailed in Chapter 5. Using this methodology, $k_{(611)}$ is found to be 2.4 x 10^{-10} cm^3 s^{-1} which is in excellent agreement with the earlier measurements. [177, 178] There is no reaction between $C_2H_2^+$ and N_2, ($k < 5$ x 10^{-13} cm^3 s^{-1}). In these experiments a typical degree of dissociation of N_2 downstream from the glass wool plug was 0.4 % for pure N_2, increasing to 1.5 % for a 5 % N_2 / He mixture.

6.3: Results and Data Analysis.

Evidence for only one product channel, namely $NH_2^+ + H$, was found for reaction **(607)**, which is consistent with the thermochemistry. This pathway is the only exothermic bimolecular channel, ($\Delta H° = -97.9$ kJ mol^{-1}). The alternative proton transfer channel [reaction **(612)**] is endothermic by ~ 1 eV or + 98.7 kJ mol^{-1}, viz:

$$H_3^+ + N \Rightarrow NH^+ + H_2 - 1.0\ eV \qquad \textbf{(612)}$$

The product ion of reaction **(607)**, NH_2^+, was not directly observed as it was quickly converted to NH_3^+ and then more slowly to NH_4^+ in the presence of hydrogen, via reactions **(603)** and **(604)** respectively. H_2 was always resident in the flow tube as it is needed to convert Kr^+ to H_3^+ via reactions **(609)** and **(610)**. Most measurements were conducted using a hydrogen bath gas. In a hydrogen bath gas, all the NH_3^+ was converted to NH_4^+ via reaction **(604)**, whereas in a helium bath gas both NH_3^+ and NH_4^+ were observed.

The possibility that the observed NH_3^+ product was also produced by a three-body association reaction cannot be completely discounted, viz:

$$H_3^+ + N + M \Rightarrow NH_3^+ + M + 6.7\ eV \qquad \textbf{(613)}$$

Several hydrocarbon ions undergo termolecular association with atomic hydrogen, [350] (see Chapter 4), but two factors make association in the $H_3^+ + N$ system less likely. Firstly, 645.6 kJ mol^{-1} of energy must be apportioned

amongst six internal degrees of freedom for NH_3^+ to survive until collisional stabilization can occur. This exoergicity is significantly larger than that in any of the hydrocarbon ion-H atom reactions where association is observed. [350] Furthermore, these $C_mH_n^+$-H atom systems have more internal modes available to dissipate energy. Whilst possible, the direct association of H_3^+ and N to generate NH_3^+ is thus unlikely.

Methodology of Data Analysis

In the following discussion $\{NH_2^+\}$ represents the total ion signal measured for all the product ions that have their inception in the NH_2^+ generated via reaction **(607)**. That is, $\{NH_2^+\} = [NH_4^+]$ in a hydrogen bath gas and $\{NH_2^+\} = ([NH_3^+] + [NH_4^+])$ in a helium bath gas. It was of course essential to verify that $\{NH_2^+\}$ was derived only from reaction **(607)** and from no other source. This was achieved by demonstrating that the $\{NH_2^+\}$ signal was only present with the microwave discharge on and with H_3^+ present in the flow tube.

The determination of the rate coefficient for reaction **(607)** required a very different methodology to the usual procedure of measuring a rate coefficient in a flow tube. Usually the rate coefficient is derived from the slope of the semilogarithmic decay of the reactant ion signal with neutral reactant flow. This standard technique could not be employed in the present situation because virtually all the H_3^+ signal was depleted by N_2 and not N. Instead, the rate coefficient for the reaction between H_3^+ and atomic nitrogen was calculated from the ratio of the product ion signals of reaction **(607)**, $\{NH_2^+\}$, and the simultaneous reaction **(608)**, $[N_2H^+]$, viz:

$$\frac{\{NH_2^+\}}{[N_2H^+]} = \frac{k(H_3^+ / N)}{k(H_3^+ / N_2)} x \frac{Q(N)}{Q(N_2)} \qquad \textbf{(614)}$$

In equation **(614)**, $k(H_3^+ / N)$ and $k(H_3^+ / N_2)$ are the rate coefficient values for reactions **(607)** and **(608)** respectively. Similarly, $Q(N)$ and $Q(N_2)$ represent the respective flow rates of N and N_2, (in Torr L s^{-1}). Other symbols have been previously defined. The rate coefficient for the $H_3^+ + N_2$ reaction **(608)** is well-established [5] and was readily verified in the conventional manner with the discharge off. The measured value of the rate coefficient for reaction **(608)**, was $(1.7 \pm 0.2) \times 10^{-9}$ cm^3 s^{-1} which is within experimental error of the evaluated literature value of $(1.9 \pm 0.2) \times 10^{-9}$ cm^3 s^{-1}. [24] The $\{NH_2^+\}$ / $[N_2H^+]$ ratio was

measured with the microwave discharge on and was subsequently corrected for mass discrimination and differential diffusion of the ions. $Q(N)$ was found from the degree of dissociation of N_2 measured in additional, independent experiments utilising the calibration reaction $C_2H_2^+ + N$, **(611)**. Once $Q(N)$ was ascertained, $Q(N_2)$ was derived using the following relation:

$$\%Dissociation = \frac{Q(N)}{2 \,.\, Q(N_2)} \qquad \textbf{(615)}$$

All parameters in equation **(614)**, save $k(H_3^+ / N)$, were thus available; the rate coefficient for the reaction $H_3^+ + N$ was therefore calculated by an appropriate rearrangement of equation **(614)**.

Equation **(614)** implies that the $\{NH_2^+\} / [N_2H^+]$ ratio should be invariant and independent of N_2 flow rate, providing the degree of dissociation does not change and given that all the reactant H_3^+ ion has been converted to products. A typical set of experimental data, (Figure 6.2 below), shows that this prediction was in fact observed.

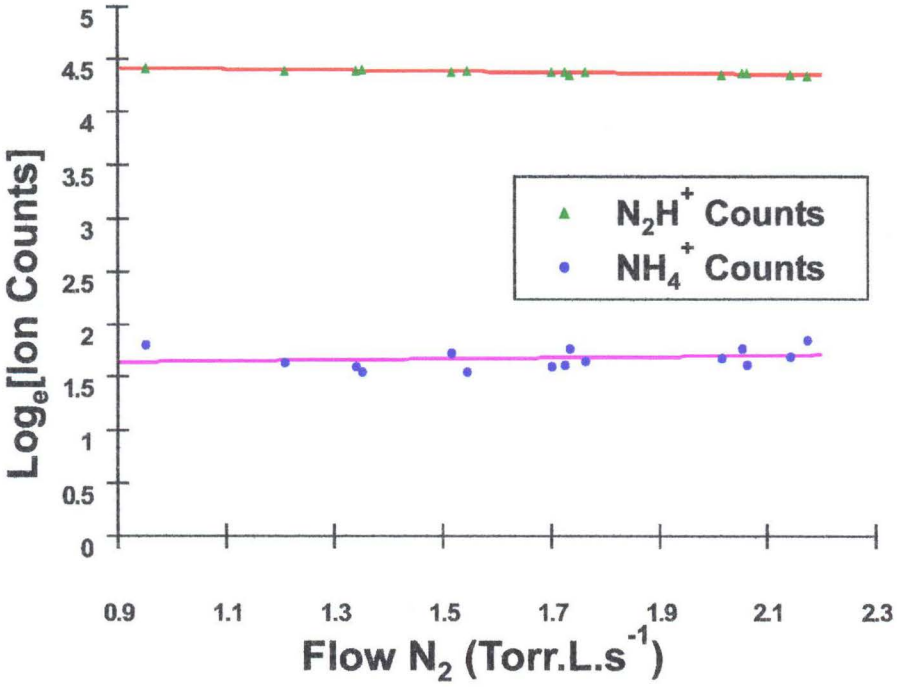

Figure 6.2. The variation in ion products $\{NH_2^+\}$ and $[N_2H^+]$ at varying N_2 flows in a hydrogen carrier using 100 % N_2 in the microwave discharge. Under these conditions $\{NH_2^+\} = [NH_4^+]$. The ratio of these ion signals provides the H_3^+ / N rate coefficient via equation (614).

Theoretical Justification of Analytical Method

The rate coefficient for the generic ion-neutral reaction,

$A^+ + B \Rightarrow$ Products is evaluated from the following conventional flow tube equation: [144]

$$Ln\left(\frac{[A^+]}{[A^+]_0}\right) = -\frac{kQ_B(z+\varepsilon)}{\pi a^2 v_0 v_i} \qquad \textbf{(616)}$$

In this expression $[A^+]$ is the count of A^+ with a given flow of neutral B, Q_B, (in Torr L s^{-1}) ; $[A^+]_0$ is the count of A^+ with zero flow of B; $(z + \varepsilon)$ is the reaction distance, corrected for inlet port perturbation; a is the flow tube radius; v_0 is the bulk flow velocity of the bath gas; and v_i is the average ion velocity. In accordance with the general mathematical formalism used by Tosi and colleagues [154] equation **(616)** can be simplified as follows:

$$[A^+] = [A^+]_0 \exp\left(-R(B)\ .\ Q(B)\right) \qquad \textbf{(617)}$$

In equation **(617)**, $R(B) = k\left(\frac{z+\varepsilon}{\pi a^2 v_0 v_i}\right)$

Applying equation **(617)** to the particular case of H_3^+ loss via concomitant reactions with N_2 and N, [reactions **(607)** and **(608)**], generates the following equations for $[N_2H^+]$ and $\{NH_2^+\}$:

$$[N_2H^+] = \left([H_3^+]_0 - [H_3^+]\right) \cdot \frac{R(N_2)Q(N_2)}{\left(R(N_2)Q(N_2) + R(N)Q(N)\right)} \qquad \textbf{(618)}$$

$$\{NH_2^+\} = \left([H_3^+]_0 - [H_3^+]\right) \cdot \frac{R(N)Q(N)}{\left(R(N_2)Q(N_2) + R(N)Q(N)\right)} \qquad \textbf{(619)}$$

In the above expressions, $[H_3^+]_0$ is the count rate of H_3^+ with zero flow of the neutrals N_2 and N. Similarly, $[H_3^+]$ is the count rate of H_3^+ at specific discrete flow rates of N_2 and N. All other symbols have been defined previously. Equation **(614)** is obtained by taking the ratio of equation **(619)** and equation **(618)**. Alternatively, relation **(614)** may also be derived by taking the ratio of the formation rates of $\{NH_2^+\}$ and $[N_2H^+]$ and integrating, viz:

$$k(H_3^+ / N)[N]d[N_2H^+] = k(H_3^+ / N_2)[N_2]d\{NH_2^+\} \qquad \textbf{(620)}$$

Value of the Rate Coefficient for $H_3^+ + N$

The average of sixteen separate experimental measurements gave a value for the rate coefficient of the reaction between H_3^+ and N, [reaction **(607)**], of $(4.5 \pm 1.8) \times 10^{-10}$ cm^3 s^{-1}. The Langevin collision rate for this reaction is 1.6×10^{-9} cm^3 s^{-1}.

6.4: Why Should H_3 + N be Fast?

The theoretical study of the NH_3^+ potential surface by Herbst and co-workers predicted that reaction **(607)** has a large activation barrier and concluded that this reaction was unimportant. [184] The authors of this paper argued that as N has ^4S symmetry and H_3^+ has $^1A_1'$ symmetry, then the reactive encounter must occur on a surface that is characterised by quartet multiplicity, ie:

$$H_3^+(^1A_1') + N(^4S) \Rightarrow NH_3^+(^4) \Rightarrow NH_2^+(^3B_1) + H(^2S) \quad \textbf{(621)}$$

The reactants cannot access the ground ($^2A_2''$) electronic state of NH_3^+. With these spin conservation constraints, Herbst et al. concluded that the pathways they investigated, corresponding to three distinct entrance and exit channel geometries, all contained barriers. They did however qualify this conclusion by stating that their calculations could have missed "a low energy pathway of quartet multiplicity". Furthermore they commented that "given the number of degrees of freedom in the problem, the possibility of missing such a pathway cannot be dismissed out of hand". [184] Recently, Maclagan surveyed several lowered symmetry pathways in an effort to find a viable route from reactants ($H_3^+ + N$) to products ($NH_2^+ + H$). [351] Unfortunately this study was unsuccessful and the precise details of the mechanism for reaction **(607)** are still unclear.

There is also considerable doubt as to the inviolability of spin conservation in ion-atom reactions. Ferguson [254] and Federer et al. [178] have observed a number of rapid ion-N atom reactions that do not conserve spin. Spin does appear to be conserved in the $H_3^+ + N$ reaction, certainly in terms of the macroscopic conversion of reactants to products. It is however conceivable that spin conservation may be violated during some facet of the reactive encounter. Indeed, Federer and colleagues have conjectured that multiple curve crossings between surfaces of different multiplicities may not be rare in ion-atom reactions and can occur within the orbiting complexes formed in collision. [178]

6.5: Interstellar Ammonia Synthesis.

The measurement of a fast rate coefficient for the $H_3^+ + N$ reaction suggests that the synthesis of ammonia in interstellar clouds may be initiated by reaction **(607)**, in addition to the $N^+ + H_2$ process, **(601)**. These two synthetic pathways are readily compared, as reactions **(603)** through **(605)** are common to both routes. Reaction **(602)** is fast at 20 K, hence computation of the relative rates of reactions **(601)** and **(607)**, [ie. **R(601)** and **R(607)**], under typical interstellar conditions gives a quantitative comparison of the two synthetic schemes for ammonia. Using the number densities calculated by Lee et al. [16] in their new standard model, and tabulated below in Table 6.1, the relative rates at 10 K, are **R(607) / R(601)** ~ 6.3, and at 50 K, **R(607) / R(601)** ~ 1.1. Concomitant changes to the number densities of ammonia and various other species, (eg. NH_2CN, HNC^+ and NH_2CNH^+), also occur when the rate coefficient for the reaction of $H_3^+ + N$ is incorporated into standard models. [352]

Species / nH_2	**10 K**	**50 K**
N	1.9×10^{-5}	6.6×10^{-6}
N^+	2.3×10^{-11}	9.7×10^{-14}
H_3^+	3.5×10^{-9}	6.6×10^{-9}
R(601) / (particle cm^{-3} s-1)	1.2×10^{-16}	4.4×10^{-16}
R(607) / (particle cm^{-3} s^{-1})	7.5×10^{-16}	4.9×10^{-16}
R(607) / R(601)	6.25	1.11

Table 6.1. Number Densities evaluated by Lee et al, [16] in their new standard model for steady state conditions at 10 K and 50 K, relative to a H_2 density of 5×10^3 cm^{-3}. The calculated rates of reactions (601) and (607), [R(601) and R(607)], using this data are also tabulated.

If the observed rate coefficient for reaction **(607)** is approximately invariant with temperature change (which is usual for exothermic bimolecular ion-molecule reactions dependent on charge induced dipole interactions) then increased ammonia production will occur in models utilising the $H_3^+ + N$

reaction. Reaction **(607)** may be the primary production source for NH_3 at temperatures around 10 K with both mechanisms having equal roles around 50 K. Should present estimates of the low temperature rate coefficient for the $N^+ + H_2$ reaction be inflated, then the $H_3^+ + N$ mechanism will have the dominant role.

6.6: Conclusions.

The rapid rate coefficient measured for the reaction between $H_3^+ + N$ is contrary to the theoretical prediction for this reaction. [184] It is perhaps not too remarkable that ab-initio calculations have failed to identify the pathway for this process, given the complexity of the potential surface. The $H_3^+ + N$ reaction seems to conserve spin, but to accomplish this the reactive encounter must occur on a quartet potential surface of NH_3^+. If so, the ground state ($^2A_2''$) NH_3^+ surface, lying ~ 646 kJ mol^{-1} below the entrance level of the reactants, is inaccessible.

The reaction between $H_3^+ + N$ to yield $NH_2^+ + H$ is unusual for reactions of H_3^+ which invariably proceed by proton transfer. In this case an H_2^+ fragment has been transferred from the ion to the neutral species, or alternatively one may view such a reaction as loss of a hydrogen atom from the collision complex. Only one other such reaction is known, namely that of $H_3^+ + O$ which is also rapid and has two exothermic channels, viz: [24, 180]

$$H_3^+ + O \Rightarrow OH^+ + H_2 + 0.7\ eV \qquad \textbf{(622a)}$$

$$\Rightarrow H_2O^+ + H + 1.7\ eV \qquad \textbf{(622b)}$$

$k_{(624)\ 300K} = (8 \pm 4) \times 10^{-10}\ cm^3\ s^{-1}$

The weighting of each channel could not be determined by Fehsenfeld as both product ions were depleted by secondary reaction with the H_2 present in the flow tube, forming the "terminal ion", H_3O^+. [180] Currently, only these two fast ion-atom reactions of H_3^+, ($H_3^+ + N$ and $H_3^+ + O$), are known to proceed via an H atom loss mechanism. [24, 180]

The observation for the first time of H_3^+ in interstellar clouds [22] at roughly the densities predicted by models [13, 16] provides additional support for an ion-molecule mechanism of formation for many molecules known to reside in interstellar clouds. A long overdue laboratory measurement of the rate

coefficient for the reaction between H_3^+ ions and atomic nitrogen has been performed. The value for this rate constant is $(4.5 \pm 1.8) \times 10^{-10}$ cm^3 s^{-1}. This experimental result confirms that the reaction between $H_3^+ + N$ forming $NH_2^+ + H$ is fast and provides a significant new source of ammonia in cold dark interstellar clouds.

CHAPTER 7.

REACTIONS OF SOME CATIONS WITH ATOMIC AND MOLECULAR OXYGEN.

7.1: Introduction.

The first experimental study of a reaction between an ion and atomic oxygen was reported by Ferguson and colleagues in 1965. [189] These workers measured a rate constant and determined the product channel for the reaction between N_2^+ cations and O atoms, viz:

$$N_2^+ + O \Rightarrow NO^+ + N + 3.1\ eV \qquad \textbf{(701)}$$

$$k_{(701)\ 300K} = (2.5 \pm 1.0) \times 10^{-10}\ cm^3\ s^{-1}$$

The impetus for studying this process was the suggestion that it played an important role in the E and F1 regions of the Earth's ionosphere. [189] Aeronomy therefore, rather than interstellar chemistry, sparked the first efforts to characterise cation-O atom reactions.

To date, relatively few reactions involving cations and atomic oxygen have been investigated, [24, 50] despite more than thirty years having elapsed since the first experiment was conducted in this field. Indeed the paucity of reliable experimental measurements for cation-O atom reactions is a large and obvious gap in the database of ion-neutral reactions.

The principal reason for the lack of experimental data on cation-O atom reactions is that the experiments are quite difficult to perform. Atomic oxygen is not a trivial reagent to generate and monitor. Generally O atoms have been produced by forming atomic nitrogen in a microwave discharge of N_2 and then titrating the N atoms with measured flow rates of nitric oxide to form known fluxes of atomic oxygen. [161, 177, 179, 180, 189] This technique has been previously

discussed in Chapter 5 of this thesis and the pertinent reaction is repeated here for the convenience of the reader: [85]

$$N + NO \Rightarrow N_2 + O + 3.3\ eV \qquad \textbf{(702)}$$

$k_{(702)\ 298K} = (3.4 \pm 1.0) \times 10^{-11}\ cm^3\ s^{-1}$

The neutral-neutral reaction between N and NO is very efficient, indeed Fehsenfeld and Ferguson suggested it is so rapid that in a properly designed apparatus the conversion of over 98 % of N atoms to O atoms should be attained. [161]

There are several obvious problems with this experimental methodology for the production of atomic oxygen. Firstly the flux of O atoms generated via this method is obviously small, as the precursor flux of N atoms is typically ~ 0.5 %. [161, 177] Secondly the number density of O atoms is affected by the processes of gas phase, (or "volume"), recombination and recombination on quartz / Pyrex or metal surfaces. The recombination coefficient for O atoms on quartz is quite large, being 3.75 s^{-1}. [353, 354] Ferguson and Fehsenfeld have suggested that this recombination may result in a reduction of the perceived rate constants for the reaction of ions with O atoms by typically ~ 20 %. [135, 161] Furthermore, this phenomenon of a significant amount of O-O recombination means that O_2 is entering the reaction zone of the flow tube in sufficient concentrations to possibly contaminate the results. [161] For this reason it is critical to know how a given cation reacts with O_2 when ion experiments are being conducted with atomic oxygen.

Oxygen atoms have two low-lying metastable states, namely ^1D and ^1S; these states are 1.97 eV and 4.19 eV above the ground state respectively. [135] In itself, reaction **(702)** is sufficiently exothermic to allow the formation of the ^1D excited state, however merged beam experiments indicate that the NO titration technique produces essentially pure O ^3P ground state atoms with only very small amounts of metastable atoms present. [355] To obviate difficulties with the presence of metastable atoms some researchers have preferred to produce atomic oxygen by the thermal dissociation of O_2. [356] At least one experiment has also been performed in which O atoms have been generated by subjecting a dilute mixture of O_2 in helium to a microwave discharge. [186] The disadvantage with this method is that excitation by the microwave discharge will produce a finite

concentration of metastable oxygen molecules, (O_2 a $^1\Delta_g$). The additional question of the reactivity of this metastable molecule with the cation being studied must therefore be addressed. [157, 357]

Although the first reaction between a cation and atomic oxygen was examined because of its relevance to aeronomy, [189] subsequent work in this area has concentrated on reactions that are applicable to the chemistry of planetary atmospheres, (eg. Mars and Venus), [161, 181] and interstellar clouds. [177, 178, 180] In terms of elemental abundances oxygen is a major constituent of dense molecular clouds. In their new standard model Lee et al. tabulate the number density of atomic oxygen in dense clouds as 1.5×10^{-4} atoms cm^{-3} at 10 K, and 9.0×10^{-5} atoms cm^{-3} at 50 K, relative to H_2 (= 1.0). [16] This species is thus relatively plentiful in interstellar molecular clouds and is therefore likely to be implicated in much of the chemistry occurring in these objects.

Aside from CO there are no substantial reservoir species for oxygen, hence atomic oxygen is present in high concentrations, (compared to most chemical species except H_2, H and CO), throughout a molecular cloud for the lifetime of the object. [205] In order to fully consider the chemistry occurring in the interstellar medium, it is important to investigate the reactions between ions likely to reside in the interstellar medium and O atoms. Although outside the scope of this thesis, some interstellar cloud ion-chemical modellers believe that neutral-neutral reactions involving O atoms may impact upon the interstellar formation of complex molecules. [205] Both ion-O atom and neutral-O atom reactions may be especially important in discrete regions of space such as the Orion compact ridge, which has abnormally high abundances of oxygen-containing organic molecules. [358] This clump within the Orion Molecular Cloud is adjacent to IRc2, a luminous infra-red source with an oxygen-rich outflow. [358]

In several research laboratories the reactions of many ions with O atoms and N atoms have been studied concurrently. [177, 180] The compendium of data on cation-O atom reactions is severely limited however, with no experiments having been performed on the reactivity of mid-range hydrocarbon cations, ($C_mH_n^+$; $m = 3 - 6$, $n \geq 1$), nitrile cations, or the HCO^+ and HCO_2^+ species with atomic oxygen. [24, 50, 135] Most of the small number of cation-O atom reactions which have been investigated demonstrate quite rapid kinetics, which further highlights

the importance of this class of reactions. Nevertheless the observed rate coefficients are all substantially less than the limiting Langevin collision rate. [24, 50, 135] In their 1980 paper Viggiano et al. suggested that such reactions often showed a strong correlation with negative temperature dependence, hence many cation-O atom reactions may well be more rapid at the temperatures of interstellar space. [177, 359] A further intriguing aspect of these processes is the propensity shown by many small hydrocarbon species to form C-O bonds when reacting with atomic oxygen. [24, 50, 135] It is of considerable interest to determine whether this trend continues as the size and complexity of the reactant hydrocarbon species is increased. The formation of C-O bonds may have relevance to the synthesis of such species as ketene, $H_2C{=}C{=}O$, which has been observed in the interstellar medium. [358]

The current study investigated the reaction of a number of cations with atomic oxygen. Most cations selected had not been the subject of prior experimental investigations although a small number, for which data currently exists in the chemical literature, were re-examined. These cations were CH_3^+, $C_2H_2^+$, H_2O^+ and N_2^+. The results obtained from the reaction of these "revisited" species with O atoms were compared with literature data and provided a check on the reliability of the experimental methods and data analysis procedures used.

Experimental data for the reaction of all cations studied with molecular oxygen and nitric oxide is also presented in this section of work. Since O_2 and NO were both present in the neutral reaction "soup", it was deemed necessary to obtain rate coefficients and product distributions for the reaction of all reactant cations with these neutral reagents. This additional experimentation was a necessary adjunct to the primary task of confirming the rate coefficients and product distributions for the reaction of the selected cations with O atoms.

Nitric oxide is an observed interstellar molecule but O_2 has no dipole moment and therefore has not been detected in the interstellar medium. [13, 17] Lee et al., in their new standard model, list the number density of molecular oxygen as 3.0×10^{-5} molecules cm^{-3} at 10 K, and 5.7×10^{-5} molecules cm^{-3} at 50 K, relative to H_2 (= 1.0). [16] They similarly estimate the number density of nitric oxide as 5.7×10^{-8} molecules cm^{-3} at 10 K, and 1.8×10^{-7} molecules cm^{-3} at 50 K, relative to H_2 (= 1.0). [16] A large body of data exists in the scientific literature for

the reaction of positive ions with both O_2 and NO and the reactions reported here further enlarge this database. [24, 50]

7.2: Experimental.

The experimental methodology and data analysis techniques used in the current study are well established and have been previously employed by several research groups.

The NO Titration Procedure

The NO titration procedure [177, 179] outlined in Chapter 5 of this thesis was used for all O atom reactions considered in the present work. For the sake of completeness, and as an aid to the reader, the salient points of this experimental method are reiterated below.

A microwave discharge in pure, (100 %), nitrogen was established to provide a small flux of atomic nitrogen, (~ 0.5 % fractional dissociation was typical). A small plug of glass wool, located a short distance downstream of the discharge region, served to remove vibrationally excited N_2 molecules and metastable N atoms, (^2D and ^2P), from the neutral flow. [135, 179] Nitric oxide was subsequently introduced into the neutral mixture in measured flow rates, thereby forming ground state O atoms via reaction **(702)**.

The probe was designed and constructed to ensure that, under all operating conditions, sufficient flow time was available for all neutral reactions to proceed to completion in the side tube. [85] The "tertiary N atom probe" was used to perform all the cation-O atom experiments discussed below. A comprehensive description of this probe, together with a labelled photograph, (Figure 5.1), is presented in Chapter 5 of this thesis.

The stoichiometry of reaction **(702)** indicates that for each NO molecule reactively consumed, one N atom is replaced by one O atom. Measured NO flow rates were added to the N_2 / N flow, under flowmeter control. The endpoint of the NO + O titration reaction was clearly visible for most systems as the intersection between two linear decays on a Ln[Cation$^+$] versus NO flow rate plot. Figures 7.1 to 7.3, (p. 168, p. 170, and p. 171), illustrate this phenomenon. For any particular experiment, at the precise endpoint of the titration the recorded NO flow was equal to the "original" flux of N atoms, (ie. the N atom flow before any NO had been added). Furthermore, at this point, all of the N atoms were

consumed and the O atom flow rate was equal to the endpoint flow of nitric oxide. This last statement is only approximately correct, as atomic oxygen recombines much more rapidly than does atomic nitrogen on surfaces. [353, 354] The gas phase recombination rate coefficient for atomic oxygen at 300 K, (in N_2), is however slow, being 2.8×10^{-33} cm^6 s^{-1}. [360] Due to surface recombination the rate coefficient data presented in this chapter for the reaction of selected cations with O atoms may be low by up to ~ 20 %. [135, 161] Determination of the titration endpoint facilitated the calculation of N and O atom fluxes for any measured NO flow rate. Simply put, any NO flow rate less than the endpoint of the titration was equivalent to the flow of O atoms. Similarly, the N atom flux for any point prior to the endpoint was given by the difference between the original flux of N atoms and the flow of NO. These atomic fluxes were required to calculate the cation-atom reaction rate coefficients.

It is important to appreciate that the neutral flow consisted of a mixture of N_2, N atoms, O atoms, and a small O_2 impurity, (from O-O recombination [161]), for all flow rates less than the titration endpoint. [177] Likewise, for all flow rates in excess of the endpoint the neutral flow was a mixture of O atoms, NO, N_2, and a small O_2 impurity. Under all circumstances the overwhelming bulk of the neutral flow was N_2, however as demonstrated in Chapter 5 most non-noble gas cations are unreactive with molecular nitrogen. [177]

The simultaneous presence of atomic nitrogen and oxygen precludes the determination of accurate product ratios except for systems in which the ionic products produced by the O atom reaction are unreactive with N atoms. This situation arises because as the O atom flux is extrapolated to zero flow, the N atom flux tends to its maximum value. This deleterious complicating feature of the NO titration procedure has not been previously discussed in the chemical literature but it may potentially skew product distribution data.

For many cation-O atom reactions the endpoint of the NO titration could also be determined by monitoring the appearance of product ion(s), provided they had been unequivocally identified. For complex systems, where the primary ion undergoes a simultaneous reaction with N_2, (eg. (ac)-$C_6H_5^+$), it may be more convenient and accurate to evaluate the rate constant by analysing the *product* ion count rate as a function of NO flow rate. Specifically, this variant on the standard method of primary ion analysis allows the fraction of primary

ions that react with the atomic reagent to be quantified. This type of approach was useful in deconvoluting the data obtained from the reaction of N_2, N atoms, and atomic oxygen with the isomeric species (c) and (ac)-$C_6H_5^+$. The employment of this mode of analysis required that due cognisance be paid to mass discrimination and indeed this procedure has tolerable accuracy only when the primary and product ions are of similar mass.

The Interpretation of Raw Data Obtained From NO Titrations of Several Cations

During the NO titration, reactions occur simultaneously between the cation of interest and the three, (or four if the small flux of O_2 is included), neutral reagents which are present in the reaction zone of the main flow tube. The raw data for three sample reactions is presented below to give some insight into how the separate rate coefficients for the respective neutrals, N atoms, O atoms, and NO, are obtained. In addition, Figures 5.2 and 5.4, (in Chapter 5), graphically depict data obtained from NO titrations involving the reactant cations O_2^+ and $C_2H_2^+$, respectively.

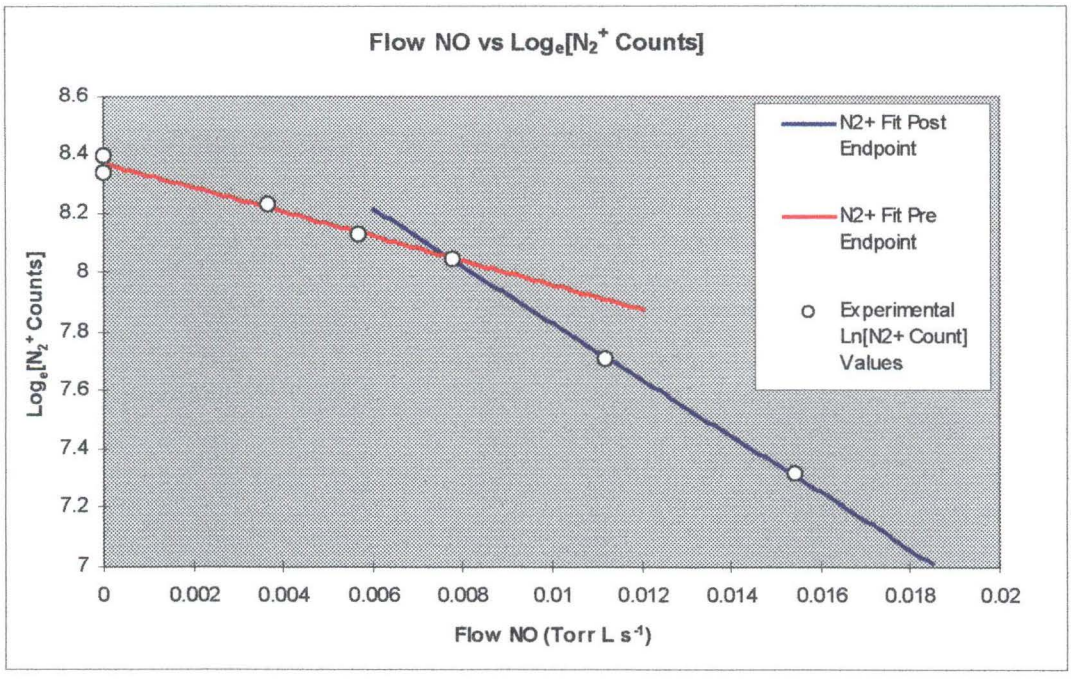

Figure 7.1. Data obtained for the reaction of N_2^+ with N atoms, O atoms and NO. The endpoint of the NO titration is clearly visible as the intersection of the red and blue lines. The difference in the N_2^+ signal at zero NO flow, with N_2 on and off is slight, indicating a very slow reaction between N_2^+ and N atoms.

Figure 7.1 shows data collected from the reaction of N_2^+ cations with N atoms, O atoms, and NO. The rate coefficients for the separate reactions were determined in the following manner. The difference in the N_2^+ signal with the N_2 flow on and off, at zero NO flow, is due to the $N_2^+ + N$ reaction. The microwave discharge was "initiated" for both of these "zero NO flow" points and indeed for all data points recorded during this run. In this case the N_2^+ count rate, (accepting small statistical fluctuations), is approximately constant, irrespective of whether the N_2 is flowing into the reaction zone of the flow tube or not. This indicates that the reaction between N_2^+ and N is quite slow, as reported in Chapter 5 of this thesis, [$k = (1.4 \pm 0.4) \times 10^{-11}$ cm^3 s^{-1}]. Note that the rate for the $N_2^+ + N$ reaction was actually determined by monitoring the appearance of the N_3^+ product ion, rather than the removal of the N_2^+ primary ion. As the NO flow is progressively increased the N atom flux reduces while the O atom flux rises. The decline of the N_2^+ signal is due to a combination of loss terms reflecting the N atom reaction, (decreasing or minor factor), and the O atom reaction, (increasing or major factor). Precisely at the endpoint, the flow rate of N atoms is zero and the flow rate of O atoms is equal to the flow rate of NO, (ie. $Q\{NO_{[END]}\}$). In this reaction, the difference between the initial N_2^+ signal with both the N_2 and NO flow off, and the N_2^+ signal at the titration endpoint, is due to the O atom reaction. Since these count rates are known, along with the O atom flux at the endpoint, the $N_2^+ + O$ rate coefficient can be deduced. At NO flows in excess of the titration endpoint, the N atom flux is zero, the O atom flux is unchanged from $Q\{NO_{[END]}\}$, and the decay in the N_2^+ signal is solely due to the $N_2^+ + NO$ reaction.

Figure 7.2 shows a different situation in which the reactant cation, (c)-$C_6H_6^+$, reacts at approximately the same rate with both N atoms and O atoms. The (c)-$C_6H_6^+$ species was generated via electron impact on benzene. The difference between the $C_6H_6^+$ signal at zero NO flow with N_2 on and off is due to the (c)-$C_6H_6^+ + N$ reaction. As the NO flow rate is progressively increased the N atom flux begins to fall while the O atom flux rises. It can clearly be seen that the primary ion count remains essentially constant throughout the pre-endpoint flow range. This outcome indicates that the (c)-$C_6H_6^+$ cation reacts with N and O atoms at similar rates. Finally, at the endpoint the (c)-$C_6H_6^+$ signal drops

sharply as the primary ion begins to react rapidly with NO. The slope of this decay gives the $C_6H_6^+$ + NO rate coefficient in the standard manner. The endpoint flow rate of NO is equivalent to the initial flux of atomic nitrogen that produced the difference between the (c)-$C_6H_6^+$ signals with N_2 on and off. These parameters allow the straightforward evaluation of the rate coefficient for the $C_6H_6^+$ + N reaction. Again in this system the difference between the initial (c)-$C_6H_6^+$ signal with both the N_2 and NO flow off, and the $C_6H_6^+$ signal at the titration endpoint, is due to the O atom reaction. These count rates, along with the O atom flux at the endpoint, enable the (c)-$C_6H_6^+$ + O reaction rate coefficient to be readily determined.

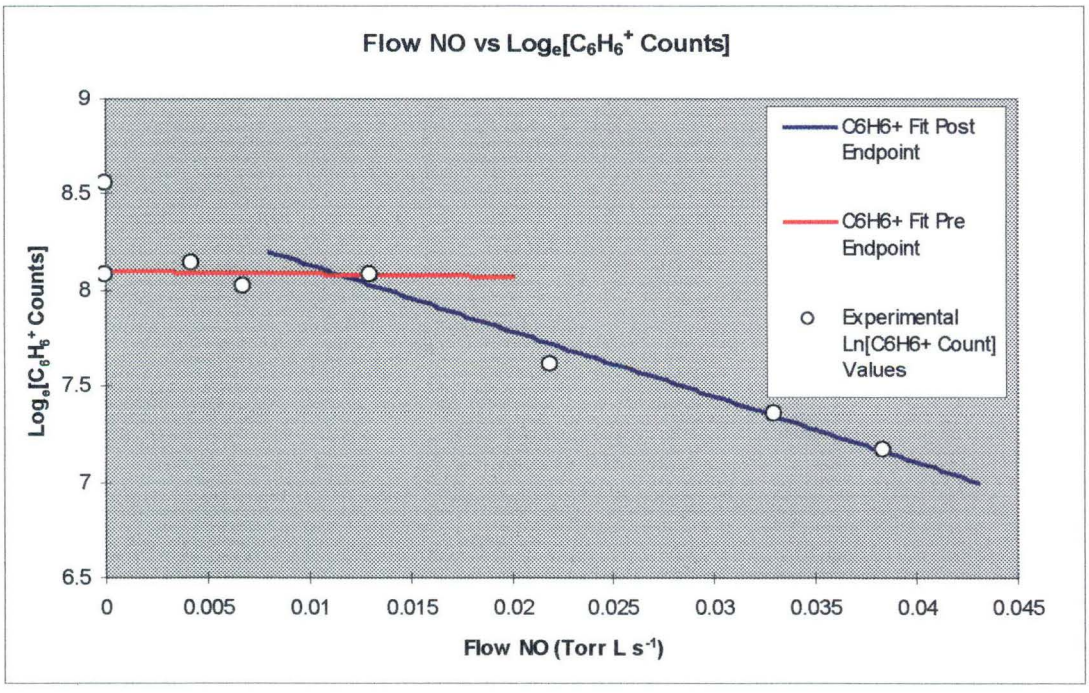

Figure 7.2. Data obtained for the reaction of (c)-$C_6H_6^+$ with N atoms, O atoms and NO. The endpoint of the NO titration is clearly visible as the intersection of the red and blue lines. The uppermost left data point at zero NO flow is the $C_6H_6^+$ signal with no N_2 flowing, ie. zero flux of N atoms.

Finally, Figure 7.3 shows the data obtained from a NO titration of the (c,ac)-$C_3H_3^+$ species, (produced from electron impact on ethylene in a high-pressure ion source). This is a relatively straightforward situation as it appears that this mixture of isomeric $C_3H_3^+$ cations does not react at measurable rates with N atoms. As the NO flow rate is increased the (c,ac)-$C_3H_3^+$ signal decays as the N atom flux falls and the O atom flux rises. Since there is ostensibly "no reaction" between the (c,ac)-$C_3H_3^+$ cations and N atoms, the slope of this initial

decline yields the $C_3H_3^+$ + O atom rate directly. As the endpoint is exceeded, the N atom flux is zero and the O atom flux does not increase above its endpoint value. Post-endpoint, only the NO flow rate increases, however the flat line of best fit through the (c,ac)-$C_3H_3^+$ data points indicates that there is no reaction between these species and nitric oxide.

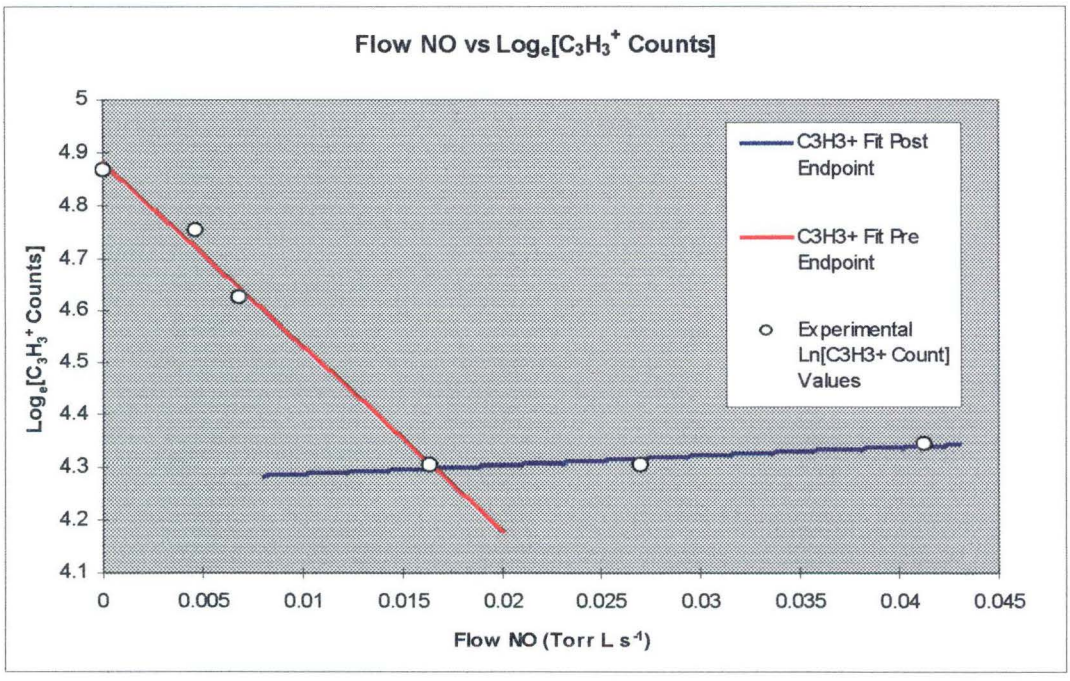

Figure 7.3. Data obtained for the reaction of (c,ac)-$C_3H_3^+$ with N atoms, O atoms and NO. The endpoint of the NO titration is clearly visible as the intersection of the red and blue lines. The data point at zero NO flow is the (c,ac)-$C_3H_3^+$ signal with N_2 flowing. A separate experiment determined that this species, (generated from C_2H_4 in a high-pressure ion source), did not react at a measurable rate with N_2.

Reagents and Experimental Conditions

Most reagents used in this chapter were as previously detailed in Chapter 5 to this thesis.

Diacetylene, C_4H_2, was the only "new" reagent that was used in the experiments conducted in this section of research. Diacetylene was synthesised according to the method of Brandsma. [361]

Experimental Uncertainty

The uncertainty in the rate coefficients for the O atom reactions detailed below is estimated as ± 30 %. This is a larger uncertainty than is generally reported for stable neutral reactants, (± 15 %), due primarily to the difficulty in accurately establishing the O atom number density in the main flow tube.

Several workers who previously conducted experiments involving atomic oxygen have noted ion signal instabilities. [177, 189] Viggiano and colleagues ascribed these signal fluctuations to "changes in the ion sampling efficiencies arising from atom-surface reactions in the vicinity of the mass spectrometer sampling aperture". [177] No such instability in the ion signal was observed in the current batch of experiments.

7.3: Results.

A summary of all the results obtained in this work are presented in Tables 7.1 to 7.6. Table 7.1 details the results obtained for the reaction between atomic oxygen and a small number of non-hydrocarbon cations. Table 7.2 tabulates the data obtained for the reaction of several hydrocarbon cations with O atoms. Tables 7.3 and 7.4 list data obtained for the reaction of O_2 with some hydrocarbon cations and several non-hydrocarbon cations, respectively. Finally, Tables 7.5 and 7.6 give the data obtained from the reaction of nitric oxide, NO, with a number of hydrocarbon cations and several non-hydrocarbon cations, respectively. Previous measurements, where they exist, are catalogued in column 4 of each Table.

Reactant Ion	Products and Branching Ratio	k_{obs} [a]	k_{prev} [b]	k_{coll} [c]	ΔH^o (kJ mol^{-1}) [d]
$HCNH^+$	No Reaction	< 0.25		6.55	
HC_3N^+	$C_3NO^+ + H$ 0.50 $HC_2N^+ + CO$ 0.40 HC_3NO^+ 0.10	4.1		5.99	- - 301.4 - 651.1 [e]
$H_2C_3N^+$	No Reaction	< 0.25		5.97	
H_2O^+	No Reaction	< 0.57		7.18	
N_2^+	$NO^+ + N$ 0.95 $O^+ + NO$ 0.05	1.4	1.4 [f] 2.5 [g]	6.55	- 295.3 - 98.3
HCO^+	No Reaction	< 0.25		6.51	
HCO_2^+	No Reaction	< 0.25		6.08	

Table 7.1. Reaction rate coefficients and product distributions for the reaction of the specified cations with atomic oxygen.

[a] Observed rate coefficient in units of 10^{-10} cm^3 s^{-1}. [b] Rate coefficients determined in other laboratories, in units of 10^{-10} cm^3 s^{-1}. [c] Langevin collision rate in units of 10^{-10} cm^3 s^{-1}. k_{coll} values were calculated according to the parameterised theory of Su and Chesnavich. [118]

[d] The listed exothermicities are taken from Lias et al. [31] [e] Thermochemistry for the NCCH=C=O$^+$ cation. [f] References 181, 186, and 291. [g] Reference 189.

Reactant Ion	Products and Branching Ratio		k_{obs} [a]	k_{prev} [b]	k_{coll} [c]	ΔH^o (kJ mol^{-1}) [d]
CH_3^+	$H_3^+ + CO$		4.1	4.4[e]	7.51	- 346.5
	$HOC^+ + H_2$					- 380.4
	$HCO^+ + H_2$					- 517.2
$C_2H_2^+$	$HCO^+ + CH$	0.50	2.0	1.7[f]	6.64	- 156.1[g]
	$HC_2O^+ + H$	0.50				- 263.2
$C_2H_3^+$	$H_2CCO^+ + H$	0.85	1.0		6.59	- 264.4[h]
	$C_2H_3O^+$	0.10				- 520.9[i]
	$CH_3^+ + CO$	0.05				- 379.1
$C_2H_4^+$	$HCO^+ + CH_3$	0.60	2.4		6.55	-344.3[g]
	$CH_3^+ + HCO$	0.15				-177.3
	$HC_2O^+ + H_2 + H$	0.10				-1.2
	$C_2H_3O^+ + H$	0.05				- 256.4[i]
	$H_2CCO^+ + H_2$	0.05				- 435.9[h]
	$CH_2^+ + H_2CO$	0.05				-39.2
$C_2H_5^+$	No Reaction		< 0.25		6.51	
(c,ac)-$C_3H_3^+$	$C_3H_2O^+ + H$	0.30	1.5		6.20	- 236.4[j]
	$C_2H_3^+ + CO$	0.30				- 427.3[k]
	$C_2H_2^+ + HCO$	0.25				- 56.5[k]
	$HC_3O^+ + H_2$	0.15				- 458.6[l]
(c,ac)-$C_3H_5^+$	No Reaction		< 0.25		6.16	
$C_4H_2^+$	$C_4HO^+ + H$	0.50	2.7		6.00	-
	$C_3H_2^+ + CO$	0.40				- 45.2[m]
	$C_3HO^+ + CH$	0.05				- 105.5[n]
	$C_4H_2O^+$	0.05				-
$C_4H_3^+$	No Reaction		< 0.5		5.99	
(c)-$C_6H_5^+$	$C_5H_5^+ + CO$	0.60	1.0		5.74	- 432.3[o]
	$C_3H_3^+ + C_3H_2O$	0.40				- 204.7[p]
(ac)-$C_6H_5^+$	No Reaction		< 0.25		5.74	
(c)-$C_6H_6^+$	$C_5H_6^+ + CO$	0.90	1.4		5.73	- 377.5[q]
	$C_4H_4O^+ + C_2H_2$	0.10				- 174.9[r]

Table 7.2. Reaction rate coefficients and product distributions for the reaction of the specified hydrocarbon cations with atomic oxygen.

[a] Observed rate coefficient in units of 10^{-10} cm^3 s^{-1}. [b] Rate coefficients determined in other laboratories, in units of 10^{-10} cm^3 s^{-1}. [c] Langevin collision rate in units of 10^{-10} cm^3 s^{-1}. k_{coll} values were calculated according to the parameterised theory of Su and Chesnavich. [118]

[d] The listed exothermicities are taken from Lias et al. [31] [e] References 180 and 187.

[f] Reference 177. [g] Thermochemistry for the HCO^+ cation, (not HOC^+). [h] Thermochemistry for the H_2CCO^+ cation. [i] Thermochemistry for the oxiranyl radical cation. [j] Thermochemistry for the (ac)-$C_3H_3^+$ cation and $H_2C{=}C{=}C{=}O^+$. [k] Thermochemistry for the (ac)-$C_3H_3^+$ cation. [l] Thermochemistry for the (ac)-$C_3H_3^+$ cation and $HC{\equiv}C\text{-}C{=}O^+$. [m] Thermochemistry for the $HC{\equiv}CCH^+$ cation. [n] Thermochemistry for the $HC{\equiv}CC{=}O^+$ cation. [o] Thermochemistry for the cyclopentadienyl cation. [p] Thermochemistry for the cyclopropenyl cation, [(c)-$C_3H_3^+$], and propadienone. [q] Thermochemistry for the cyclopentadiene cation. [r] Thermochemistry for the furan cation.

Reactant Ion	Products and Branching Ratio	k_{obs} [a]	k_{prev} [b]	k_{coll} [c]	ΔH^o (kJ mol^{-1}) [d]
CH_3^+	$CH_3.O_2^+$ 1.0	0.002[e]	0.43[f] < 0.001[g] < 0.0008[h]	9.18	
$C_2H_2^+$	$HCO^+ + HCO$ 0.70 $C_2H_2O^+ + O$ 0.25 $C_2H_2^+.O_2$ 0.05	0.014	< 0.1[i]	7.75	-457.7[j] -45.1[k] -566.5
$C_2H_3^+$	No Reaction	< 0.005		7.67	
$C_2H_4^+$	No Reaction	< 0.005		7.59	
$C_2H_5^+$	No Reaction	< 0.005		7.52	
(c,ac)-$C_3H_3^+$	No Reaction	< 0.005		7.00	
(c,ac)-$C_3H_5^+$	No Reaction	< 0.005		6.93	
$C_4H_2^+$	No Reaction	< 0.005		6.64	
$C_4H_3^+$	No Reaction	< 0.005		6.62	
(c)-$C_6H_5^+$	$C_4H_5^+ + 2CO$ 0.90 $C_5H_5O^+ + CO$ 0.10	0.54		6.17	- 356.2[l] -
(ac)-$C_6H_5^+$	No Reaction	< 0.006		6.17	
(c)-$C_6H_6^+$	No Reaction	< 0.005		6.16	

Table 7.3. Reaction rate coefficients and product distributions for the reaction of the specified hydrocarbon cations with molecular oxygen.

[a] Observed rate coefficient in units of 10^{-10} cm^3 s^{-1}. [b] Rate coefficients determined in other laboratories, in units of 10^{-10} cm^3 s^{-1}. [c] Langevin collision rate in units of 10^{-10} cm^3 s^{-1}. k_{coll} values were calculated according to the parameterised theory of Su and Chesnavich. [118]
[d] The listed exothermicities are taken from Lias et al. [31] [e] Pseudo-bimolecular reaction. The rate constant shown is for a flow tube pressure of 0.32 Torr. The termolecular rate for the three-body association process is estimated as $k_3 \geq 1.9 \times 10^{-29}$ cm^6 s^{-1}. [f] Reference 344. [g] Reference 39. The termolecular rate for the three-body association process was reported as 1×10^{-29} cm^6 s^{-1}.
[h] Reference 287. The termolecular rate for the three-body association process was reported as 7.3×10^{-30} cm^6 s^{-1}. [i] Reference 24. [j] Thermochemistry based on the HCO^+ cation, (not HOC^+).

[k] Thermochemistry based on the $HC{\equiv}COH^+$ cation, (not H_2CCO^+). [l] Thermochemistry for the methyl cyclopropenyl radical cation.

Reactant Ion	Products and Branching Ratio	k_{obs} [a]	k_{prev} [b]	k_{coll} [c]	ΔH^o (kJ mol^{-1})[d]
$HCNH^+$	No Reaction	< 0.005		7.59	
HC_3N^+	$HCO^+ + CO + CN$ 0.55 $HC_3N^+.O_2$ 0.45	0.05	0.025[e]	6.62	-322.7[f] -
$H_2C_3N^+$	No Reaction	< 0.005		6.59	
H_2O^+	$O_2^+ + H_2O$ 1.0	2.5	1.5[g], 4.3[h] 5.2[i], 3.3[j], 12.9[k], 2.0[l] 4.6[m]	8.64	-51.5
N_2^+	$O_2^+ + N_2$ 1.0	0.51	0.98[n], 0.49[o] 0.51[p] 0.47[q] 0.457[r] 0.50[s] 0.90[t],0.60[u] 0.65[v], 1.0[x] 1.1[y], 0.42[z]	7.59	-338.1
HCO^+	No Reaction	< 0.005	< 0.5[A] < 0.002[B]	7.52	
HCO_2^+	No Reaction	< 0.005		6.78	

Table 7.4. Reaction rate coefficients and product distributions for the reaction of the specified cations with molecular oxygen.

[a] Observed rate coefficient in units of 10^{-10} cm^3 s^{-1}. [b] Rate coefficients determined in other laboratories, in units of 10^{-10} cm^3 s^{-1}. [c] Langevin collision rate in units of 10^{-10} cm^3 s^{-1}. k_{coll} values were calculated according to the parameterised theory of Su and Chesnavich. [118]
[d] The listed exothermicities are taken from Lias et al. [31] [e] Reference 362. [f] Thermochemistry based on the HCO^+ cation, (not HOC^+). [g] Reference 363. [h] Reference 364. [i] Reference 24. [j] Reference 365. [k] Reference 294. [l] Reference 234. [m] Reference 366. [n] Reference 35. [o] Reference 367. [p] Reference 42 and 368. [q] Reference 140, 143, 200, 369 and 370. [r] Reference 371. [s] Reference 372. [t] Reference 373. [u] Reference 374. [v] Reference 375. [x] References 179 and 284. [y] Reference 376. [z] Reference 377. [A] Reference 304. [B] Reference 238.

Reactant Ion	Products and Branching Ratio	k_{obs}[a]	k_{prev}[b]	k_{coll}[c]	ΔH^o (kJ mol^{-1})[d]
CH_3^+	$NO^+ + CH_3$ 1.0	10.0	10.0[e], 9.4[f], 11.0[g]	10.18	- 54.4
$C_2H_2^+$	$NO^+ + C_2H_2$ 1.0	0.98	1.1[h], 1.2[i]	8.63	- 206.7
$C_2H_3^+$	No Reaction	< 0.005		8.54	
$C_2H_4^+$	$NO^+ + C_2H_4$ 1.0	4.7	3.6[g]	8.46	- 120.4
$C_2H_5^+$	No Reaction	< 0.005		8.38	
(c,ac)-$C_3H_3^+$	$C_3H_3^+$.NO 1.0	0.014		7.82	- 129.0[j]
(c,ac)-$C_3H_5^+$	No Reaction	< 0.05		7.74	
$C_4H_2^+$	$NO^+ + C_4H_2$ 1.0	3.80		7.44	- 90.0
$C_4H_3^+$	No Reaction	< 0.15		7.41	
(c)-$C_6H_5^+$	(c)-$C_6H_5^+$.NO 1.0	1.9		6.93	- 234.9[k]
(ac)-$C_6H_5^+$	No Reaction	< 0.005		6.93	
(c)-$C_6H_6^+$	NO^+ + (c)-C_6H_6 0.25 (c)-$C_6H_5^+$.NO 0.75	1.4		6.92	+ 0.4 - 192.5[l]

Table 7.5. Reaction rate coefficients and product distributions for the reaction of the specified hydrocarbon cations with nitric oxide.

[a] Observed rate coefficient in units of 10^{-10} cm^3 s^{-1}. [b] Rate coefficients determined in other laboratories, in units of 10^{-10} cm^3 s^{-1}. [c] Langevin collision rate in units of 10^{-10} cm^3 s^{-1}. k_{coll} values were calculated according to the parameterised theory of Su and Chesnavich. [118]
[d] The listed exothermicities are taken from Lias et al. [31] [e] Reference 177. [f] Reference 344. [g] Reference 378. [h] Reference 379 @ 15 K. [i] Reference 177. [j] Thermochemistry based on (c)-$C_3H_3^+$ and the isoxazole cation. [k] Thermochemistry based on the nitrosobenzene cation. [l] Thermochemistry based on the protonated nitrosobenzene cation.

Reactant Ion	Products and Branching Ratio	k_{obs} [a]	k_{prev} [b]	k_{coll} [c]	ΔH^o (kJ mol^{-1}) [d]
$HCNH^+$	No Reaction	< 0.14		8.46	
HC_3N^+	$NO^+ + HC_3N$ 1.0	1.8		7.41	-228.0
$H_2C_3N^+$	No Reaction	< 0.23		7.38	
H_2O^+	$NO^+ + H_2O$ 1.0	3.6	4.4[e], 4.5[f] 5.9[g], 3.6[h] 11.[i]	9.60	-323.4
N_2^+	$NO^+ + N_2$ 1.0	3.6	3.0[j], 4.40[k] 4.8[l], 3.3[m] 5.0[n]	8.46	-610.0
HCO^+	No Reaction	< 0.005		8.38	
HCO_2^+	$HNO^+ + CO_2$ 1.0	0.18	< 1.0[o]	7.59	-2.4[p]

Table 7.6. Reaction rate coefficients and product distributions for the reaction of the specified cations with nitric oxide.

[a] Observed rate coefficient in units of 10^{-10} cm^3 s^{-1}. [b] Rate coefficients determined in other laboratories, in units of 10^{-10} cm^3 s^{-1}. [c] Langevin collision rate in units of 10^{-10} cm^3 s^{-1}. k_{coll} values were calculated according to the parameterised theory of Su and Chesnavich. [118]
[d] The listed exothermicities are taken from Lias et al. [31] [e] Reference 363. [f] References 365 and 380. [g] Reference 364. [h] Reference 177. [i] Reference 294. [j] Reference 381. [k] Reference 369. [l] Reference 373. [m] Reference 181 and 291. [n] Reference 179 and 284. [o] Reference 329.
[p] Themochemistry based on the HNO^+ cation, (not NOH^+).

7.4: Discussion of Results.

(i). $CH_3^+ + O / O_2 / NO$. The methyl cations used in these experiments were generated from methyl bromide, CH_3Br. CH_3^+ undergoes a rapid reaction with atomic oxygen, [$k = (4.1 \pm 1.2) \times 10^{-10}$ cm^3 s^{-1}]. This value for the rate coefficient is in excellent agreement with the two previously reported values for this reaction. [180, 187] The only product ion observed has a mass to charge, (m/z), ratio of 29. One other product channel, namely $H_3^+ + CO$, is also accessible on energy grounds but the H_3^+ product cation could not be identified because of the experimental conditions under which the reaction was studied, (ie. excess N_2 present in the neutral flow). In summary, the viable channels are:

$$CH_3^+(^1A) + O(^3P) \Rightarrow H_3^+(^1A_1') + CO(^1\Sigma^+) + 3.6\text{ eV} \quad \textbf{(703a)}$$

$$\Rightarrow HCO^+(^1\Sigma_g) + H_2(^1\Sigma_g^+) + 5.4\text{ eV} \quad \textbf{(703b)}$$

$$\Rightarrow HOC^+(^1\Sigma^+) + H_2(^1\Sigma_g^+) + 3.9\text{ eV} \quad \textbf{(703c)}$$

$k_{(703)\ 300K}$ = $(4.1 \pm 1.2) \times 10^{-10}$ cm^3 s^{-1}

In channel **(703a)** the H_3^+ product ion is undetectable due to an immediate collision rate reaction with N_2 to form N_2H^+, [$k = (1.86 \pm 0.19) \times 10^{-9}$ cm^3 s^{-1}]. [24] Note that unfortunately N_2H^+ has a m/z ratio of 29, ie. the same m/z ratio as HCO^+ and HOC^+ produced in channels **(703b)** and **(703c)** respectively. The HOC^+ cation generated in channel **(703c)**, similarly undergoes a fast secondary reaction with N_2 to form N_2H^+, [$k = (6.7 \pm 1.3) \times 10^{-10}$ cm^3 s^{-1}]. [24] The formyl radical cation, (HCO^+), produced in channel **(703b)** is unreactive with N_2. [238] Thus, the presence of secondary chemistry makes the precise determination of the product channels(s) impracticable for reaction **(703)**.

Fragmentation of the collision complex occurs in all three pathways, **(703a) – (703c)**. Channel **(703a)** proceeds by C atom transfer from cation to neutral and presumably requires extensive rearrangement of the collision complex. The other two channels, **(703b)** and **(703c)** require minimal atomic rearrangement and hence are more easily contrived. The principle of spin conservation is violated in all three product channels detailed above.

In accordance with the chemical literature, CH_3^+ participates in a fast charge transfer reaction with NO, [$k = (1.0 \pm 0.15) \times 10^{-9}$ cm^3 s^{-1}] [177, 344, 378], and a very slow termolecular association process with O_2, ($k_3 = 1.9 \times 10^{-29}$ cm^6 s^{-1}). [39, 287, 344] The observed pseudo-bimolecular rate coefficient, (at 0.32 Torr), is $k = 2 \times 10^{-13}$ cm^3 s^{-1}.

(ii). $C_2H_2^+$ + O / O_2 / NO. The $C_2H_2^+$ cations used in these measurements were formed directly by electron impact on acetylene. This species participates in a moderately fast two-channel reaction with O atoms, viz:

$C_2H_2^+(^2\Sigma)$ + $O(^3P)$ $\Rightarrow$ $HCO^+(^1\Sigma_g)$ + $CH(^2\Pi)$ + 1.6 eV (0.50) **(704a)**

$\Rightarrow$ $HC_2O^+(^1A')$ + $H(^2S)$ + 2.7 eV (0.50) **(704b)**

$k_{(704)\ 300K}$ = $(2.0 \pm 0.6) \times 10^{-10}$ cm^3 s^{-1}

Note that spin is conserved in both product channels and the observed rate coefficients are slightly less than (2/6 k_L x 0.5), [ie. k_L multiplied by the statistical weight of the spin allowed doublet reaction pathway and the "fraction" of each channel, **(704a)** and **(704b)**]

Thermochemistry dictates that the m/z = 29 cation in channel **(704a)** could also be HOC^+ (ΔH^o for $C_2H_2^+ + O \Rightarrow HOC^+ + CH$ is - 19.3 kJ mol^{-1}). The rate

coefficient and product ratio obtained from the current study are in good agreement with the sole previous investigation of this reaction. [177] Channel **(704a)** involves O atom attack on the triple C≡C bond of the $C_2H_2^+$ species followed by fragmentation, whilst the other channel, **(704b)**, involves O atom-H atom exchange.

The $C_2H_2^+$ cation undergoes a slow charge transfer reaction with NO, [$k = (9.8 \pm 1.5) \times 10^{-11}$ cm^3 s^{-1}]. This outcome is in reasonable agreement with the previous SIFT investigation of Viggiano et al., [177] and the 1990 free jet flow reactor measurement of Hawley and co-workers. [379]

A slow reaction, [$k = (1.4 \pm 0.2) \times 10^{-12}$ cm^3 s^{-1}], with three product channels, was observed in the reaction between $C_2H_2^+$ and molecular oxygen. The major channel, (0.70), involved the fragmentation of the collision complex into a HCO neutral and either HCO^+, (most likely due to minimal rearrangement), or HOC^+, (ΔH^o for $C_2H_2^+ + O_2 \Rightarrow HOC^+ + HCO$ is - 320.9 kJ mol^{-1}). The other pathways were O atom abstraction, (0.25), and a very small termolecular association pathway, (0.05). These observations are in broad agreement with the single reported examination of this process using the ICR technique, (in 1977 Huntress reported "no reaction" for the $C_2H_2^+ + O_2$ process with $k < 1 \times 10^{-11}$ cm^3 s^{-1}). [24]

(iii). $C_2H_3^+ + O / O_2 / NO$. The $C_2H_3^+$ species was formed by the collisional dissociation of the $C_2H_5^+$ cation produced following electron impact on ethyl bromide, C_2H_5Br. A moderately fast three-channel reaction is observed between $C_2H_3^+$ and O atoms, ie.

$C_2H_3^+(^1A) + O(^3P) \Rightarrow H_2CCO^+(^2B_1) + H(^2S) + 2.7$ eV[a] (0.85) **(705a)**

$\Rightarrow CH_3CO^+(^1A_1) + 5.4$ eV[b] (0.10) **(705b)**

$\Rightarrow CH_3^+(^1A) + CO(^1\Sigma^+) + 3.9$ eV (0.05) **(705c)**

$k_{(705)\ 300K} = (1.0 \pm 0.3) \times 10^{-10}$ cm^3 s^{-1}

Spin is not conserved in either of the minor channels, **(705b)** or **(705c)**, however it is conserved in the predominant channel, **(705a)**.

Again, the major channel, **(705a)**, proceeds via O-H exchange, whereby the O atom inserts into the carbon skeleton of the hydrocarbon cation. Note that in

---

[a] Thermochemistry for the H_2CCO^+ cation.

[b] Thermochemistry for the oxiranyl radical cation.

this channel both $C_2H_2O^+$ species are thermodynamically accessible, however H_2CCO^+ has been assumed to be the likely product cation as it involves the least rearrangement, (ΔH^o for the alternative reaction: $C_2H_3^+ + O \Rightarrow HC{\equiv}COH^+ + H$, is - 110.4 kJ mol^{-1}).

The other two minor channels are termolecular association, **(705b)**, and a fragmentation channel with associated rearrangement forming CH_3^+ and the very stable carbon monoxide molecule, ie. **(705c)**. All three known $C_2H_3O^+$ cations are accessible in the association pathway, **(705b)**, however production of the oxiranyl cation involves minimal rearrangement. The standard enthalpy change for the reaction of $C_2H_3^+ + O$ to form CH_3CO^+ is - 709.2 kJ mol^{-1} or alternatively to form $CH_2{=}COH^+$ is - 558.6 kJ mol^{-1}.

$C_2H_3^+$ does not react with either O_2 or NO, ($k < 5 \times 10^{-13}$ cm^3 s^{-1}).

(iv). $C_2H_4^+ + O / O_2 / NO$. The $C_2H_4^+$ cation, which was formed directly by electron impact on ethylene, undergoes a fast six-channel reaction with atomic oxygen, viz:

$C_2H_4^+(^2A) + O(^3P) \Rightarrow HCO^+(^1\Sigma_g) + CH_3(^2A_2'') + 3.6\ eV^c$ (0.60) **(706a)**

$\Rightarrow CH_3^+(^1A) + HCO(^2A') + 1.8\ eV$ (0.15) **(706b)**

$\Rightarrow HC_2O^+(^1A') + H_2(^1\Sigma_g^+) + H(^2S) + 0.01\ eV$ (0.10) **(706c)**

$\Rightarrow CH_3CO^+(^1A_1) + H(^2S) + 2.7\ eV^d$ (0.05) **(706d)**

$\Rightarrow H_2CCO^+(^2B_1) + H_2(^1\Sigma_g^+) + 4.5\ eV^e$ (0.05) **(706e)**

$\Rightarrow CH_2^+(^2A_1) + H_2CO(^1A_1) + 0.4\ eV$ (0.05) **(706f)**

$k_{(706)\ 300K} = (2.4 \pm 0.7) \times 10^{-10}$ cm^3 s^{-1}

Note that in channel **(706a)** the alternative CHO^+ cation, HOC^+, is also thermodynamically accessible, (ΔH^o for the alternative reaction: $C_2H_4^+ + O \Rightarrow HOC^+ + CH_3$, is - 207.5 kJ mol^{-1}). Additionally, all three CH_3CO^+ cations, (CH_3CO^+, $CH_2{=}COH^+$, and the oxiranyl radical cation), are thermodynamically accessible in the minor channel, **(706d)**. In channel **(706e)** the thermochemistry indicates that both the H_2CCO^+ and $HC{\equiv}COH^+$ cations are accessible, (ΔH^o for the alternative reaction: $C_2H_4^+ + O \Rightarrow HC{\equiv}COH^+ + H_2$, is - 281.9 kJ mol^{-1}).

Channels, **(706a)** and **(706b)**, proceed by CH^+ and CH transfer respectively, from cation to atom. Channel, **(706c)**, presumably requires a major change in

---

[c] Thermochemistry for the HCO^+ cation, (not HOC^+).
[d] Thermochemistry for the oxiranyl cation.
[e] Thermochemistry for the H_2CCO^+ cation.

configuration during the lifetime of the collision complex, whilst the minor channel **(706d)** occurs via O-H exchange. The minor channels **(706e)** and **(706f)** appear to require O atom attack at the C=C double bond followed by fragmentation of the collision complex.

Spin is conserved in all channels, **(706a)** – **(706f)**, with the observed rate coefficients being slightly greater than 2/6 k_L x f[Channel][f], this being the Langevin collision rate factored by the statistical weight of the spin allowed doublet reaction pathway and multiplied by the "fraction" of the each channel.

The ethylene cation is unreactive with O_2, ($k < 5 \times 10^{-13}$ cm^3 s^{-1}), but does participate in a moderately fast, [$k = (4.7 \pm 0.7) \times 10^{-10}$ cm^3 s^{-1}], charge transfer reaction with nitric oxide. The rate coefficient obtained from the present study is somewhat faster, (~ 30 %), than the value reported previously by Sieck and Futrell in 1968. [378]

(v). $C_2H_5^+$ + O / O_2 / NO. Electron impact on ethyl bromide, followed by injection at low ion energies, generated the $C_2H_5^+$ cation. No reaction is observed for the reaction of this species with atomic oxygen, O_2, or nitric oxide, ($k < 2.5 \times 10^{-11}$ cm^3 s^{-1} for $C_2H_5^+$ + O, and $k < 5 \times 10^{-13}$ cm^3 s^{-1} for the reaction of $C_2H_5^+$ with O_2 and NO).

(vi). $C_3H_3^+$ and $C_3H_5^+$ + O / O_2 / NO. The (c,ac)-$C_3H_3^+$ and (c,ac)-$C_3H_5^+$ cations were both produced by electron impact on ethylene in a high-pressure ion source. It is known from previous work, (see Chapter 4 to this thesis), that this mode of generation produces an approximately 60 % (ac)-$C_3H_3^+$: 40 % (c)-$C_3H_3^+$ mixture. The ratio of acyclic / cyclic $C_3H_5^+$ species generated from this precursor is not known.

The **(c,ac)-$C_3H_3^+$** species react moderately rapidly with atomic oxygen via four product channels, ie.

$C_3H_3^+(^1A)$ + $O(^3P)$ $\Rightarrow$ $C_3H_2O^+(^2A')$ + $H(^2S)$ + 2.5 eV[g] (0.31) **(707a)**

$\Rightarrow$ $C_2H_3^+(^1A)$ + $CO(^1\Sigma^+)$ + 4.4 eV[h] (0.31) **(707b)**

$\Rightarrow$ $C_2H_2^+(^2\Sigma)$ + $HCO(^2A')$ + 0.6 eV[h] (0.22) **(707c)**

$\Rightarrow$ $C_3OH^+(^3A')$ + $H_2(^1\Sigma_g^+)$ + 4.8 eV[i] (0.16) **(707d)**

---

[f] f[Channel] denotes the "fraction" of each doublet product channel, **(706a)** - **(706d)**.

[g] Thermochemistry for (ac)-$C_3H_3^+$ and $H_2C{=}C{=}C{=}O^+$.

[h] Thermochemistry for (ac)-$C_3H_3^+$.

[i] Thermochemistry for (ac)-$C_3H_3^+$ and $HC{\equiv}C{-}C{=}O^+$.

$k_{(707)\ 300K}$ = $(1.5 \pm 0.5) \times 10^{-10}$ cm^3 s^{-1}

All product channels, except **(707b)**, conserve spin.

The two major channels, **(707a)** and **(707b)**, proceed via O-H exchange and C atom transfer from cation to neutral, respectively. Reaction **(707c)** involves CH transfer from cation to neutral atom while the minor channel, **(707d)**, involves oxygen atom insertion into the hydrocarbon skeleton followed by loss of H_2 from the collision complex. It is of interest to note that all product channels **(707a)** through **(707d)** result in the formation of a C-O bond.

Three $C_3H_2O^+$ isomers are known, namely $HC{\equiv}CCHO^+$, $H_2C{=}C{=}C{=}O^+$ and 2-cyclopropen-1-one. For channel **(707a)** the thermochemistry indicates that all three isomers are accessible from (ac)-$C_3H_3^+$, however the formation of $HC{\equiv}CCHO^+ + H$ is + 48.1 kJ mol^{-1} endothermic from (c)-$C_3H_3^+$. Channels **(707b)** and **(707d)** are accessible from both $C_3H_3^+$ isomers, however only the higher energy (ac)-$C_3H_3^+$ cation can give rise to reaction **(707c)**, [ΔH^0 for (c)-$C_3H_3^+ + O \Rightarrow C_2H_2^+ + HCO$ is + 48.1 kJ mol^{-1}].

(c,ac)-$C_3H_3^+$ is unreactive with O_2 but does participate in a slow termolecular association reaction with NO, [$k = (1.4 \pm 0.2) \times 10^{-12}$ cm^3 s^{-1}].

The **(c,ac)-$C_3H_5^+$** species is unreactive with atomic and molecular oxygen, ($k < 2.5 \times 10^{-11}$ cm^3 s^{-1} and $k < 5 \times 10^{-13}$ cm^3 s^{-1}, respectively). This species is also unreactive with nitric oxide, ($k < 5 \times 10^{-12}$ cm^3 s^{-1}).

(vii). $C_4H_2^+$ and $C_4H_3^+$ + O / O_2 / NO. Electron impact on acetylene in a high-pressure ion source was the mode of generation for the $C_4H_2^+$ and $C_4H_3^+$ cations. The $C_4H_2^+$ cation was also generated from diacetylene in a separate block of experiments. Within experimental error, there was no difference in the behaviour of the $C_4H_2^+$ arising from either precursor.

The **$C_4H_3^+$** species is unreactive with O atoms, O_2 and NO, ($k < 5 \times 10^{-11}$ cm^3 s^{-1}, $k < 5 \times 10^{-13}$ cm^3 s^{-1} and $k < 1.5 \times 10^{-11}$ cm^3 s^{-1}, respectively).

In contrast, a moderately fast reaction with four product channels is observed between **$C_4H_2^+$** and atomic oxygen, viz:

$C_4H_2^+(^2\Pi_g) + O(^3P) \Rightarrow C_4HO^+ + H(^2S)$ (0.50) **(708a)**

$\Rightarrow C_3H_2^+(^2A') + CO(^1\Sigma^+) +$ 0.5 eV[j](0.40) **(708b)**

$\Rightarrow C_3OH^+(^3A') + CH(^2\Pi) +$ 1.1 eV (0.05) **(708c)**

$\Rightarrow C_4H_2O^+$ (0.05) **(708d)**

$k_{(708)\ 300K} = (2.7 \pm 0.8) \times 10^{-10}$ cm^3 s^{-1}

No thermochemical data is available for either the C_4HO^+ or C_3HO^+ species, hence the ergicities of these channels cannot be evaluated. Both the c-$C_3H_2^+$ and the $HC{\equiv}CCH^+$ cations are thermochemically accessible in channel **(708b)**, (ΔH^o for $C_4H_2^+ + O \Rightarrow C_2H_2^+ + CO$ is 250.2 kJ mol^{-1}).

The ground electronic states for both the C_4HO^+ and $C_4H_2O^+$ species have not been reported in the chemical literature. In the case of C_4HO^+ the ground electronic state is likely to be a singlet, whereas $C_4H_2O^+$ is probably a doublet. The major channel, **(708a)**, is thus probably spin allowed with an observed rate coefficient > 2/6 k_L x f[Channel][k], (this is the Langevin collision rate factored by the statistical weight of the spin allowed doublet reaction pathway and multiplied by the "fraction" of the major channel). The other major channel, **(708b)**, is spin allowed with a rate coefficient > 2/6 k_L. The minor channel, **(708c)**, is also spin allowed and it is likely that spin is conserved in the other minor channel, **(708d)**. Channel **(708c)** has an observed rate coefficient < 4/6 k_L, this being the Langevin collision rate factored by the statistical weight of the spin allowed quartet reaction pathway. In contrast, the observed rate coefficient for the minor channel, **(708d)**, is > 2/6 k_L x f[Channel][k], (ie. the Langevin collision rate factored by the statistical weight of the spin allowed doublet reaction pathway and multiplied by the "fraction" of the minor channel, **(708c)**).

The predominant channel, **(708a)**, once again proceeds either by O atom insertion or attachment to the carbon skeleton of the hydrocarbon cation, with attendant loss of atomic hydrogen. The minor channels, **(708b)** and **(708c)**, involve O atom insertion into the cation followed by CH loss from the collision complex, and termolecular association, respectively.

Nitric oxide undergoes a moderately rapid charge transfer reaction with $C_4H_2^+$, ($k = 3.8 \times 10^{-10}$ cm^3 s^{-1}), however O_2 is unreactive with this hydrocarbon

---

j Thermochemistry for the $HC{\equiv}CCH^+$ cation.

k f[Channel] denotes the "fraction" of each doublet product channel, **(708a)** and **(708c)**.

cation, ($k < 5 \times 10^{-13}$ cm^3 s^{-1}).

(viii). (c)-$C_6H_5^+$ and (ac)-$C_6H_5^+$ + O / O_2 / NO. An isomeric mixture of (c,ac)-$C_6H_5^+$ cations, was generated from bromobenzene vapour, C_6H_5Br. A double exponential decay is observed for the reaction of the (c,ac)-$C_6H_5^+$ species with a variety of neutral reagents including N_2, NO, O_2, N_2 / N atoms and O_2 / O atoms. The last two mixtures, namely N_2 / N atoms and O_2 / O atoms, were generated by subjecting molecular nitrogen and oxygen gas, (both 100 %), respectively, to a microwave discharge. Fitting the data obtained from these experiments to a double exponential function allows the (c)-$C_6H_5^+$: (ac)-$C_6H_5^+$ ratio from the bromobenzene precursor to be evaluated as ~ 70 % : 30 %. In accordance with the findings of Ausloos and colleagues the unreactive isomer was assumed to be (ac)-$C_6H_5^+$ for all reactions examined. [253]

The **(ac)-$C_6H_5^+$** isomer is apparently unreactive with all neutrals examined in the present study, [k{(ac)-$C_6H_5^+$ + O} < 2.5 x 10^{-11} cm^3 s^{-1} ; k{(ac)-$C_6H_5^+$ + NO}< 5 x 10^{-13} cm^3 s^{-1}; and k{(ac)-$C_6H_5^+$ + O_2}< 6 x 10^{-13} cm^3 s^{-1}]. The rate coefficients for the reaction of (ac)-$C_6H_5^+$ with N_2 and N atoms were previously reported in Chapter 5 of this thesis.

The phenylium cation, (c)-$C_6H_5^+$, cation reacts at a moderate rate with atomic oxygen via two products channels:

$$(c)\text{-}C_6H_5^+(^1A_1) + O(^3P) \Rightarrow C_5H_5^+(^3A'_2) + CO(^1\Sigma^+) + 4.5\ eV^{l}\ (0.60)\ \textbf{(709a)}$$

$$\Rightarrow C_3H_3^+(^1A) + C_3H_2O(^1A') + 2.1\ eV^{m}\ (0.40)\ \textbf{(709b)}$$

$$k_{(709)\ 300K} = (1.0 \pm 0.5) \times 10^{-10}\ \text{cm}^3\ \text{s}^{-1}$$

The simultaneous presence of two $C_6H_5^+$ isomers meant that it was necessary to obtain the overall rate coefficient for reaction **(709)** by analysing the appearance of the product ions. The rate constant obtained from this method of data analysis is only considered accurate to ± 50 %, due primarily to the complicating effect of mass discrimination.

The mode of reaction for the major channel, **(709a)**, is carbon atom transfer from cation to neutral, thereby forming the low energy CO molecule. Spin is conserved in this channel.

---

l Thermochemistry for the cyclopentadienyl cation.

m Thermochemistry for the cyclopropenyl, [(c)-$C_3H_3^+$] cation and propadienone.

Significant fragmentation of the collision complex is evident in the minor channel, **(709b)**, which results in the production of the stable $C_3H_3^+$ ion and a C_3H_2O neutral, (propadienone, propynal or cyclopropenone). The principle of spin conservation is violated in the minor channel, **(709b)**.

Three stable $C_5H_5^+$ species are known to exist, namely the cyclopentadienyl radical cation, the $HC{\equiv}CCHCH{=}CH_2^+$ species, and the vinylcyclopropenyl radical cation. Sufficient energy exists in the reactants to form any of these $C_5H_5^+$ isomers via channel **(709a)**, [ΔH^o for (c)-$C_6H_5^+ + O \Rightarrow C{\equiv}CCHCH{=}CH_2^+ + CO$ is - 352.8 kJ mol^{-1}, and ΔH^o for (c)-$C_6H_5^+ + O \Rightarrow$ vinylcyclopropenone radical cation + CO is - 474.2 kJ mol^{-1}]. In channel **(709b)** all six combinations of the two isomeric $C_3H_3^+$ cations and three C_3H_2O neutrals are thermodynamically accessible.

Cyclic $C_6H_5^+$ also undergoes a fast termolecular association reaction with NO, [$k = (1.9 \pm 0.3) \times 10^{-10}$ cm^3 s^{-1}], and reacts moderately slowly with O_2 via two channels, ie.

$$(c)\text{-}C_6H_5^+ + O_2 \Rightarrow C_4H_5^+ + 2CO + 3.7\ eV^n \quad (0.90) \quad \textbf{(710a)}$$

$$\Rightarrow C_5H_5O^+ + CO \quad (0.10) \quad \textbf{(710b)}$$

$$k_{(710)\ 300K} = (5.4 \pm 0.8) \times 10^{-11}\ cm^3\ s^{-1}$$

The driving force for reaction **(710)** appears to be the formation of the carbon monoxide molecule, with one mole of CO formed for every mole of reactants in the predominant channel, **(710a)**, and two moles formed in the minor pathway, **(710b)**.

In the major channel, **(710a)**, all four known $C_4H_5^+$ isomers, ($CH_3C{\equiv}CCH_2^+$, $CH{\equiv}CCHCH_3^+$, $CH_2{=}CCH{=}CH_2^+$, and the methyl cyclopropenyl radical cation), are thermochemically accessible. No thermochemical data is available for the $C_5H_5O^+$ species, hence the ergicity of reaction **(710b)** cannot be evaluated.

(ix). (c)-$C_6H_6^+$ + O / O_2 / NO. Cyclic $C_6H_6^+$ ions were formed by electron impact on benzene vapour.

No reaction is observed between the $C_6H_6^+$ cation and molecular oxygen, ($k < 5 \times 10^{-13}$ cm^3 s^{-1}), however this species does undergo a rapid reaction with atomic oxygen, viz:

---

[n] Thermochemistry for the methyl cyclopropenyl cation.

$(c)\text{-}C_6H_6^+(^2E_{1g}) + O(^3P) \Rightarrow C_5H_6^+(^2A_2) + CO(^1\Sigma^+) + 3.9\ eV^o$ (0.89) **(711a)**

$\Rightarrow C_4H_4O^+(^2A_2) + C_2H_2(^1\Sigma_g^+) + 1.8\ eV^p$ (0.11)**(711b)**

$k_{(711)\ 300K} = (1.4 \pm 0.4) \times 10^{-10}\ cm^3\ s^{-1}$

Spin is conserved in both of the above channels and the observed rate coefficients are $< 2/6\ k_L \times f$[channel]^q, this being the Langevin collision rate factored by the statistical weight of the spin allowed doublet reaction pathway and multiplied by the "fraction" of the respective channels.

The predominant channel, **(711a)**, involves C atom transfer from cation to neutral thereby forming CO, while acetylene is produced in the secondary channel, **(711b)**, along with a $C_4H_4O^+$ cation, (possibly the furan cation?). Channel **(711b)** clearly involves major fragmentation of the collision complex. Note that both reaction pathways involve the formation of small stable neutral molecules, ie. CO in **(711a)** and C_2H_2 in **(711b)**.

There are 9 known $C_5H_6^+$ isomers, all of which are accessible in reaction **(711a)**, according to the thermochemical data. Thermochemical calculations dictate that only 11 of the 16 known $C_4H_4O^+$ isomers may be formed in reaction **(711b)**, [in order to be generated by the $(c)\text{-}C_6H_6^+ + O$ process, a $C_4H_4O^+$ species must have a ΔH_f^o value of $\sim \leq 997.1$ kJ mol^{-1}].

The $(c)\text{-}C_6H_6^+$ species also reacts with nitric oxide by charge transfer and termolecular association pathways, ie.

$(c)\text{-}C_6H_6^+ + NO \Rightarrow NO^+ + C_6H_6 - 0.004\ eV$ (0.27) **(712a)**

$\Rightarrow C_6H_6.NO^+ + 2.0\ eV^r$ (0.73) **(712b)**

$k_{(712)\ 300K} = (1.4 \pm 0.2) \times 10^{-10}\ cm^3\ s^{-1}$

Note that the charge transfer process, **(712a)**, is essentially thermoneutral.

(x). The Nitrile Cations, $HCNH^+$, HC_3N^+, and $H_2C_3N^+$ + O / O_2 / NO.

The $HCNH^+$ cation was formed via electron impact on hydrogen cyanide, HCN, whilst the HC_3N^+ and $H_2C_3N^+$ cations were both produced following electron impact on cyanoacetylene, HC_3N.

The $HCNH^+$ and $H_2C_3N^+$ cations are unreactive with all three neutral species considered in the current study, [ie. the upper limits for the reaction of

---

o Thermochemistry for the cyclopentadiene cation.

p Thermochemistry for the furan cation.

q f[Channel] denotes the "fraction" of each doublet product channel, **(711a)** and **(711b)**.

r Thermochemistry for the protonated nitrosobenzene cation.

both species with O and O_2 are 2.5 x 10^{-11} cm^3 s^{-1} and 5 x 10^{-13} cm^3 s^{-1}, respectively ; the upper limit for the reaction of $HCNH^+$ with NO is 1.4 x 10^{-11} cm^3 s^{-1}; and the upper limit for the reaction of $H_2C_3N^+$ with NO is 2.3 x 10^{-11} cm^3 s^{-1}].

Atomic oxygen and the cyanoacetylene cation, HC_3N^+, cation react via a rapid three-channel process, viz:

$HC_3N^+(^2\Pi) + O(^3P) \Rightarrow C_3NO^+ + H(^2S)$ (0.50) **(713a)**

$\Rightarrow HC_2N^+(^2A) + CO(^1\Sigma^+) + 3.1$ eV (0.40) **(713b)**

$\Rightarrow NCCHCO^+(^2A'') + 6.8$ eV (0.10) **(713c)**

$k_{(713)\ 300K}$ = (4.1 ± 1.2) x 10^{-10} cm^3 s^{-1}

The ergicity of the major channel, **(713a)**, could not be evaluated due to the unavailability of a heat of formation for the C_3NO^+ product cation.

The ground electronic state of C_3NO^+ is not known but it is likely to be a singlet. This means that all product channels conserve spin and all have observed rate coefficients that are greater than 2/6 k_L x f[Channel][s]. This expression is simply the Langevin collision rate factored by the statistical weight of the spin allowed doublet reaction pathway and multiplied by the "fraction" of each channel, **(713a) - (713c)**.

The two major channels, **(713a)** and **(713b)** proceed via H-O exchange and C atom transfer from cation to neutral, respectively. Pathway **(713b)** continues the trend of cation-O atom reactions producing carbon monoxide as a neutral fragment. A minor termolecular association channel, **(713c)**, is also present.

The HC_3N^+ cation also undergoes a moderately rapid charge transfer reaction with NO, [k = (1.8 ± 0.3) x 10^{-10} cm^3 s^{-1}], and a slow two-channel reaction with molecular oxygen, ie.

$HC_3N^+ + O_2 \Rightarrow HCO^+ + CO + CN + 3.3$ eV (0.55) **(714a)**

$\Rightarrow HC_3N^+.O_2$ (0.45) **(714b)**

$k_{(714)\ 300K}$ = (5.0 ± 0.8) x 10^{-12} cm^3 s^{-1}

The rate coefficient obtained from the present study is double that previously reported by Fox et al., however the product branching ratios obtained in the two measurements are in tolerable agreement. [362]

---

[s] f[Channel] denotes the "fraction" of each doublet product channel, **(713a) - (713c)**.

No thermochemical data is available for the $HC_3N^+.CO$ adduct cation, therefore the ergicity of channel **(714b)** cannot be determined.

(xi). $H_2O^+ + O / O_2 / NO$. The water cation is unreactive with O atoms, ($k < 5.7 \times 10^{-11}$ cm^3 s^{-1}), however this species participates in moderately rapid charge transfer reactions with both O_2 and NO, [$k = (2.5 \pm 0.4) \times 10^{-10}$ cm^3 s^{-1}, and $k = (3.6 \pm 0.5) \times 10^{-10}$ cm^3 s^{-1}, respectively].

(xii). $N_2^+ + O / O_2 / NO$. The nitrogen cation undergoes a moderately rapid two-channel reaction with atomic oxygen reacts, viz:

$$N_2^+(^2\Sigma_g^+) + O(^3P) \Rightarrow NO^+(^1\Sigma) + N(^4S) + 3.1 \text{ eV } (0.95) \textbf{ (715a)}$$

$$\Rightarrow O^+(^4S) + NO(^2\Pi) + 1.0 \text{ eV } (0.05) \textbf{ (715b)}$$

$$k_{(715)\,300K} = (1.4 \pm 0.4) \times 10^{-10} \text{ cm}^3 \text{ s}^{-1}$$

The rate coefficient and product distribution obtained from the current study are in excellent agreement with the two most recent prior investigations of this reaction carried in the early 1970s.[181, 186, 291]

Spin is conserved in the predominant channel, **(715a)**, however this parameter is violated in the minor charge transfer pathway, **(715b)**. Moreover, the observed rate coefficient for channel **(715a)** is $< 4/6\ k_L$, which is the statistical weight of the spin allowed quartet channel.

In the major channel, **(715a)**, a N^+ fragment is transferred from the primary cation to the reactant neutral atom, thereby forming the stable NO^+ cation and a nitrogen atom. The minor channel, **(715b)**, proceeds via simple charge transfer from cation to atom. Reaction **(715b)** is one of the few charge transfer molecular ion-atom processes known.[24, 50, 135]

N_2^+ also undergoes charge transfer reactions with the molecules O_2 and NO, [$k = (5.1 \pm 0.8) \times 10^{-11}$ cm^3 s^{-1} and $k = (3.6 \pm 0.5) \times 10^{-10}$ cm^3 s^{-1}, respectively]. These results are in accordance with the evaluated data of Anicich for gas phase bimolecular ion-molecule reactions.[24]

(xiii). HCO^+ and $HCO_2^+ + O / O_2 / NO$. Both HCO^+ and HCO_2^+ are unreactive with atomic and molecular oxygen, (the upper limit for the reaction of both cations with O is $k < 2.5 \times 10^{-11}$ cm^3 s^{-1}; and the upper limit for the reaction of both species with O_2 is $k < 5 \times 10^{-13}$ cm^3 s^{-1}). HCO^+ is also unreactive with NO, ($k < 5 \times 10^{-13}$ cm^3 s^{-1}), however HCO_2^+ reacts with this neutral via a slow proton transfer reaction, [$k = (1.8 \pm 0.3) \times 10^{-11}$ cm^3 s^{-1}]. The observation of a

slow proton transfer reaction is in agreement with the sole previous measurement of the reaction by Roche and co-workers. [329]

7.5: Implications of this Study to Extraterrestrial Chemistry.

As has been remarked upon above, atomic oxygen is a relatively plentiful component of interstellar clouds, [16] indeed in dark clouds the aggregate amount of oxygen present is greater than the total amount of carbon. [205] This assertion is based on observations made of the depletion of elements, relative to solar abundances, through a diffuse cloud in front of ζ Oph. [382, 383] Throughout the lifetime of an interstellar cloud there is always an excess of oxygen over carbon and, furthermore, a significant proportion of the total oxygen is present in the atomic form. [205] Even at "steady state" ~ 10 % of total oxygen exists as O atoms. [205] The number density of atomic oxygen is significantly elevated above even these number densities in certain discrete regions of the interstellar medium such as the Orion compact ridge, near the luminous infra-red source IRc2. [358]

The widespread occurrence of O atoms in interstellar molecular clouds demands that modellers consider ion-neutral and neutral-neutral reactions involving this species. In 1991 Bettens and Brown published an article which discussed the influence of atomic oxygen on the interstellar chemistry occurring in interstellar clouds. [205] Their study concluded that the effect of ion-O atom reactions on the overall chemistry of interstellar clouds is relatively small. This paper did however suggest that neutral-neutral reactions involving O atoms, if viable, could curtail the interstellar synthesis of complex chemical species. The theoretical study of Bettens and Brown focused upon the O atom chemistry in dense dark interstellar clouds, [205] however the influence of atomic oxygen may be more pronounced in diffuse interstellar clouds. [177] In these objects the number densities of most chemical species, (barring atomic species), are somewhat lower than in dense clouds. [17] Ion-atom reactions, whilst possibly of only modest importance in dark interstellar clouds, may be quite significant processes in diffuse clouds. [17]

Molecular oxygen has not been detected in interstellar clouds, [13, 17] (presumably due to its lack of a permanent dipole moment), although it is almost certainly present in comparatively high abundance. Nitric oxide has been

observed in the interstellar medium, [13, 17] although it is not especially abundant. [16] Reactions between these molecular species and various cations are relevant to the chemistry occurring within a variety of regimes, including interstellar clouds and the atmospheres of gas giant planets, inner ("terrestrial") planets and large satellites.

Implications of the Reactions of Hydrocarbon Cations with O Atoms, O_2 and NO to Extraterrestrial Chemistry

The small hydrocarbon cations, ($C_mH_n^+$, where $m \leq 2$), tend to undergo relatively rapid reactions with atomic oxygen, producing both HCO^+ and $C_mH_nO^+$ type cations. As the size of the reactant hydrocarbon cation is progressively increased, the pattern of reactivity with atomic oxygen changes. The $C_3H_n^+$ and $C_4H_n^+$ ions that are reactive with atomic oxygen do not generate HCO^+ but do still form the $C_mH_nO^+$ cations. With the $C_6H_n^+$ species, (n = 5 and 6), there seems to be a preponderance for the formation of carbon monoxide and a smaller hydrocarbon cation. One characteristic is common to all $C_mH_n^+$ cation-O atom reactions, and that is the presence of multiple product channels. This multiplicity of reaction pathways is not seen to anywhere near the same extent in reactions between cations and H atoms or N atoms, and is curious.

These observations suggest that there is no overall preferred mode of reaction for $C_mH_n^+$ cations reacting with atomic oxygen, rather each process is quite specific to the cation involved. The data provided by the current study supports the contention of Bettens and Brown that H_mC_nO and C_nO molecules could be formed by oxygen atoms reacting with hydrocarbon ions to produce $H_mC_nO^+$, followed by electron-ion recombination. [205] An example of such a process is the synthesis of ketene, $H_2C{=}CO$, (an observed interstellar molecule [13, 17]), via gas phase ion-neutral pathways. In 1991 Millar et al. suggested that this molecule might be made by the following processes: [358]

$C_2H_4^+ + O \Rightarrow CH_3CO^+ + H + 2.7\ eV$ **(706d)**

followed by:

$CH_3CO + e^- \Rightarrow H_2C{=}CO + H + \leq 5.0\ eV$ **(716)**

This proposal appears to gain some degree of validation from the results of the current study, although reaction **(706d)** is only observed to be a 5 % channel in the reaction between ethylene cations and O atoms. The experimental data from

the current research indicates that similar processes to reaction **(706d)** are also viable for the reaction of other hydrocarbon cations with atomic oxygen, eg. $C_3H_3^+$ and $C_4H_2^+$. Carbon-oxygen bonds are forged in every cation-O atom reaction studied in the present work. This outcome indicates that hydrocarbon cation-O atom reactions are a useful interstellar route to the formation of carbonyl compounds.

The fact that several of the cation-O atom reactions produce either HCO^+ and a smaller hydrocarbon neutral, or, alternatively, CO and a smaller hydrocarbon cation is also interesting as CO and HCO^+ are plentiful interstellar species and probably act as "sinks" for oxygen. [205] Indeed carbon monoxide is the second most abundant molecule in the cosmos, (behind H_2), and therefore a large proportion of the oxygen present in the universe is tied up in this form. [13, 16] The formyl cation, HCO^+, being unreactive with H_2, [24] is the most abundant interstellar ion [16] and it is readily generated by ionised CO reacting with H_2. [24]

With few exceptions hydrocarbon cations are unreactive with O_2 and only mildly reactive with NO. Only two hydrocarbon cations in this study reacted at measurable rates with O_2, namely $C_2H_2^+$ and (c)-$C_6H_5^+$. This finding indicates that ion chemistry involving O_2 is likely to be unimportant in the interstellar medium, despite the relatively high number density of O_2 in this environment. [16] In general, hydrocarbon ions are more reactive with nitric oxide. These processes proceed by charge transfer, forming NO^+, (which has been detected in interstellar clouds [13, 17]), or termolecular association generating larger adduct cations. Termolecular association processes involving molecular oxygen or nitric oxide are unimportant under the low density regimes encountered in interstellar molecular clouds, although they are indicative that analogous radiative association reactions may be viable. [384]

Implications of the Reactions of Non-Hydrocarbon Cations with O Atoms, O_2, and NO to Extraterrestrial Chemistry

An examination of the data in Table 7.2 indicates that few of the non-hydrocarbon species examined in the current study are reactive with O atoms. In particular, $HCNH^+$, HCO^+, HCO_2^+, H_2O^+, and $H_2C_3N^+$are unreactive with atomic oxygen. The first three of the ions are observed interstellar species, [13, 17] and interestingly this triumvirate are unreactive with H_2, N_2, N, and O [24, 50] ,(as

also is $H_2C_3N^+$). It appears then that these cations are somewhat inert, particularly when located in an environment where these four neutrals are amongst the most neutral plentiful species. [13, 16] Only HC_3N^+ and N_2^+ undergo reactions with O; neither of these cations have been detected in the interstellar medium to date, [13, 17] although they are both almost certainly present. Note that the neutral HC≡CCN molecule has been detected in interstellar clouds [13, 17] which implies that its cation will also be present.

This general lack of reactivity by nitrile cations and other non-hydrocarbon species towards atomic oxygen is in contrast to the high degree of reactivity displayed by hydrocarbon cations towards this reagent. As only seven reactions between non-hydrocarbon cations and O atoms have been characterised in the present study, the database is too small to make a credible assessment of the overall importance of these processes to interstellar synthesis.

Several non-hydrocarbon cations participate in reactions with O_2, including HC_3N^+, H_2O^+ and N_2^+. These last two reactions proceed by charge transfer, generating O_2^+, which, whilst not yet detected in the interstellar medium, [13, 17] is very likely to be present. These same cations, along with HCO_2^+, also react with NO mainly via charge transfer processes, producing the observed interstellar species, NO^+. [13, 17]

7.6: Concluding Remarks.

The rate coefficients for most cation-O atom reactions are significantly less than the limiting Langevin collision rate constant. This finding is not particularly startling as the effect was also observed for the reactions between various cations and both atomic hydrogen and nitrogen. It appears, therefore, that nearly all ion-atom processes react at rates that are at best 70 % of the Langevin collision rate. One exception to this statement is the electron detachment reaction between chloride anions and atomic hydrogen. [43, 167-171] This phenomenon is somewhat perplexing, as Langevin theory should provide an adequate description of the reactive encounter between an ion and a neutral atom, which obviously has no permanent dipole moment. [1, 105] Indeed this particular class of reaction is one of the few known examples of an ion-induced dipole process where Langevin theory *apparently* fails to provide expectation values for rate coefficients that are in good agreement with experimental results. [52, 107, 108]

It should be noted that Langevin theory in particular, simplistically treats both reactant species as point masses and does not consider the individual quantum states of the reagents. [1, 105]

An alternative, but equally valid explanation as to why the overwhelming majority of cation-atom reactions proceed at rates that are less than k_L is that a significant proportion of collisions are elastic and do not result in reaction. Why this might be so is as yet unknown and any comment is somewhat conjectural. For ion-atom reactions the coupling of orbital angular momenta between ion and atom during the collision may be especially important. Stereochemical effects, ie. the *specific* trajectories of approach of the reactant species, may also be much more critical for reactions between cations and atoms. These statements are quite speculative but what is relatively certain is that existing theories inadequately describe this class of reaction and theoretical input is required to develop a new quantitative theory that satisfactorily reproduces the experimental results.

To further complicate the picture the "true" physical situation may lie somewhere between the two explanations proffered above. Langevin theory may not constitute an adequate description of the collision frequency between atoms and cations and, additionally, there may also be a barrier to reaction during the collision process itself.

Most cations examined in the current study reacted with O atoms relatively quickly, in fact no slow, ($k \sim 10^{-11}$ cm^3 s^{-1}), cation-O atom reactions were observed. The other intriguing aspect of these reactions is the existence of multiple product channels, suggesting that the potential energy surfaces for the transition states may be complex. Moreover, in several cases, eg. $C_2H_2^+ + O$, (c,ac)-$C_3H_3^+ + O$, $C_4H_2^+ + O$, and (c)-$C_6H_5^+ + O$ there is no clear predominant product channel. This result further indicates that the geometry and energy with which the reagents approach the encounter may result in the collision complex adopting subtly different configurations, thereby leading to disparate products. The systems examined in the present work also show little propensity to participate in termolecular association processes. Obvious exceptions to this statement include the cation-O atom reactions involving $C_2H_3^+$, $C_4H_2^+$ and HC_3N^+, which exhibit minor termolecular association pathways. This outcome is different from that observed for the reactions between various cations and

either H or N atoms, however the reasons for the divergent behaviour are unclear. Also, several cation-O atom reactions demonstrate a tendency to generate the particularly stable carbon monoxide molecule as a neutral product.

Of the 19 cation-O atom reactions reported in the present research only three have been the subject of previous investigations. [24, 50, 135] In these three cases excellent agreement was obtained between the current data and literature values; this concurrence between results engenders confidence that the "new" data presented here for the various cation-O atom reactions is likely to be accurate.

This study has reinforced the trend evident in the chemical literature that many cations are unreactive with molecular oxygen. [24, 50] Again, of the 19 reactions between various cations and O_2 that are reported herein, 6 have been previously investigated. Once more the current data is well in accord with any previous measurements. Where cations react with molecular oxygen there is no clear trend in the product channels observed. A small number of species participate in charge transfer processes with this neutral, eg. H_2O^+ and N_2^+, whilst hydrocarbon and nitrile cations seem to react via either complex fragmentation or termolecular association pathways, eg. CH_3^+, $C_2H_2^+$, (c)-$C_6H_5^+$ and HC_3N^+.

Many more cations are reactive with nitric oxide and occasionally these reactions are rapid. Nineteen reactions between a series of cations and NO are reported in this chapter, of which data exists in the literature for six processes. [24, 50] These reactions primarily proceed via charge transfer, (nitric oxide is readily ionised, the IP being only 9.26 eV), and / or termolecular adduct formation. Excellent agreement is again obtained between the current results and historical data.

Much of the chemistry discussed in this chapter is pertinent to processes occurring in quiescent interstellar clouds, shocked regions of the interstellar medium, and extraterrestrial atmospheres. Indeed, the incorporation of the data presented in this work into contemporary interstellar ion-chemical models is likely to produce amendments to the calculated abundances of many known interstellar species.

CHAPTER 8.

SOME PRELIMINARY EXPERIMENTS BETWEEN IONS AND ATOMIC CARBON.

8.1: Introduction.

Atomic carbon is a relatively minor constituent of the interstellar medium, however its number density is elevated above "normal" levels in the vicinity of C-rich giant stars. [385] These "metal-rich"[a] stars are plentiful and ubiquitous throughout the Milky Way galaxy, (and therefore by extrapolation, presumably other galaxies), and apparently act as effusive sources of carbon. [385] The standard model of Lee and associates tabulates the nominal steady state fractional abundance of atomic carbon in dense interstellar clouds as 3.9×10^{-8} at 10 K, and 7.3×10^{-9} at 50 K, (all numbers relative to $H_2 = 1$). [16] Note that at "early times", ($\sim 10^5$ years), the fractional abundance of interstellar elemental carbon is considerably higher, ie. $\sim 5 \times 10^{-5}$ relative to $H_2 = 1$. [16] As an interstellar cloud evolves, the concentration of atomic carbon is depleted, due mainly to chemical reactions. Also, the relative ease with which atomic carbon is photo-ionised means that a proportion of the initial interstellar complement of this species is converted to C^+ cations. [386]

Carbon is a component of the vast majority of chemical species that have been identified in interstellar clouds. [13, 17] The mechanism of how carbon is "fixed", or incorporated into interstellar molecules is thus a question that has long occupied the minds of many scientists interested in interstellar chemistry. Several commentators have suggested that the inception point for the formation

---

[a] Astrophysicists use the term "metals" to refer to all elements other than H and He.

of simple hydrocarbon molecules and ions is the proposed reaction between H_3^+ and atomic carbon, viz: [17, 386, 387]

$$H_3^+ + C \Rightarrow CH^+ + H_2 + 2.1\ eV \qquad \textbf{(801)}$$

This key reaction has not yet been investigated in laboratory experiments, but it is known from numerous experiments that exothermic proton transfer reactions, like process **(801)**, are invariably rapid. [17] Furthermore, in 1991, the $H_3^+ + C$ interaction was studied theoretically and found to be viable and fast. [388] The generation of CH^+ activates the entire ion-neutral gas phase synthetic sequence for the production of hydrocarbon molecules. [17] Atomic carbon may also participate in ion-atom reactions with larger hydrocarbon cations, eg. [387]

$$CH_3^+ + C \Rightarrow C_2H_2^+ + H + 2.7\ eV \qquad \textbf{(802)}$$

A search of the chemical literature reveals that, to date, there are no reported laboratory studies of reactions between ions and atomic carbon. [24, 50] The primary reason for this deficiency is that, experimentally, atomic carbon is an extraordinarily difficult neutral reagent to generate in known flow rates. [17, 386] Furthermore, discrete carbon atoms have a known penchant for clustering into C_2 units, (and higher clusters if conditions are conducive to such a condensation). Whilst presenting formidable problems, any measurements in this unexplored avenue of ion-C atom chemistry would be worth the necessary expenditure of time and effort.

In contrast to the dearth of available data on ion-carbon reactions, several measurements of reactions between neutral species and C atoms have been reported. Husain and co-workers have carried out a number of successful investigations into neutral-neutral chemical systems involving atomic carbon. In these experiments atomic carbon was produced by pulsed flash photolysis of carbon suboxide, C_3O_2. [389, 390] A Japanese group have also formed atomic carbon and characterised its reactivity with several molecules, including NO, NO_2, and HI. These Japanese researchers formed ground state C atoms, [C (^{3}P)], by dissociating carbon monoxide with metastable argon atoms which had been produced in a microwave discharge. [391-393] In yet another study, Kaiser and colleagues have examined the reactions of C (^{3}P) with actetylene, methylacetylene, ethylene, and propene in a crossed-beam apparatus. The

atomic carbon used in these experiments was generated by focussing a neodymium YAG laser onto a rotating carbon rod and then seeding the C atoms into a Ne or He carrier gas. [394]

The objective of the current experiments was to establish techniques to produce a useable flux of ground state C (^{3}P) atoms and efficiently admit this species into the reaction zone of the main flow tube.

8.2: Experimental.

Essentially, two different experimental methodologies were trialed in this section of work.

Microwave Discharge of Dilute CO / Ar and CO / He Mixtures

In the first batch of experiments dilute mixtures of carbon monoxide, in either helium or argon gas, were subjected to a microwave discharge and the resulting neutral mixture admitted into the flow tube. A monitor cation, (eg. N_2O^+ or Ar^+), was simultaneously injected into the flow tube in the usual manner and the resulting mass spectrum observed.

Initially an ~ 1.6 % mixture of CO in Ar was used, and then subsequently an ~ 0.7 % mixture of CO in He was employed. The abbreviated N-atom probe used to perform the $H_3^+ + N$ measurements, (Chapter 6), was modified for this sequence of experiments. This probe was coated with the halocarbon wax / chloroform mixture as previously described in Chapters 4 - 7 in an attempt to reduce atom-atom surface recombination. The glass wool plug that had been present for all cation-N atom reactions was removed from the probe.

Production of C (^{3}P) via the Reaction of CO with Ar Metastable Atoms

In a second sequence of experiments Ar* atoms were used to dissociate CO gas into C atoms. [391-393]

This technique required the designing and construction of a new atom probe, which is depicted in Figure 8.1. This new probe was in fact a reincarnation of the short N atom probe utilised for the initial study detailed above, in which CO was directly subjected to a microwave discharge. Two substantial alterations were made to this "secondary" N atom probe. The first modification involved incorporating a carbon monoxide inlet into the atom probe. This inlet was of the type used to introduce NO for the studies between

various cations and O and N atoms, and consequently has been previously described in some detail in Chapters 5 and 7. For a small number of initial experiments the quartz discharge section was standard 13 mm o.d., 10 mm i.d. tubing, however this original design was also transformed by incorporating a much thinner ~ 3 cm long section of 4 mm o.d., 2 mm i.d., quartz tubing in the middle of the vertical discharge section of the probe. The rationale for this modification was a bid to optimise the flux of Ar* metastable species generated in the microwave discharge. Broida had previously discovered that an extremely thin section of quartz tubing markedly increases the flux of metastable atoms produced by the action of a microwave discharge. [395] The interior of this probe was coated with a halocarbon wax / chloroform mixture downstream of the discharge region.

The experimental procedure involved subjecting pure, (100 %), argon gas to a microwave discharge, thereby forming Ar* ($^3P_{2,0}$) metastable atoms. A small flow of carbon monoxide gas was then introduced into the atom probe a short distance, (~ 3.4 cm), downstream of the probe's elbow and the following reactions ensued: [391-393]

$$Ar^*(^3P_{2,0}) + CO \Rightarrow C(^3P) + O + Ar + < 0.5\ eV \quad \textbf{(803)}$$

$$Ar^*(^3P_{2,0}) + CO \Rightarrow CO^*[(A\ ^1\Pi), \text{and } (b\ ^3\Sigma^+)] + Ar + < 1.1\ eV \quad \textbf{(804)}$$

followed by; [396]

$$CO^*(a\ ^3\Pi) + CO \Rightarrow CO_2 + C(^3P) + 0.4\ eV \quad \textbf{(805)}$$

Note that firstly, some ground state C atoms are formed directly from the reaction of CO with metastable argon atoms, Ar* ($^3P_{2,0}$), ie. reaction **(803)**. The energies of the Ar* metastable atoms, ($^3P_2$ = 11.55 eV and $^3P_0$ = 11.72 eV), are insufficient to generate excited state C (^1D) or (^1S) atoms. [391] Secondly, C atoms are also generated indirectly by the reaction of metastable carbon monoxide molecules with ground state CO molecules, [reaction **(805)**]. [396] As noted above, reaction **(804)** produces two excited states of CO*, namely the (A $^1\Pi$), and (b $^3\Sigma^+$) states. [391] Whilst the (A $^1\Pi$) state rapidly relaxes to the ground state, the (b $^3\Sigma^+$) state only relaxes as far as the (a $^3\Pi$) metastable state, [392] which has a lifetime of ~ 10^{-3} seconds. [397] The ultimate fate of the (a $^3\Pi$) state is somewhat contentious in that some workers maintain that it radiates into the v'' = 1 vibrational state [398] while others suggest that it reacts

with ground state CO molecules forming atomic carbon and CO_2, viz reaction (**805**). [396]

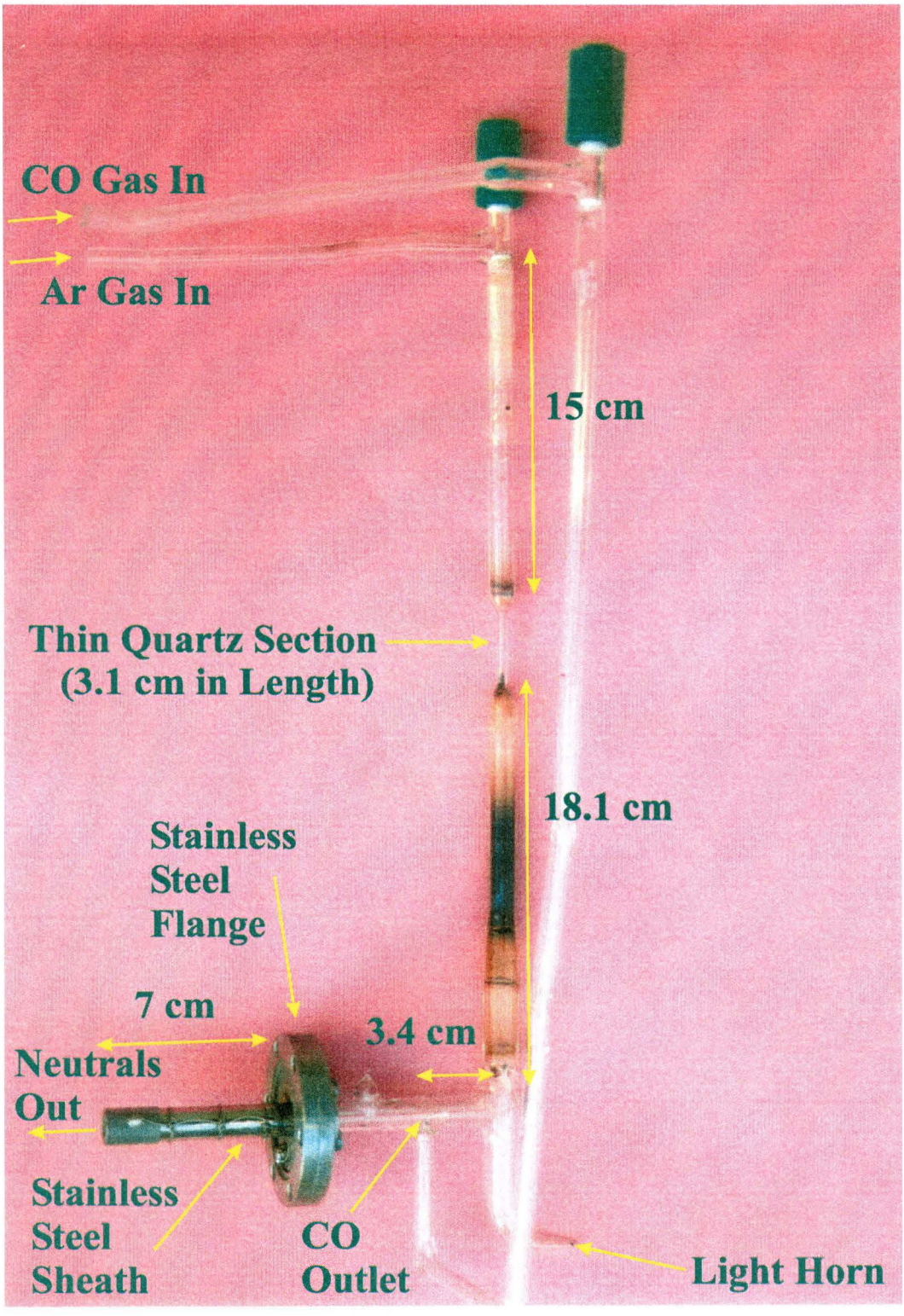

Figure 8.1. The carbon atom probe used to generate C atoms from the reaction of Ar* ($^3P_{2,0}$) metastable atoms with CO. Carbon deposition may be clearly seen on the interior surfaces of the probe.

Having supposedly produced a flux of atomic carbon using the combined reaction sequence **(803)** through **(805)**, a series of cations, (eg. CO^+, Ar^+), were SIFT injected into the flow tube in an attempt to observe a reaction between the ion and either C or O atoms.

8.3: Results.

Neither of the experimental methodologies trialed produced satisfactory results, in that no definitive reaction between a cation and atomic carbon was detected. During the course of this research many observations were made, the salient points of which are noted below.

Results Obtained by Discharging CO / Ar and CO / He Mixtures

The first experiments that were attempted involved directly discharging dilute mixtures of carbon monoxide in noble gases, in an effort to generate atomic carbon. This mode of operation quickly resulted in the interior of the atom probe becoming coated in black soot for some considerable distance downstream of the microwave discharge region.

The N_2O^+ cation was used as monitor ion during an experiment in which an ~ 1.6 % CO in Ar mixture was discharged. This particular cation was selected because it was hoped that the following reaction with C atoms might ensue:

$$N_2O^+ + C \Rightarrow CN^+ + NO + 1.6\ eV \qquad \textbf{(806)}$$

This nitrous oxide cation was selected as an ideal monitor ion because the reactions between CO, (the predominant constituent of the neutral reagent mixture), and both the primary cation, N_2O^+, and postulated product ion of reaction **(806)**, CN^+, have been previously characterised, viz: [399]

$$N_2O^+ + CO \Rightarrow CO_2^+ + N_2 + 2.9\ eV\ (0.37) \qquad \textbf{(807a)}$$

$$\Rightarrow NO^+ + NCO + 0.8\ eV\ (0.63) \qquad \textbf{(807b)}$$

$k_{(807)\ 300K} = (3.0 \pm 0.6) \times 10^{-10}\ cm^3\ s^{-1}$

and; [24]

$$CN^+ + CO \Rightarrow CO^+ + CN + 0.08\ eV \qquad \textbf{(808)}$$

$k_{(808)\ 300K} = (4.4 \pm 2.6) \times 10^{-10}\ cm^3\ s^{-1}$

Note that neither channel of reaction **(807)** produces an ion which has the same m/z ratio as CN^+, ie. m/z = 26, or CO^+, (which is the ion formed as a result

of the secondary reaction between CN^+ and CO), ie. m/z = 28. Thus the observation of an ion at m/z = 26 and / or m/z = 28 in this experiment would strongly suggest that the postulated process **(806)** between N_2O^+ and C did in fact proceed.

When this experiment was performed the expected ions at m/z = 30, (NO^+), and m/z = 44, (CO_2^+), were observed but no ion products at m/z = 26 or 28 were seen. This negative result suggests either no significant flux of C atoms was delivered into the main flow tube, or that reaction **(806)** does not occur.

Interestingly, a spectrum recorded when the monitor ion was prevented from entering the main flow tube, (achieved by deselecting the upstream quadrupole mass filter), shows a peculiar periodicity of mass peaks, ie. m/z= 44, m/z= 56, m/z = 68 etc. Note that this mass spectrum corresponds solely to the discharge of a dilute carbon monoxide mixture in an argon bath gas, or alternatively it may be attributed to the action of the microwave discharge on the black carbon deposit, (soot), on the inside of the probe. The major mass peaks in this spectrum were provisionally assigned to O_2^+, (m/z = 32) CO_2^+, (m/z = 44), $C_2.O_2^+$, (m/z = 56), $C_3.O_2^+$, (m/z = 68), with a smaller $C_4.O_2^+$ peak (m/z = 80). It would also appear that there is an N_2 contaminant in this CO / Ar mixture as evidenced by the "fingerprint" peak at m/z = 30, (NO^+). A typical mass spectrum obtained from this experiment is shown in Figure 8.2.

This type of experiment was repeated using an ~ 0.68 % CO in He mixture with similarly negative results. In this particular experiment, Ar^+ was selected as the monitor ion as it was hoped to detect the presence of O_2^+, (produced via the recombination of oxygen atoms formed by the microwave discharge of CO), at m/z = 32. Alternatively, whilst unlikely, it is thermochemically possible for Ar^+ cations to charge transfer to C atoms, hence there was a small possibility that a m/z = 12 peak might be observed. The IP's of Ar and C are 15.76 eV and 11.26 eV respectively, thus the likelihood of charge transfer is remote, as atomic species generally only participate in such reactions when the IP's are near resonance.

Unfortunately when this experiment was performed a small peak was present at m/z = 32, even with the Ar^+ monitor ion deselected. This suggested that O_2^+ was generated directly in the atom probe due to action of the microwave discharge on either the CO / He mixture or the soot deposit. Under the same

operating conditions, (ie. Ar^+ monitor ion deselected), further masses were observed at m/z ratios of 12, 16, 18, 28, 32, and 44. Intriguingly the small m/z = 12 peak indicates that some C^+ was being produced in the atom probe.

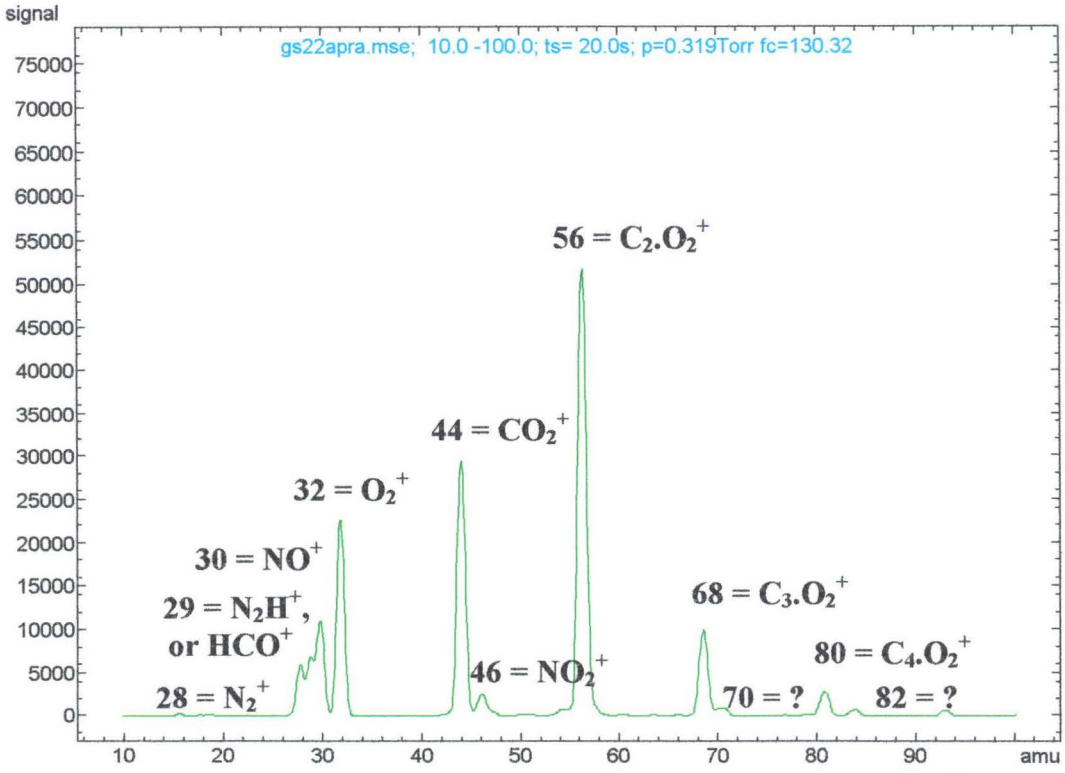

Figure 8.2. Mass spectrum obtained from the discharge of a dilute ~ 1.6 % mixture of CO in Ar. Note that the analyser quadrupole response is somewhat non-linear, in that peaks at high m/z ratios appear to be ~ 1 amu high.

At this point, because of the fouling of the atom probe, and the complexity of the mass spectra being generated it was decided to forgo any further experiments conducted using this specific mode of operation.

Results Obtained by Producing C (^{3}P) via the Reaction of CO with Ar*

In an effort to observe an ion-C atom reaction, a series of monitor cations were injected into the flow tube whilst ground state carbon atoms were supposedly produced by the action of Ar* metastable atoms on CO.

Prior to the inclusion of the thin section of quartz tubing in the middle of the discharge section of the probe, both $C_2N_2^+$, and $C_2H_2^+$ were SIFT injected and the mass spectra monitored for any evidence of a reaction between either ion and C atoms. Unfortunately no ionic products consistent with the reaction of these species with atomic carbon were apparent.

In a further experiment a small flow of ethylene, C_2H_4, was added to the flow tube through an upstream inlet, whilst Ar* metastable atoms were simultaneously generated in the microwave discharge. Ionic products created by the Penning ionisation of ethylene were detected and hence this investigation conclusively showed that a moderate flux of Ar* metastable atoms was indeed entering the flow tube. The largest "product" ions detected from this procedure were $C_3H_5^+$, (from the reaction of $C_2H_4^+ + C_2H_4$ [24]), and $C_2H_5^+.C_2H_4$, at ~ 2000 counts per second for each cation. Note that the $C_2H_5^+$ cation was presumably formed in this system by the reaction of $C_2H_3^+$, (formed directly via Penning ionisation of C_2H_4), with the parent molecule C_2H_4. [24]

The C atom probe with the thin quartz section in the centre of the discharge region was subsequently installed on the SIFT instrument and a series of measurements performed.

Ethylene was once more admitted to the flow tube through an upstream inlet and the Penning ionisation of this neutral by Ar* metastables examined. This experiment demonstrated considerably greater levels of ionic products, (~ 30,000 counts per second of ions such as $C_3H_5^+$ and $C_2H_5^+.C_2H_4$), thereby indicating that the flow rate of metastable Ar* atoms had been greatly enhanced by modifying the probe.

Next, a number of reactant cations were SIFT injected in an attempt to observe a reaction between any of these species and atomic carbon. These species were CO^+, Ar^+, HCN^+, $C_2H_2^+$, $C_4H_3^+$, $C_4H_2^+$, CS^+, and CS_2^+. During these experiments no ionic products that could have arisen from the reaction of any of these monitor cations with C atoms were observed.

It is interesting to record however, that during the experiments performed with both CO^+ and Ar^+ as monitor ions, a peak at m/z = 44 was observed which was assigned to CO_2^+. The presence of this peak indicated that CO_2 was seemingly entering the reaction zone of the flow tube and subsequently being ionised by the SIFT injected CO^+ or Ar^+ monitor cations. [24] This carbon dioxide flow was most likely the result of reaction **(805)**, ie. the reaction of CO* metastable molecules with ground state carbon monoxide molecules. [396] The stoichiometry of this reaction indicates that for every CO_2 molecule produced, one carbon atom should be formed, hence if the above reasoning is correct, C atoms should also have been entering the flow tube.

The fact that no cation-C atom reactions were apparent with any of the monitor species employed may indicate that all of the examined processes are not viable. Alternatively, the more credible explanation for these observations is that despite the apparent production of CO_2 in the side arm, C atoms are not entering the reaction zone of the flow tube for reasons that are currently unknown.

8.4: Conclusions.

This block of experiments appears to have confirmed what many researchers working in the field of ion-neutral reactions have known and appreciated for years; ion-C atom processes are not easily studied in the laboratory. It is somewhat unsatisfactory to conclude the research detailed in this thesis with an unsuccessful segment of work.

Notwithstanding the above comments some useful facts have been gathered during this investigation. It has been demonstrated that directly discharging dilute mixtures of carbon monoxide in noble gases leads to a deposition of carbonaceous soot inside the atom probe. Furthermore, complex mass spectra obtained from these experiments show that a plethora of ionic species are generated under these circumstances.

The evidence provided by the second mode of generating atomic carbon, namely via the reaction of Ar* metastable atoms with CO, is more confusing. The observed production of CO_2 would tend to indicate that C atoms are being formed using this technique but, if so, why are no ionic products observed that can be attributed to the reaction between the various monitor ions trialed and C atoms? As remarked upon above it may be that none of these species react with atomic carbon, but in all likelihood some of them probably do and additional developmental work needs to be done on efficiently admitting atomic carbon into the reaction zone of the main flow tube.

This study will hopefully qualify as the starting point for the first ever measurement of a reactions between an ion and atomic carbon at the University of Canterbury, rather than a plaintive investigation of little enduring merit. The carbon atom probe depicted in Figure 8.1 is currently undergoing further modifications before being reinstalled on an upgraded FA / SIFDT instrument.

These alterations include reversing the direction with which CO is admitted into the atom probe, (to hopefully prevent CO from permeating upstream into the vicinity of the microwave discharge). That section of the probe downstream of the CO inlet is also being extended by approximately 5 cm to allow time for complete reaction of Ar* metastable atoms with carbon monoxide. This modification is required as eventually rate coefficients for the reaction of various ions with C atoms need to be evaluated and it is therefore essential to achieve a point source of the neutral, (C atoms), at their entry point into the main flow tube. If C atoms continue to be created in the flow tube by the action of Ar* metastable atoms on CO, the standard mathematical expressions for the evaluation of rate coefficients in flow tube experiments are invalidated. Finally, carbonaceous deposits were observed to accumulate on the concentric dimples immediately upstream of the probe's elbow, (used to locate the glass wool plug used in the N and O atom experiments), and consequently this feature is to be removed.

CHAPTER 9.

CONCLUDING REMARKS AND SUGGESTIONS FOR FUTURE WORK.

At this juncture it is appropriate to briefly review the entirety of work presented in this thesis and offer some suggestions for future endeavours.

9.1: A Summary.

It is not perhaps immediately apparent that this research does have a certain coherence and is not merely a disjointed miscellany of unrelated projects.

The first project tackled was a combined experimental and theoretical investigation of the $C_3H_3O^+$ system. Two $C_3H_3O^+$ isomers were examined experimentally and, additionally, the $C_3H_3O^+$ potential energy surface was characterised. This was an ideal initial assignment as it provided excellent exposure to many techniques that were later employed during the atom research.

The aim of the $C_3H_3O^+$ work was to determine whether the association product between $C_2H_3^+$ and carbon monoxide has the same isomeric structure as protonated propynal, $HC{\equiv}C\text{-}CHOH^+$. Propynal, $HC{\equiv}C\text{-}CHO$ is an observed interstellar molecule, [13, 17, 202] and several eminent commentators have suggested that the condensation of $C_2H_3^+$ and CO followed by dissociative electron recombination might yield this species in the interstellar medium. [203] In actuality, a combination of experimental measurements and theoretical calculations clearly showed that the $C_2H_3^+$.CO association product has the structure of C2-protonated propadienone, $H_2C{=}CH\text{-}C{=}O^+$. Furthermore, this work enabled the proton affinity of propynal to be bracketed between 759 and 736 kJ mol^{-1}, and that of propadienone to be constrained within the limits of 896 to 868 kJ mol^{-1}.

This work showed that it was extremely unlikely that propynal was formed in interstellar clouds via the $C_2H_3^+ + CO$ association pathway, and that an alternative synthetic route must be sought.

The remainder of the research discussed in this thesis is concerned with the characterisation of a number of ion-atom processes. In particular, data has been presented for the reactions of a number of cations with H, N and O atoms. These studies may partially redress the current paucity of experimental results that are available on these very important ion-atom processes. [24, 50, 135] The reaction of many cations with H_2, N_2, O_2, and NO were also measured as a necessary adjunct to the investigation of the ion-atom systems.

It is of particular interest to note that no ion-atom reaction studied proceeded at a rate that approached the limiting Langevin collision rate. This apparent aberration may be attributed to unknown barriers to reaction during the ion-atom encounter, or, alternatively, may be because Langevin theory provides an overly simplistic description of the ion-atom collision process. Spin conservation appears to have minimal effect on the outcome of ion-atom reactions, as has been previously noted by several distinguished workers in the field. [162, 177]

The ion-H atom study determined that most hydrocarbon cations react with atomic hydrogen via either a hydrogen atom transfer route, or a termolecular association pathway. No clear trends were established with regard to the reactivity of non-hydrocarbon cations with H atoms, as each system found its own unique reaction pathway. With regard to the reactions of cations with H_2 it is observed that H atom abstraction, (where exothermic), is the prevalent mechanistic pathway. The only qualification to this statement is that saturated hydrocarbon cations tend to be unreactive with molecular hydrogen. These cation-H / H_2 reactions are particularly pertinent to gas phase ion-neutral interstellar synthesis, as both H and H_2 are very plentiful in molecular and diffuse clouds.

The reactions of in excess of 30 cations with atomic and molecular nitrogen have been characterised. This investigation has indicated that, in general, smaller $C_mH_n^+$ species react with N atoms by forming C-N bonds and the attendant elimination of atomic or molecular hydrogen. Larger hydrocarbon species usually react somewhat differently with atomic nitrogen, producing the

stable HCN neutral and a lower mass $C_mH_n^+$ fragment. Several non-hydrocarbon cations also undergo moderately rapid reactions with N atoms, however there are no obvious patterns to this reactivity. In contrast, most cations are unreactive with N_2. These processes are variously applicable to interstellar chemistry [177] and aeronomy occurring within extraterrestrial nitrogenous atmospheres. [282, 283]

The critical reaction between H_3^+ and N atoms has been examined in the laboratory and found to proceed rapidly. The product channel is almost certainly $NH_2^+ + H$. This ion-atom process provides an alternative, and more facile, synthetic pathway to ammonia in interstellar clouds at low temperatures than the conventional $N^+ + H_2$ route. [14]

The reactions between 12 hydrocarbon and 7 non-hydrocarbon cations with O atoms, O_2, and NO have been studied in laboratory experiments. Hydrocarbon cations react with atomic oxygen via a variety of channels including forming $C_mH_nO^+$ species and an H or H_2 fragment. This generalisation holds for $C_mH_n^+$ cations of small and medium size, ie. $C_mH_n^+$, where $m \leq 4$. Larger hydrocarbon cations interact with O atoms, producing the stable carbon monoxide molecule and a smaller hydrocarbon cation fragment. Only two of the seven non-hydrocarbon cations examined, are reactive with atomic oxygen.

Many ions are unreactive with O_2, however those that do react tend to proceed via charge transfer or association pathways. Nitric oxide is a more reactive neutral, with many ionic species participating in charge transfer and / or termolecular association reactions with this reagent.

Several preliminary experiments were conducted in an effort to measure the first ion-C atom reaction. The techniques for generating atomic carbon included discharging dilute mixtures of CO in argon or helium, and dissociating carbon monoxide using Ar* ($^3P_{2,0}$) metastable atoms. [391-393]

Laboratory studies of ion-atom processes are somewhat challenging and hence the totality of work presented herein is significant. This conglomeration of ion-atom data is applicable to chemical processes occurring in most of the regions in which plasma exist.

9.2: Suggestions for Further Work.

The experimental / theoretical investigation into the $C_3H_3O^+$ system was unable to identify a viable ion-molecule route to propynal. Petrie has made the credible suggestion that the radical / neutral reaction between C_2H and H_2CO might provide the route to this observed interstellar molecule. [227] It is desirable that an experiment be undertaken to verify, (or repudiate), this pathway to HC≡C-CHO.

The Boulder research group headed by Bierbaum is currently pursuing the study of reactions between naphthalene ions and H, N, and O atoms. [175] These investigations are extremely interesting as they augment the ion-atom data presented in this thesis. There is certainly tremendous scope for measuring the reactions of many more cations with atoms. In particular, it is very important to remeasure the reaction of H_3^+ with atomic oxygen and check on the accuracy of the sole measurement for this process reported by Fehsenfeld in 1976. [180] There would also be considerable merit in other laboratories remeasuring any of the processes examined in the current work as an independent check on the veracity of the data presented herein.

Whilst probably not applicable to interstellar chemistry, it would be quite novel to investigate the reaction of various cations with halogen atoms, eg. F or Cl. This work would probably be extremely difficult as the generation of halogen atoms and introduction of such species into a flow tube, has not yet been attempted by any workers in the field.

The apparent problem of virtually no ion-atom processes proceeding at the kinetic theoretical limit, ie. the Langevin collision rate, needs to be explained. The reaction between Cl^- anions and H atoms is rapid, [43, 167-171] but this particular reaction is somewhat atypical in that it is an associative detachment process, which involves the emission of a stabilising electron from the collision complex. The detailed mechanism for associative detachment reactions is not well elucidated, [43-46] but it may well be substantially different from that encountered in the many cation-atom systems studied in the current research. In any case the development of a cogent theoretical treatment of ion-atom interactions would be extremely valuable.

The cation-atom data collated in this thesis needs to be incorporated into interstellar ion-chemical models. To some extent this work has already been commenced due to collaborations with researchers who are currently engaged in modelling the chemical environment and evolution of interstellar clouds. [400] It may be that several of the reactions investigated during the course of the current research have a significant effect on the "chemical balance sheet" that is generated by these models.

Finally, the ion-C atom research that was commenced during the current work needs to be pursued with vigour. The technique of generating of C atoms by using Ar* ($^3P_{2,0}$) metastable atoms to dissociate CO needs to be optimised [391-393, 396] or, alternatively, a new methodology, (perhaps involving the pulsed flash photolysis photolysis of carbon suboxide, C_3O_2 [389, 390]), developed. The characterisation of the critical reaction between H_3^+ and carbon atoms is undoubtedly the final goal of this project. Only when this process is finally measured will researchers in the field of interstellar chemistry be certain that $H_3^+ + C$ is the primary reaction which initiates the formation of hydrocarbon species in the interstellar medium. [17, 386, 387]

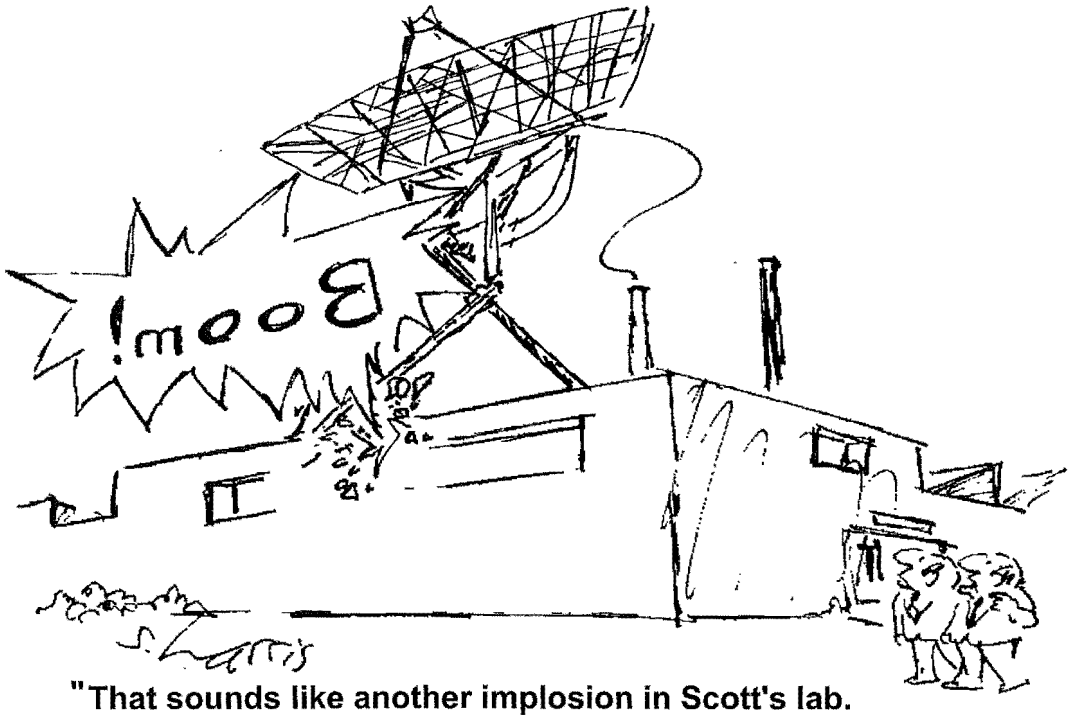

"That sounds like another implosion in Scott's lab. He's trying to make ammonia in interstellar clouds you know."

REFERENCES

1. Langevin, P.M., *Ann. Chim. Phys.*, **5**, 245, (1905).
2. Thomson, J.J., *Phil. Mag.*, **24**, 209, (1912).
3. Hogness, T.R., and Lunn, E.G., *Phys. Rev.*, **26**, 44, (1925).
4. Eyring, H., Hirschfelder, J.O., and Taylor, H.S., *J. Chem. Phys.*, **4**, 479 (1936).
5. Gutbier, H., *Z. Naturforsch*, **12a**, 499, (1957).
6. Tal'roze, V.L., and Lyubimova, A.K., *Doklady Akad. S.S.S.R.*, **86**, 909, (1952).
7. Stevenson, D.P., and Schissler, D.O., *J. Am. Chem. Soc.*, **23**, 1353, (1955).
8. Field, F.H., Franklin, J.L., and Lampe, F.W., *J. Am. Chem. Soc.*, **78**, 5697, (1956).
9. Meisels, G.G., Hamill, W.H., and Williams, R.R. Jr., *J. Chem. Phys.*, **25**, 790, (1956).
10. Dunham, T. Jr., *Publications of the Astronomical Society of the Pacific*, **49**, 26, (1937).
11. Dunham, T. Jr., and Adams, W.S., *Am. Astr. Soc. Publs.*, **9**, 5, (1937).
12. Swings, P., and Rosenfeld, L., *Astrophys. J.*, **86**, 483, (1937).
13. Millar, T.J., Farquhar, P.R.A., and Willacy, K., *Astron. Astrophys. Suppl. Ser.*, **121**, 139, (1997).
14. Herbst, E., and Klemperer, W., *Astrophys. J.*, **185**, 505, (1973).
15. Watson, W.D., *Astrophys. J.*, **188**, 35, (1974).
16. Lee, H-H., Bettens, R.P.A., and Herbst, E., *Astron. Astrophys. Suppl. Ser.*, **119**, 111, (1996).
17. Smith, D., *Chem. Rev.*, **92**, 1473, (1992).
18. Petrie, S.A.H., *A Selected-Ion Flow Tube Study of Some Gas-Phase Ion-Molecule Reactions of Potential Relevance to the Chemistry of Dense Interstellar Clouds*, Ph. D. Thesis, University of Canterbury, New Zealand, (1991).
19. Dyson, J.E., and Williams, D.A., *The Physics of the Interstellar Medium*, Manchester University Press, Manchester, 1980.

20. Zeilik, M., and Smith, E. v. P., *Introductory Astronomy and Astrophysics*, Saunders College Publishing, Philadelphia, 1987.
21. Goldsmith, P.F., in *Interstellar Processes*, edited by Hollenbach, D.J., and Thronson, H.A. Jr., D. Reidel Publishing Co., Dordrecht, Holland, 1987, p. 51.
22. Gaballe, T.R., and Oka, T., *Nature*, **384**, 334, (1996).
23. Marquette, J.B., Rowe, B.R., Dupeyrat, G., and Roueff, E., *Astron. Astrophys.*, **147,** 115, (1985).
24. Anicich, V.G., *J. Phys. Chem. Ref. Data*, **22,** 1469, (1993).
25. Dotan, I., Albritton, D.L., Fehsenfeld, F.C., Streit, G.C., and Ferguson, E.E., *J. Chem. Phys.*, **68**, 5414, (1978).
26. Ervin, K.M., and Armentrout, P.B., *J. Chem. Phys.*, **86,** 6240, (1987).
27. Villinger, H., Futrell, J.H., Richter, R., Saxer, A., Niccolini, S.T., and Lindinger, W., *Int. J. Mass Spectrom. Ion Phys.*, **47**, 175, (1983).
28. Betowski, D., Payzant, J.D., Mackay, G.I., and Bohme, D.K., *Chem. Phys. Lett.*, **31**, 312, (1975).
29. Bohme, D.K., in *Interactions between Ions and Molecules*, edited by Ausloos, P., Plenum, New York, 1975, p. 489.
30. Adams, N.G., in *Atomic, Molecular and Optical Physics Handbook*, edited by Drake, G.W.F., AIP Press, New York, USA, 1996, p. 441.
31. Lias, S.G., Bartmess, J.E., Liebman, J.F., Holmes, J.L., Levin, R.D., and Mallard, W.G., *J. Phys. Chem. Ref. Data*, **17**, Suppl. 1, (1988).
32. Adams, N.G., and Smith, D., *Chem. Phys. Lett.*, **54**, 530, (1978).
33. Mackay, G.I., Betowski, L.D., Payzant, J.D., Schiff, H.I., and Bohme, D.K., *J. Phys. Chem.*, **80**, 2919, (1976).
34. Pollard, J.E., Johnson, L.K., Lichtin, D.A., and Cohen, R.B., *J. Chem. Phys.*, **95**, 4894, (1991).
35. Schultz, R.H., and Armentrout, P.B., *J. Chem. Phys.*, **95**, 121, (1991).
36. Anicich, V.G., Huntress, W.T. Jr., and McEwan, M.J., *J. Phys. Chem.*, **90**, 2446, (1986).
37. Gerlich, D., and Kaefer, G., 5th International Swarm Seminar, Birmingham, U.K., (1987).
38. Huntress, W.T. Jr., Pinizzotto, R.F. Jr., and Laudenslager, J.B., *J. Am. Chem. Soc.*, **95**, 4107, (1973).

39. Smith, D., and Adams, N.G., *Chem. Phys. Lett.*, **54**, 535, (1978).
40. Herbst, E., Schubert, J.G., and Certain, P.R., *Astrophys. J.*, **213**, 696, (1977).
41. Herd, C.R., and Babcock, L.M., *J. Phys. Chem.*, **93**, 245, (1989).
42. Adams, N.G., Smith, D., and Paulson, J.F., *J. Chem. Phys.*, **72**, 288, (1980).
43. Howard, C.J., Fehsenfeld, F.C., McFarland, M., *J. Chem. Phys.*, **60**, 5086, (1974).
44. Bierbaum, V.M., Ellison, G.B., and Leone, S.R., in *Gas Phase Ion Chemistry*, edited by Bowers, M.T., Academic Press, New York, 1984, Vol. 3, p. 2.
45. Fehsenfeld, F.C., in *Interactions between Ions and Molecules*, edited by Ausloos, P., Plenum, New York, 1975, p. 387.
46. Viggiano, A.A., and Paulson, J.F., in *Swarms of Ions and Electrons in Gases,* edited by Lindinger, W., Mark, T.D., and Howorka, F., Springer-Verlag, Wien, 1984, p. 218.
47. Clary, D.C., Smith, D., and Adams, N.G., *Chem. Phys. Lett.*, **119**, 320, (1985).
48. Marquette, J.B., Rowe, B.R., Dupeyrat, G., Poissant, G., and Rebrion, C., *Chem. Phys. Lett.*, **122**, 431, (1985).
49. Adams, N.G., and Smith, D., in *Reactions of Small Transient Species*, edited by Fontijn, A., Academic Press, London, 1983, p. 311.
50. Ikezoe, Y., Matsuoka, S., Takebe, M., and Viggiano, A., *Gas Phase Ion-Molecule Reaction Rate Constants Through 1986*, Maruzen, Tokyo, Japan, 1987.
51. McEwan, M.J., Denison, A.B., Huntress, W.T. Jr, Anicich, V.G., Snodgrass, J., and Bowers, M.T., *J. Phys. Chem.*, **93**, 4064, (1989).
52. Meot-Ner, M., in *Gas Phase Ion Chemistry*, edited by Bowers, M.T., Academic Press, New York, 1979, Vol 1, p. 198.
53. Viggiano, A.A., and Paulson, J.F., *J. Phys. Chem.*, **95**, 10719, (1991).
54. Herbst, E., and McEwan, M.J., *Astron. Astrophys.*, **229**, 201, (1990).
55. Mitchell, J.B.A., *Phys. Rep.*, **186**, 216, (1990).
56. Andersen, L.H., Heber, O., Kella, D., Pederson, H.B., Vejbychristensen, L., and Zajfman, D., *Phys. Rev. Lett.*, **77**, 4891, (1996).

57. Smith, D., and Adams, N.G., in *Swarms of Ions and Electrons in Gases*, edited by Lindinger, W., Mark, T.D., and Howorka, F., Springer-Verlag, Wien, 1984, p. 284.
58. Williams, T.L., Adams, N.G., Babcock, L.M., Herd, C.R., and Geoghegan, M., *Mon. Not. R. astr. Soc.*, **282**, 413, (1996).
59. Johnsen, R., *Int. J. Mass Spectrom. Ion Proc.*, **81**, 67, (1987).
60. Adams, N.G., and Smith, D., in *Rate Coefficients in Astrochemistry*, edited by Millar, T.J., and Williams, D.A., Kluwer, Dordrecht, 1988, p. 173.
61. Fergusson, E.E., Fehsenfeld, F.C., and Schmeltekopf, A.L., *Phys. Rev.*, **138**, A381, (1965).
62. Bates, D.R., *Phys. Rev.*, **78**, 492, (1950).
63. Bardsley, J.N., *J. Phys. B 1*, **349**, 365, (1968).
64. Bardsley, J.N., and Biondi, M.A., *Adv. At. Mol. Phys.*, **6**, 1, (1970).
65. Guberman, S.L., in *Dissociative Recombination: Theory, Experiment and Applications*, edited by Rowe, B.R., Mitchell, J.B.A., and Canosa, A., Plenum, New York, 1993, p. 47.
66. Tabli, D., and Ellinger, Y., in *Dissociative Recombination: Theory, Experiment and Applications*, edited by Rowe, B.R., Mitchell, J.B.A., and Canosa, A., Plenum, New York, 1993, p. 59.
67. Bates, D.R., *Astrophys. J.*, **344**, 531, (1989).
68. Galloway, E.T., and Herbst, E., *Astrophys. J.*, **376**, 531, (1991).
69. Adams, N.G., Herd, C.R., Geoghegan, M., Smith, D., Canosa, A., Rowe, B.R., Queffelec, J.L., and Morlais, M., *J. Chem. Phys.*, **94**, 4852, (1991).
70. Herd, C.R., Adams, N.G., and Smith, D., *Astrophys. J.*, **349**, 388, (1990).
71. Adams, N.G., and Babcock, L.M., *J. Phys. Chem.*, **98**, 4564, (1994).
72. Smith, D., and Adams, N.G., in *Physics of Ion-Ion and Electron-Ion Collisions*, edited by Brouillard, F., and McGowan, J.W., Plenum, New York, 1983, p. 501.
73. Olsen, R.E., *J. Chem. Phys.*, **56**, 2979, (1972).
74. Smith, D., and Adams, N.G., *Geophys. Res. Lett.*, **9**, 1085, (1982).
75. Smith, D., Adams, N.G., and Church, M.J., *J. Phys. B*, **11**, 4041, (1978).
76. Smith, D., and Church, M.J., *Int. J. Mass Spectrom. Ion. Phys.*, **19**, 185 (1976).

77. Christophorou, L.G., McCorkle, D.L., and Christodoulides, A.A., in *Electron-Molecule Interactions and their Applications*, edited by Christophorou, L.G., Academic, Orlando, 1984, Vol. 1.

78. Herd, C.R., Adams, N.G., and Smith, D., *Int. J. Mass Spectrom. Ion Proc.*, **87**, 331, (1989).

79. Naff, W.T., Compton, R.N., and Cooper, C.D., *J. Chem. Phys.*, **54**, 212, (1971).

80. Warman, J.M., and Sauer, M.C., *Int. J. Radiat. Chem.*, **3**, 273, (1971).

81. Smith, D., Herd, C.R., Adams, N.G., and Paulson, J.F., *Int. J. Mass Spectrom. Ion Proc.*, **96**, 341, (1990).

82. Sims, I.R., Queffelec, J.-L., Defrance, A., Rebrion-Rowe, C., Travers, D., Bocheri, P., Rowe, B.R., and Smith, I.W.M., *J. Chem. Phys.*, **100,** 4229, (1994).

83. Sims, I.R., Smith, I.W.M., Bocheri, P., Defrance, A., Travers, D., and Rowe, B.R., *J. Chem. Soc. Faraday Trans.*, **90**, 1473, (1994).

84. Liao, Q., and Herbst, E., *Astrophys. J.*, **444**, 694, (1995).

85. DeMore, W.B., Sander, S.P., Golden, D.M., Hampson, R.F., Kurylo, M.J., Howard, C.J., Ravishankara, A.R., Kolb, C.E., and Molina, M.J., *Chemical Kinetics and Photochemical Data for Use in Stratospheric Modeling, Evaluation Number10, JPL Publication 92-20*, JPL, CIT, Pasadena, California, 1992.

86. Herbst, E., in *Advances in Gas Phase Ion Chemistry Vol. 3*, edited by Babcock, L., and Adams, N.G., JAI Press, Greenwich, Connecticut, (in press 1997).

87. Herbst, E., Lee, H-H., Howe, D.A., Millar, T.J., *Mon. Not. R. astr. Soc.*, **268**, 335, (1994).

88. Bettens, R.P.A., Lee, H-H., and Herbst, E., *Astrophys. J.*, **443**, 664, (1995).

89. Clary, D.C., Haider, N., Husain, D., and Kabir, M., *Astrophys. J.*, **422**, 416, (1994).

90. Takahashi, J., and Yamashita, K., *J. Chem. Phys.*, **104**, 6613, (1996).

91. Herbst, E., *Chem. Phys. Lett.*, **222**, 297, (1994).

92. Herbst, E., in *Dust and Chemistry in Astronomy*, edited by Millar, T.J., and Williams, D.A., Institute of Physics, Philadelphia, 1993, p. 183.

93. Langmuir, I., *Trans. Faraday Soc.*, **17**, 621, (1922).

94. Bonzel, H.P., and Ku, R., *Surf. Sci.*, **33**, 91, (1972).

95. Eley, D.D., *Chem. and Ind.*, **1**, 12, (1976).

96. Somarjai, G.A., in *Introduction to Surface Chemistry and Catalysis*, Wiley, New York, 1994, p. 454.

97. Tielens, A.G.G.M., Hagen, W., *Astron. Astrophys.*, **114**, 245, (1982).

98. de Jong, T., *Astron. Astrophys.*, **20**, 263, (1972).

99. Gould, R.J., and Salpeter, E.E., *Astrophys. J.*, **138**, 393, (1963).

100. Fehsenfeld, F.C., Howard, C.J., and Fergusson, E.E., *J. Chem. Phys.*, **58**, 5841, (1973).

101. Ramaker, D.E., and Peek, J.M., *Phys. Rev. A.*, **13**, 58, (1976).

102. Karpas, Z., Anicich, V.G., and Huntress, W.T. Jr, *J. Chem. Phys.*, **70**, 2877, (1979).

103. Hasegawa, T.I., Herbst, E., Leung, C.M., *Astrophys. J. Suppl. Ser.*, **82**, 167, (1992).

104. Williams, D.A., in *Dust and Chemistry in Astronomy*, edited by Millar, T.J., and Williams, D.A., Institute of Physics, Philadelphia, 1993, p. 143.

105. Gioumousis, G., and Stevenson, D.P., *J. Chem. Phys.*, **29**, 294, (1958).

106. McDaniel, E.W., *Collision Phenomena in Ionised Gases*, Wiley, New York, 1964, p. 701.

107. Rowe, R.B., Marquette, J.B., Depeyrat, G., and Ferguson, E.E., *Chem. Phys. Lett.*, **113**, 403, (1985).

108. Rebrion, C., Marquette, J.B., Rowe, B.R., Adams, N.G., and Smith, D., *Chem. Phys. Lett.*, **136**, 495, (1987).

109. Su, T., and Bowers, M.T., in *Gas Phase Ion Chemistry*, edited by Bowers, M.T., Academic Press, New York, 1979, Vol. 1, p. 83.

110. Su, T., and Bowers, M.T., *J. Chem. Phys.*, **58**, 3027, (1973).

111. Moran, T.F., and Hamill, W.H., *J. Chem. Phys.*, **39**, 1413, (1963).

112. Gupta, S.K., Jones, E.G., Harison, A.G., and Myher, J.J., *Can. J. Chem.*, **45**, 3107, (1967).

113. Su, T., and Bowers, M.T., *Int. J. Mass Spectrom. Ion Phys.*, **12**, 347, (1973).

114. Su, T., and Bowers, M.T., *Int. J. Mass Spectrom. Ion Phys.*, **17**, 211, (1975).

115. Su, T., Su, E.C.F., and Bowers, M.T., *J. Chem. Phys.*, **69**, 2243, (1978).

116. Hseih, E.T., and Castleman, A.W., *Int. J. Mass Spectrom. Ion Phys.*, **40**, 295, (1981).

117. Chesnavich, W.J., Su, T., and Bowers, M.T., *J. Chem. Phys.*, **72**, 2641, (1980).

118. Su, T., and Chesnavich, W.J., *J. Chem. Phys.*, **72**, 5183, (1982).

119. Su, T., *J. Chem. Phys.*, **88**, 4102, (1988).

120. Clary, D.C., *Mol. Phys.*, **54**, 605, (1985).

121. Adams, N.G., Smith, D., and Clary, D.C., *Astrophys. J.*, **296**, L31, (1985).

122. McDaniel, E.W., Cermak, V., Dalgarno, A., Ferguson, E.E., and Friedman, L., *Ion-Molecule Reactions*, Wiley, New York, 1970, p. 159.

123. Arthurs, A.M., and Dalgarno, A., *Proc. Royal Soc. (London)*, **A256**, 540, (1960).

124. Robinson, F.N.H., *J. Sci. Instr.*, **36**, 481, (1959).

125. Kemper, P.R., and Bowers, M.T., in *Techniques for the Study of Ion Molecule Reactions*, edited by Farrar, J.M., and Saunders, W.H., Techniques of Chemistry Vol. XX, Wiley, New York, 1988, p. 1.

126. Kemper, P.R., and Bowers, M.T., *Rev. Sci. Instrum.*, **53**, 989, (1982).

127. Wronka, J., and Ridge, D.P., *Rev. Sci. Instrum.*, **53**, 491 (1982).

128. Wobschall, D., *Rev. Sci. Instrum.*, **36**, 466, (1965).

129. McIver, R.T., and Dunbar, R.C., *Int. J. Mass Spectrom. Ion Phys.*, **7**, 471, (1971).

130. Wilson, P.F., *Experimental Studies of Gas-Phase Ion-Molecule Reactions*, Ph. D. Thesis, University of Canterbury, New Zealand, (1994).

131. Buchanan, M.V., and Comisarov, M.B., in *Fourier Transform Mass Spectrometry*, edited by Buchanan, M.V., ACS Symposium Series Vol. 359, ACS, Washington, 1987, p. 1.

132. Freiser, B.S., in *Techniques for the Study of Ion Molecule Reactions*, edited by Farrar, J.M., and Saunders, W.H., Techniques of Chemistry Vol. XX, Wiley, New York, 1988, p. 61.

133. Squires, R.R., *Chem. Rev.*, **87**, 623, (1987).

134. Eller, K., Schwarz, H., *Chem. Rev.*, **91**, 1121, (1991).

135. Sablier, M., and Rolando, C., *Mass Spectrom. Rev.*, **12**, 285, (1993).

136. Ferguson, E.E., Fehsenfeld, F.C., Dunkin, D.B., Schmeltekopf, A.L., and Schiff, H.I., *Planet. Space Sci.*, **12**, 1169, (1964).

137. Ferguson, E.E., Fehsenfeld, F.C., Schmeltekopf, A.L., *Adv. At. Mol. Phys.*, **5**, 1, (1969).

138. Fehsenfeld, F.C., *Int. J. Mass. Spectrom. Ion Phys.*, **16**, 151, (1975).

139. Smith, D., and Adams, N.G., in *Gas Phase Ion Chemistry*, edited by Bowers, M.T., Academic Press, New York, 1979, Vol. 1, p. 1.

140. Dunkin, D.B., Fehsenfeld, F.C., Schmeltekopf, A.L., and Ferguson, E.E., *J. Chem. Phys.*, **49**, 1365, (1968).

141. Adams, N.G., and Smith, D., in *Techniques for the Study of Ion Molecule Reactions*, edited by Farrar, J.M., and Saunders, W.H., Techniques of Chemistry Vol. XX, Wiley, New York, 1988, p. 165.

142. Adams, N.G., in *Advances in Gas Phase Ion Chemistry*, Vol. 1, JAI Press, Greenwich, Connecticut, 1992, p. 271.

143. Adams, N.G., and Smith, D., *Int. J. Mass Spectrom. Ion Phys.*, **21**, 349, (1976).

144. Smith, D., and Adams, N.G., *Adv. At. Mol. Phys.*, **24**, 1, (1988).

145. Smith, D., and Adams, N.G., *J. Phys. D.*, **13**, 1267, (1980).

146. Van Doren, J.M., Barlow, S.E., Depuy, C.H., and Bierbaum, V.M., *Int. J. Mass Spectrom. Ion Proc.*, **81**, 85, (1987).

147. Graul, S.T. and Squires, R.R., *Mass Spec. Rev.*, **7**, 263, (1988).

148. Farrar, J.M., in *Techniques for the Study of Ion Molecule Reactions*, edited by Farrar, J.M., and Saunders, W.H., Techniques of Chemistry Vol. XX, Wiley, New York, 1988, p. 325.

149. Gentry, W.R., in *Gas Phase Ion Chemistry*, edited by Bowers, M.T., Academic Press, New York, 1979, Vol. 2, p. 221.

150. Gentry, W.R., McClure, D.J., and Douglas, C.H., *Rev. Sci. Instrum.*, **46**, 367, (1976).

151. Sieck, L.W., Searles, S.K., and Ausloos, P., *J. Am. Chem. Soc.*, **91**, 7627, (1969).

152. Meot-Ner, M., and Sieck, L.W., *J. Am. Chem. Soc.*, **105**, 2956, (1983).

153. Meot-Ner, M., and Sieck, L.W., *J. Am. Chem. Soc.*, **113**, 4448, (1991).

154. Tosi, P., Ianotta, S., Bassi, D., Villinger, H., Dobbler, W., and Lindinger, W., *J. Chem. Phys.*, **80**, 1905, (1984).

155. Fehsenfeld, F.C., and Fergusson, E.E., *Planet. Space Sci.*, **20**, 295, (1972).

156. Adams, N.G., and Smith, D., *Astrophys. J.*, **294**, L63, (1985).

157. Tsai, C., Berlanger, S.M., Kim, J.T., Lord, J.R., and McFadden, J.L., *J. Phys. Chem.*, **93**, 1916, (1989).

158. Hsu, W.L., and Tung, D.M., *Rev. Sci. Instrum.*, **63**, 4138, (1992).

159. Fehsenfeld, F.C., and Fergusson, E.E., *J. Geophys. Res.*, **76**, 8453, (1971).

160. Federer, W., Dobler, W., Lindinger, W., Tosi, P., and Bassi, D., in *Proceedings of the 3rd International Swarm Seminar*, Aug 3-5, Innsbruck, 1983, p. 191.

161. Fehsenfeld, F.C., and Fergusson, E.E., *J. Chem. Phys.*, **56**, 3066, (1972).

162. Federer, W., Villinger, H., Howarka, F., Lindinger, W., Tossi, P., Bassi, D., and Ferguson, E., *Phys. Rev. Lett.*, **52**, 2084, (1984).

163. Federer, W., Villinger, H., Tossi, P., Bassi, D., Ferguson. E.E., and Lindinger, W., in *Molecular Astrophysics*, edited by Diercksen G.H.F., Huebner, W.F., and Langhoff, P.W., D. Reidel Publishing Company, Boston, 1985, p. 649.

164. Hansel, A., Richter, R., Lindinger, W., and Ferguson, E.E., *Int. J. Mass Spectrom. Ion Proc.*, **94**, 251, (1989).

165. Petrie, S., Javahery, G., and Bohme, D.K., *J. Am. Chem. Soc.*, **114**, 9205, (1992).

166. Millar, T.J., Adams, N.G., Smith, D., Lindinger, W., and Villinger, H., *Mon. Not. R. astr. Soc.*, **221**, 673, (1986).

167. McDonald, R.N., Chowdhury, A.K., and Schell, P.L., *Organometallics*, **3**, 644, (1984).

168. Ferguson, E., *Acc. Chem. Res.*, **3**, 402, (1970).

169. Fehsenfeld, F.C., Ferguson, E.E., and Schmeltekopf, A.L., *J. Chem. Phys.* **45**, 1844, (1966).

170. Fehsenfeld, F.C., *J. Chem. Phys.*, **54**, 438, (1971).

171. Smith, D., and Adams, N.G., *J. Phys. B*, **20**, 4903, (1987).

172. Schmeltekopf, A.L., Fehsenfeld, F.C., and Ferguson, E.E., *Astrophys. J.*, **148**, L155, (1967).

173. Petrie, S., Javahery, G., Wang, J., and Bohme, D.K., *J. Am. Chem. Soc.*, **114**, 6268, (1992).

174. Petrie, S., Becker, H., Baranov, V.I., and Bohme, D.K., *Int J. Mass Spectrom. Ion Proc.*, **145**, 79, (1995).

175. Le Page, V., Keheyan, Y., Bierbaum, V. M., and Snow, T.P., *J. Am. Chem. Soc., (submitted)*, (1997).

176. Brenner, W., Shane, E.C., *J. Phys. Chem.*, **75**, 1552, (1971).

177. Viggiano, A.A., Howorka, F., Albritton, D.L., Fehsenfeld, F.C., Adams, N.D., and Smith, D., *Astrophys. J.*, **236**, 492, (1980).

178. Federer, W.,Villinger, H., Lindinger, W., and Ferguson, E.E., *Chem. Phys. Lett.*, **123**, 12, (1986).

179. Goldan, P.D., Schmeltekopf, A.L., Fehsenfeld, F.C., Schiff, H.I., and Ferguson, E.E., *J. Chem. Phys.*, **44**, 4095, (1966).

180. Fehsenfeld, F.C., *Astrophys. J.*, **209**, 638, (1976).

181. Fehsenfeld, F.C., Dunkin, D.B., and Ferguson, E.E., *Planet. Space Sci.*, **18**, 1267, (1970).

182. Fehsenfeld, F.C., *Planet. Space Sci.*, **25**, 195, (1977).

183. Fehsenfeld, F.C., Schmeltekopf, A.L., Schiff, H.I., and Ferguson, E.E., *Planet. Space Sci.*, **15**, 373, (1967).

184. Herbst, E., DeFrees, D.J., and McLean, A.D., *Astrophys. J.*, **321**, 898, (1987).

185. Millar, T.J., and Freeman, A., *Mon. Not. R. astr. Soc.*, **207**, 405, (1984).

186. McFarland, M., Albritton, D.L., Fehsenfeld, F.C., Fergusson, E.E., and Schmeltekopf, A.L., *J. Geophys. Res.*, **79**, 2925, (1974).

187. Viggiano, A.A., Morris, R.A., Paulson, J.F., and Ferguson, E., *Chem. Phys. Lett.*, **148**, 296, (1988).

188. Bohme, D.K., Mackay, G.I., and Schiff, H.I., *J. Chem. Phys.*, **73**, 4976, (1980).

189. Ferguson, E.E., Fehsenfeld, F.C., Goldan, P.D., Schmeltekopf, A.L., and Schiff, H.I., *Planet. Space Sci.*, **13**, 823, (1965).

190. McFarland, M., Albritton, D.L., Fehsenfeld, F.C., and Fergusson, E.E., *J. Geophys. Res.*, **79**, 2005, (1974).

191. Fehsenfeld, F.C., Ferguson, E.E., and Bohme, D.K., *Planet. Space Sci.*, **17**, 1759, (1969).

192. Knight, J.S., *Selected-Ion Flow Tube Studies of Some Gaseous Ion-Molecule Reactions*, Ph. D. Thesis, University of Canterbury, New Zealand, (1986).

193. Howorka, F., Fehsenfeld, F.C., and Albritton, A.L., *J. Phys. B*, **12**, 4189, (1979).

194. Mackay, G.I., Vlachos, G.D., Bohme, D.K., and Schiff, H.I., *Int. J. Mass Spectrom. Ion Phys.*, **36**, 259, (1980).

195. Dahl, D.A., and Delmore, J.E., SIMION PC/PS2 version 3.1.

196. McGilvery, D.C., Ph.D. Thesis, LaTrobe University, (1978).

197. Upschulte, B.L., Schul, R.J., Passarella, R., Keesee, R.G., and Castleman, A.W. Jr., *Int. J. Mass Spectrom. Ion Proc.*, **75**, 27, (1987).

198. Fehsenfeld, F.C., Evenson, K.M., and Broida, H.P., *Rev. Sci. Instr.*, **36**, 294, (1965).

199. Morrison, M., *Ion-Neutral Interactions in a Flow Tube*, Ph.D. First Year Progress Report, University of Canterbury, New Zealand, (1991).

200. Adams, N.G., and Smith, D., *J. Phys. B*, **9**, 1439, (1976).

201. Bohme, D.K., Hemsworth, R.S., Rundle, H.W., and Schiff, H.I., *J. Chem. Phys.*, **58**, 3504, (1973).

202. Irvine, W.M., Brown, R.D., Cragg, D.M., Friberg, P., Godfrey, P.D., Kaifu, N., Matthews, H.E., Ohishi, M., Suzuki, H., and Takeo, H., *Astrophys. J.*, **335**, L89, (1988).

203. Adams, N.G., Smith, D., Giles, K., and Herbst, E., *Astron. Astrophys.*, **220**, 269, (1989).

204. Herbst, E., Smith, D., and Adams, N.G., *Astron. Astrophys.*, **138**, L13, (1984).

205. Bettens, R.P.A., and Brown, R.D., *Mon. Not. R. astr. Soc.*, **258**, 347, (1992).

206. Bates, D.R., *Astrophys. J.*, **306**, L45, (1986).

207. Kharasch, M.S., McNab, M.C., and Mayo, F.R., *J. Am. Chem. Soc.*, **55**, 2521, (1933).

208. Sauer, J.C., in *Organic Syntheses, Coll. Vol. IV*, edited by Rabjohn, N., New York, John Wiley & Sons Inc., 1963, p. 813.

209. Petrie, S., Knight, J.S., Freeman, C.G., Maclagan, R.G.A.R., McEwan, M.J., and Sudkeaw, P., *Int. J. Mass Spectrom. Ion Proc.*, **105**, 43, (1991).

210. Bouchoux, G., Hoppilliard, Y., and Flament, J-P., *Organic Mass Spectrom.*, **20**, 560, (1985).

211. Holmes, J.L., Terlouw, J.K., and Burgers, P.C., *Organic Mass Spectrom.*, **15**, 140, (1980).

212. Hopkinson, A.C., and Lien, M.H., *J. Am. Chem. Soc.*, **108**, 2843, (1986).

213. Komornicki, A., Dykstra, C.E., Vincent, M.A., and Radom, L., *J. Am. Chem. Soc.*, **103**, 1652, (1981).

214. Brown, R.D., and Dittman, R.G., *Chem. Phys.*, **83**, 77, (1984).

215. Brown, R.D., Godfrey, P.D., Champion, R., and McNaughton, D., *J. Am. Chem. Soc.*, **103,** 5711, (1981).

216. Frisch, M.F., Head-Gordon, M., Trucks, G.W., Foresman, J.B., Schlegel, H.B., Raghavachari, K., Robb, M.A., Binkley, J.S., Gonzalez, C., DeFrees, D.J., Fox, D.J., Whiteside, R.A., Seeger, R., Melius, C.F., Baker, J., Martin, R.L., Kahn, L.R., Stewart, J.J.P., Topiol, S., and Pople, J.A., GAUSSIAN 90, Gaussian Inc., Pittsburgh PA, 1990.

217. Frisch, M.F., Trucks, G.W., Head-Gordon, M., Gill, P.M.W., Wong, M.W., Foresman, J.B., Johnson, B.G., Schlegel, H.B., Robb, M.A., Replogle, E.S., Gomperts, R., Andres, J.L., Raghavachari, K., Binkley, J.S., Gonzalez, C., Martin, R.L., Fox, D.J. DeFrees, D.J., Baker, J., Stewart, J.J.P., and Pople, J.A., GAUSSIAN 92, Gaussian Inc., Pittsburgh PA, 1992.

218. Curtiss, L.A., Raghavachari, K., Trucks, G.W., and Pople, J.A., *J. Chem. Phys.*, **94**, 7221, (1991).

219. Winnewisser, G., *J. Mol. Spec.*, **46**, 16, (1973).

220. Benson, R.C., Flygare, W.H., Oda, M., and Breslow, R., *J. Am. Chem. Soc.*, **95**, 2772, (1973).

221. Herbst, E., and Leung, C.M., *Astrophys. J. Suppl.*, **69**, 271, (1989).

222. Mackay, G.I., Tanaka, K., and Bohme, D.K., *Int. J. Mass Spectrom. Ion Proc.*, **24**, 125, (1977).

223. Bohme, D.K., Raksit, A.K., and Fox, A.J., *J. Am. Chem. Soc.*, **105**, 5481, (1983).

224. DePuy, C., Private Communication, (1995).

225. Maclagan, R.G.A.R., McEwan, M.J., and Scott, G.B.I., *Chem. Phys. Lett.*, **40**, 185, (1995).

226. Scott, G.B.I., Fairley, D.A., Freeman, C.G., Maclagan, R.G.A.R., and McEwan, M.J., *Int. J. Mass Spectrom. Ion Proc.*, **149/150**, 251, (1995).

227. Petrie, S., *Astrophys. J.*, **454**, L165, (1995).

228. Ekern, S., Szczepanski, J., and Vala, M., *J. Phys. Chem.*, **100**, 16109, (1996).

229. Ekern, S., and Vala, M., *J. Phys. Chem.*, **101**, 3601, (1997).

230. Irvine, W.M., Goldsmith, P.F., and Hjalmarson, Å., in *Interstellar Processes*, edited by Hollenbach, D.J., Thronson, H.A., D. Reidel Publishing Co., Dordrecht, Holland, 1987, p. 561.

231. Miller, T.J., and Williams, D.A., in *Dust and Chemistry in Astronomy*, edited by Millar, T.J., and Williams, D.A., Institute of Physics Pub., Philadelphia, 1993, p. 1.

231. Janz, G.J., Inorganic Syntheses, Vol. V, edited by Moeller, T., McGraw-Hill, New York, 1957, p. 43.

233. Brandsma, L., Preparative Acetylenic Chemistry, Studies in Organic Chemistry Vol. 34, Elsevier, Amsterdam, 1988, p. 167.

234. Fehsenfeld, F.C., Schmeltekopf, A.L., and Ferguson, E.E., *J. Chem. Phys.*, **46**, 2802, (1967).

235. McAllister, T., *Int. J. Mass Spectrom. Ion Phys.*, **9**, 127, (1972).

236. Ryan, K.R., *J. Chem. Phys.*, **61**, 1559, (1974).

237. Kim, J.K., Theard, L.P., and Huntress, W.T., *J. Chem. Phys.*, **62**, 45 (1975).

238. Adams, N.G., Smith, D., and Grief, D., *Int. J. Mass Spectrom. Ion Phys.*, **26**, 405, (1978).

239. Freeman, C.G., Knight, J.S., Love, J.G., and McEwan, M.J., *Int. J. Mass Spectrom. Ion Proc.*, **80**, 255, (1987).

240. Smith, D.L., and Futrell, J.H., *Int. J. Mass Spectrom. Ion Phys.*, **10**, 405, (1972).

241. McAllister, T., and Pitman, P., *Int. J. Mass Spectrom. Ion Phys.*, **19**, 423, (1976).

242. Copp, N.W., Hamdan, M., Jones, J.D.C., Birkinshaw, K., and Twiddy, N.D., *Chem. Phys. Lett.*, **88**, 508, (1982).

243. Raksit, A.B., Schiff, H.I., and Bohme, D.K., *Int. J. Mass Spectrom. Ion Proc.*, **56**, 321, (1984).

244. Petrie, S., Freeman, C.G., McEwan, M.J., and Ferguson, E.E., *Mon. Not. R. astr. Soc.*, **248**, 272, (1991).

245. Petrie, S.A.H., Freeman, C.G., McEwan, M.J., and Meot-Ner, M., *Int. J. Mass Spectrom. Ion Proc.*, **90**, 241, (1989).

246. Adams, N.G., and Smith, D., *Chem. Phys. Lett.*, **47**, 383, (1977).

247. Bohme, D.K., and Wlodek, S., *Int. J. Mass Spectrom. Ion Proc.*, **102**, 133, (1990).

248. Buttrill, S.E., Kim, J.K., Huntress, W.T., LeBreton, P.R., and Williamson, A., *J. Chem. Phys.*, **61**, 2122, (1974).

249. Herbst, E., Adams, N.G., and Smith, D., *Astrophys. J.*, **269**, 329, (1983).

250. McEwan, M.J., McConnell, C.L., Freeman, C.G., and Anicich, V.G., *J. Phys. Chem.*, **98**, 5068, (1994).

251. Giles, K., Adams, N.G., and Smith, D., *Int. J. Mass Spectrom. Ion Proc.*, **89**, 303, (1989).

252. Lammertsma, K., Pople, J.A., and Schleyer, P. v-R., *J. Amer. Chem. Soc.*, **108**, 7, (1986).

253. Ausloos, P., Lias, S.G., Buckley, T.J., and Rogers, E.E., *Int. J. Mass Spectrom. Ion Proc.*, **92**, 65, (1989).

254. Ferguson, E., *Chem. Phys. Lett.*, **99**, 89, (1983).

255. Bemand, P.P., and Clyne, M.A.A., *J. Chem. Soc. Faraday Trans. II*, **73**, 394, (1977).

256. Petrie, S., Freeman, C.G., Meot-Ner, M., McEwan, M.J., and Ferguson, E.E., *J. Am. Chem. Soc.*, **112**, 7121, (1990).

257. Ferguson, E., Private communication, (1996).

258. Smith, D., Glosik, J., Skalsky, V., Spanel, P., and Lindinger, W., *Int. J. Mass Spectrom. Ion Proc.*, **129**, 145, (1993).

259. Wong, M.W., and Radom, L., *J. Am. Chem. Soc.*, **115**, 1507, (1993).

260. Maluendes, S.A., McLean, A.D., Yamashita, K., and Herbst, E., *J. Chem. Phys.*, **99**, 2812, (1993).

261. Skancke, A., *J. Phys. Chem.*, **99**, 13886, (1995).

262. Koch, W., Lin, B., and Schleyer, P. v-R, *J. Am. Chem. Soc.*, **111**, 3479, (1989).

263. Lavell, S., Feller, D., and Davidson, E.R., *Theor. Chim. Acta*, **77**, 111, (1990).

264. Anicich, V.G., Sen, A.D., Huntress, W.T., and McEwan, M.J., *J. Chem. Phys.*, **93**, 7163, (1990).

265. Knight, J.S., Freeman, C.G., McEwan, M.J., Anicich, V.G., and Huntress, W.T., *J. Phys. Chem.*, **91**, 3898, (1987).

266. Bates, D.R., and Herbst, E., in *Reaction Rate Coefficients in Astrophysics*, edited by Miller, T.J., and Williams, D.A., Kluwer Academic Pub., Dordrecht, 1988, p. 17.

267. Bernardi, F., Grandinetti, F., Guarino, A., and Robb, M.A., *Chem. Phys. Lett.*, **153**, 309, (1988).

268. Ziurys, L.M., and Apponi, A.P., *Astrophys. J.*, **455**, L73, (1995).

269. Freeman, C.G., and McEwan, M.J., in *Chemistry and Spectroscopy of Interstellar Molecules*, edited by Bohme, D.K., Herbst, E., Kaifu, N., and Saito, S., University of Tokyo Press, Tokyo, Japan, 1992, p. 187.

270. Herbst, E., and Woon, D.E., *Astrophys. J.*, **463**, L113, (1996).

271. Anicich, V.G., and McEwan, M.J., *Planet. Space Sci.*, **45**, 897, (1997).

272. Magnani, L., Onello, J.S., Adams, N.G., Hartman, D., and Thaddeus, P., *Astrophys. J. (submitted)*, (1997).

273. Smith, D., and Adams, N.G., *Int. J. Mass Spectrom. Ion Proc.*, **76**, 307, (1987).

274. Adams, N.G., and Smith, D., *Astrophys. J.*, **317**, L25, (1987).

275. Hammerum, S., *Mass Spectrom. Rev.*, **7**, 123, (1988).

276. Stirk, K.M., Kiminkinen, L.K.M., and Kenttämaá, H.I., *Chem. Rev.*, **92**, 1649, (1992).

277. Black, J.H., and Dalgarno, A., *Astrophys. J. Suppl.*, **34**, 405, (1977).

278. Iglesias, E., *Astrophys. J.*, **218**, 697, (1977).

279. Vidaud, P.H., and Wayne, R.P., *J. Chem. Soc. Faraday Trans. II*, **72**, 1185, (1976).

280. Wright, A.N., and Winkler, C.A., *Active Nitrogen*, Academic Press, New York, 1968, p. 83.

281. Lin, C-L., and Kaufman, F., *J. Chem. Phys.*, **55**, 3760, (1971).

282. Yung, Y.L., Allen, M., and Pinto, J.P., *Astrophys. J. Suppl.*, **55**, 465, (1984).

283. Toublanck, D., Parisot, J.P., Brillet, J., Gautier, D., Raulin, F., and McKay, C.P., *Icarus*, **113**, 2, (1995).

284. Fehsenfeld, F.C., Schmeltekopf, A.L., and Ferguson, E.E., *Planet. Space Sci.*, **13**, 219, (1965).

285. Melville, H.W., and Gowenlock, B.G., *Experimental Methods in Gas Reactions*, Macmillan & Co., London, 1964, p. 205.

286. Moreu, C., and Bongrand, J.C., *Ann. Chemie*, **14**, 47, (1920).

287. Adams, N.G., and Smith, D., *Chem. Phys. Lett.*, **79**, 563, (1981).

288. Raksit, A.B., and Bohme, D.K., *Int. J. Mass Spectrom. Ion Proc.*, **55**, 69, (1983/1984).

289. Lias, S.G., Liebman, J.F., and Levin., R.D., *J. Phys. Chem. Ref. Data*, **13**, 695, (1984).

290. Ferguson, E.E., *Adv. Electron. Electron Phys.*, **24**, 1, (1968).

291. Fehsenfeld, F.C., and Ferguson, E.E., *Radio Sci.*, **7**, 113, (1972).

292. McEwan, M.J., Anicich, V.G., Huntress, W.T., Kemper, P.R., and Bowers, M.T., *Int. J. Mass Spectrom. Ion Spectrom.*, **50**, 179, (1983).

293. McEwan, M.J., Anicich, V.G., and Huntress, W.T., *Int. J. Mass Spectrom. Ion Phys.*, **37**, 273, (1981).

294. Karpas, Z., and Huntress, W.T., *Chem. Phys. Lett.*, **59**, 87, (1978).

295. McCrumb, J.L., and Warneck, P., *J. Chem. Phys.*, **67**, 5006, (1977).

296. Mark, T.D., and Oskam, H.J., *Phys. Rev. A*, **4**, 1445, (1971).

297. Bohme, D.K., Dunkin, D.B., Fehsenfeld, F.C., and Ferguson, E.E., *J. Chem. Phys.*, **51**, 863, (1969).

298. Adams, N.G., Smith, D., Lister, D.G., Rakshit, A.B., and Twiddy, N.D., *Chem. Phys. Lett.*, **61**, 608, (1979).

299. Bohringer, H., Arnord, F., Smith, D., and Adams, N.G., *Int. J. Mass Spectrom. Ion Phys.*, **52**, 25, (1983).

300. Smith, D., Adams, N.G., and Alge, E., *Chem. Phys. Lett.*, **105**, 317, (1984).

301. Rowe, B.R., Marquette, J.B., and Dupeyrat, G., in *Molecular Astrophysics*, edited by Diercksen, G.H.F., Huebner, W.F., and Langhoff, P.W., D. Reidel Publishing Company, Boston, 1985, p. 631.

302. van Koppen, P.A.M., Jarrold, M.F., Bowers, M.T., Bass, L.M., and Jennings, K.R., *J. Chem. Phys.*, **81**, 288, (1984).

303. Ferguson, E.E., Adams, N.G., and Smith, D., *Chem. Phys. Lett.*, **128**, 84, (1986).

304. Wagner-Redeker, W., Kemper, P.R., Jarrold, M.F., and Bowers. M.T., *J. Chem. Phys.*, **83**, 1121, (1985).

305. Ferguson, E.E., Fehsenfeld, F.C., Goldan, P.D., and Schmeltekopf, A.L., *J. Geophys. Res.*, **70**, 4323, (1965).

306. Ferguson, E.E., *At. Data. Nucl. Data Tables*, **12**, 159, (1973).

307. Adams, N.G., Bohme, D.K., Dunkin, D.B., Fehsenfeld, F.C., and Ferguson, E.E., *J. Chem. Phys.*, **52**, 3133, (1970).

308. Howard, C.J., Bierbaum, V.M., Rundle, H.W., and Kaufman, F., *J. Chem. Phys.*, **57**, 3491, (1972).

309. Matsuoka, S., Nakamura, H., Tamura, T., *J. Chem. Phys.*, **75**, 681, (1981).

310. Viggiano, A.A., van Doren, J.M., Morris, R.A., and Paulson, J.F., *J. Chem. Phys.*, **93**, 4761, (1990).

311. Rowe, B.R., Marquette, J.B., and Rebrion, C., *J. Chem. Soc. Trans. II*, **85**, 1631, (1989).

312. Rebrion, C., Rowe, B.R., and Marquette, J.B., *J. Chem. Phys.*, **91**, 6142, (1989).

313. Shul, R.J., Passarella, R., Upschulte, B.L., Keesee, R.G., and Castleman, A.W. Jr., *J. Chem. Phys.*, **86**, 4446, (1987).

314. Smith, D., and Adams, N.G., *Phys. Rev. A*, **23**, 2327, (1981).

315. Lindinger, W., Howarka, F., Kuhn, S., Villinger, H., Alge, E., and Ramler, H., *Phys. Rev. A*, **23**, 2319, (1981).

316. Dotan, I., and Lindinger, W., *J. Chem. Phys.*, **76**, 4972, (1982).

317. Laudenslager, J.B., Huntress, W.T., and Bowers, M.T., *J. Chem. Phys.*, **61**, 4600, (1974).

318. Anicich, V.G., Laudenslager, J.B., Huntress, W.T., and Futrell, J.H., *J. Chem. Phys.*, **67**, 4340, (1977).

319. Adams, N.G., Dean, A.G., and Smith, D., *Int. J. Mass Spectrom. Ion Phys.*, **10**, 63, (1972).

320. Adams, N.G., Bohme, D.K., Dunkin, D.B., and Fehsenfeld, F.C., *J. Chem. Phys.*, **52**, 1951, (1970).

321. Fehsenfeld, F.C., Ferguson, E.E., and Schmeltekopf, A.L., *J. Chem. Phys.*, **45**, 404, (1966).

322. Hyatt, D., and Knewstubb, P.F., *J. Chem. Soc. Faraday Trans. II*, **68**, 202, (1972).

323. Thomas, R., Barassin, A., and Burke, R.R., *Int. J. Mass Spectrom. Ion Phys.*, **28**, 275, (1978).

324. Rakshit, A.B., Stock, H.M.P., Wareing, D.P., and Twiddy, N.D., *J. Phys. B, Atom Molec. Phys.*, **11**, 4237, (1978).

325. Rakshit, A.B., and Warneck, P., *J. Chem. Phys.*, **73**, 2673, (1980).

326. Warneck, P., *J. Chem. Phys.*, **46**, 513, (1967).

327. Kaneko, Y., Kobayashi, N., and Kanomata, I., *J. Phys. Soc. Jpn.*, **27**, 982, (1969).

328. Howorka, F., *J. Chem. Phys.*, **68**, 804, (1978).

329. Roche, A.E., Sutton, M.M., Bohme, D.K., and Schiff, H.I., *J. Chem. Phys.*, **55**, 5480, (1971).

330. Fehsenfeld, F.C., Lindinger, W., Schiff, H.I., Hemsworth, R.S., and Bohme, D.K., *J. Chem. Phys.*, **64**, 4887, (1976).

331. McKnight, L.G., McAfee, K.B., and Sipler, D.P., *Phys. Rev.*, **164**, 62, (1967).

332. Good, A., Durden, D.A., and Kebarle, P., *J. Chem. Phys.*, **52**, 212, (1970).

333. Knight, J.S., Freeman, C.G., McEwan, M.J., Smith, S.C., Adams, N.G., and Smith, D., *Mon. Not. R. astr. Soc.*, **219**, 89, (1986).

334. Cheung, A.C., Rank, D.M., Townes, C.H., Thornton, D.D., and Welch, W.J., *Phys. Rev. Lett.*, **21**, 1701, (1968).

335. Morris, M., Zuckerman, B., Palmer, P., and Turner, B.E., *Astrophys. J.*, **186**, 501, (1973).

336. Marquette, J.B., Rebrion, C., and Rowe, B.R., *J. Chem. Phys.*, **89**, 2041, (1988).

337. Adams, N.G., Smith, D., and Millar, T.J., *Mon. Not. R. astr. Soc.*, **211**, 857, (1984).

338. Yee, J.H., Lepp, S., and Dalgarno, A., *Mon. Not. R. astr. Soc.*, **227**, 461, (1987).

339. Galloway, E.T., and Herbst, E., *Astron. Astrophys.*, **211**, 413, (1989).

340. Le Bourlot, J., *Astron. Astrophys.*, **242**, 235, (1991).

341. Herbst, E., DeFrees, D.J., Talbi, D., Pauzat, F., Koch, W., and McLean, A.D., *J. Chem. Phys.*, **94**, 7842, (1991).

342. Bates, D.R., *J. Phys. B*, **24**, 3267, (1991).

343. Dalgarno, A., in *Interactions between Ions and Molecules,* edited by Ausloos, P., Plenum Press, N.Y.,1975, p. 341.

344. Huntress, W.T., *Astrophys. J. Suppl.*, **33**, 495, (1977).

345. Graedel, T.E., Langer, W.D., and Frerking, M.A., *Astrophys. J. Suppl.*, **48**, 321, (1982).

346. Millar, T.J., Leung, C.M., and Herbst, E., *Astron. Astrophys.*, **183**, 109 (1987).

347. Pineau des Forets, G., Roueff, E., and Flowers, D.R., *Mon. Not. R. astr. Soc.*, **244**, 668, (1990).

348. Pauls, T.A., Wilson, T.L., Bieging, J.H., and Martin, R.N., *Astron. Astrophys.*, **124**, 23, (1983).

349. Smith, D., and Spanel, P., *Chem. Phys. Lett.*, **211**, 454, (1993).

350. Scott, G.B.I., Fairley, D.A., Freeman, C.G., McEwan, M.J., Adams, N.G., and Babcock, L.M., *J. Phys. Chem.*, **101**, 4973, (1997).

351. Maclagan, R.G.A.R., Private Communication, (1997).

352. Herbst, E., Private Communication, (1997). E. Herbst advised that incorporation of the rate coefficient for reaction **(607)** into the "new standard model" produced significant increases in the number densities of NH_3, NH_2CN, HNC^+ and NH_2CNH^+ at intermediate and steady state times.

353. Graves, J.C., and Linnett, J.W., *Trans. Faraday Soc.*, **55**, 1346, (1959).

354. Linnett, J.W., and Marsden, D.G.H., *Proc. Roy. Soc. (London)*, **A234**, 489, (1956).

355. McClure, D.J., Douglass, C.H., and Gentry, W.R., *J. Chem. Phys.*, **66**, 2362, (1977).

356. Rutherford, J.A., and Vroom, D.A., *J. Chem. Phys.*, **61**, 2514, (1974).

357. Schmitt, R.J., Bierbaum, V.M., and DePuy, C.H., *J. Am. Chem. Soc.*, **101**, 6443, (1979).

358. Millar, T.J., Herbst, E., and Charnley, S.B., *Astrophys. J.*, **369**, 147, (1991).

359. Ferguson, E.E., Bohme, D.K., Fehsenfeld, F.C., and Dunkin, D.B., *J. Chem. Phys.*, **50**, 5039, (1969).

360. Morgan, J.E., and Schiff, H.I., *J. Chem. Phys.*, **38**, 1495, (1963).

361. Brandsma, L., *Preparative Acetylenic Chemistry*, Elsevier, Amsterdam, 1971, p. 122.

362. Fox, A., Raksit, A.B., Dheandhanoo, S., and Bohme, D.K., *Can. J. Chem.*, **64**, 399, (1986).

363. Shul, R.J., Passarella, R., DiFazio, L.T. Jr., Keesee, R.G., and Castleman, A.W. Jr., *J. Phys. Chem.*, **92**, 4947, (1988).

364. Jones, J.D.C., Birkinshaw, K., and Twiddy, N.D., *Chem. Phys. Lett.*, **77**, 484, (1981).

365. Dotan, I., Lindinger, W., Rowe, B., Fahey, D.W., Fehsenfeld, F.C., and Albritton, D.L., *Chem. Phys. Lett.*, **72**, 67, (1980).

366. Rakshit, A.B., and Warneck, P., *J. Chem. Soc. Faraday Trans. II*, **76**, 1084, (1980).

367. Alge, E., and Lindinger, W., *J. Geophys. Res.*, **86**, 871, (1981).

368. Smith, D., Adams, N.G., and Miller, T.M., *J. Chem. Phys.*, **69**, 308, (1978).

369. Tichy, M., Rakshit, A.B., Lister, D.G., Twiddy, N.D., Adams, N.G., and Smith, D., *Int. J. Mass. Spectrom. Ion Phys.*, **29**, 231, (1979).

370. Lindinger, W., Fehsenfeld, F.C., Schmeltekopf, A.L., and Ferguson, E.E., *J. Geophys. Res.*, **79**, 4753, (1974).

371. McFarland, M., Albritton, D.L., Fehsenfeld, F.C., Ferguson, E.E., and Schmeltekopf, A.L., *J. Chem. Phys.*, **59**, 6620, (1973).

372. Warnech, V.P., *Berichte Der Bunsen-Gesellschaft*, **76**, 413, (1972).

373. Johnsen, R., Brown, H.L., and Biondi, M.A., *J. Chem. Phys.*, **52**, 5080, (1970).

374. Farragher, A.L., *Trans. Faraday Soc.*, **66**, 1411, (1970).

375. Fehsenfeld, F.C., Schmeltekopf, A.L., and Ferguson, E.E., *Planet. Space Sci.*, **13**, 219, (1965).

376. Warneck, P., *J. Chem. Phys.*, **46**, 502, (1967).

377. Dreyer, J.W., and Perner, D., *Chem. Phys. Lett.*, **12**, 299, (1971).

378. Sieck, L.W., and Futrell, J.H., *J. Chem. Phys.*, **48**, 1409, (1968).

379. Hawley, H., Mazely, T.L., Randeniya, L.K., Smith, R.S., Zeng, X.K., and Smith, M.A., *Int. J. Mass Spectrom. Ion Proc.*, **97**, 55, (1990).

380. Durup-Ferguson, M., Bohringer, H., Fehey, D.W., and Ferguson, E.E., *J. Chem. Phys.*, **79**, 265, (1983).

381. Villinger, H., Lukac, P., Howarka, F., Alge, E., Ramler, H., and Lindinger, W., *Czech. J. Phys.*, **B31**, 832, (1981).

382. Morton, D.C., *Astrophys. J. Lett.*, **193**, L35, (1974).

383. Morton, D.C., *Astrophys. J.*, **197**, 85, (1975).

384. Smith, D., *Int. J. Mass Spectrom. Ion Proc.*, **129**, 1, (1993).

385. Tielens, A.G.G.M., in *Dust and Chemistry in Astronomy*, edited by Millar, T.J., and Williams, D.A., Institute of Physics, Philadelphia, 1993, p. 103.

386. Herbst, E., *Angew. Chem. Int. Ed. Engl.*, **29**, 595, (1990).

387. Winnewisser, G., and Herbst, E., *Topics in Current Chemistry*, **139**, 119, (1987).

388. Talbi, D., DeFrees, D.J., Egolf, D.A., and Herbst, E., *Astrophys. J.*, **374**, 390, (1991).

389. Haider, N., and Husain, D., *Combustion and Flame*, **93**, 327, (1993).

390. Haider, N., and Husain, D., *J. Chem. Soc. Faraday Trans. II*, **89**, 7, (1993).

391. Sekiya, H., Tsuji, M., and Nishimura, Y., *J. Chem. Phys.*, **83**, 2857, (1985).

392. Sekiya, H., Tsuji, M., and Nishimura, Y., *J. Chem. Phys.*, **84**, 3739, (1986).

393. Nishimura, Y., Sekiya, H., and Tsuji, M., *J. Chem. Phys.*, **84**, 5213, (1986).

394. Kaiser, R.I., Stranges, D., Lee, Y.T., and Suits, A.G., *Astrophys. J.*, **477**, 982, (1997).

395. Phillips, L.F., Private Communication, (1997).

396. Luiti, G., Dondes, S., Hartek, P., *J. Chem. Phys.*, **44**, 4052, (1966).

397. Stedman, D.H., Setser, D.W., *J. Chem. Phys.*, **52**, 3957, (1970).

398. Donovan, R.J., Hussain, D., *Trans. Faraday Soc.*, **63**, 2879, (1967).

399. Kemper, P.R., and Bowers, M.T., *Int. J. Chem. Kin.*, **16**, 707, (1984).

400. Herbst, E., Private Communication, (1997).

401. Hierl, P.M., and Herman, Z., *Chem. Phys.*, **50**, 249, (1980).

402. Douglass, C.H., McClure, D.J., and Gentry, W.R., *J. Chem. Phys.*, **67**, 4931, (1977).

403. Krenos, J.R., Lehmann, K.K., Tulley, J.C., Hierl, P.M., and Smith, G.P., *Chem. Phys.*, **16**, 109, (1976).

404. Petrie, S., Bettens, R.P.A., Freeman, C.G., and McEwan, M.J., *Mon. Not. R. astr. Soc.*, **264**, 862, (1993).

405. Petrie, S., Bettens, R.P.A., Freeman, C.G., and McEwan, M.J., *J. Phys. Chem.*, **97**, 13673, (1993).

406. Herbst, E., *Annu. Rev. Phys. Chem.*, **46**, 27, (1995).

407. Petrie, S., Freeman, C.G., McEwan, M.J., and Ferguson, E.E., *Mon. Not. R. astr. Soc.*, **248**, 272, (1991).

APPENDICES

I. Maclagan, R.G.A.R., McEwan, M.J., and Scott, G.B.I., *Chem. Phys. Lett.*, **240**, 185, (1995).
Ab-initio calculations related to the formation of propynal and propadienone in interstellar clouds.

II. Scott, G.B.I., Fairley, D.A., Freeman, C.G., Maclagan, R.G.A.R., and McEwan, M.J., *Int. J. Mass Spectrom. Ion Proc.*, **149/150**, 251, (1995).
The association reaction $C_2H_3^+$ + CO and interstellar propynal.

III. Scott, G.B., Fairley, D.A., Freeman, C.G., McEwan, M.J., Spanel, P., and Smith, D., *J. Chem. Phys.*, **106**, 3982, (1997).
Gas phase reactions of some positive ions with atomic and molecular hydrogen at 300 K.

IV. Scott, G.B.I., Fairley, D.A., Freeman, C.G., McEwan, M.J., Adams, N.G., and Babcock, L.M., *J. Phys. Chem. A*, **101**, 4973, (1997).
$C_mH_n^+$ Reactions with H and H_2: An Experimental Study.

V. Scott, G.B.I., Fairley, D.A., Freeman, C.G., and McEwan, M.J., *Chem. Phys. Lett.*, **269**, 88, (1997).
The reaction H_3^+ + N: a laboratory measurement.

VI. Scott, G.B.I., Freeman, C.G., and McEwan, M.J., *Mon. Not.,R. astr. Soc.*, **290**, 636, (1997).
The Interstellar Synthesis of Ammonia.

Reprinted from

APPENDIX I

CHEMICAL PHYSICS LETTERS

Chemical Physics Letters 240 (1995) 185–192

Ab initio calculations related to the formation of propynal and propadienone in interstellar clouds

Robert G.A.R. Maclagan, Murray J. McEwan, Graham B.I. Scott

Department of Chemistry, University of Canterbury, Christchurch, New Zealand

Received 3 March 1995; in final form 19 April 1995

ELSEVIER

Contributions should, preferably, be sent to a member of the Advisory Editorial Board (addresses are given in the first issue of each volume) who is familiar with the research reported, or to one of the Editors:

A.D. BUCKINGHAM
D.A. KING
Editor of Chemical Physics Letters
University Chemical Laboratory
Lensfield Road
Cambridge CB2 1EW, UK
FAX 44-1223-336362

A.H. ZEWAIL
Editor of Chemical Physics Letters
A.A. Noyes Laboratory of Chemical Physics
California Institute of Technology
Mail Code 127-72
Pasadena, CA 91125, USA
FAX 1-818-4050454

Important: manuscripts should normally not exceed 2500 words, the abstract should not exceed 100 words and there should be no more than 5 figures. (For details, see the instructions to authors, to be found on the last pages of each volume.)

After acceptance of the paper for publication, all further correspondence should be sent to the publishers (Ms. S.A. Hallink, Editorial Department, Chemistry & Chemical Engineering Department, P.O. Box 330, 1000 AH Amsterdam, The Netherlands; telephone 31-20-4852664, FAX 31-20-4852459, telex 10704 espom nl; electronic mail X400: C=NL; A=400NET; P=SURF; O=ELSEVIER; S=HALLINK, I=S or RFC822: S. HALLINK@ELSEVIER.NL).

Chemical Physics Letters (ISSN 0009-2614). For 1995, volumes 229–245 are scheduled for publication. Subscription prices are available upon request from the publisher. Subscriptions are accepted on a prepaid basis only and are entered on a calendar year basis. Issues are sent by surface mail except to the following countries where air delivery via SAL is ensured: Argentina, Australia, Brazil, Canada, Hong Kong, India, Israel, Japan, Malaysia, Mexico, New Zealand, Pakistan, PR China, Singapore, South Africa, South Korea, Taiwan, Thailand, USA. For all other countries airmail rates are available upon request. Claims for missing issues must be made within six months of our publication (mailing) date. Please address all your requests regarding orders and subscription queries to: Elsevier Science B.V., Journal Department, P.O. Box 211, 1000 AE Amsterdam, The Netherlands. Tel.: 31-20-4853642, fax: 31-20-4853598.

US mailing notice – Chemical Physics Letters (ISSN 0009-2614) is published weekly by Elsevier Science B.V., Molenwerf 1, P.O. Box 211, 1000 AE Amsterdam. Annual subscription price in the USA US$ 5279.00, including air speed delivery, valid in North, Central and South America only. Second class postage paid at Jamaica, NY 11431. USA POSTMASTERS: Send address changes to Chemical Physics Letters, Publications Expediting, Inc., 200 Meacham Avenue, Elmont, NY 11003. Airfreight and mailing in the USA by Publication Expediting.

Printed in The Netherlands | Published weekly | Library of Congress Catalog Card Number 68–26532

ELSEVIER

23 June 1995

Chemical Physics Letters 240 (1995) 185–192

CHEMICAL PHYSICS LETTERS

Ab initio calculations related to the formation of propynal and propadienone in interstellar clouds

Robert G.A.R. Maclagan, Murray J. McEwan, Graham B.I. Scott

Department of Chemistry, University of Canterbury, Christchurch, New Zealand

Received 3 March 1995; in final form 19 April 1995

Abstract

The proposal that propynal, CHCCHO, observed in interstellar clouds is formed by the ion molecule reaction of $C_2H_3^+$ and CO has been investigated in a G2 study. The calculations show that propadienone CH_2CCO could be formed by this reaction but not propynal. At the G2 level of theory, propadienone is calculated to be lower in energy than propynal.

1. Introduction

Propynal has been observed in interstellar clouds [1], but its isomer propadienone has not been observed. It has been postulated that propynal is formed by the same association reaction proposed for the formation of C_3O [2,3],

$$C_2H_3^+ + CO \rightarrow C_3H_3O^+,$$

followed by the dissociative electron recombination reaction,

$$C_3H_3O^+ + e \rightarrow C_3H_2O + H.$$

Dissociative electron recombination reactions are assumed to be fast, with the least possible rearrangement reactions occurring [4].

There have been a number of earlier ab initio studies of the $C_3H_3O^+$ species, but only that of Bouchoux et al. [5] carried out calculations beyond the Hartree–Fock level of theory. Bouchoux et al. carried out a series of calculations on eleven diffferent structures. They found the lowest energy structure to be C-protonated propadienone (**VI**), followed by the cyclic structure (**VII**), O-protonated propynal (**VIII, IX**) and O-protonated propadienone (**X**). Their highest level calculations were at the CIPSI/4-31G*//HF/3-21G level of theory. Holmes et al. [6] used collisional activation (CA) mass spectrometry to obtain values for the heats of formation of five structures. Their experimental work was coupled with HF/DZ calculations. Hopkinson and Lien [7] reported HF/6-31G* calculations.

There have been a number of ab initio studies on the unprotonated species, propadienone, propynal, and the cyclic isomer cyclopropenone. At the Hartree–Fock level of theory the structure of propadienone is predicted to have C_{2v} symmetry [8], but the inclusion of correlation terms leads to a bent structure [9] in agreement with the experimental microwave structure [10]. At the Hartree–Fock level of theory the lowest a′ frequency is predicted to be very small. Brown and Dittman [9] attributed the kinked nature of propadienone to the influence of a doubly excited σ electron configuration. Propadienone and propynal are predicted to be very close in energy. At the Hartree–Fock level of theory propynal is slightly lower in energy than propa-

SSDI 0009-2614(95)00503-X

dienone. Cyclopropenone is higher in energy than the other two isomers.

2. Computational details

All calculations were performed using the GAUSSIAN 90 and GAUSSIAN 92 programs [11,12]. The calculations follow the prescription detailed in the original description of the G2 procedure [13].

3. Results and discussion

The MP2/6-31G* optimised geometries of all C_3H_2O species discussed are shown in Fig. 1, and those of $C_3H_3O^+$ species are shown in Fig. 2. The G2 energies and the energies relative to $C_2H_3^+ + CO$, and calculated enthalpies of formation at 298 K for all $C_3H_3O^+$ species and possible precursors are given in Table 1. The enthalpies of formation were calculated using the values of -110.5 and $+1112.5$ kJ mol^{-1} for the enthalpies of formation of CO and $C_2H_3^+$ [14]. Values calculated using the tabulated enthalpies of formation of C_2H_2 and HOC^+ are 4.4 kJ mol^{-1} more positive. The G2 procedure was chosen because of the established reliability of the calculations. Curtiss et al. [13] give absolute deviations from experimental values of 3.85 kJ mol^{-1} for atomisation energies and 4.4 kJ mol^{-1} for proton affinities of first row species. In Table 2 the calculated proton affinities for the C_3H_2O species **I–III** to form the ions **VI–XIII** are given.

3.1. C_3H_2O isomers

At the HF/6-31G* level of theory, propynal (**II**) is 12.8 kJ mol^{-1} lower in energy than propadienone (**I**). With the same basis set, it is calculated to be

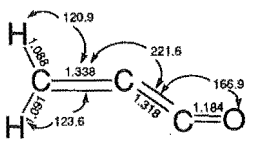

I

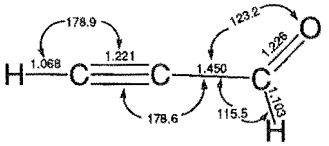

II

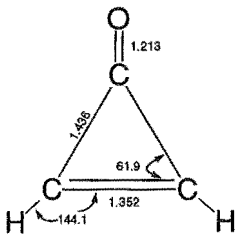

III

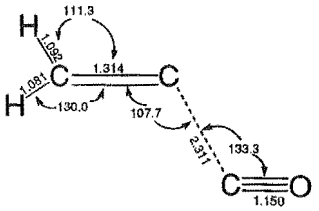

IV

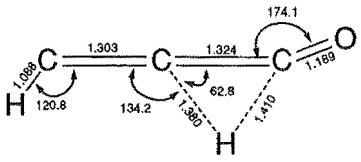

V

Fig. 1. MP2/6-31G* optimised structures of C_3H_2O species.

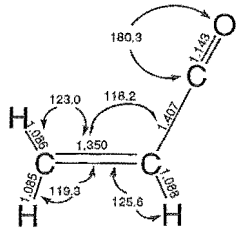

VI

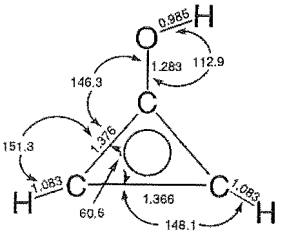

VII

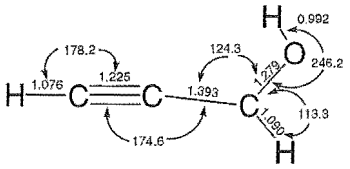

VIII

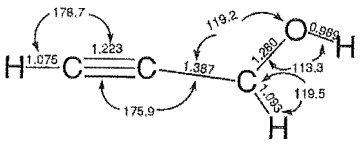

IX

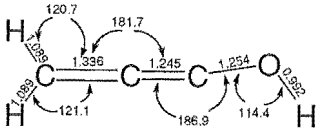

X

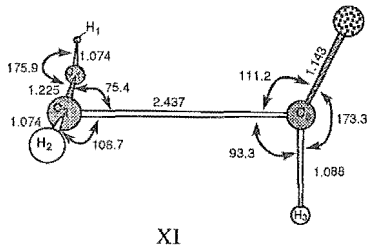

XI

$\omega(H_2C_2C_3H_3) = 89.9°$

$\omega(C_1C_2C_3O) = 95.8°$

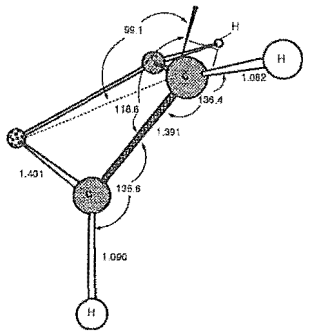

XII

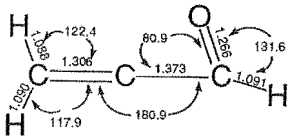

XIII

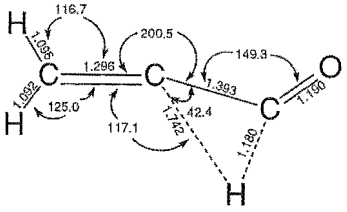

XIV

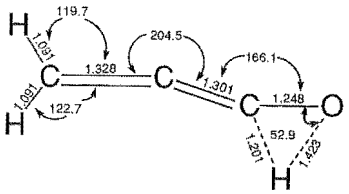

XV

Fig. 2. MP2/6-31G* optimised structures of $C_3H_3O^+$ species.

Table 1
G2 energies and relative energies for $C_3H_3O^+$ species and possible precursors

Structure	E(G2)	ΔE(G2) [a]	ΔH_f^0 (kJ mol^{-1})	
		(kJ mol^{-1})	this work	other work
$C_2H_3^+ + CO$	−190.60807	0.0	1002.0	
I	−190.35709	+659.0	137.0	
II	−190.35443	+665.9	131.6	
III	−190.34372	+694.1	163.6	
IV TS (**I** → $C_2H_2 + CO$)	−190.29177	+830.4	302.8	
V TS(**II** → $C_2H_2 + CO$)	−190.25259	+933.3	404.5	
$C_2H_2 + CO$	−190.36323	+642.8	116.5	
$C_2H + COH$	−190.10401	+1323.4	798.7	
VI	−190.69611	−231.1	766.1	749 [b,c]
VII	−190.65804	−131.2	865.1	858 [b], 900 [c]
VIII	−190.64114	−86.8	911.0	
IX	−190.64025	−84.4	913.2	833 [b], 814 [c]
X	−190.62399	−41.8	956.8	882 [b], 857 [c]
XI	−190.60706	+2.7	1002.0	995 [c]
XII	−190.60258	+14.4	1011.0	986 [c]
XIII	−190.60108	+18.3	1017.8	982 [c]
XIV TS (**VI** → **XIII**)	−190.58767	+53.6	1051.1	1061 [c]
XV TS(**X** → **XIII**)	−190.53586	+189.6	1189.1	
$C_2H_2 + COH^+$	−190.52784	+210.7	1213.7	
$C_2H_2 + HCO^+$	−190.58683	+55.8	1055.9	
$C_2H_2 + HCOH^+ - H$	−190.61248	−11.6	986.1	
$C_2H_2 + H_2COH^+ - H_2$	−190.62712	−50.0	945.2	
$C_3H_2^+ + OH$	−190.44467	+429.0	1429.9	
$C_3H^+ + H_2O$	−190.47262	+355.6	1359.2	

[a] With respect to $C_2H_3^+ + CO$.
[b] Ref. [6]. [c] MNDO calculations of Ref. [5].

only 0.4 kJ mol^{-1} lower at the MP2/6-31G* level of theory which includes some correlation terms. Increasing the size of the basis set to the 6-311G** basis set lowers the energy of propadienone to 2.8 kJ mol^{-1} below that of propynal. Increasing the level of theory to MP4SDTQ puts propadienone 14.1 kJ mol^{-1} below propynal. At the G2 level of theory propadienone is calculated to be 7.0 kJ mol^{-1} below

Table 2
Calculated proton affinities of C_3H_2O

	Proton affinity (298 K)					
	I		**II**		**III**	
	(kJ mol^{-1})	(eV)	(kJ mol^{-1})	(eV)	(kJ mol^{-1})	(eV)
VI	895.5	9.28				
VII					828.5	8.59
VIII			756.1	7.84		
IX			753.8	7.81		
X	704.8	7.30				
XI			665.0	6.89		
XII	650.6 [a]	6.74 [a]				
XIII	643.8	6.67	649.2	6.73		

[a] Ion **XII** cannot be formed directly, without rearrangements, from **I**–**VI**.

propynal, with the D(QCI) correction favouring propynal. This relative ordering differs from that given by Komornicki et al. [8]. Cyclopropenone (**III**) is calculated to be 35.1 kJ mol^{-1} above propadienone, which is a larger separation than the 13.4 kJ mol^{-1} of Komornicki et al.

For propadienone the rotational constants (GHz) are calculated to be: $A = 299.6$, $B = 4.26$, $C = 4.20$ at the HF/6-31G* level of theory and $A = 126.2$, $B = 4.414$, $C = 4.264$ at the MP2/6-31G* level of theory, compared with the experimental values [10] of $A = 149.83$, $B = 4.387$, $C = 4.258$. The large variation in the A constant is due to the change of symmetry. The rotational constants (GHz) for propynal are calculated to be: $A = 69.7$, $B = 4.89$, $C = 4.57$ at the HF/6-31G* level of theory and $A = 65.137$, $B = 4.786$, $C = 4.459$ at the MP2/6-31G* level of theory, compared with the experimental values [15] of $A = 68.04$, $B = 4.826$, $C = 4.500$. For cyclopropenone, the rotational constants (GHz) are calculated to be $A = 32.9$, $B = 8.03$, $C = 6.45$ at the HF/6-31G* level of theory, and $A = 31.90$, $B = 7.739$, $C = 6.228$ at the MP2/6-31G* level of theory, compared with the experimental values of $A = 32.05$, $B = 7.825$, $C = 6.281$ obtained by Benson et al. [16]. The calculated dipole moments of 3.00 D for propadienone and 3.35 D for propynal are not in very good agreement with the experimental values of 2.297 D [10] and 2.46 D [15], respectively. The calculated dipole moment for cyclopropenone of 4.69 is closer to the experimental value of 4.39 [16].

3.2. $C_3H_3O^+$ isomers

The energies relative to $C_2H_3^+ + CO$ of various $C_3H_3O^+$ species are shown in Fig. 3. The lowest energy $C_3H_3O^+$ isomer is C_2-protonated propadienone (**VI**). This isomer can be directly formed by the association of $C_2H_3^+$ and CO, with a C–H bond broken and a C–O bond formed. There is a large contribution (29 kJ mol^{-1}) from the zero-point vibrational energy difference to the calculated proton affinity, which lowers the calculated value. The next lowest isomer is O-protonated cyclopropenone (**VII**). The difference in energy between isomers **VI** and **VII** of 99.9 kJ mol^{-1} is in better agreement with Holmes et al.'s estimated value of 109 kJ mol^{-1} than their calculated value of 151 kJ mol^{-1}. Bouchoux et al. give a value of 117 kJ mol^{-1} at the CI/4-31G*//HF/3-21G level of theory. The difference is increased by increasing the level of theory, but decreased by increasing the size of the basis set. For O-protonated propynal there is the possibility of cis or trans isomers around the C–O bond. The trans isomer **VIII** is lower in energy than the cis isomer **IX**. The trans isomer is the lowest energy form of protonated propynal. Holmes et al. used a value of 795 kJ mol^{-1} for the proton affinity in their calculations of the enthalpies of formation, compared with our value of 753.8 kJ mol^{-1} for isomer **IX**, which led to the much lower value for ΔH_f^0. Bouchoux et al. give a value for the difference in energy beween isomers **VI** and **IX** of only 65 kJ mol^{-1} based on

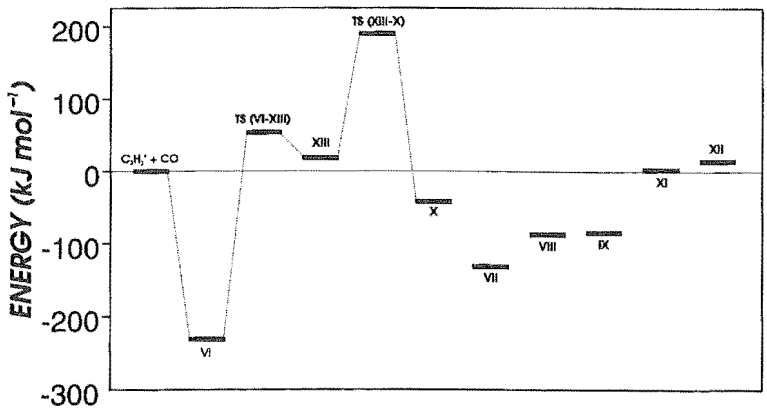

Fig. 3. Relative energies of $C_3H_3O^+$ species.

their MNDO calculations, compared with 171 kJ mol^{-1} at the CI/4-31G*//HF/3-21G level of theory, which is closer to our value of 146.7 kJ mol^{-1}. Isomer **X** is O-protonated propadienone. The difference in the energy between isomers **VI** and **X** is 189.3 kJ mol^{-1}, compared with the values of 133 kJ mol^{-1} estimated by Holmes et al. and 108 kJ mol^{-1} (MNDO) and 218 kJ mol^{-1} (CI/4-31G*) of Bouchoux et al. Our calculations lead to a higher value for the enthalpy of formation of propynal than the MNDO value of Bouchoux et al. and that of Holmes et al. The calculated proton affinities were important in identifying particular isomers observed in mass spectrometric experiments which will be published elsewhere [17]. Isomer **XI** is C_2-protonated propynal. Our calculations indicate that this isomer has approximately the same energy as the reactants $C_2H_3^+ + CO$. They also indicate that C_2 protonation is favoured over C_3 protonation in contrast to the calculations of Bouchoux et al. The C_1C_2 bond is particularly long, which means that this is essentially an association complex of C_2H_2 and HCO^+. Isomer **XII** involves a four-membered C_3O ring. The reaction to form it from $C_2H_3^+ + CO$ is calculated to be just endothermic. Isomer **XIII** can be regarded as either C_1-protonated propadienone or C_3-protonated propynal. The reaction to form **XIII** from $C_2H_3^+ + CO$ is also calculated to be endothermic. For propadienone the relative proton affinities at 298 K at O, C_1 and C_2 are 190.7, 251.7 and 0.0 kJ mol^{-1}, compared with the Bouchoux et al. HF/4-31G*//HF/3-21G values of 213, 285 and 0 kJ mol^{-1}. For propynal the relative values at O, C_2 and C_3 are 0.0, 91.1 and 106.9 kJ mol^{-1} compared with 0, 126 and 109 of Bouchoux et al. A number of other cyclic structures were investigated, but none had energies within 100 kJ mol^{-1} of that for $C_2H_3^+ + CO$. An attempt to optimise the structure of C_2-protonated cyclopropadienone led to structure **VI**.

The three lowest energy protonated forms of propadienone, propynal, and cyclopropanone are the ions **VI**, **VIII**, and **VII** respectively. On protonation of propadienone the CCC angle changes at the MP2/6-31G* level of theory from 138.4° to 118.2°, the C_1C_2 bond length increases from 1.318 to 1.407 Å, as the bond changes from being a double bond, to a single bond. The C_2C_3 bond length also changes from 1.338 to 1.350 Å. At the HF/6-31G* level of theory the rotational constants (GHz) for ion **VI** are: $A = 46.45$, $B = 5.03$, $C = 4.54$. At the MP2/6-31G* level of theory they are: $A = 45.17$, $B = 4.933$, $C = 4.447$. On protonation the C_1O bond in propynal increases slightly, from 1.226 to 1.279 Å, and the C_1C_2 bond decreases from 1.450 to 1.393 Å, as it gains some double bond character. The rotational constants (GHz) for ion **VIII** at the HF/6-31G* level of theory are $A = 56.54$, $B = 4.82$, $C = 4.44$, and at the MP2/6-31G* level of theory: $A = 56.14$, $B = 4.679$, $C = 4.319$. For cyclopropenone, on protonation the CO bond is lengthened from 1.213 to 1.283 Å, and the C_1C_2 bond decreases from 1.436 to 1.376 Å. The rotational constants (GHz) are $A = 30.43$, $B = 7.62$, $C = 6.09$ at the HF/6-31G* level of theory and $A = 29.53$, $B = 7.418$, $C = 5.929$ at the MP2/6-31G* level of theory. The dipole moments of ions **VI**, **VIII**, and **VII** were calculated to be 3.11, 1.44, and 2.58 D, respectively at the HF/6-311 + G(3df, 2p) level of theory.

3.3. Products of the reaction of $C_2H_3^+ + CO$

Based on thermodynamics alone, structures **VI** to **X** could all be formed from the reaction of $C_2H_3^+ + CO$. Without extensive rearrangements, ions **VI**, **VII**, and **X** would not yield propynal in a dissociative electron recombination reaction. For ion **VI** the loss of a hydrogen atom from C_2 gives propadienone while the loss of a hydrogen atom from C_3 would lead to a pentavalent carbon atom at C_2 in a major resonance structure. For isomer **VII** the loss of a hydrogen atom from the O atom would give cyclopropenone, while the loss from C_2 would either give a cyclopropadiene ring or, if ring opening occurred, a pentavalent carbon atom at C_2. For ion **X** either propadienone is formed by the loss of a H atom from the O atom or the structure formed by the loss of a H atom from C_2 in ion **VII** is produced. This leaves only the two $HCCCHOH^+$ isomers **VIII** and **IX** and possibly isomer **XI** which may form propynal by dissociative electron recombination. To form propynal one requires a mechanism by which ion **VI** can rearrange to form either **VIII** (or **IX**), **XI** or **XIII**. Any rearrangement from **VI** to **XI** would involve a transition state higher in energy than $C_2H_3^+ + CO$. At the temperature of interstellar clouds such a rear-

rangement is not possible. The rearrangement of **VI** to form **XIII** involves the shift of the H atom from C_2 to C_1. The transition state for this rearrangement (**XIV**) lies 53.6 kJ mol^{-1} above the energy of $C_2H_3^+ + CO$. Again at the temperature of interstellar clouds such a rearrangement is not possible. Moreover at the G2 level of theory the formation of ion **XIII** from $C_2H_3^+ + CO$ is endothermic. Under conditions very different from those prevailing in interstellar clouds, ion **XIII** could rearrange further to form O-protonated propadienone **X**. The energy of the transition state for this rearrangement (**XV**) is even higher above the energy of $C_2H_3^+ + CO$ than the transition state **XIV**.

$C_2H_3^+$ and CO appear to be the obvious precursors of propynal and propadienone in the interstellar medium. Herbst and Leung [18] in their standard model calculate the abundance of $C_2H_3^+$ and CO relative to H_2 to be 6.7×10^{-12} and 1.5×10^{-4}, respectively. C_2H_2 and HCO^+ have calculated relative abundances of 1.5×10^{-8} and 9.5×10^{-9}, respectively, giving, if reaction rates are similar, an order of magnitude smaller rate of reaction to form propadienone or propynal. The reaction to form ion **XIII** from C_2H_2 and HCO^+ is exothermic, and if ion **VI** is the initial association product, the arrangement to form **XIII** is just possible at interstellar temperatures. At room temperature however a collision rate proton transfer reaction is the only channel observed [19]. Another possibility is the reaction of the ion $HCOH^+$ with acetylene to form either **VIII** or **IX**, with the loss of a hydrogen atom. Alternatively, protonated formaldehyde could react with acetylene, forming H_2 and ions **VIII** or **IX**. The reaction of $C_3H_2^+$ and OH is thermodynamically favourable and could lead to the direct formation of ions **VIII** or **IX**. Ion **VII** could also be formed by this reaction. However the calculated relative abundances of $C_3H_2^+$ and OH are 8.4×10^{-13} and 2.4×10^{-7}, giving a rate of reaction four orders of magnitude slower than $C_2H_3^+ + CO$. For $C_3H^+ + H_2O$ a similar situation exists, where the calculated relative abundances are 7.0×10^{-15} and 1.3×10^{-6} for C_3H^+ and H_2O, respectively, giving a rate five orders of magnitude slower than $C_2H_3^+ + CO$. At room temperature the main product of this reaction is HCO^+ [20].

If, as our calculations suggest, protonated propadienone is formed by the reaction of $C_2H_3^+ + CO$, why is propynal, not propadienone observed in interstellar clouds? A possible reason for the non observation of propadienone is that there is sufficient energy released in the dissociative electron recombination reaction to allow the unimolecular decomposition of propadienone to acetylene and carbon monoxide to occur. At the G2 level of theory, we calculate the energy released by this reaction to be 438.8 kJ mol^{-1}.The decomposition of propadienone to HCCH + CO is 16.1 kJ mol^{-1} exothermic. The transition state for the unimolecular dissociation of propadienone is calculated to be 171.4 kJ mol^{-1} above propadienone, which means that there is sufficient energy released in the recombination reaction to allow the dissociation to proceed. Komornicki et al. [8] gave an estimate of 134.7 kJ mol^{-1} for this transition state energy. The energy available from recombination reactions is always large, and what we have argued for propadienone could also be argued for propynal. For example, although dissociation into C_2H and COH is endothermic with a calculated dissociation energy of 657.5 kJ mol^{-1}, other dissociative channels are available. A dissociation into $C_2H_2 + CO$ is possible if there is sufficient energy released to allow a 1,2 H transfer from C_1 to C_2. The transition state for this H transfer is calculated to be 267.4 kJ mol^{-1} above propynal, which is within the available energy constraints of the dissociative electron recombination reaction. The decomposition of propynal to $C_2H_2 + CO$ is 23.1 kJ mol^{-1} exothermic. We conclude therefore, that the route to the formation of propynal in interstellar clouds via ion molecule reactions is uncertain.

4. Conclusions

The calculations performed in this study suggest that the reaction of $C_2H_3^+$ and CO forms C_2-protonated propadienone. Experiments in this laboratory [17] using the SIFT apparatus, combined with our calculations of proton affinities, have shown that the product is ion **VI** and not protonated propynal (**VIII** or **IX**). Rearrangement of **VI** to form an ion which would yield propynal in a dissociative electron recombination reaction is not possible under the conditions of an interstellar cloud. The nonobservation of

propadienone could be due to it undergoing unimolecular decomposition to $C_2H_2 + CO$ following the dissociative electron recombination reaction of **VI**. Other ion–molecule based syntheses that we have considered seem to be ruled out on the grounds of low abundance of the reactants.

It is apparent that polyatomic ions exist in many different isomeric forms. Without detailed ab initio calculations it is not obvious which isomeric species are formed in a particular radiative association process. To further complicate the picture, it is not apparent what are the products of a dissociative recombination. The large amount of energy released into the complex during recombination certainly produces fragmentation [21], but the longer time scale of the isomerisation process makes it less likely.

References

[1] W.M. Irvine, R.D. Brown, D.M. Cragg, P. Friberg, P.D. Godfrey, N. Kaifu, H.E. Matthews, M. Ohishi, H. Suzuki and H. Takeo, Ap. J. 335 (1988) L89.
[2] E. Herbst, D. Smith and N.G. Adams, Astron. Astophys. 138 (1984) L13.
[3] N.G. Adams, D. Smith, K. Giles and E. Herbst, Astron. Astrophys. 220 (1989) 269.
[4] D.R. Bates, Ap. J. 306 (1986) L45.
[5] G. Bouchoux, Y. Hoppilliard and J.-P. Flament, Org. Mass Spectrom. 20 (1985) 560.
[6] J.L. Holmes, J.K. Terlouw and P.C. Burgers, Org. Mass Spectrom. 15 (1980) 140.
[7] A.C. Hopkinson and M.H. Lien, J. Am. Chem. Soc. 108 (1986) 2843.
[8] A. Komornicki, C.E. Dykstra, M.A. Vincent and L. Radom, J. Am. Chem. Soc. 103 (1981) 1652.
[9] R.D. Brown and R.G. Dittman, Chem. Phys. 83 (1984) 77.
[10] R.D. Brown, P.D. Godfrey, R. Champion and D. McNaughton, J. Am. Chem. Soc. 103 (1981) 5711.
[11] M.F. Frisch, M. Head-Gordon, G.W. Trucks, J.B. Foresman, H.B. Schlegel, K. Raghavachari, M.A. Robb, J.S. Binkley, C. Gonzalez, D.J. DeFrees, D.J. Fox, R.A. Whiteside, R. Seeger, C.F. Melius, J. Baker, R.L. Martin, L.R. Kahn, J.J.P. Stewart, S. Topiol and J.A. Pople, GAUSSIAN 90 (Gaussian, Pittsburgh, 1990).
[12] M.F. Frisch, G.W. Trucks, M. Head-Gordon, P.M.W. Gill, M.W. Wong, J.B. Foresman, B.G. Johnson, H.B. Schlegel, M.A. Robb, E.S. Replogle, R. Gomperts, J.L. Andres, K. Raghavachari, J.S. Binkley, C. Gonzalez, R.L. Martin, D.J. Fox, D.J. DeFrees, J. Baker, J.J.P. Stewart and J.A. Pople, GAUSSIAN 92 (Gaussian, Pittsburgh, 1992).
[13] L.A. Curtiss, K. Raghavachari, G.W. Trucks and J.A. Pople, J. Chem. Phys. 94 (1991) 7221
[14] S.G. Lias, J.E. Bartmess, J.F. Liebman, J.L. Holmes, R.D. Levin and W.G. Mallard, J. Phys. Chem. Ref. Data 17 (1988) Suppl. 1.
[15] G. Winnewisser, J. Mol. Spectry. 46 (1973) 16.
[16] R.C. Benson, W.H. Flygare, M. Oda and R. Breslow, J. Am. Chem. Soc. 95 (1973) 2772.
[17] G.B.I. Scott, D.A. Fairley, C.G. Freeman, R.G.A.R. Maclagan and M.J. McEwan, to be submitted for publication.
[18] E. Herbst and C.M. Leung, Ap. J. Suppl. 69 (1989) 271.
[19] G.I. Mackay, K. Tanaka and D.K. Bohme, Int. J. Mass Spectrom. Ion Proc. 24 (1977) 125.
[20] D.K. Bohme, A.K. Raksit and A.J. Fox, J. Am. Chem. Soc. 105 (1983) 5481.
[21] N.G. Adams in: Advances in gas phase ion chemistry, Vol. 1, eds. N.G. Adams and L.M. Babcock (JAI Press, Greenwich, 1992) p.271.

Reprinted from

APPENDIX II

International Journal of

Mass Spectrometry and Ion Processes

International Journal of Mass Spectrometry and Ion Processes 149/150 (1995) 251–255

The association reaction $C_2H_3^+ + CO$ and interstellar propynal☆

Graham B.I. Scott, David A. Fairley, Colin G. Freeman*, Robert G.A.R. Maclagan, Murray J. McEwan*

Department of Chemistry, University of Canterbury, Private Bag 4800, Christchurch, New Zealand

Received 24 April 1995; accepted 17 June 1995

ELSEVIER

INTERNATIONAL JOURNAL OF MASS SPECTROMETRY AND ION PROCESSES

GENERAL INFORMATION

Scope of the journal

The journal contains papers which consider fundamental aspects of mass spectrometry and ion processes, and the application of mass spectrometric techniques to specific problems in chemistry and physics. The following topics, amongst others, can be found in the journal: theoretical and experimental studies of ion formation (i.e. by electrons, laser or other forms of radiation, heavy ions, high-energy particles, etc.), ion separation and ion detection processes; the design and performance of instruments (or their parts) and accessories; measurements of natural isotopic abundances, precise isotopic masses, ionization, appearance and excitation energies, ionization cross-sections; development of techniques related to determining molecular structures, geological age determination, studies of thermodynamic properties, chemical kinetics, surface phenomena, radiation chemistry, and chemical analyses; theory of mass spectra, application of computer techniques to mass spectral data; chemistry and physics of cluster ions; spectroscopy of gaseous ions including studies related to interstellar chemistry; mechanistic studies of unimolecular processes and ion/molecule reactions in the gas phase including computational aspects (ion trajectory calculations, quantum mechanical studies of potential energy surfaces); physical organic chemistry of isolated ions; biological applications of mass spectrometry.

The journal is of interest to all mass spectrometrists and other scientists interested in the chemistry and physics of charged particles.

Categories of manuscripts

The journal welcomes the following types of papers.

Full-length articles: Comprehensive description and discussion of original research investigations; the experimental techniques must be described in detail.

Short Communications: Complete but concise articles, fully documented, both by reference to the literature and by description of the experimental procedures. Short Communications should not exceed 4–5 printed pages.

Letters: Brief reports (no longer than 4 printed pages or 2000 words) of significant, original and timely research. In considering the suitability of a letter for publication, the editors pay particular attention to the originality of the research and the desirability of rapid publication. **Letters will be published within 6–8 weeks** after acceptance of the article by the editor concerned. No proofs will be sent to the authors.

Reviews: Timely, critical reviews will focus on recent developments while keeping historical documentation to a minimum. Reviews will often be solicited, but prospective authors are also encouraged to contact the editors or editorial board members regarding the appropriateness of the subject matter. In general the length should not exceed 30–40 printed pages. The publisher provides authors of Reviews with a modest honorarium.

Book Reviews: Normally invited by the editors, the style should conform to that of previously published Book Reviews.

0168-1176/95/$09.50

This issue is printed on acid-free paper.

PRINTED IN THE NETHERLANDS

ELSEVIER International Journal of Mass Spectrometry and Ion Processes 149/150 (1995) 251–255

The association reaction $C_2H_3^+ + CO$ and interstellar propynal☆

Graham B.I. Scott, David A. Fairley, Colin G. Freeman*, Robert G.A.R. Maclagan, Murray J. McEwan*

Department of Chemistry, University of Canterbury, Private Bag 4800, Christchurch, New Zealand

Received 24 April 1995; accepted 17 June 1995

Abstract

Two different $C_3H_3O^+$ ions were generated in a selected-ion flow tube operating at room temperature. C-2 protonated propadienone, $H_2C{=}CHCO^+$, was produced by the association reaction between $C_2H_3^+$ and CO. Protonated propynal, $HC{\equiv}C{-}CHOH^+$, was produced by proton transfer to propynal, $HC{\equiv}C{-}CHO$. The ions were identified by their proton transfer reactions with $C_2H_5NH_2$, CH_3NH_2, C_4H_5N, NH_3, $(n\text{-}C_4H_9)_2O$, $(C_2H_5)_2CO$, $C_6H_{10}O$, C_6H_6 and C_2H_5I. Rate coefficients and branching ratios are reported for these reactions. The implications of this work for the synthesis of $HC{\equiv}C{-}CHO$ in interstellar clouds are discussed.

Keywords: Association; $C_3H_3O^+$ ions; Interstellar propynal; SIFT

1. Introduction

Propynal, $HC{\equiv}C{-}CHO$, is one of the molecules possessing a carbon chain skeleton in a growing list of such molecules that have been identified in interstellar clouds. Propynal was first detected in the cold interstellar cloud TMC-1 from its rotational line emission between 18 and 19 GHz [1]. A search was also made for an isomer of propynal, propadienone, $H_2C{=}C{=}C{=}O$, both in TMC-1 and in Sgr B2 molecular clouds, but in each cloud it was below the limit of detection [1].

Sequences of ion/molecule reactions have provided a cogent synthetic route for the formation of most molecular species thus far observed in the interstellar medium [2].

Among the processes suggested for the synthesis of propynal are the ion/molecule association reaction [3]

$$C_2H_3^+ + CO \rightarrow C_3H_3O^+ + h\nu \qquad (1)$$

and the reactions of hydrocarbon ions with atomic oxygen [4], e.g.

$$C_3H_5^+ + O \rightarrow C_3H_3O^+ + H_2 \qquad (2)$$

$HC{\equiv}C{-}CHO$ may then be produced from the $C_3H_3O^+$ ion in dissociative electron

☆ Dedicated to Professor David Smith FRS in recognition of the outstanding contribution he has made to the physics and chemistry of ion/molecule reactions, electron attachment and electron/ion recombination processes. We have all enjoyed stimulating conversations with Professor Smith and benefited greatly from his wide experience, his enthusiasm and his helpful and encouraging comments.

* Corresponding authors.

SSDI 0168-1176(95)04253-9

Table 1
G2 energies calculated for C_3H_2O isomers summarized from Ref. [8]

Molecule	Description	ΔH_f° (kJ mol^{-1})	PA (kJ mol^{-1})
HC≡CCHO	Propynal	132	756[a]
$H_2C{=}C{=}C{=}O$	Propadienone	137	705[b]
			896[c]
HCCOCH	Cyclopropenone	164	829[d]

[a] Refers to the trans isomer of O-protonated propynal.
[b] Refers to O-protonated propadienone.
[c] Refers to C-2 protonated propadienone.
[d] Refers to O-protonated cyclopropenone.

recombination:

$$C_3H_3O^+ + e \rightarrow HC{\equiv}C{-}CHO + H \quad (3)$$

Each of these suggestions is eminently reasonable on the grounds that the precursor ion in each case, $C_2H_3^+$ or $C_3H_5^+$, is unreactive with H_2. What is not known, however, is the isomeric form of the $C_3H_3O^+$ ion formed in reactions (1) and (2).

In this work, we examine the feasibility of reaction (1) producing protonated propynal in an experimental study using a selected-ion flow tube (SIFT). We have also undertaken a theoretical examination of the $C_3H_3O^+$ potential surface. The combined approach, experimental and theoretical, leads to some interesting conclusions. In the experiments that follow, the $C_3H_3O^+$ ion is formed by collisional stabilization of the $(C_3H_3O^+)^*$ intermediate, whereas in interstellar clouds the ion is produced by radiative stabilization of the complex (reaction (1)). It is conceivable (although unlikely) that the two processes may have different products.

2. Experimental

All experiments were made at room temperature (298 ± 5 K) using the Canterbury SIFT system which has been described previously [5,6]. The $C_3H_3O^+$ association ion from reaction (1) was produced in the flow tube by injecting $C_2H_3^+$ and adding CO at the first inlet jet. Propynal was prepared by standard techniques from 2-propyn-1-ol [7] and was injected into the flow tube in its protonated form from the source region. Several experiments were also carried out by injecting HCO^+ and adding HC≡C–CHO at the first inlet port, thereby allowing proton transfer to occur within the flow tube. No difference in behaviour was found in the $C_3H_3O^+$ ion generated from HC≡C–CHO in these two different ways. Most experiments with protonated propynal were undertaken by injecting the self-protonated ion from the ion source.

All other reagents were obtained from commercial suppliers and were further purified by freeze–pump–thaw cycles.

Table 2
G2 energies calculated for isomers of $C_3H_3O^+$

Ion	Description	ΔH_f° (kJ mol^{-1})
$H_2CCHC\overline{O}^+$	C-2 protonated propadienone	766
$HC\overline{COHCH}^+$	O-protonated cyclopropenone	865
$HCCC\overline{HOH}^+$	O-protonated propynal	911
$H_2CCC\overline{OH}^+$	O-protonated propadienone	957

3. Results

Our ab initio studies have identified several $C_3H_3O^+$ structures corresponding to minima on the potential surface [8]. A summary of the heats of formation, ΔH_f°, and proton affinities, PA, of the relevant neutral structures calculated according to the G2 procedure [9] are summarized in Table 1. The energies of some relevant $C_3H_3O^+$ isomers are summarized in Table 2. It is evident from these tables that, whereas the relative stabilities of propynal and propadienone are very close, the same is not true of their protonated ions. C-2 protonated propadienone is about 100 kJ mol^{-1} more stable than O-protonated cyclopropenone and about 191 kJ mol^{-1} more stable than O-protonated propadienone. The very different proton affinities calculated for the neutral C_3H_2O isomers suggest that a convenient way of distinguishing between isomeric $C_3H_3O^+$ ions is to compare their relative ease of proton transfer.

We have carried out a series of comparative reactions of $C_3H_3O^+$ ion chemistry by forming $C_3H_3O^+$ in two ways: from the association reaction between $C_2H_3^+$ and CO and from protonated propynal. The results of this study are summarized in Table 3.

4. Discussion

There is little doubt from the comparative behaviour of the two $C_3H_3O^+$ ions shown in Table 3 that the product of the association reaction between $C_2H_3^+$ and CO (reaction (1)) is not protonated propynal. The experiments listed in Table 3 show that the proton transfer behaviour of the two $C_3H_3O^+$ ions is very different. Both ions transfer a proton at close to the collision rate to $C_2H_5NH_2$ (PA, 908 kJ mol^{-1}) and CH_3NH_2 (PA, 896 kJ mol^{-1}), but only protonated propynal transferred a proton to pyrrole and ammonia. In the case of ammonia, $C_2H_3 \cdot CO^+$ is unreactive ($k = 3.0 \times 10^{-11}$ cm^3 s^{-1}) whereas $HC{\equiv}C{-}CHOH^+$ undergoes a proton transfer reaction at close to the collision rate ($k = 1.6 \times 10^{-9}$ cm^3 s^{-1}). No proton transfer was observed from the $C_2H_3 \cdot CO^+$ ion to any neutral with a proton affinity less than that of CH_3NH_2 (PA, 896 kJ mol^{-1}). The observation of proton transfer with CH_3NH_2 but not with C_4H_5N (pyrrole) brackets the PA of C_3H_2O formed after proton transfer from $C_2H_3 \cdot CO^+$ as 896 kJ mol^{-1} > PA(C_3H_2O) > 868 kJ mol^{-1}. A comparison of the calculated PA values from the ab initio calculations summarized in Table 1 allows us to identify the $C_2H_3 \cdot CO^+$ ion as C-2 protonated propadienone, H_2CCHCO^+, which is at the global minimum on the $C_3H_3O^+$ potential surface. Further, the calculated value for PA($H_2C{=}C{=}C{=}O$) with the proton attaching at the C-2 position is 896 kJ mol^{-1} which is in good agreement with the results of our bracketing experiments.

The experimental results are also consistent with the findings of the theoretical study which predicted that C-2 protonated propadienone could be formed directly from the association of $C_2H_3^+$ and CO [8]. Although the proton affinity of propadienone at O is substantially lower than protonation at the C-2 position, the much deeper potential well for the C-2 position encountered when entering the $C_3H_3O^+$ surface at the $C_2H_3^+ + CO$ entrance favours C-2 protonation. Also, the transition state between the C-2 and O-protonated forms of propadienone cannot be accessed with the energy available from the $C_2H_3^+$ and CO reactants.

The experiments with protonated propynal, $HC{\equiv}C{-}CHOH^+$, summarized in Table 3, enable PA($HC{\equiv}C{-}CHO$) to be evaluated. Rapid proton transfer from $HC{\equiv}C{-}CHOH^+$ occurs to C_6H_6 (PA, 759 kJ mol^{-1}) but not to C_2H_5I (PA ≈ 736 kJ mol^{-1} [10,11] and this observation

Table 3
Reaction rate coefficients and product ratios for the $C_3H_3O^+$ isomeric ions $C_2H_3 \cdot CO^+$ and $HC{\equiv}C{-}CHOH^+$ with the specified reactant

Reactant	Product distribution		k_{coll} [a]	k_{obs} [a]	PA neutral [g] (kJ mol^{-1})
	Proton transfer	Adduct			
$C_2H_5NH_2$	0.85	0.15	1.8	1.7 [b]	908
	0.85	0.15		1.8 [c]	
CH_3NH_2	0.75	0.25	1.8	1.5 [b]	896
	0.90	0.10		2.0 [c]	
C_4H_5N [d]	0	1.0	2.0	2.0 [b]	868
	0.8	0.2		2.2 [c]	
NH_3	0	1.0	2.3	0.03 [b]	854
	1.0	0		1.6 [c]	
$(n\text{-}C_4H_9)_2O$	0	$\leqslant$0.25 [e]	1.9	1.6 [b]	852
	1.0	0		2.0 [c]	
$(C_2H_5)_2CO$	0	1.0	2.8	1.3 [b]	843
	1.0	0		2.5 [c]	
$C_6H_{10}O$ [f]	0	1.0	2.7	2.9 [b]	843
	1.0	0		3.2 [c]	
C_6H_6	0.20	0.80	1.3	1.0 [c]	759
C_2H_5I	0	1.0	1.9	0.1 [c]	≈736

[a] In units 10^{-9} cm^3 s^{-1}.
[b] $C_2H_3 \cdot CO^+$.
[c] $HC{\equiv}C{-}CHOH^+$.
[d] Pyrrole.
[e] Other products include $C_4H_9{-}O{-}C_4H_8^+$ (major peak) and $C_4H_9O^+$.
[f] Cyclohexanone.
[g] From Ref. [10].

brackets the proton affinity of propynal as 759 kJ mol^{-1} > PA(HC≡C–CHO) > 736 kJ mol^{-1}. The calculated proton affinity PA(HC≡C–CHO) = 756 kJ mol^{-1} is in excellent agreement.

5. Conclusions

The $C_3H_3O^+$ ion formed from the association of $C_2H_3^+$ and CO has the C-2 protonated propadienone structure and not the protonated propynal structure. This result makes the proposed mechanism for the interstellar synthesis of propynal from the radiative association of $C_2H_3^+$ and CO followed by dissociative recombination (reactions (1) and (3) unlikely. If propynal is made during dissociative recombination then so also should

propadienone, yet the latter has not been observed [1]. Although the products of dissociative recombination are not known, it is highly unlikely that preferential isomerization would occur in view of the fragmentation products of dissociative recombination observed from smaller ions [12]. Instead, $H_2C{=}C{=}C{=}O$ and not $HC{\equiv}C{-}CHO$ is the more plausible outcome of recombination.

In view of the projected rate of reaction (1) under interstellar cloud conditions [3], the non-detection of propadienone presents as much of a dilemma as does the detection of propynal. We also point out that the experiments reported here do not rule out the production of C_3O in reaction (3) as proposed by Herbst et al. [13]. It is quite feasible that three H atoms could be eliminated from the C_3O skeleton during the recombination reaction. Perhaps the non-observation of $H_2C{=}C{=}C{=}O$ in TMC-1 is evidence for dissociation of the C-2 protonated propadienone ion back to C_2H_3 and CO or $C_2H_2 + H + CO$ during recombination.

What then is the mechanism by which propynal and not propadienone is produced in interstellar clouds? The selective synthesis of $HC{\equiv}C{-}CHO$ over $H_2C{=}C{=}C{=}O$ requires a pathway specific in its selection of $HC{\equiv}C{-}CHOH^+$ and not $H_2C{=}CHCO^+$ if an ion/molecule mechanism is the source. This specificity in turn requires entry to the $C_3H_3O^+$ potential surface in the vicinity of $HC{\equiv}C{-}CHOH^+$ and away from $H_2C{=}CHCO^+$. No transition state between C-2 protonated propadienone and O-protonated propynal was identified [8]. An appropriate entry point to the $C_3H_3O^+$ potential surface which could access protonated propynal and not protonated propadienone, might be reaction (2) as suggested by Bettens and Brown [3] or a reaction of the type [14]

$$C_3H_2^+ + H_2O \rightarrow C_3H_3O^+ + H$$

These reactions will need to be investigated further before the solution to the problem is found.

Acknowledgements

We would like to thank David Smith and Patrik Spanel for their advice and help during a recent visit to this Department.

References

[1] W.M. Irvine, R.D. Brown, D.M. Cragg, P. Friberg, P.D. Godfrey, N. Kaifu, H.E. Matthews, M. Ohishi, H. Suzuki and H. Takeo, Astrophys. J., 335 (1988) L89.
[2] D. Smith, Chem. Rev., 92 (1992) 1473.
[3] N.G. Adams, D. Smith, K. Giles and E. Herbst, Astron. Astrophys., 220 (1989) 269.
[4] R.P.A. Bettens and R.D. Brown, Mon. Not. R. Astron. Soc., 258 (1992) 347.
[5] J.S. Knight, C.G. Freeman, M.J. McEwan, N.G. Adams and D. Smith, Int. J. Mass Spectrom. Ion Processes, 67 (1985) 317.
[6] M.J. McEwan, in N.G. Adams and L.M. Babcock (Eds.), Advances in Gas Phase Ion Chemistry, Vol. 1, J.A.I. Press, Greenwich, CT, 1992, p. 1.
[7] J.C. Sauer, in N. Rabjohn (Editor in Chief), Organic Syntheses, Collected Vol. IV, Wiley, New York, 1963, p. 813.
[8] R.G.A.R. Maclagan, M.J. McEwan and G.B.I. Scott, Chem. Phys. Lett., 240 (1995) 185.
[9] L.A. Curtiss, K. Raghavachari, G.W. Trucks and J.A. Pople, J. Chem. Phys., 94 (1991) 7221.
[10] S.G. Lias, J.E. Bartmess, J.F. Liebman, J.L. Holmes, R.D. Levin and W.G. Mallard, J. Phys. Chem. Ref. Data, 17 (1988) Suppl. 1.
[11] S. Petrie, J.S. Knight, C.G. Freeman, R.G.A.R. Maclagan, M.J. McEwan and P. Sudkeaw, Int. J. Mass Spectrom. Ion Processes, 105 (1991) 43.
[12] N.G. Adams, in N.G. Adams and L.M. Babcock (Eds.), Advances in Gas Phase Ion Chemistry, Vol. 1, J.A.I. Press, Greenwich, CT, 1992, p. 271.
[13] E. Herbst, D. Smith and N.G. Adams, Astron. Astrophys., 138 (1984) L13.
[14] C. DePuy, personal communication, 1994.

Submission of papers (in English, French or German (English is preferred))

Papers should be sent to:

M.T. BOWERS, Department of Chemistry, University of California, Santa Barbara, CA 93106, USA (Fax: +1 805 893 8703)

or to: H. SCHWARZ, Department of Chemistry, Technical University, Strasse des 17. Juni 135, +1 D-10623 Berlin, Germany (Fax: +49 30 3142 1102)

or to: J.F.J. TODD, University Chemical Laboratory, University of Kent, Canterbury, Kent CT2 7NH, UK (Fax: +44 227 475475)

Submission of an article is understood to imply that the article is original and unpublished and is not being considered for publication elsewhere. Upon acceptance of an article by the journal, author(s) will be asked to transfer the copyright of the article to the publisher. This transfer will ensure the widest possible dissemination of information.

Publication

International Journal of Mass Spectrometry and Ion Processes (ISSN 0168-1176). For 1995 volumes 141–151 are scheduled for publication. Subscription prices are available on request from the publisher.

Subscriptions are accepted on a prepaid basis only and are entered on a calendar year basis. Issues are sent by surface mail except to the following countries where air delivery via SAL (Surface Air Lift) mail is ensured: Argentina, Australia, Brazil, Canada, Hong Kong, India, Israel, Japan, Malaysia, Mexico, New Zealand, Pakistan, PR China, Singapore, South Africa, South Korea, Taiwan, Thailand, USA. For all other countries airmail rates are available upon request. Claims for missing issues must be made within six months of our publication (mailing) date.

Please address all your requests regarding orders and subscription queries to: Elsevier Science B.V., Journal Department, P.O. Box 211, 1000 AE Amsterdam, The Netherlands (Tel: +31 20 5843 642; Fax: +31 20 5803 598).

Reprints

Fifty reprints will be supplied free of charge. Additional reprints (minimum 100) can be ordered at quoted prices. They must be ordered on order forms which are sent together with the proofs.

Advertisements

For rates apply to the publisher.

Subscriptions should be sent to: ELSEVIER SCIENCE B.V., Journals Department, P.O. Box 211, 1000 AE Amsterdam, The Netherlands (Tel: +31 20 5803 911; Telex: 18582).

US mailing notice—International Journal of Mass Spectrometry and Ion Processes (ISSN 0168-1176) is published semi-monthly (except in January when it will appear monthly) by Elsevier Science B.V., Molenwerf 1, Postbus 211, 1000 AE Amsterdam. Annual subscription price in the USA US$2432.00 (valid in North, Central and South America only), including air speed delivery. Second class postage is paid at Jamaica, NY 11431.

USA POSTMASTERS: Send address changes to International Journal of Mass Spectrometry and Ion Processes, Publications Expediting, Inc., 200 Meacham Avenue, Elmont, NY 11003. Airfreight and mailing in the USA by Publication Expediting.

INSTRUCTIONS TO AUTHORS

Manuscripts

Authors should submit the original and two copies in double-spaced type with adequate margins on pages of uniform size. Instructions for the preparation of compuscripts are available from the publisher.

Acknowledgements and references should be placed at the end of the paper. It is recommended that authors use the nomenclature and symbols adopted by IUPAC (Quantities, Units and Symbols in Physical Chemistry, Blackwell Scientific, Oxford, 1988). See also the IUPAC Recommendations for Symbolism and Nomenclature for Mass Spectrometry, Pure Appl. Chem., 50 (1978) 65, and reprinted in Int. J. Mass Spectrom. Ion Phys., 29 (1979) 392.

Tables should be typed on separate pages and numbered with Arabic numerals in the order in which they are mentioned in the text. All tables should have descriptive titles. The use of chemical formulae and conventional abbreviations is encouraged in tables and figures but chemical formulae should not be used in the text unless they are necessary for clarity. Units of weight, volume, etc., when used with numerals should be abbreviated and unpunctuated (e.g. 2%, 2 ml, 2 g, 2 μl, 2 μg, 2 ng, 2 cm, 200 nm).

Figures should be drawn in black, waterproof drawing ink on drawing or tracing paper. Standard symbols should be used in line drawings; the following are available to the typesetter:

○ ⊕ ● × + △ ▲ ◇ ◆ □ ■ ☆ ★ –

Photographs should be submitted as clear black-and-white glossy prints. Figures and photographs should be of the same size as the typed pages. Legends for figures should be typed on a separate page. Figures should be numbered with Arabic numerals in the order in which they are mentioned in the text.

References in text should be numbered (on the line and in square brackets) in the order of their appearance. The reference list at the end of the article should be in numerical order of appearance in the text. Abbreviations of journal titles should conform to those adopted by the Chemical Abstract Service (Bibliographic Guide for Editors and Authors, The American Chemical Society, Washington, DC, 1974). The recommended form for references to journal papers and books is as follows: 1 J.J. Lingane and A.M. Hartley, Anal. Chim. Acta, 11 (1954) 475. 2 F. Feigl, Spot Tests in Organic Analysis, 7th edn., Elsevier, Amsterdam, 1966, p. 516. For multi-author references, all authors must be named, and initials given, in the reference list, although the use of, for example, Smith et al., is desirable in the text.

An abstract of not more than 500 words should be provided in the language of the paper. The abstract should be a concise and factual description of the contents and conclusions as well as an indication of any new findings. References should be avoided in the abstract if at all possible. If they are necessary, they should be given in full and not included as part of the numbered list. Illustrations (e.g. formulae and schemes which cannot be typeset) should be avoided in the abstract if at all possible. For papers in French or German, an English abstract should also be provided. No abstract is needed for Short Communications.

Detailed suggestions and instructions to authors are published in Int. J. Mass Spectrom. Ion Processes, 128 (1993) 209–212. A free copy of these instructions is available from the publisher on request.

Gas phase reactions of some positive ions with atomic and molecular hydrogen at 300 K

Graham B. Scott, David A. Fairley, Colin G. Freeman, and Murray J. McEwan
Department of Chemistry, University of Canterbury, Christchurch, New Zealand

Patrik Spanel and David Smith
Department of Biomedical Engineering and Medical Physics, University of Keele, Stoke on Trent ST4 7QB, United Kingdom

(Received 18 July 1996; accepted 3 December 1996)

The reactions of CO^+, CO_2^+, SO_2^+, NO_2^+, CS_2^+, CN^+, $C_2N_2^+$, and $C_2H_3^+$ with H atoms and H_2 molecules have been studied in a selected ion flow tube operated at (300±5) K. The H atom reactions proceed variously by the processes of atom exchange and charge transfer (when allowed), none proceed at the Langevin rate, and the rates of several of them appear to be influenced by the spin states of the product species. Most of the H_2 reactions proceed by H atom abstraction and at a large fraction of the Langevin rate. © *1997 American Institute of Physics.*
[S0021-9606(97)00210-9]

I. INTRODUCTION

Laboratory investigations into the reactions of ions with atoms have an interesting history. Whereas a large number of ion–molecule reactions have been measured in the laboratory only few ion–atom reactions have been studied.[1] Two problems, inherent in all ion–atom studies (with the exception of the inert gases), are the difficulties of generating atoms in the reaction region and the problem of detecting them.

Atomic hydrogen is readily made by passing a mixture of helium and hydrogen through a microwave cavity but it is not an easy reactant to monitor in the laboratory. Most of the difficulties associated with the measurement of ion–H atom reactions are associated with the determination of H atom number densities.[2,3] Considerable efforts have been expended by various groups in overcoming these problems and some ion–H atom reactions have now been studied, mostly utilizing flow tube techniques. Fehsenfeld and Ferguson calibrated the H atom flow by using a titration reaction with NO_2 (Refs. 2 and 3) and also a theoretical rate coefficient for the associative detachment reaction

$$F^- + H \rightarrow HF + e \qquad (1)$$

and later for the analogous reaction,[4,5]

$$Cl^- + H \rightarrow HCl + e. \qquad (2)$$

Another technique also used by this group was to monitor the heat released by the recombining H atoms on a platinum surface.[6]

Some ions react with both H_2 and H and since a microwave discharge source produces a mixture of H_2 and H, then two simultaneous reactions may occur. As long as a different product ion is produced in each reaction, it is possible to determine the H atom densities by comparing the reactant ion loss and product formation in the presence and absence of H atoms (discharge on/off). Thus, the H/H_2 ratio in a flow tube has been determined by observing the different products of the reactions of H and H_2 with CO_2^+.[7] More recently, both reaction (2) and the reaction of Ar^+ ions with H_2 have been used to establish the H/H_2 ratio in the flow tube of a SIFT.[8] Also, Cl^- and SF_6^- ions have been used to determine the H/H_2 and D/D_2 ratios in a SIFT experiment in which the exchange of H and D atoms was studied in some ion-neutral reactions of interstellar interest.[9] Much of the laboratory chemistry of ion–atom reactions has been reviewed recently by Sablier and Rolando.[10]

The method selected for the present study was that involving the $CO_2^+ + H_2$, H reactions (producing HCO_2^+ and HCO^+, respectively) which has been used successfully in several laboratories[7,11] and additionally the $CO^+ + H_2$, H reactions [producing (HCO^+, HOC^+) and H^+, respectively] (see Tables I and II). It was a convenient choice for the present study because the SIFT apparatus is configured for positive ions (see Experiment).

We report here the results of a study of a number of ion–H atom reactions, including some which have been studied previously in other laboratories.

II. EXPERIMENT

All the measurements of the rate coefficients reported here were made using the selected ion flow tube (SIFT) at the University of Canterbury, operated at room temperature (300±5) K, which has been described elsewhere.[12] Hydrogen atoms were generated in a microwave discharge through either a 10% mixture of hydrogen in helium or, alternatively, through pure hydrogen, in a Pyrex side tube with a quartz discharge section connected to the main flow tube. That part of the 13 mm o.d., 10 mm i.d. Pyrex tube that was inserted into the carrier gas and exposed to the ion swarm was sheathed in stainless steel on the outside and coated with halocarbon wax on the inside in order to reduce atom/atom surface recombination. A light horn reduced the number of photons from the discharge reaching the main flow tube. The microwave cavity was situated about 28 cm from the flow tube but even at this distance, some He $2\,^3S$ metastables reached the carrier gas at high flows of the H_2/He mixtures

 0021-9606/97/106(10)/3982/6/$10.00

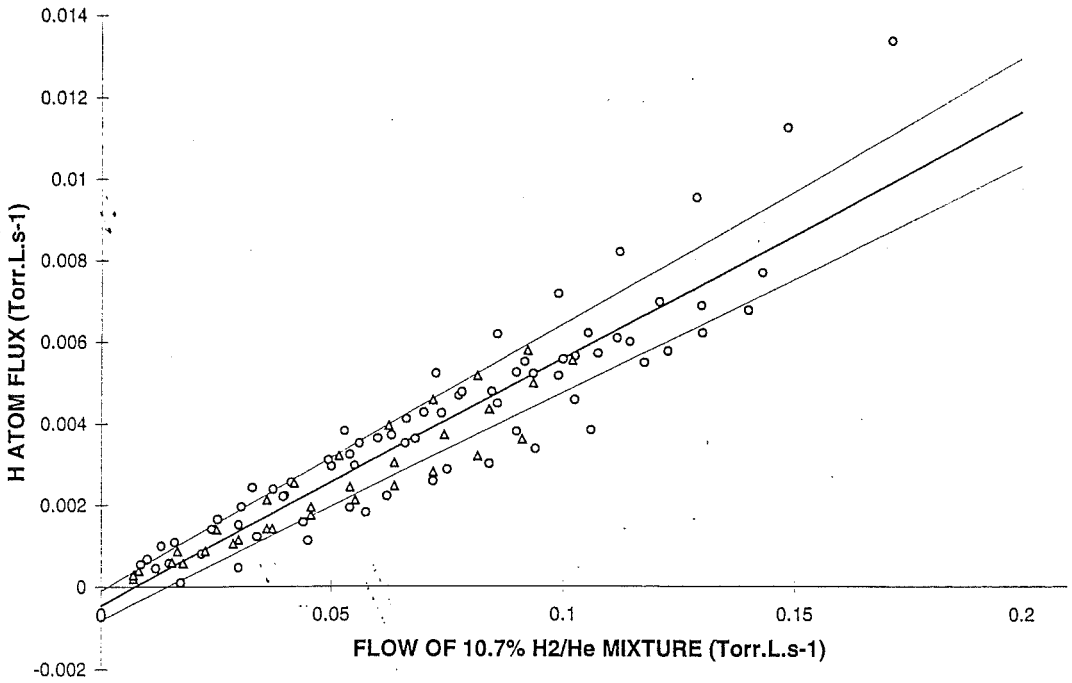

FIG. 1. The variability in H atom flux with flow of 10.7% H_2/He mixture through the microwave discharge cavity. The H atom fluxes shown were determined from the $CO_2^+ + H_2/H$ (circles) and $CO^+ + H_2/H$ (triangles) reactions as described in the text.

causing Penning ionization of the neutral reactant. When interference from He ($2\,^3S$) Penning ionization occurred, pure hydrogen was substituted for the H_2/He mixture.

Other workers have noted that the fractional dissociation of H_2 to H atoms in a discharge varies in an unpredictable manner.[3] This fraction was frequently monitored in our experiments using the reference CO_2^+/H_2, H and CO^+/H_2, H reactions which provide an absolute measure of the H atom number density within the flow tube. During the course of some 20 or so measurements of the reference reactions, a variation of $\leqslant 8\%$ in the fraction of the H_2 dissociated was noted (in a series of runs over several weeks) as is shown in Fig. 1. A typical degree of dissociation of hydrogen in the flow tube was 20%–30% using the 10% H_2/He mixture. The degree of dissociation remained constant with H_2/He flow over the range of flows used. We also compared the degree of dissociation found using the CO_2^+ and CO^+ reactions with those found using several other reactions including the CN^+ and $C_2N_2^+$ reactions which give different products when reacting with H_2 and H (see Tables I and II). All systems investigated yielded the same H atom densities (within experimental error) thus providing evidence that possible contamination from $H_2(v)$ in the discharge was not a significant source of error. Had $H_2(v)$ been present, then variations in the apparent degree of dissociation of H_2 might have been observed from the different systems. A similar argument can be made for the absence of vibrational excitation in the CO_2^+ and CO^+ monitor ions. It should also be noted that all the reactant ions undergo multiple collisions with the He carrier gas atoms before they react with the H_2 and H in the SIFT experiments and this, whilst not guaranteeing that excess vibrational energy has been quenched, must surely tend to do so. In some cases it was necessary to substitute D_2 for H_2 in the He/H_2 mixture to assist in product determination because of the difficulty in detecting H^+ ions.

We estimate the uncertainty in the rate coefficients for H atom reactions as ±30%. This is a larger uncertainty than is usually reported for stable neutral reactants (±15%) due to the difficulty in determining the H atom number density in the main flow tube.

III. RESULTS AND DISCUSSION

A. $CO_2^+ + H_2/H$

The reaction between $CO_2^+ + H$ was one of the first atomic hydrogen–ion reactions to be investigated,[3] but such measurements are complicated by the simultaneous rapid reaction of CO_2^+ with the H_2 which is also present in the flow tube,

$$CO_2^+ + H_2 \rightarrow HCO_2^+ + H. \tag{3}$$

It is somewhat surprising that the previously measured values of the rate coefficient for reaction (3) should exhibit such a considerable spread ranging from 4.0×10^{-10} to 1.4×10^{-9} $cm^3\ s^{-1}$.[13–19] Our value for this rate coefficient (the mean of more than 20 measurements) is $k=8.7\times10^{-10}\ cm^3\ s^{-1}$ which is in good agreement with Tosi *et al.*[7]

The first measurement of the rate coefficient for the overall reaction (4) between CO_2^+ and H by Fehsenfeld and Ferguson[3] indicated a value of $(6\pm3)\times10^{-10}\ cm^3\ s^{-1}$ but they did not measure a branching ratio—although indirect

evidence supported a HCO^+/H^+ ratio of 5/1. Both HCO^+ and H^+ are energetically allowed products thus,

$$CO_2^+(^2\Pi_g)+H(^2S)\rightarrow HCO^+(^1A)+O(^3P) \quad (4a)$$

$$\rightarrow H^+(^1S)+CO_2(^1\Sigma_g^+). \quad (4b)$$

Tosi *et al.*[7] distinguished between reactions (3) and (4) which occur simultaneously, by comparing the relative ion signals of CO_2^+ and the product ion of the reaction with H_2, HCO_2^+, with the microwave discharge on and off. Since the rate coefficient for reaction (3) is known (it is readily determined with the discharge off), then the H atom density can be determined.[7] The rate coefficient obtained by Tosi *et al.* for reaction (4) is 2.9×10^{-10} cm^3 s^{-1}.[7] Our measured rate coefficient for reaction (4) (the mean of over 20 measurements) is $k=4.7\times10^{-10}$ cm^3 s^{-1}. This value is not inconsistent with both of the earlier measurements,[3,7] considering the collective large uncertainties in these three experiments.

Two isomeric structures of $(CHO)^+$, viz. HOC^+ and HCO^+, are energetically accessible in reaction (4a). We probed the structure of the $(CHO)^+$ product ion by examining its reactivity with N_2O, having established earlier that HOC^+ reacts rapidly with N_2O whereas HCO^+ does not.[20] The $(CHO)^+$ product of reaction (4a) was found to be exclusively HCO^+. We also measured the H^+/HCO^+ branching ratio for reaction (4) by reacting CO_2^+ with a 10% deuterium/helium mixture. With the microwave discharge on, no D^+ product was observed even though the channel is exothermic by 17 kJ mol^{-1}. This allowed us to place a limit of $<5\%$ for the branching ratio for the D^+ channel and by inference a similar limit is placed on the H^+ product of the $CO_2^+ + H$ reaction. The Langevin rate coefficient for reaction (4) is $k_L=1.9\times10^{-9}$ cm^3 s^{-1}. When spin conservation is accounted for, the spin-weighted fraction of channel (4a) has an upper limit of 3/4 k_L, i.e., 1.4×10^{-9} cm^3 s^{-1}, whereas the unobserved channel (4b) has an upper limit of 1/4 k_L, i.e., 4.8×10^{-10} cm^3 s^{-1}. These upper limit values clearly exceed our measured values, and thus other, unknown factors are diminishing the rate of reaction below the collision rate.

B. $CO^+ + H_2/H$

The rate coefficient for the reaction (5) between CO^+ and H_2 has been well characterized in many laboratories with $k=1.4\times10^{-9}$ cm^3 s^{-1}.[1] Our measurement indicated a rate coefficient of $k=1.5\times10^{-9}$ cm^3 s^{-1}. We have earlier reported that the product ions for this reaction are the isomers HCO^+ and HOC^+ in equal proportions,[20]

$$CO^+ + H_2 \rightarrow HOC^+ + H(0.50) \quad (5a)$$

$$\rightarrow HCO^+ + H(0.50). \quad (5b)$$

One earlier measurement of the reaction between CO^+ and H has been recorded in which the products are reported as $H^+ + CO$.[21] In our study the only observed product ion is H^+ (confirmed by studying the analogous D reaction as before). Federer *et al.*[21] noted that only singlet products of reaction (6) are energetically accessible,

$$CO^+(^2\Sigma)+H(^2S)\rightarrow H^+(^1S)+CO(^1\Sigma). \quad (6)$$

Thus if spin is conserved then $k\leqslant 1/4k_L$ (i.e., $k\leqslant 4.8\times10^{-10}$ cm^3 s^{-1}) which is the statistical weight ratio of singlet-to-total products. The rate coefficient reported by Federer *et al.* of $k=7.5\times10^{-10}$ cm^3 s^{-1} (Ref. 21) is larger than the spin weighted collision rate and these workers then argued for some spin conversion to occur during the collision. Our measured rate coefficient for reaction (6) is $k=4.0\times10^{-10}$ cm^3 s^{-1} which supports spin conservation. We noted previously that reactions (5) and (6) can be utilized to provide absolute H atom number densities in the flow tube in a similar manner to that described for the $CO_2^+ + H_2/H$ reactions. H atom number densities from both sets of reactions were utilized to obtain the rate coefficient for reaction (6).

C. $SO_2^+ + H_2/H$

One previous measurement [using the ion cyclotron resonance (ICR) technique] of the rate coefficient for reaction (7) between SO_2^+ and H_2 has been reported, a value of $k=1.7\times10^{-11}$ cm^3 s^{-1} (Ref. 1) being indicated,

$$SO_2^+ + H_2 \rightarrow HSO_2^+ + H. \quad (7)$$

Our study shows that the reaction does apparently occur, but very slowly, the rate coefficient k being about 5.0×10^{-12} cm^3 s^{-1}, and the product ion being identified as HSO_2^+.

However, a relatively rapid reaction occurs between SO_2^+ and H atoms ($k=4.2\times10^{-10}$ cm^3 s^{-1}), the only product ion being SO^+,

$$SO_2^+(^2A_1)+H(^2S)\rightarrow SO^+(^2\Pi)+OH(^2\Pi). \quad (8)$$

Spin is conserved in this reaction but the observed rate coefficient is only 20% of k_L (which$=1.9\times10^{-9}$ cm^3 s^{-1}). This may be an indication that the reaction proceeds via a singlet potential surface. A number of spin-allowed ion–atom reactions have been observed that exhibit similar characteristics.[21,22]

D. $NO_2^+ + H_2/H$

This SIFT study shows that NO_2^+ is unreactive with both H_2 ($k<1\times10^{-12}$ cm^3 s^{-1}) and H ($k<1\times10^{-11}$ cm^3 s^{-1}) at thermal energies, even though exothermic channels are available for both reactions ($NO^+ + H_2O$ for the H_2 reaction) and for the H reaction,

$$NO_2^+(^1\Sigma)+H(^2S)\nrightarrow NO^+(^1\Sigma)+OH(^2\Pi). \quad (9)$$

In this unobserved exothermic reaction (9), ($\Delta H°=-169$ kJ mol^{-1}) spin is conserved, and so this unreactivity indicates either the presence of a substantial barrier on the $(NO_2H^+)^*$ surface, or, that the selection rule for orbital angular momentum conservation is more stringent than might be expected. It is interesting to note that the analogous neutral reaction of H with NO_2 (giving OH+NO) is fast[23] as is also the reaction between NO_2^- and H.[24]

E. $CS_2^+ + H_2/H$

No previous studies of either of these reactions have been reported. In the present study, no reaction was observed

TABLE I. Reactions of the given reactant ion with H_2.

Reactant ion	Products	Branching ratio	k^a	$k_{prev}{}^b$	$-\Delta H^0$/(kJ mol^{-1})
CO^+	$HOC^+ + H$	0.5		20,[c] 11.9,[d] 14[e]	61.3
			15	13.9,[f] 18,[g] 13,[h] 15[i]	
	$HCO^+ + H$	0.5			198.1
CO_2^+	$HCO_2^+ + H$	1.0	8.7	14,[c] 10.1,[d] 4,[j] 8[e] 7.2,[k] 5.8,[l] 9.5,[m] 4.7[n] 9.0[o]	127.5
SO_2^+	$HSO_2^+ + H$	1.0	0.05	0.17[n]	74.9
NO_2^+	...	...	NR[p]	...	...
CS_2^+	...	...	NR[q]	...	...
CN^+	$HCN^+ + H$	0.5			128.8
			16	12.4,[n] 10.0,[r] 11[s]	
	$HNC^+ + H$	0.5			170.7
$C_2N_2^+$	$HC_2N_2^+ + H$	1.0	8.8	9.6[t]	219.6

[a]Observed rate coefficient in units of 10^{-10} cm^3 s^{-1}. The Langevin capture rate coefficient for all reactions in this table is 1.5×10^{-9} cm^3 s^{-1}.
[b]Rate coefficients determined in other laboratories, in units of 10^{-10} cm^3 s^{-1}.
[c]Reference 34.
[d]Reference 17.
[e]Reference 18.
[f]Reference 35.
[g]Reference 36.
[h]Reference 21.
[i]Reference 20.
[j]Reference 37.
[k]Reference 19
[l]Reference 13.
[m]Reference 15.
[n]Reference 1.
[o]Reference 7.
[p]No reaction observed ($k<1\times10^{-12}$ cm^3 s^{-1}).
[q]No reaction observed ($k<5\times10^{-13}$ cm^3 s^{-1}).
[r]Reference 25.
[s]Reference 26.
[t]Reference 27.

TABLE II. Reaction of given reactant ion with H.

Reactant ion	Products	Branching ratio	k^a	$k_{prev}{}^b$	$-\Delta H^0$/(kJ mol^{-1})
CO^+	$H^+ + CO$	1.0	4.0	7.5[c]	40.1
CO_2^+	$HCO^+ + O$	>0.95			
			4.7	6,[d] 1.1[e], 2.9[f]	78.6
	$H^+ + CO_2$	<0.05			17.0
SO_2^+	$SO^+ + OH$	1.0	4.2	...	69.4
NO_2^+	...	...	NR[g]	...	...
CS_2^+	$HCS^+ + S$	1.0	2.8	...	12.1
CN^+	$H^+ + CN$	1.0	6.4	...	77.4
$C_2N_2^+$	$HNC^+ + CN$	0.8			7[h]
			6.2	...	
	$C_2H^+ + N_2$	0.2			120.1
$C_2H_3^+$	$C_2H_2^+ + H_2$	1.0	0.68	<0.1,[e] 1.0[i]	5.8[h]

[a]Observed rate coefficient in units of 10^{-10} cm^3 s^{-1}. The Langevin capture rate coefficient for all reactions in this table is 1.9×10^{-9} cm^3 s^{-1}.
[b]Rate coefficients determined in other laboratories in units of 10^{-10} cm^3 s^{-1}.
[c]Reference 21.
[d]Reference 3.
[e]Reference 13.
[f]Reference 7.
[g]No reaction observed ($k<1\times10^{-11}$ cm^3 s^{-1}).
[h]See text.
[i]Reference 31.

between CS_2^+ and H_2 ($k<5\times10^{-13}$ cm^3 s^{-1}), but a moderately fast reaction (10) with H atoms was observed in which the product ion is HCS^+ and $k=2.8\times10^{-10}$ cm^3 s^{-1},

$$CS_2^+(^1\Sigma)+H(^2S)\rightarrow HCS^+(^1A)+S(^3P). \quad (10)$$

Spin is not conserved for ground state products and the reaction is not sufficiently exothermic ($\Delta H=-12$ kJ mol^{-1}) to produce metastable $S(^1D)$ atoms.

F. $CN^+ + H_2/H$

Previously it has been observed that CN^+ reacts with H_2 (Ref. 25) at the collision rate ($k_L=1.5\times10^{-9}$ cm^3 s^{-1}), and that the product ions are the two isomers HCN^+ and HNC^+ in equal proportion.[26] Both of these isomers then undergo further reaction with H_2 to produce $HCNH^+$. Therefore, the method of analysis used to obtain the H/H_2 ratio and hence to obtain the rate coefficient for reaction (11) required that we monitored both HCN^+/HNC^+ and their product ion $HCNH^+$. Again, to determine the reaction products we used D atoms (using a 10% deuterium helium mixture). The only ion product observed in the reaction between CN^+ and D, analogous to reaction (11), was D^+, this being the only exothermic channel. The exothermicity arises from the difference in ionization potentials, viz., IP(CN)−IP(H)=47.4 kJ mol^{-1},

$$CN^+(^1\Sigma)+H(^2S)\rightarrow H^+(^1S)+CN(^2\Sigma^+). \quad (11)$$

This reaction is fast with $k=6.4\times10^{-10}$ cm^3 s^{-1} and spin is conserved. It has been suggested previously[13] that D^+ can be produced in the reaction between $HCN^+ + D$. We did not observe any D^+ arising from this reaction.

G. $C_2N_2^+ + H_2/H$

No previous studies have been reported for the reaction of $C_2N_2^+$ with H atoms. Reaction (12) with H_2 occurs close to the collision rate ($k=8.8\times10^{-10}$ cm^3 s^{-1}) with H atom abstraction being the only channel, producing $HC_2N_2^+$, in agreement with an earlier measurement,[27]

$$C_2N_2^+ + H_2\rightarrow HC_2N_2^+ + H. \quad (12)$$

Two product channels were observed in the $C_2N_2^+ + H$ reaction (13) which has a total rate coefficient of $k=6.2\times10^{-10}$ cm^3 s^{-1},

$$C_2N_2^+(^2\Sigma)+H(^2S) \xrightarrow{0.80} HNC^+(^2\Sigma)+CN(^2\Sigma^+) \quad (13a)$$

$$\xrightarrow{0.20} C_2H^+(^1\Sigma)+N_2(^1\Sigma_g^+). \quad (13b)$$

If the multiplicities of all ground state reactants and products in reaction (13a) are doublets, then the reaction conserves spin. The thermodynamic data in Lias *et al.*[28] suggests that reaction (13a) is endothermic by 27 kJ mol^{-1}. However, more recent data suggests that the reaction is exothermic by 12 kJ mol^{-1} in the first instance.[29,30] This value arises from the observation that charge transfer does not occur between HNC^+ and O_2 which constrains the heat of formation of HNC^+ as $\Delta H_f^0(HNC^+)\leq1373$ kJ mol^{-1}.[29] Also very recently Ferguson has estimated $\Delta H_f^0(HNC^+)=1368$ kJ mol^{-1} from an Arrhenius plot of the slightly endothermic reaction between $HNC^+ + CO$.[30] Energy constraints dictate that only the lower energy isomer HNC^+ is accessible to thermal energy reactants in reaction (13a). Further in this reaction, end attack by H followed by C–C bond cleavage leads to HNC^+ rather than HCN^+.

H. $C_2H_3^+ + H$

Two previous room temperature studies of this reaction have been attempted. In one study[13] no reaction was observed, and in the other a rate coefficient of $k=1.0\times10^{-10}$ cm^3 s^{-1} (Ref. 31) was reported,

$$C_2H_3^+ + H\rightarrow C_2H_2^+ + H_2. \quad (14)$$

The latter result has been applied to the evaluation of the energetics of the reaction between $C_2H_2^+ + H_2$ by Smith *et al.*,[32] this reaction being a critical step in the synthesis of hydrocarbons in interstellar clouds.[33] Our rate coefficient for this reaction, although not drastically different from that of Hansel *et al.*[31] (in view of the uncertainty in the determination of atom densities), is sufficiently different to be reported. The mean of five determinations is $k=6.8\times10^{-11}$ cm^3 s^{-1}. The rate coefficient for the "forward" direction of the reaction,

$$C_2H_2^+ + H_2 \rightleftharpoons C_2H_3^+ + H \quad (15)$$

measured by Smith *et al.*[32] is $k=2.6\times10^{-12}$ cm^3 s^{-1} at 300 K. When this is combined with the present rate coefficient for (the "reverse") reaction (14), it yields an equilibrium constant for reaction (15) of $K=3.8\times10^{-2}$ and hence $\Delta G^\circ=8.16$ kJ mol^{-1} for the reactions at 300 K. Assuming a value for $\Delta S^\circ=-7.9$ J K^{-1} mol^{-1} as calculated from total partition functions,[32] then reaction (15) is endothermic by $\Delta H^\circ=+5.8$ kJ mol^{-1}. Hence this reaction cannot proceed at a significant rate in cold interstellar clouds, which is in agreement with earlier conclusions.[32,33]

All the reactions with H_2 included in this study are summarized in Table I, and those with H are given in Table II.

IV. CONCLUDING REMARKS

It is interesting to note that all ion-H atom reactions measured in this work have rate coefficients substantially less than the Langevin capture rate. In several reactions the smaller observed rate coefficients are a consequence of spin statistics. The same may be true of other reactions (e.g., $SO_2^+ + H$) but the potential surfaces of such reactions need to be better defined before any definite conclusions can be drawn.

Molecular and atomic hydrogen, the two neutral reactants of this study, are very abundant species in the universe. The chemistry summarized in Tables I and II for these species has some relevance to extraterrestrial chemistry. The reactions of CO^+ and CO_2^+ with H_2 have been the subject of many earlier studies. The two isomeric product ions observed in the reaction of $CO^+ + H_2$, viz., HOC^+ and HCO^+ have both been unambiguously identified in the interstellar

medium with HOC^+ being confirmed quite recently.[38] This confirmation of interstellar HOC^+ poses the difficulty of rationalizing the laboratory observation of a rapid reaction between HOC^+ and H_2 (Ref. 39) with the interstellar observation. This apparent conflict has now been satisfactorily resolved by Herbst and Woon[41] who have shown, using theoretical considerations, that the rate coefficient for $HOC^+ + H_2$ drops to $<1\times10^{-10}$ $cm^3.s^{-1}$ at temperatures under 100 K. Of the remaining reactant ions in Table I, CN^+ and $C_2N_2^+$ have rapid reactions with H_2 and thus they should have low concentrations in dense interstellar clouds. In contrast NO_2^+, SO_2^+, and CS_2^+ may reach appreciable number densities due to their unreactivity with H_2.

Only three of the ion–H atom reactions shown in Table II have been measured previously. The reaction with CO^+ proceeds exclusively by charge transfer to yield $H^+ + CO$ which is the only exothermic channel available. In contrast, the reaction with CO_2^+ proceeds, as far as we can tell, by dissociative H atom exchange even though the charge transfer channel is exothermic. A series of molecules and ions containing a C–S bond have been observed in the interstellar medium (e.g., CS, HCS^+, OCS, H_2CS, and C_3S).[33] Presumably CS_2 is also present but it has not been detected due to its lack of a permanent dipole moment. The efficient reaction between CS_2^+ and H yields HCS^+ as the product ion which is an observed interstellar ion.[33] The detection of HCS^+ in the interstellar medium is consistent with its unreactivity with H_2. The reactions of CN^+ and $C_2N_2^+$ with H atoms are relevant to the ion chemistry of Titan's atmosphere[41] as well as the chemistry of interstellar clouds.

ACKNOWLEDGMENTS

We thank Leon Phillips and Bryce Williamson for helpful discussions and the Marsden Fund for financial support. P.S. and D.S. thank the Department of Chemistry at the University of Canterbury for financial support which allowed them to spend an enjoyable and scientifically profitable few weeks in New Zealand.

[1] V. G. Anicich, J. Phys. Chem. Ref. Data **22**, 1469 (1993).
[2] F. C. Fehsenfeld and E. E. Ferguson, Planet. Space Sci. **20**, 295 (1972).
[3] F. C. Fehsenfeld and E. E. Ferguson, J. Geophys. Res. **76**, 8453 (1971).
[4] F. C. Fehsenfeld, in *Interaction Between Ions and Molecules*, edited by P. Ausloos (Plenum, New York, 1975), p. 387.
[5] F. C. Fehsenfeld, C. J. Howard, and E. E. Ferguson, J. Chem. Phys. **58**, 5841 (1973).
[6] C. J. Howard, F. C. Fehsenfeld, and M. McFarland, J. Chem. Phys. **60**, 5086 (1974).
[7] P. Tosi, S. Iannotta, D. Bassi, H. Villinger, W. Dobler, and W. Lindinger, J. Chem. Phys. **80**, 1905 (1984).
[8] D. Smith and N. G. Adams, J. Phys. B **20**, 4903 (1987).
[9] N. G. Adams and D. Smith, Astrophys. J. **294**, L63 (1985).
[10] M. Sablier and C. Rolando, Mass Spectrom. Rev. **12**, 285 (1993).
[11] S. Petrie, G. Javahery, and D. K. Bohme, J. Am. Chem. Soc. **114**, 9205 (1992).
[12] M. J. McEwan, in *Advances in Gas Phase Ion Chemistry*, edited by N. G. Adams and L. M. Babcock (JAI, Greenwich, 1992), Vol. 1, p. 1.
[13] Z. Karpas, V. G. Anicich, and W. T. Huntress, J. Chem. Phys. **70**, 2877 (1979).
[14] F. C. Fehsenfeld, A. L. Schmeltekopf, and E. E. Ferguson, J. Chem. Phys. **46**, 2802 (1967).
[15] N. W. Copp, M. Hamdan, J. D. C. Jones, K. Birkinshaw, and N. D. Twiddy, Chem. Phys. Lett. **88**, 508 (1982).
[16] D. L. Smith and J. H. Futrell, Int. J. Mass Spectrom. Ion Phys. **10**, 405 (1972).
[17] T. McAllister, Int. J. Mass Spectrom. Ion Phys. **9**, 127 (1972).
[18] K. R. Ryan, J. Chem. Phys. **61**, 1559 (1974).
[19] T. McAllister and P. Pitman, Int. J. Mass Spectrom. Ion Phys. **19**, 423 (1976).
[20] C. G. Freeman, J. S. Knight, J. G. Love, and M. J. McEwan, Int. J. Mass Spectrom. Ion Proc. **80**, 255 (1987).
[21] W. Federer, H. Villinger, F. Howorka, W. Lindinger, P. Tosi, D. Bassi, and E. Ferguson, Phys. Rev. Lett. **52**, 2084 (1984).
[22] E. Ferguson, Chem. Phys. Lett. **99**, 89 (1983).
[23] P. P. Bemand and M. A. A. Clyne, J. Chem. Soc. Faraday Trans. II **73**, 394 (1977).
[24] F. C. Fehsenfeld and E. E. Ferguson, Planet. Space Sci. **20**, 295 (1972).
[25] A. B. Raksit, H. I. Schiff, and D. K. Bohme, Int. J. Mass Spectrom. Ion Proc. **56**, 321 (1984).
[26] S. Petrie, C. G. Freeman, M. J. McEwan, and E. E. Ferguson, Mon. Not. R. Astron. Soc. **248**, 272 (1991).
[27] S. A. H. Petrie, C. G. Freeman, M. J. McEwan, and M. Meot-Ner, Int. J. Mass Spectrom. Ion Proc. **90**, 241 (1989).
[28] S. G. Lias, J. E. Bartmess, J. F. Liebman, J. L. Holmes, R. D. Levin, and W. G. Mallard, J. Phys. Chem. Ref. Data **17**, Suppl. 1 (1988).
[29] S. Petrie, C. G. Freeman, M. Meot Ner, M. J. McEwan, and E. E. Ferguson, J. Am. Chem. Soc. **112**, 7121 (1990).
[30] E. Ferguson (private communication, 1996).
[31] A. Hansel, R. Richter, W. Lindinger, and E. E. Ferguson, Int. J. Mass Spectrom. Ion Proc. **94**, 251 (1989).
[32] D. Smith, J. Glosik, V. Skalsky, P. Spanel, and W. Lindinger, Int. J. Mass Spectrom. Ion Proc. **129**, 145 (1993).
[33] D. Smith, Chem. Rev. **92**, 1473 (1992).
[34] F. C. Fehsenfeld, A. L. Schmeltekopf, and E. E. Ferguson, J. Chem. Phys. **46**, 2802 (1967).
[35] J. K. Kim, L. P. Theard, and W. T. Huntress, J. Chem. Phys. **62**, 45 (1975).
[36] N. G. Adams, D. Smith, and D. Grief, Int. J. Mass Spectrom. Ion Phys. **26**, 405 (1978).
[37] D. L. Smith and J. H. Futrell, Int. J. Mass Spectrom. Ion Phys. **10**, 405 (1972/73).
[38] L. M. Ziurys and A. P. Apponi, Astrophys. J. **455**, L73 (1995).
[39] C. G. Freeman and M. J. McEwan, in *Chemistry and Spectroscopy of Interstellar Molecules*, edited by D. K. Bohme, E. Herbst, N. Kaifu, and S. Saito (University of Tokyo, Tokyo, Japan, 1992), p. 187.
[40] E. Herbst and D. E. Woon, Astrophys. J. **463**, L113 (1996).
[41] V. G. Anicich and M. J. McEwan, Planet. Space Sci. (submitted).

J. Phys. Chem. A **1997**, *101*, 4973−4978

$C_mH_n^+$ Reactions with H and H_2: An Experimental Study

Graham B. I. Scott, David A. Fairley, Colin G. Freeman, and Murray J. McEwan*

Department of Chemistry, University of Canterbury, Christchurch, New Zealand

Nigel G. Adams and Lucia M. Babcock

Department of Chemistry, University of Georgia, Athens, Georgia 30602

Received: February 25, 1997; In Final Form: May 1, 1997[⊗]

We report measurements of the reactions of a number of hydrocarbon ions with atomic and molecular hydrogen made using a selected ion flow tube (SIFT) operating at room temperature. Results, including branching ratios and rate coefficients, are reported for $C_mH_n^+$ ions ($m = 2-6$, $n = 0-9$). Highly unsaturated hydrocarbon ions undergo mainly H atom abstraction reactions with H_2 forming $C_mH_{n+1}^+ + H$ products. More saturated ions are unreactive. Two types of reactions occur for H atoms: H atom transfer to give $C_mH_{n-1}^+ + H_2$ (if exothermic) and association (to give $C_mH_{n+1}^+$).

Introduction

The most ubiquitous and abundant species in the universe are molecular and atomic hydrogen. The enormous clouds of gas and dust that exist in the interstellar medium are composed largely of H_2 and H. Radioastronomy techniques have discovered significant densities of hydrocarbon molecules and ions in these interstellar clouds,[1] and models have been constructed showing how the chemistry taking place within the clouds can lead to the various hydrocarbon species observed.[2] Moreover, the precursor ion in many synthetic schemes, H_3^+, has recently been detected for the first time.[3] The physical conditions existing within a typical dense cloud (viz. low temperatures 10−50 K) and low densities (10^3-10^6 particles cm^{-3}) mean that conventional chemical processes are very slow.[2] Chemical models, involving a mixture of ion−molecule, radical−radical, and some heterogeneous reactions occurring on grain surfaces have been developed, and these provide reasonable estimates of the observed abundances for many species.[2,4] These models use results from experimental studies as input. Although many laboratory investigations of ions reacting with molecular hydrogen relevant to interstellar cloud chemistry have been made, the same is not true for ion−H atom processes. Atomic hydrogen is not an easy reactant to monitor in the laboratory, and this is the main reason reported ion reactions with H_2 outnumber those with H by about a factor of 20.[5]

In addition to the relevance of ion−H_2, H chemistry to interstellar clouds, there is a more fundamental aspect. Reactions of hydrocarbon ions with H atoms and H_2 provide information on ion stabilities and on the mode of hydrogen addition to hydrocarbon species.

Efforts have been made in the past by different groups to overcome the problems of monitoring H-atom densities with by far the majority of attempts using flow-tube techniques.[6] Early ion−H atom studies applied conventional methods from neutral−H atom studies,[7,8] but later, methods unique to ion−H atom reactions were developed. One such technique utilizes the reaction of CO_2^+ with a mixture of H_2 and H.[9,10] We recently compared this method for determining H atom concentrations with those using other systems (e.g., CO^+, H_2/H; $C_2N_2^+$, H_2/H; CN^+, H_2/H) and obtained good agreement between the different systems.[10] In the present study, we apply the CO_2^+, H_2/H technique to examine the reactions of a series of hydrocarbon ions, $C_mH_n^+$ ($m = 2-6$; $n = 0-9$) with H atoms. As part of the study we have also measured the reactions of the same ions with H_2. The ions were chosen on the basis of their importance to gas-phase molecular synthesis in interstellar clouds. Primarily, although not exclusively, we have concentrated on reactions that have not been previously studied. In several cases we have repeated work performed in other laboratories to verify the accuracy of our methods.

Experimental Section

The details of the selected ion flow tube (SIFT) at the University of Canterbury that was used in this work have been described elsewhere.[11] Only a brief summary of that part of the equipment pertinent to the present study will be given here. The $C_mH_n^+$ reactant ions are generated by electron impact on an appropriate hydrocarbon gas and, after mass selection by the upstream quadrupole mass filter, are injected into the flow tube. H atoms are generated in a quartz side tube by a microwave discharge of either a 10% mixture of hydrogen in helium or, alternatively, pure hydrogen as is discussed elsewhere.[10] A typical degree of dissociation of the He/H_2 mixture is 25− 40%. The reactions of CO_2^+ with H_2 and H

$$CO_2^+ + H_2 \rightarrow HCO_2^+ + H \quad (1)$$

$$CO_2^+ + H \rightarrow HCO^+ + O \quad (2a)$$

$$\rightarrow H^+ + CO_2 \quad (2b)$$

are used to calibrate the H atom number density within the flow tube as described by Tosi et al.[9] and also in our earlier paper.[10] As the extent of dissociation of H_2 in the microwave discharge is always less than 100%, a mixture of H_2 and H enters the flow tube. It is therefore necessary in each case to establish the outcome of the reaction of the $C_mH_n^+$ ion with H_2 first (microwave discharge off) before examining its reactivity with H atoms (microwave discharge on). Small fluxes of minor species formed in the discharge (e.g. H^+, H_2^+, H_3^+), metastable atoms (e.g., He 2 ^3S), and electrons are produced concomitantly with H atoms. Ion−electron recombination and surface neutralization reduce the concentration of charged species to an insignificant level compared with the reacting molecular and

[⊗] Abstract published in *Advance ACS Abstracts*, June 15, 1997.

S1089-5639(97)00694-4 CCC: $14.00

TABLE 1: Reaction of the Designated $C_mH_n^-$ Ion with H_2

reactant ion	products	branching ratio	k^a	$k_{prev}{}^b$	$-\Delta H°$/(kJ mol^{-1})^c
C_2^+	$C_2H^+ + H$	1.0	11	11,[d] 14,[e] 12[f]	88
C_2H^+	$C_2H_2^+ + H$	1.0	11	7.8,[d] 17[e]	149
$C_2H_3^+$	NR		<0.05	<0.01,[g] <0.001[h]	
$HCCCH_2^+$	NR		<0.05	<0.05[i]	
c-$C_3H_3^+$	NR		<0.05	<0.05[i]	
$H_2CCCH_2^+$	NR		<0.05	<0.001[j]	
$HCCCH_3^+$	NR		<0.005	<0.001[j]	
$C_3H_5^+$	NR		<0.005	NR[k]	
$C_3H_7^+$	NR		<0.05	NR[k]	
C_4H^+	$C_4H_2^+ + H$	1.0	1.8	<0.001,[k] 1.5,[l] 1.8[f]	~137[m]
$C_4H_2^+$	NR		<0.04		
$C_4H_3^+$	NR		<0.02		
$C_4H_4^+$	NR		<0.03		
$C_4H_5^+$	NR		<0.03		
$C_4H_6^+$	NR		<0.04		
$C_4H_8^+$	NR		<0.005		
$C_4H_9^+$	NR		<0.005		
ac-$C_6H_4^+$	NR		<0.005		
c-$C_6H_4^+$	NR		<0.03		
ac-$C_6H_5^+$	NR		<0.01	<0.01[n]	
c-$C_6H_5^+$	$C_6H_7^+$	1.0	0.38[o]	0.15,[p] 0.5[l,n]	273
c-$C_6H_6^+$	NR		<0.05	<0.01[n]	

[a] Observed rate coefficient in units of 10^{-10} cm^3 s^{-1}. The Langevin capture rate coefficient for all reactions in this table is 1.5×10^{-9} cm^3 s^{-1}. [b] Rate coefficients determined in other laboratories in units of 10^{-10} cm^3 s^{-1}. [c] The listed exothermicities are taken from ref 12. [d] Reference 13 [e] Reference 14. [f] Reference 15. [g] Reference 16. [h] Reference 17. No bimolecular reaction was observed, but a limit to termolecular association of $k \lesssim 1 \times 10^{-30}$ cm^6 s^{-1} at 80 K was reported. [i] Reference 18. [j] Reference 17. Results are measured at 80 K. Isomeric form of $C_3H_4^+$ not specified. No bimolecular reaction was observed, but a limit to termolecular association of $k < 1 \times 10^{-30}$ cm^6 s^{-1} was reported. [k] Reference 17. A limit to termolecular association of $k < 1 \times 10^{-30}$ cm^6 s^{-1} at 80 K was reported. [l] Reference 19. [m] Exothermicity from refs 12 and 20. [n] Reference 21. [o] Pseudobimolecular reaction. The rate constant shown is for a flow tube pressure of 0.30 Torr. The termolecular rate for the three body association process is estimated as $\geq 3.9 \times 10^{-27}$ cm^6 s^{-1}. [p] Reference 22.

atomic hydrogen. He 2 ^{3}S atoms are not so easily removed, and although the flux of such metastables is several orders of magnitude below that of H and H_2, they can be effectively excluded only by discharging pure hydrogen.

All reactions reported here were carried out at 300 ± 5 K and at a flow tube pressure of 0.30−0.35 Torr. We estimate the uncertainty in the rate coefficients reported in this work for H atoms as ±30% (unless specified otherwise) where the increase in uncertainty over the ±15% usually specified for SIFT measurements arises from the uncertainties associated with the determination of H-atom densities.

Results and Discussion

A summary of all the results obtained in this work for $C_mH_n^+$ reactions are presented in Table 1 for H_2 and Table 2 for H atoms. Previous measurements, where they exist, are indicated in column 5 of each table.

C_2^+ and C_2H^+. Each of these ions was generated by electron impact on a He/C_2H_2 mixture. In both cases the determination of the rate coefficient with H was hampered by a rapid reaction with H_2:

$$C_2^+ + H_2 \rightarrow C_2H^+ + H \qquad (3)$$

$$k = 1.1 \times 10^{-9} \text{ cm}^3 \text{ s}^{-1}$$

$$C_2H^+ + H_2 \rightarrow C_2H_2^+ + H \qquad (4)$$

$$k = 1.1 \times 10^{-9} \text{ cm}^3 \text{ s}^{-1}$$

The apparent rate coefficients for reactions 3 and 4 decreased with the discharge on, to rate coefficient values equivalent to that expected for diluting H_2 with a nonreacting gas in the reaction mixture at the same level as H atoms. No new products appeared, and we thus conclude that no reaction with H occurs at measurable rates for either ion. These results are consistent with the fact that no exothermic binary channels are available for either reaction.

$C_2H_3^+$. The $C_2H_3^+$ ion in this study was generated by a sequential process from $C_2H_5^+$ which was produced by electron impact on C_2H_5Br. $C_2H_5^+$ was mass selected and injected into the flow tube at just sufficient energy for fragmentation to $C_2H_3^+$ to occur by collision-induced dissociation with the helium bath gas during injection. No reaction was found with H_2 but $C_2H_3^+$ does undergo reaction with H:

$$C_2H_3^+ + H \rightarrow C_2H_2^+ + H_2 \qquad (5)$$

$$k = 6.8 \times 10^{-11} \text{ cm}^3 \text{ s}^{-1}$$

The significance of this measurement to establishing the endothermicity of the reverse of reaction 5 has been commented on elsewhere.[10,24,25]

$C_3H_3^+$. There are two low-energy forms of $C_3H_3^+$: the acyclic propargyl ion, $HCCCH_2^+$, and the cyclopropenylium ion, c-$C_3H_3^+$. Mixtures of these ions (typically 60% acyclic, 40% cyclic) are readily made from reactions ensuing after initial electron impact on C_2H_4. The primary ion, $C_2H_4^+$, reacts with C_2H_4 in a high-pressure ion source producing $C_3H_5^+$, which fragments after mass selection into the two isomeric forms of $C_3H_3^+$ during the injection process. We have discussed previously methods based on differing reactivities for distinguishing between the two isomers of $C_3H_3^+$:[18] in all cases $HCCCH_2^+$ is more reactive than c-$C_3H_3^+$. In the present study neither ion was found to be reactive with H_2. Similarly, no reaction was found with H atoms despite each isomeric ion having an apparent exothermic binary reaction channel available[12] leading to their respective cyclic and acyclic $C_3H_2^+$ isomers (+H_2). However extensive ab initio calculations of the $C_3H_2^+$ and $C_3H_3^+$ surface[26,27] have shown both H-atom-transfer reactions to be endothermic which is in keeping with our observations. The endothermicity of the ac-$C_3H_3^+$/H atom-transfer reaction is calculated as only 8 kJ mol^{-1}.[26]

TABLE 2: Reactions of the Designated $C_mH_n^+$ Ion with H

reactant ion	products	branching ratio	k^a	k_{prev}^b	$-\Delta H°$/(kJ mol^{-1})^c
C_2^+	NR		<1.0		
C_2H^+	NR		<1.0		
$C_2H_3^+$	$C_2H_2^+ + H_2$	1.0	0.68	<0.1;[d] 1.0[e]	5.8[f]
$HCCCH_2^+$	NR		<0.03		
c-$C_3H_3^+$	NR		<0.03		
$H_2CCCH_2^+$	$C_3H_3^+ + H_2$	1.0	1.7		164[g]
$HCCCH_3^+$	$C_3H_3^+ + H_2$	1.0	3.0		224[g]
$C_3H_5^+$	$C_3H_6^+$	1.0	1.6[h,i]		206[j]
$C_3H_7^+$	$C_3H_6^+ + H_2$	1.0	0.32		59[k]
C_4H^+	$C_4H_2^+$	1.0	~5.8[h,l]		~574[m]
$C_4H_2^+$	$C_4H_3^+$	1.0	2.6[h,n]		~420
$C_4H_3^+$	$C_4H_4^+$	1.0	~0.5[h,o]		~206[s]
$C_4H_5^+$	NR		<0.4		
$C_4H_6^+$	$C_2H_3^+ + C_2H_4$	~0.15			38[p]
	$C_2H_5^+ + C_2H_2$	~0.65	1.9		73[p]
	$C_4H_5^+ + H_2$	~0.20			174[q]
$C_4H_8^+$	$C_4H_7^+ + H_2$	1.0	1.1		193[r]
$C_4H_9^+$	NR		<0.2		
ac-$C_6H_4^+$	NR		<0.05		
c-$C_6H_4^+$	$C_6H_5^+$	1.0	0.33[h,s]		400[t]
ac-$C_6H_5^+$	NR		<0.05	0.05[u]	
c-$C_6H_5^+$	NR		<0.1	0.01[u]	
c-$C_6H_6^+$	$C_6H_5^+ + H_2$	~0.35			67[v]
			2.1[w]	2.5[u]	
	$C_6H_7^+$	~0.65			340[x]

[a] Observed rate coefficient in units of 10^{-10} cm^3 s^{-1}. The Langevin capture rate coefficient for all reactions in this table is 19×10^{-10} cm^3 s^{-1}. [b] Rate coefficients determined in other laboratories in units of 10^{-10} cm^3 s^{-1}. [c] Unless specified otherwise, the listed exothermicities are taken from ref 12. [d] Reference 23. [e] Reference 24. [f] See reference 10. [g] Thermochemistry for acyclic isomers. [h] Pseudobimolecular reaction. The rate coefficient shown is for a flow tube pressure of 0.30 Torr. [i] The termolecular rate for the three body association process is estimated as $\geq 1.6 \times 10^{-26}$ cm^6 s^{-1}. [j] Thermochemistry for lowest energy acyclic isomers. [k] This value corresponds to the iso $C_3H_7^+$ structure converted to the acyclic C_3H_6 species. [l] The termolecular rate for the three-body association process is estimated as $\geq 6 \times 10^{-26}$ cm^6 s^{-1}. [m] References 12 and 20. [n] The termolecular rate for the three-body association process is estimated as $\geq 2.7 \times 10^{-26}$ cm^6 s^{-1}. [o] The termolecular rate for the three body association process is estimated as $\geq 5.1 \times 10^{-27}$ cm^6 s^{-1}. [p] Thermochemistry based on (*E*)-1,3-butadiene ion. [q] Thermochemistry as for (*p*) and CH_2=CCH=CH_2. [r] Thermochemistry based on (*E*)-2-$C_4H_8^+$ and $CH_3CCHCH_3^+$. [s] The termolecular rate for the three body association process is estimated as $\geq 3.4 \times 10^{-27}$ cm^6 s^{-1}. [t] Thermochemistry based on benzyne ion and phenyl radical ion. [u] Reference 21. [v] Thermochemistry based on benzene ion and phenyl radical ion. [w] The termolecular rate for the three body association channel between c-$C_6H_6^+$ + H is estimated as $\geq 1.4 \times 10^{-26}$ cm^6 s^{-1}. [x] Thermochemistry based on benzene ion and protonated benzene ion.

$H_2CCCH_2^+$ and $HCCCH_3^+$. The ions $H_2CCCH_2^+$ and $HCCCH_3^+$ were made by electron impact on their parent precursors, allene and propyne, respectively. No reaction was observed with H_2 for either ion. Both ions underwent efficient H atom transfer with H:

$$H_2CCCH_2^+ + H \rightarrow ac\text{-}C_3H_3^+ + H_2 \quad (6)$$

$$k = 1.7 \times 10^{-10}\ cm^3\ s^{-1}$$

$$HCCCH_3^+ + H \rightarrow ac\text{-}C_3H_3^+ + H_2 \quad (7)$$

$$k = 3.0 \times 10^{-10}\ cm^3\ s^{-1}$$

The $C_3H_3^+$ products of reactions 6 and 7 are shown as ac-$C_3H_3^+$ (acyclic $C_3H_3^+$) on the basis that the precursor ions are acyclic, although this was not confirmed by experiment.

$C_3H_5^+$. The $C_3H_5^+$ ion was generated by electron impact on C_2H_4 in a high pressure ion source. $C_3H_5^+$ is also the major product ion from the reaction between $C_2H_4^+$ and C_2H_4 as discussed previously for $C_3H_3^+$. After mass selection, $C_3H_5^+$ was injected into the flow tube (using sufficiently low energies to prevent fragmentation into $C_3H_3^+$). No reaction was observed with H_2 ($k < 5 \times 10^{-13}$ cm^3 s^{-1}), but an observable reaction did occur with H atoms, the major channel resulting from an association reaction:

$$C_3H_5^+ + H \rightarrow C_3H_6^+ \quad (8)$$

$$k = 1.6 \times 10^{-10}\ cm^3\ s^{-1}$$

A curved semilogarithmic decay of Ln($C_3H_5^+$) count versus H-atom flow indicates at least two $C_3H_5^+$ isomers may be present. The rate coefficient shown here is that for the more reactive isomer. No reaction was observed for the less reactive isomers.

$C_3H_7^+$. This ion was generated by electron impact on either 1-bromopropane or 2-bromopropane, C_3H_7Br. There was no difference in the behavior of the $C_3H_7^+$ arising from either precursor with H_2 and H. No reaction was found between $C_3H_7^+$ and H_2, which is consistent with the lack of a bimolecular exothermic channel. The slow reaction with H atoms proceeded via H atom transfer:

$$C_3H_7^+ + H \rightarrow C_3H_6^+ + H_2 \quad (9)$$

$$k = 3.2 \times 10^{-11}\ cm^3\ s^{-1}$$

The fact that the H-atom-transfer reaction appears independent of ion structure is an interesting result. If the $C_3H_7^+$ ions generated from 1- and 2-bromopropane retain the structural distinction of their precursor, then the slow rate coefficient observed for each ion may suggest a similar kinetic barrier. Alternatively, the $C_3H_7^+$ ions from the two precursors may have the same structure. Energies and geometries of the $C_3H_6^+$, $C_3H_7^+$ and $C_3H_8^+$ ions have been characterized using quantum chemistry ab initio methods.[28-30] A study of the [$C_3H_7^+ \cdots$H] transition states has not to our knowledge been undertaken and would be valuable in clarifying the details of reaction 9.

C_4H^+, $C_4H_2^+$, $C_4H_3^+$. All three ions were produced by

electron impact on acetylene in a high-pressure ion source. $C_4H_2^+$ and $C_4H_3^+$ are the primary product ions from the reaction of $C_2H_2^+$ on C_2H_2, and C_4H^+ is the product ion of the reaction between C_2^+ and C_2H_2.

C_4H^+ undergoes an H-atom abstraction with H_2 at about 10% of the collision rate:

$$C_4H^+ + H_2 \rightarrow C_4H_2^+ + H \quad (10)$$

$$k = 1.8 \times 10^{-10}\ \text{cm}^3\ \text{s}^{-1}$$

and also exhibits an efficient association reaction with H atoms:

$$C_4H^+ + H \rightarrow C_4H_2^+ \quad (11)$$

$$k \sim 5.8 \times 10^{-10}\ \text{cm}^3\ \text{s}^{-1}$$

The higher uncertainty in the rate coefficient for reaction 11 (±50%) is a consequence of the presence of both H_2 and H atoms together in the reaction mixture when the microwave discharge is on. C_4H^+ produces the same product ion with H_2 (H-atom abstraction) as with H (association). The observation of reaction 10 allows us to place an estimate for $\Delta H°_f(C_4H^+) \geq 1640$ kJ mol^{-1} which is consistent with the best theoretical estimate of $\Delta H°_f(C_4H^+) = 1779$ kJ mol^{-1}.[20] To separate the C_4H^+ loss via H_2 from the H atom loss, it was necessary to computer-model the observed total decay of C_4H^+ using the rate coefficient for reaction 10 (measured with the microwave discharge off) as input.

$C_4H_2^+$ and $C_4H_3^+$ do not undergo reaction with H_2 but in both cases show association with H atoms (reactions 12 and 13) with pseudobimolecular rate coefficients of 2.6×10^{-10} cm^3 s^{-1} and 5×10^{-11} cm^3 s^{-1}, respectively:

$$C_4H_2^+ + H \rightarrow C_4H_3^+ \quad (12)$$

$$k = 2.6 \times 10^{-10}\ \text{cm}^3\ \text{s}^{-1}$$

$$C_4H_3^+ + H \rightarrow C_4H_4^+ \quad (13)$$

$$k = (5 \pm 3) \times 10^{-11}\ \text{cm}^3\ \text{s}^{-1}$$

The higher uncertainty in the rate coefficient for reaction 13 stems from a small contribution to $C_4H_3^+$ from reaction 12. The decrease in association rate with number of H atoms in the series $C_4H_n^+$ ($n = 1-3$) is possibly a consequence of the decreasing well depth of the $(C_4H_{n+1}^+)^*$ collision complex as n increases. If this occurs, the complex lifetime is shortened thus allowing less time for complex stabilization. Assuming the most stable structures for the acyclic ions $C_4H_n^+$ ($n = 1-4$) the well depths are[12,20] reaction 11 (≥574 kJ mol^{-1}); reaction 12; ~420 kJ mol^{-1}, and reaction 13 (~205 kJ mol^{-1}).

$C_4H_5^+$, $C_4H_6^+$. These ions were generated by electron impact on 1,3-butadiene and injected into the flow tube after mass selection, in company with lesser amounts of $C_4H_7^+$. Neither $C_4H_5^+$ nor $C_4H_6^+$ undergo reaction with H_2. Although $C_4H_5^+$ is produced in the fast reaction of $C_4H_6^+ + H$, it does not appear to react with atomic hydrogen, and we assess an upper limit for its reaction as $k < 4 \times 10^{-11}$ cm^3 s^{-1}. The fast reaction of $C_4H_6^+$ with H atoms yields three products including a 20% H-atom-transfer channel:

$$C_4H_6^+ + H \rightarrow C_2H_3^+ + C_2H_4\ (\sim 0.15) \quad (14a)$$

$$\rightarrow C_2H_5^+ + C_2H_2\ (\sim 0.65) \quad (14b)$$

$$\rightarrow C_4H_5^+ + H_2\ (\sim 0.20) \quad (14c)$$

$$k = 1.9 \times 10^{-10}\ \text{cm}^3\ \text{s}^{-1}$$

The fact that this reaction is substantially different in terms of dissociative reaction pathways, from all other $C_mH_n^+/H$ reactions studied thus far indicates a different reaction mechanism is in operation. Insertion of H into $C_4H_6^+$ to form the $(C_4H_7^+)^*$ collision complex results in rapid dissociation of the complex before stabilization can occur. The ~360 kJ mol^{-1} of available excitation energy above the $C_4H_7^+$ well is sufficient to cause fragmentation at the C2 position of a protonated 1,3-butadiene type ion, $CH_3CHCH{=}CH_2^+$, giving rise to the two fragmentation channels observed.

$C_4H_8^+$, $C_4H_9^+$. These ions were each generated by electron impact on 2-butene. Neither ion was reactive with H_2. $C_4H_9^+$ was also unreactive with H atoms ($k < 2 \times 10^{-11}$ cm^3 s^{-1}), but $C_4H_8^+$ exhibited H-atom transfer:

$$C_4H_8^+ + H \rightarrow C_4H_7^+ + H_2 \quad (15)$$

$$k = 1.1 \times 10^{-10}\ \text{cm}^3\ \text{s}^{-1}$$

$C_6H_4^+$, $C_6H_5^+$, $C_6H_6^+$. These $C_6H_n^+$ ions were generated either by electron impact on benzene or following electron impact on C_2H_2 in a high-pressure source ($C_6H_4^+$, $C_6H_5^+$). With the latter method, $C_4H_2^+$ and $C_4H_3^+$ are produced from C_2H_2 as described previously and injected into the flow tube. C_2H_2 is then added at the first inlet port, forming $C_6H_4^+$ and $C_6H_5^+$ as the primary products of the reactions of $C_4H_2^+$ and $C_4H_3^+$, respectively, with C_2H_2.[31] Two stable isomeric structures are known to exist for $C_6H_4^+$ and $C_6H_5^+$ when prepared from $C_2H_2^+$. These two structures are thought to be the cyclic and acyclic isomers which are readily distinguished by their different reactivities. The more reactive isomer of $C_6H_5^+$ was originally attributed to acyclic $C_6H_5^+$,[32,33] but later work has shown that the lower energy phenylium ion is more reactive than the acylic isomer.[22] Accordingly, we attribute the $C_6H_5^+$ isomer which is more reactive with H_2, to c-$C_6H_5^+$ as also did Petrie et al.[21] Similarly the $C_6H_4^+$ ion derived from benzene was found to have a higher reactivity with C_2H_2 than did the $C_6H_4^+$ isomer produced in the reaction between $C_4H_2^+$ and C_2H_2.[32] We therefore also attribute the more reactive $C_6H_4^+$ isomer, derived from benzene, to c-$C_6H_4^+$.

No reaction of either isomer of $C_6H_4^+$ with H_2 was observed. An association reaction (almost certainly three-body) with H atoms was observed for the cyclic isomer, c-$C_6H_4^+$, only:

$$\text{c-}C_6H_4^+ + H \rightarrow \text{c-}C_6H_5^+ \quad (16)$$

$$k = 3.3 \times 10^{-11}\ \text{cm}^3\ \text{s}^{-1}$$

Acyclic $C_6H_5^+$ did not react with either H_2 or H atoms. c-$C_6H_5^+$ did not react with H, but a reaction with H_2 was observed. Again this is almost certainly a three-body process, resulting from the collisional stabilization of the $(\text{c-}C_6H_7^+)^*$ complex by the bath gas:

$$c\text{-}C_6H_5^+ + H_2 \rightarrow c\text{-}C_6H_7^+ \quad (17)$$

$$k = 3.8 \times 10^{-11}\ cm^3\ s^{-1}$$

$c\text{-}C_6H_6^+$ did not react with H_2 but underwent a comparatively fast two-channel reaction with H atoms. Association is the major channel (65%), but a significant amount of H-atom transfer also occurred:

$$c\text{-}C_6H_6^+ + H \rightarrow c\text{-}C_6H_5^+ + H_2(0.35) \quad (18a)$$

$$\rightarrow c\text{-}C_6H_7^+ (0.65) \quad (18b)$$

$$k = 2.1 \times 10^{-10}\ cm^3\ s^{-1}$$

These results are in good accord with Petrie et al.[21] except that they did not report the 35% H-atom-transfer channel. Petrie et al. have argued that the efficiency of association of the $c\text{-}C_6H_5^+$ isomer with H_2 stems from H_2 bond insertion into the vacant sp^2 orbital on the ipso carbon of the phenylium ion.[21] This orbital is not vacant for the $c\text{-}C_6H_6^+$ ion, and there is no observable association of $c\text{-}C_6H_6^+$ with H_2. They also argued that the absence of association of $c\text{-}C_6H_5^+$ with atomic H might be explained by the formation of an excited electronic state of $(c\text{-}C_6H_6^+)^*$. This excited state lowers the well depth of the $(c\text{-}C_6H_6^+)^*$ complex to $\leq$130 kJ mol^{-1}, thereby reducing the complex lifetime.[21] It is interesting to note that both $c\text{-}C_6H_4^+$ and $c\text{-}C_6H_6^+$ show the same behavior: neither associate with H_2, yet both associate with H atoms. The potential surface of $C_6H_4^+$ is not well characterized, and a more detailed comparison must wait until this has been done.

Concluding Remarks

Sufficient reactions of $C_mH_n^+$ with H_2 and H atoms have now been measured in the laboratory for some interesting trends to appear. A comparison of the present results with those already known[5,13,15] shows that highly unsaturated ions ($C_mH_n^+$, m = 1−4, n = 0−1) undergo largely H atom abstraction reactions with H_2. As m approaches 4, the rate coefficient decreases to $\leq$10% of the capture rate. More saturated hydrocarbon ions ($n \geq 2$) do not undergo reactions with H_2, which is largely a consequence of the lack of exothermic channels available for H atom abstraction. The only option for reaction other than H atom abstraction, is association—when H_2 inserts into the hydrocarbon ion. However, as Table 1 shows, these association reactions are rare, occurring only for $c\text{-}C_6H_5^+$, although association also occurs with C_3H^+,[34] which is not included in the ions in this study. Association with H_2 generally leads to a product ion that is more stable by at least 100 kJ mol^{-1}. Why then does it not occur for a wider range of $C_mH_n^+$ ions? The association reaction $C_3H^+ + H_2$ has been studied in some detail using ab initio techniques.[27] The conclusion of that study was that the reaction proceeds because $C_3H^+ + H_2$ can access the deep potential well of $ac\text{-}HCCCH_2^+$.[27] For an association ion to be observed in a flow tube, the association complex must first be stabilized by collision with the bath gas. Access to deep wells on the potential surface lengthens the lifetime of the complex so that collisional stabilization can occur. The time between collisions in the flow tube is typically ~70 ns. It is evident then that for most ions, the $(C_mH_n^+\cdots H_2)^*$ complex is not surviving long enough for stabilization to take place. When association does occur (e.g., $C_3H^+ + H_2$, $c\text{-}C_6H_5^+ + H_2$), the products are new covalently bound $C_mH_{n+2}^+$ ions.

H atom reactions of $C_mH_n^+$ behave very differently from the corresponding reactions with H_2. Two types of reaction are common: H-atom transfer and association. If an exothermic pathway is available for H-atom transfer, it usually occurs. H-atom transfer results in a decrease in hydrogenation of the ion, whereas H-atom abstraction, which occurs with H_2, results in an increase in hydrogenation. Highly unsaturated ions, such as C_2^+ and C_2H^+, are unreactive with H atoms but larger unsaturated ions, such as C_4H^+ and $C_4H_2^+$, which are intermediate in size, undergo association reactions. The larger number of atoms increases the number of modes among which the energy of the complex can be dissipated. The much greater propensity for association of $C_mH_n^+$ with H atoms as compared with H_2 is a consequence of the greater complex stability. It appears that H atom/$C_mH_n^+$ reactions form complexes that can access the region of the $(C_mH_{n+1}^+)^*$ potential surface above the deepest wells and which may be the result of H tunneling through barriers.

The structures of the $C_mH_n^+$ ions examined in this study were not always identified from experiment. In some cases it was loosely assumed that the structure of the ion formed by electron impact from the neutral precursor was the structure most closely resembling the precursor configuration. However, as previously noticed, sometimes cyclic ions can be made from acyclic precursors (e.g., $c\text{-}C_3H_3^+$ from C_2H_4) and acyclic ions from cyclic precursors ($ac\text{-}C_6H_5^+$ from C_6H_6). There has been some debate about the structures of many of these ions and distonic configurations of some $C_mH_n^+$ ions forming radical cations have been suggested for some radical hydrocarbon ions.[35,36]

Finally we note that whereas saturated $C_mH_n^+$ ions are unreactive with H_2, they are more reactive with H. The implication of this observation to interstellar cloud chemistry is that reactions of $C_mH_n^+$ with H_2 occur only for very unsaturated ions and quickly reach a level of saturation from which no further addition of H_2 occurs. Where regions of significant H-atom densities exist, then the termination steps for molecular hydrogen are bypassed by H-atom reactions which lead ultimately to even more saturated hydrocarbons. This has great significance to interstellar chemistry, since the H to H_2 ratio is very variable in the interstellar gas clouds. Observations of hydrocarbons might be a monitor of that ratio. Indeed, CH has been used as a monitor for H_2.[37]

Acknowledgment. We thank the Marsden Fund for financial support. N.G.A. thanks the University of Canterbury for the award of an Erskine Fellowship which allowed N.G.A. and L.M.B. to spend several weeks in New Zealand.

References and Notes

(1) See for example: Irvine, W. M.; Goldsmith, P. F.; Hjalmarson, Å. In *Interstellar Processes*; Hollenbach, D. J., Thronson, H. A., Eds.; D. Reidel Publishing Co.: Dordrecht, 1987; p 561. Miller, T.; Williams, D. A. *Dust and Chemistry in Astronomy*; Inst. Physics Pub., 1993.

(2) Bettens, R. P. A.; Lee, H.-H.; Herbst, E. *Astrophys. J.* **1995**, *443*, 664.

(3) Geballe, T. R.; Oka, T. *Nature* **1996**, *384*, 334.

(4) Millar, T. J.; Freeman, A. *Mon. Not. R. Astron. Soc.*, **1984**, *207*, 405.

(5) Anicich, V. G. *J. Phys. Chem. Ref. Data* **1993**, *22*, 1469.

(6) Sablier, M.; Rolando, C. *Mass Spectrom. Rev.* **1993**, *12*, 285.

(7) Fehsenfeld, F. C.; Ferguson, E. E. *J. Geophys. Res.* **1971**, *76*, 8453.

(8) Fehsenfeld, F. C.; Ferguson, E. E. *Planet. Space Sci.* **1972**, *20*, 295.

(9) Tosi, P.; Iannotta, S.; Bassi, D.; Villinger, H.; Dobler, W.; Lindinger, W. *J. Chem. Phys.* **1984**, *80*, 1905.

(10) Scott, G. B. I.; Fairley, D. A.; Freeman, C. G.; McEwan, M. J.; Spanel, P.; Smith, D. *J. Chem. Phys.* **1997**, *106*, 3982.

(11) McEwan, M. J. In *Advances in Gas-Phase Ion Chemistry*; Adams, N. G., Babcock, L. M., Eds.; J. A. I. Press: Greenwich, CT, 1992; Vol. 1, p 1.

(12) Lias, S. G.; Bartmess, J. E.; Liebman, J. F.; Holmes, J. L.; Levin, R. D.; Mallard, W. G. *J. Phys. Chem. Ref. Data* **1988**, *17*, Suppl. 1.

(13) Kim, J. K.; Theard, L. P.; Huntress, W. T. *J. Chem. Phys.* **1975**, *62*, 45.
(14) Adams, N. G.; Smith, D. *Chem. Phys. Lett.* **1977**, *47*, 383.
(15) Bohme, D. K.; Wlodek, S. *Int. J. Mass Spectrom. Ion Proc.* **1990**, *102*, 133.
(16) Buttrill, S. E.; Kim, J. K.; Huntress, W. T.; LeBreton, P. R.; Williamson, A. *J. Chem. Phys.* **1974**, *61*, 2122.
(17) Herbst, E.; Adams, N. G.; Smith, D. *Astrophys. J.* **1983**, 269, 329.
(18) McEwan, M. J.; McConnell, C. L.; Freeman, C. G.; Anicich, V. G. *J. Phys. Chem.* **1994**, *98*, 5068.
(19) Giles, K.; Adams, N. G.; Smith, D. *Int. J. Mass Spectrom. Ion Proc.* **1989**, *89*, 303.
(20) Lammertsma, K.; Pople, J. A.; Schleyer, P. vR. *J. Am. Chem. Soc.* **1986**, *108*, 7.
(21) Petrie, S.; Javahery, G.; Bohme, D. K. *J. Am. Chem. Soc.* **1992**, *114*, 9205.
(22) Ausloos, P.; Lias, S. G.; Buckley, T. J.; Rogers, E. E. *Int. J. Mass Spectrom. Ion Proc.* **1989**, *92*, 65.
(23) Karpas, Z.; Anicich, V. G.; Huntress, W. T. *J. Chem. Phys.* **1979**, *70*, 2877.
(24) Hansel, A.; Richter, R.; Lindinger, W.; Ferguson, E. E. *Int. J. Mass Spectrom. Ion Proc.* **1989**, *94*, 251.
(25) Smith, D.; Glosik, J.; Skalsky, V.; Spanel, P.; Lindinger, W. *Int. J. Mass Spectrom. Ion Proc.* **1993**, *129*, 145.
(26) Wong, M. W.; Radom, L. *J. Am. Chem. Soc.* **1993**, *115*, 1507.
(27) Maluendes, S. A.; McLean, A. D.; Yamashita, K.; Herbst, E. *J. Chem. Phys.* **1993**, *99*, 2812.
(28) Skancke, A. *J. Phys. Chem.* **1995**, *99*, 13886.
(29) Koch, W.; Lin, B.; Schleyer, P. v.-R. *J. Am. Chem. Soc.* **1989**, *111*, 3479.
(30) Lavell, S.; Feller, D.; Davidson, E. R. *Theor. Chim. Acta* **1990**, *77*, 111.
(31) Anicich, V. G.; Sen, A. D.; Huntress, W. T.; McEwan, M. J. *J. Chem. Phys.* **1990**, *93*, 7163.
(32) Knight, J. S.; Freeman, C. G.; McEwan, M. J.; Anicich, V. G.; Huntress, W. T. *J. Phys. Chem.* **1987**, *91*, 3898.
(33) Bates, D. R.; Herbst, E. In *Reaction Rate Coefficients in Astrophysics*; Miller, T. J., Williams, D. A., Eds.; Kluwer Academic: Dordrecht, 1988; p 17.
(34) Smith, D.; Adams, N. G. *Int. J. Mass Spectrom. Ion Proc.* **1987**, *76*, 307. Adams, N. G.; Smith, D. *Astrophys. J.* **1987**, *317*, L25.
(35) Hammerum, S. *Mass Spectrom. Rev.* **1988**, *7*, 123.
(36) Stirk, K. M.; Kiminkinen, L. K. M.; Kenttämaá, H. I. *Chem. Rev.* **1992**, *92*, 1649.
(37) Magnani, L.; Onello, J. S.; Adams, N. G.; Hartman, D.; Thaddeus, P. Astrophys. J., submitted.

APPENDIX V

Reprinted from

CHEMICAL PHYSICS LETTERS

Chemical Physics Letters 269 (1997) 88–92

The reaction $H_3^+ + N$: a laboratory measurement

Graham B.I. Scott, David A. Fairley, Colin G. Freeman, Murray J. McEwan

Department of Chemistry, University of Canterbury, Christchurch, New Zealand

Received 8 December 1996; in final form 31 January 1997

ELSEVIER

Contributions should, preferably, be sent to a member of the Advisory Editorial Board (addresses are given in the first issue of each volume) who is familiar with the research reported, or to one of the Editors:

A.D. BUCKINGHAM
D.A. KING
Editor of Chemical Physics Letters
University Chemical Laboratory
Lensfield Road
Cambridge CB2 1EW, UK
FAX 44-1223-336362

A.H. ZEWAIL
Editor of Chemical Physics Letters
A.A. Noyes Laboratory of Chemical Physics
California Institute of Technology
Mail Code 127-72
Pasadena, CA 91125, USA
FAX 1-818-4050454

After acceptance of the paper for publication, all further correspondence should be sent to the publishers (Ms. S.A. Hallink, Issue Management (Chemistry), Elsevier Science B.V., P.O. Box 2759, 1000 CT Amsterdam, The Netherlands; telephone 31-20-4852664, FAX 31-20-4852775, telex 10704 espom nl; electronic mail X400: C=NL; A=400NET; P=SURF; O=ELSEVIER; S=HALLINK, I=S or RFC822: S. HALLINK@ELSEVIER.NL).

Publication information: Chemical Physics Letters (ISSN 0009-2614). For 1997, volumes 264–280 are scheduled for publication. Subscription prices are available upon request from the publisher. Subscriptions are accepted on a prepaid basis only and are entered on a calendar year basis. Issues are sent by surface mail except to the following countries where Air delivery via SAL is ensured: Argentina, Australia, Brazil, Canada, Hong Kong, India, Israel, Japan, Malaysia, Mexico, New Zealand, Pakistan, PR China, Singapore, South Africa, South Korea, Taiwan, Thailand, USA. For all other countries airmail rates are available upon request. Claims for missing issues must be made within six months of our publication (mailing) date.

0009-2614/1997/$17.00

US mailing notice – Chemical Physics Letters (ISSN 0009-2614) is published weekly by Elsevier Science B.V., Molenwerf 1, P.O. Box 211, 1000 AE Amsterdam. Annual subscription price in the USA US$ 7818.00, including air speed delivery, valid in North, Central and South America only. Periodicals postage paid at Jamaica, NY 11431. USA POSTMASTERS: Send address changes to Chemical Physics Letters, Publications Expediting, Inc., 200 Meacham Avenue, Elmont, NY 11003. Airfreight and mailing in the USA by Publication Expediting.

Printed in The Netherlands | Published weekly | Library of Congress Catalog Card Number 68–26532

25 April 1997

ELSEVIER

Chemical Physics Letters 269 (1997) 88–92

CHEMICAL PHYSICS LETTERS

The reaction $H_3^+ + N$: a laboratory measurement

Graham B.I. Scott, David A. Fairley, Colin G. Freeman, Murray J. McEwan

Department of Chemistry, University of Canterbury, Christchurch, New Zealand

Received 8 December 1996; in final form 31 January 1997

Abstract

We report a study of the ion–atom reaction $H_3^+ + N$ using a selected ion flow tube (SIFT) operating at room temperature. The product channel is $NH_2^+ + H$ and the rate coefficient is $k = (4.5 \pm 1.8) \times 10^{-10}$ cm^3 s^{-1}. This reaction is relevant to the synthesis of ammonia in interstellar clouds.

1. Introduction

A possible step in the synthesis of NH_3 in interstellar clouds is the reaction between H_3^+ and N atoms [1]. The major ion product of the reaction is believed to be NH_2^+ which is converted to NH_4^+ in the presence of H_2 in the interstellar medium by a sequence of reactions [2]. NH_3 is then formed from NH_4^+ via the dissociative recombination step

$$NH_4^+ + e \rightarrow NH_3 + H. \quad (1)$$

It has not been possible to assess the significance of the $H_3^+ + N$ reaction in the overall scheme for interstellar ammonia synthesis because the reaction has never been measured in the laboratory. There are several reasons why this measurement has not been made. Most ion–atom reactions have been studied using flow tube techniques [3] in which N atoms are made by passing N_2 through a microwave discharge in a side entry port to the flow tube. Less than 1% dissociation of N_2 into N atoms is typical for this process [4,5] and therefore there is only a very small amount of atomic N, in a large excess of N_2, entering the flow tube. Nevertheless, in spite of the small amount of dissociation, some ion–N atom reactions have been successfully measured [4–8]. The $H_3^+ + N$ reaction has an additional difficulty due to the simultaneous and rapid proton transfer reaction between H_3^+ and N_2

$$H_3^+ + N_2 \rightarrow N_2H^+ + H_2, \quad (2)$$

$k = 1.86 \times 10^{-9}$ cm^3 s^{-1} [9].

To help offset the lack of an experimental measurement for the $H_3^+ + N$ reaction, Herbst et al. [10] have undertaken ab initio calculations of the NH_3^+ potential surface in which they searched for barrier-free pathways between reactants and products. The reactants N (^{4}S) and H_3^+ ($^1A_1$) collide on an NH_3^+ potential surface that has quartet multiplicity: this state is an excited state of the $(NH_3^+)^*$ complex which correlates with ground state products NH_2^+ ($^3B_1$) and H (^{2}S). They investigated several different entrance and exit channel geometries and arrived at the conclusion that the reaction between $H_3^+ + N$ possesses a large activation barrier and is unimportant under interstellar cloud conditions. As a consequence of this ab initio study, the $H_3^+ + N$ reaction has largely been discounted as a potential source of interstellar NH_3.

We report here the results of a laboratory measurement of $H_3^+ + N$ at room temperature (295 ± 5 K).

PII S0009-2614(97)00244-3

2. Experimental

The details of the selected ion flow tube (SIFT) used at Canterbury have been published previously [11]. Only a brief summary of that part of the equipment relevant to the present study will be given here. The reactant ion, H_3^+, is generated from Kr^+ ($^2P_{3/2}$ and $^2P_{1/2}$) which is injected into a hydrogen carrier gas or, alternatively, a helium carrier gas in which H_2 is added at the first inlet port of the flow tube. H_3^+ is then formed in the flow tube from Kr^+ via the reaction sequence:

$$Kr^+ + H_2 \rightarrow KrH^+ + H, \quad (3)$$

$$KrH^+ + H_2 \rightarrow H_3^+ + Kr. \quad (4)$$

The reason for the choice of Kr^+ (rather than H_2^+ or Ar^+) as the precursor for H_3^+ is that it offers the best source of H_3^+ in its lowest vibrational state [12].

N atoms are generated in a quartz side tube by a microwave discharge of N_2 (or, alternatively, a mixture of N_2 in He). Vibrationally excited N_2 molecules are removed from the discharged gas flow by a glass wool plug located in the side tube immediately downstream from the discharge but prior to the point of entry into the main flow tube [4]. The metastable atom ($N(^2D)$ and $N(^2P)$) number densities in the reactant gas stream entering the flow tube are also minimized with this arrangement as a maximum of only about 1% of all N atoms are expected to be metastable [13]. In addition, both $N(^2D)$ and $N(^2P)$ are known to be efficiently deactivated by wall collisions [14] and thus the presence of the glass wool plug depletes the metastable atom densities even further.

The extent of dissociation of N_2 into $N(^4S)$ atoms is conveniently monitored utilizing the reaction between $C_2H_2^+ + N$ (5), which has a known rate coefficient

$$C_2H_2^+ + N \rightarrow CH^+ + HCN\,(0.05), \quad (5a)$$

$$C_2H_2^+ + N \rightarrow C_2N^+ + H_2\,(0.35), \quad (5b)$$

$$C_2H_2^+ + N \rightarrow HC_2N^+ + H\,(0.60), \quad (5c)$$

of $k = 2.5 \times 10^{-10}$ cm^3 s^{-1} [5,8]. There was no reaction between C_2H_2 and N_2 (for which we observed $k < 5 \times 10^{-13}$ cm^3 s^{-1}). We had previously made an absolute measurement of the N atom density in our reaction tube by titrating the N atoms with NO as described by Viggiano et al. [5] and as we have outlined in more detail elsewhere [15]. Using the absolute N atom density found from the NO titration, we measured the absolute rate coefficient for reaction (5) as $k = 2.4 \times 10^{-10}$ cm^3 s^{-1} which is in excellent agreement with the earlier measurement [5,8].

We note that in our experiments a typical degree of dissociation of N_2 downstream from the glass wool plug is 0.4% for pure N_2 increasing to 1.5% for a 5% N_2/He mixture.

3. Results and discussion

Evidence for only one product was found for the $H_3^+ + N$ reaction (6)

$$H_3^+ + N \rightarrow NH_2^+ + H, \quad (6)$$

which is consistent with the thermochemistry. The products shown in reaction (6) are those of the only exothermic bimolecular channel ($\Delta H^\circ = -98$ kJ mol^{-1}). The alternative proton transfer channel, $NH^+ + H_2$, is endothermic by 98 kJ mol^{-1}. The product ion of the reaction, NH_2^+, was never observed by us as it is rapidly converted to NH_3^+ and then more slowly to NH_4^+ in the presence of H_2.

$$NH_2^+ + H_2 \rightarrow NH_3^+ + H \quad (7)$$

$k = 1.95 \times 10^{-10}$ cm^3 s^{-1},

$$NH_3^+ + H_2 \rightarrow NH_4^+ + H \quad (8)$$

$k = 4.40 \times 10^{-13}$ cm^3 s^{-1}.

H_2 is always present in our flow tube as it is required to convert Kr^+ to H_3^+ via reactions (3) and (4). The majority of our measurements were made using a hydrogen bath gas. In a hydrogen bath gas, all of the NH_3^+ is converted to NH_4^+ via reaction (8), whereas in a helium bath gas both NH_3^+ and NH_4^+ are observed.

The possibility that the observed NH_3^+ product is also formed via the association reaction

$$H_3^+ + N + M \rightarrow NH_3^+ + M, \quad (9)$$

cannot be completely discounted. We have previously observed termolecular association of hydrocarbon ions with atomic hydrogen [16] but two factors make association in the $H_3^+ + N$ system less likely.

Firstly 646 kJ mol^{-1} of energy must be distributed amongst six internal degrees of freedom for NH_3^+ to survive long enough for collisional stabilization to occur. This exothermicity is significantly larger than that in any of the hydrocarbon ion–H atom reactions where association was observed. Moreover, these $C_nH_m^+$–H atom systems have a greater number of internal modes available to dissipate energy. Whilst possible, the direct association of N and H_3^+ to form NH_3^+ is thus unlikely.

In the following discussion we designate '$[NH_2^+]$' to represent the total ion signal observed for all the product ions that have their origin in the NH_2^+ generated in reaction (6). That is, '$[NH_2^+]$' = ($[NH_3^+]$ + $[NH_4^+]$) in a helium bath gas and '$[NH_2^+]$' = $[NH_4^+]$ in a hydrogen bath gas. It is of course necessary to establish that '$[NH_2^+]$' is derived only from reaction (6) and from no other source. This is done by ascertaining that the '$[NH_2^+]$' signal is present only with the microwave discharge on and with H_3^+ present.

The experiment to determine the rate coefficient of reaction (6) requires a very different technique to the usual method of measuring a rate coefficient in a flow tube. Usually the rate coefficient is found from the slope of the semilogarithmic decay of the reactant ion signal with neutral reactant flow (see Eq. (13)). This technique cannot be used in the present case because almost all of the H_3^+ signal is depleted by N_2 and not N. Instead we obtain the rate coefficient for reaction (6) from the ratio of the product ion signals of reaction (6) ('$[NH_2^+]$') and the simultaneous reaction (2) ($[N_2H^+]$):

$$\text{viz.,}\quad \frac{\text{'}[NH_2^+]\text{'}}{[N_2H^+]} = \frac{k_{(H_3^+/N)}}{k_{(H_3^+/N_2)}} \times \frac{Q_N}{Q_{N_2}}. \qquad (10)$$

In Eq. (10), '$[NH_2^+]$' is as previously defined, and Q_N and Q_{N_2} represent the flow rates of N and N_2 respectively. As the rate coefficient for the $H_3^+ + N_2$ reaction (2) is well known [9] (it is also easily verified in the conventional manner with the discharge off) then the rate coefficient for the reaction $H_3^+ + N$ is available from Eq. (10). Our measured rate coefficient for the reaction $H_3^+ + N_2$ (2) is $k = 1.65 \times 10^{-9}$ cm^3 s^{-1}. The ratio '$[NH_2^+]$'/$[N_2H^+]$ is measured with the microwave discharge on and is subsequently corrected for mass discrimination and differential diffusion of the ions. Q_N is found from the degree of dissociation of N_2 measured in separate experiments with the calibration reaction $C_2H_2^+ + N$ (5). Implicit in Eq. (10) is the prediction that the '$[NH_2^+]$'/$[N_2H^+]$ ratio should be independent of N_2 flow rate and constant, providing the degree of dissociation does not vary and given that all the reactant H_3^+ ion has been converted to products.

We show a typical set of measured values in Fig. 1. The theoretical justification for Eq. (10) follows.

The conventional flow tube equation from which the rate coefficient for reaction

$$A^+ + B \rightarrow \text{products}, \qquad (11)$$

is found is [17]

$$\ln([A^+]/[A^+]_0) = -\frac{kQ_B(z+\varepsilon)}{\pi a^2 v_0 v_i}, \qquad (12)$$

where $[A^+]$ = count of A^+ with flow of neutral B, Q_B; $[A^+]_0$ = count of A^+ with zero flow of B; $(z+\varepsilon)$ = reaction distance, corrected for inlet port perturbation; a = flow tube radius; v_0 = bulk flow velocity of bath gas; v_i = average ion velocity. In keeping with the general mathematical formalism employed by Tosi et al [18] Eq. (12) can be rewritten as

$$[A^+] = [A^+]_0 \exp(-R_B Q_B), \qquad (13)$$

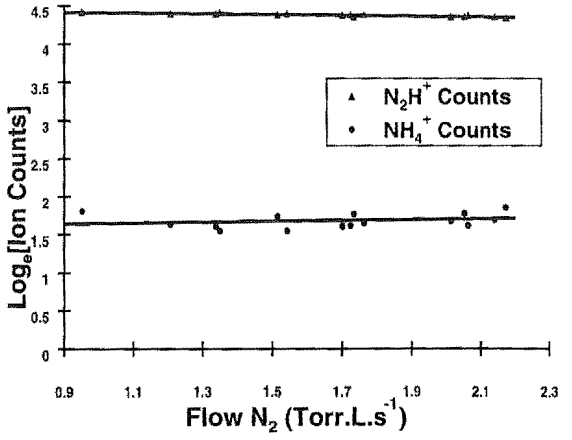

Fig. 1. The variation in ion products 'NH_2^+' and N_2H^+ at different N_2 flows in a hydrogen carrier using pure N_2 in the microwave discharge. Under these conditions, '$[NH_2^+]$' = $[NH_4^+]$. The ratio of these ion signals provides the rate coefficient as discussed in the text.

where $R_B = k(z+\varepsilon)/(\pi a^2 v_0 v_i)$

Applying Eq. (13) to the specific case of H_3^+ loss via the simultaneous reactions with N_2 and N (reactions (2) and (6)), yields the following equations for $[N_2H^+]$ and '$[NH_2^+]$':

$$[N_2H^+] = ([H_3^+]_0 - [H_3^+]) \frac{R_{N_2} Q_{N_2}}{(R_{N_2} Q_{N_2} + R_N Q_N)}, \quad (14)$$

$$'[NH_2^+]' = ([H_3^+]_0 - [H_3^+]) \frac{R_N Q_N}{(R_{N_2} Q_{N_2} + R_N Q_N)}, \quad (15)$$

Eq. (10) is then obtained by taking the ratio of Eq. (15) and Eq. (14). Alternatively (10) may be readily derived by taking the ratio of the production rates of N_2H^+ and 'NH_2^+' and integrating, viz.,

$$k_{(H_3^+/N)}[N]\,d[N_2H^+] = k_{(H_3^+/N_2)}[N_2]\,d['NH_2^+'] . \quad (16)$$

The mean of 16 separate experimental measurements gave a value for the rate coefficient of the reaction between H_3^+ and N (reaction (6)) of $k = (4.5 \pm 1.8) \times 10^{-10}$ cm^3 s^{-1}. The Langevin collision rate for the reaction is 1.6×10^{-9} cm^3 s^{-1}.

4. Conclusions

The fast rate coefficient observed for the reaction between $H_3^+ + N$ is at odds with the theoretical prediction for this reaction [10]. It is perhaps not too surprising that the ab initio calculations have not found the pathway for the reaction, given the complexity of the potential surface. As Herbst et al. comment, "given the number of degrees of freedom, the possibility of missing such a pathway cannot be dismissed out of hand" [10]. We are also undertaking additional ab initio calculations in an attempt to find a likely pathway.

The reaction between $H_3^+ + N$ to yield $NH_2^+ + H$ is unusual for reactions of H_3^+ which invariably proceed by proton transfer. Only one other such reaction has been reported, viz., that of $H_3^+ + O$ which is also rapid and which has the two exothermic channels (17) [6]:

$$H_3^+ + O \rightarrow OH^+ + H_2 \quad (17a)$$

$$H_3^+ + O \rightarrow H_2O^+ + H \quad (17b)$$

$k = 8.0 \times 10^{-10}$ cm^3 s^{-1}.

The weighting of each possible channel could not be established by Fehsenfeld as both product ions reacted further with the H_2 present in the flow tube to form H_3O^+ [6]. There are, therefore, only these two reactions of H_3^+ (the fast ion–atom reactions, $H_3^+ + N$ and $H_3^+ + O$) known in which H atom loss occurs.

Finally we note that the reaction appears to conserve spin, but to do this the reactants must collide on a quartet potential surface of NH_3^+.

$$H_3^+(^1A_1') + N(^4S) \rightarrow NH_2^+(^3B_1) + H(^2S) \quad (18)$$

If so, the ground state surface, NH_3^+ ($^2A_2''$), which lies 646 kJ mol^{-1} below the entrance level of the reactants cannot be accessed. However Federer et al. [8] have speculated that multiple curve crossings between curves of different multiplicities may not be uncommon in ion–atom reactions and can occur within the orbiting complexes formed in collision.

Acknowledgements

We thank Robert Maclagan and Leon Phillips for helpful discussions, Daniel Milligan for assisting with some measurements and the Marsden fund for financial support.

References

[1] A. Dalgarno, in: Interactions between Ions and Molecules, P. Ausloos (Ed.), Plenum Press, New York, 1975, p. 341.
[2] E. Herbst, W. Klemperer, Astrophys. J. 185 (1973) 505.
[3] M. Sablier, C. Rolando, Mass Spectrom. Rev. 12 (1993) 285.
[4] P.D. Golden, A.L. Schmeltekopf, F.C. Fehsenfeld, H.I. Schiff, E.E. Ferguson, J. Chem. Phys. 44 (1966) 4095.
[5] A.A. Viggiano, F. Howorka, D.L. Albritton, F.C. Fehsenfeld, N.G. Adams, D. Smith, Astrophys. J. 236 (1980) 492.
[6] F.C. Fehsenfeld, Astrophys. J. 209 (1976) 638.
[7] F.C. Fehsenfeld, Planet Space Sci. 25 (1977) 195.
[8] W. Federer, H. Villinger, W. Lindinger, E.E. Ferguson, Chem. Phys. Lett. 123 (1986) 12.

[9] V.G. Anicich, J. Phys. Chem. Ref. Data 22 (1993) 1469.
[10] E. Herbst, D.J. De Frees, A.D. McLean, Astrophys. J. 321 (1987) 898.
[11] M.J. McEwan, in: Advances in Gas Phase Ion Chemistry, N.G. Adams, L.M. Babcock (Eds.), J.A.I. Press, Greenwich, CT, 1992, p. 1.
[12] D. Smith, P. Spanel, Chem. Phys. Lett. 211 (1993) 454.
[13] A.N. Wright, C.A. Winkler, Active Nitrogen, Academic Press, New York, 1968, p. 83.
[14] C.-L. Lin, F. Kaufman, J. Chem. Phys. 55 (1971) 3760.
[15] G.B.I. Scott, D.A. Fairley, C.G. Freeman, M.J. McEwan, V.G. Anicich. To be submitted.
[16] G.B.I. Scott, D.A. Fairley, C.G. Freeman, M.J. McEwan, N.G. Adams, L.M. Babcock, J. Phys. Chem. submitted 1997.
[17] D. Smith, N.G. Adams, Adv. At. Mol. Phys. 24 (1988) 1.
[18] P. Tosi, S. Iannotta, D. Bassi, H. Villinger, W. Dobler, W. Lindinger, J. Chem. Phys. 80 (1984) 1905.

Orders, claims, and product enquiries: please contact the Customer Support Department at the Regional Sales Office nearest to you:

New York
Elsevier Science
P.O. Box 945
New York, NY 10159-0945
USA
Tel. (+1)212-633-3730
[Toll free number for North American customers: 1-888-4ES-INFO (437-4636)]
Fax (+1)212-633-3680
e-mail: usinfo-f@elsevier.com

Amsterdam
Elsevier Science
P.O. Box 211
1000 AE Amsterdam
The Netherlands
Tel. (+31)20-4853757
Fax (+31)20-4853432
e-mail: nlinfo-f@elsevier.nl

Tokyo
Elsevier Science
9-15 Higashi-Azabu 1-chome
Minato-ku, Tokyo 106
Japan
Tel. (+81)3-5561-5033
Fax (+81)3-5561-5047
e-mail: kyf04035@niftyserve.or.jp

Singapore
Elsevier Science
No. 1 Temasek Avenue
#17-01 Millenia Tower
Singapore 039192
Tel. (+65)434-3727
Fax (+65)337-2230
e-mail: asiainfo@elsevier.com.sg

Advertising information: Advertising orders and enquiries may be sent to: **International:** Elsevier Science, Advertising Department, The Boulevard, Langford Lane, Kidlington, Oxford OX5 1GB, UK, Tel. (+44)(0)1865 843565, Fax (+44)(0)1865 843976. **USA and Canada:** Weston Media Associates, Daniel Lipner, P.O. Box 1110, Greens Farms, CT 06436-1110, USA, Tel. (+1)(203)261-2500, Fax (+1)(203)261-0101. **Japan:** Elsevier Science Japan, Marketing Services, 1-9-15 Higashi-Azabu, Minato-ku, Tokyo 106, Japan, Tel. (+81)3-5561-5033, Fax (+81)3-5561-5047.

Electronic manuscripts: Electronic manuscripts have the advantage that there is no need for the rekeying of text, thereby avoiding the possibility of introducing errors and resulting in reliable and fast publication.

Your disk plus three, final and exactly matching printed versions should be submitted together. Double density (DD) or high density (HD) diskettes ($3^1/2$ or $5^1/4$ inch) are acceptable. It is important that the file saved is in the native format of the wordprocessor program used. Label the disk with the name of the computer and wordprocessing package used, your name, and the name of the file on the disk. Further information may be obtained from the Publisher.

Authors in Japan please note: Upon request, Elsevier Science Japan will provide authors with a list of people who can check and improve the English of their paper (*before submission*). Please contact our Tokyo office: Elsevier Science Japan, 1-9-15 Higashi-Azabu, Minato-ku, Tokyo 106; Tel. (03)-5561-5032; Fax (03)-5561-5045.

Chemical Physics Letters has no page charges.

For a full and complete Instructions to Authors, please refer to *Chemical Physics Letters,* Vol. 268, No. 5,6, pp. 566–567. The instructions can also be found on the World Wide Web: access under http://www.elsevier.nl or http://www.elsevier.com.

Mon. Not. R. Astron. Soc. 290, 636–638 (1997)

The interstellar synthesis of ammonia

Graham B. I. Scott, Colin G. Freeman and Murray J. McEwan*

Department of Chemistry, University of Canterbury, Christchurch, New Zealand

Accepted 1997 June 11. Received 1997 June 9; in original form 1997 May 9

ABSTRACT

The reaction $H_3^+ + N \rightarrow NH_2^+ + H$ has been measured in the laboratory at room temperature for the first time. It is sufficiently fast ($k = 4.5 \times 10^{-10}$ cm^3 s^{-1}) to provide a larger source of NH_3 in dense interstellar clouds at 10 K than the more widely accepted source $N^+ + H_2$. At 50 K, both ion–molecule mechanisms ($H_3^+ + N$ and $N^+ + H_2$) may provide roughly equivalent sources of NH_3.

Key words: molecular processes – ISM: abundances – ISM: atoms – ISM: molecules.

1 INTRODUCTION

Ammonia was the first polyatomic molecule to be observed in the interstellar medium. It was detected towards Sgr B2 from its emission spectrum in the microwave region (Cheung et al. 1968). NH_3 has since been found in many sources, including the Orion molecular cloud, TMC-1 and L134N, and is a widespread constituent of interstellar clouds (Morris et al. 1973; Irvine, Goldsmith & Hjalmarson 1987). In their paper reporting the first observation, Cheung et al. commented that 'since NH_3 is a fairly complex molecule, it is most likely formed by adsorbed N and H atoms on interstellar grain surfaces rather than by successive binary collisions'. Shortly afterwards, a gas-phase mechanism was postulated by Herbst & Klemperer (1973) in their pioneering paper on gas-phase ion–molecule synthesis. They proposed a synthetic scheme for NH_3 based on a reaction sequence derived from N^- ions (hereafter HK):

$$N^+ + H_2 \rightarrow NH^+ + H, \quad (1)$$

$$NH^+ + H_2 \rightarrow NH_2^+ + H, \quad (2)$$

$$NH_2^+ + H_2 \rightarrow NH_3^+ + H, \quad (3)$$

$$NH_3^+ + H_2 \rightarrow NH_4^+ + H, \quad (4)$$

$$NH_4^+ + e \rightarrow NH_3 + H. \quad (5)$$

Dalgarno (1975) proposed an alternative synthesis initiated by the reaction between H_3^+ and N atoms:

$$H_3^+ + N \rightarrow NH_2^+ + H, \quad (6)$$

which bypasses the first two reactions in the HK scheme.

Observations of high abundances of NH_3 in the hot core region of Orion were interpreted as evidence of NH_3 release from grains during heating (Pauls et al. 1983). It appears, then, from the observational data that different mechanisms may be operating in different regions of interstellar clouds. In this work we address the production of NH_3 initiated via reaction (6).

2 PRODUCTION OF NH_3 VIA $H_3^+ + N$

The gas-phase mechanism initiated by reaction (6) has largely been discounted in favour of (1) for several reasons. Huntress (1977) doubted its viability on the basis that reactions of H_3^+ invariably proceed by proton transfer and not H_2^+ transfer. Many modellers (e.g. Graedel, Langer & Frerking 1982; Millar, Leung & Herbst 1987; Bourlot 1991) have omitted any participation by reaction (6) in their models. Part of the problem in deciding whether or not to include reaction (6) was because no laboratory measurements were available. In an attempt to evaluate the contribution of reaction (6) to interstellar NH_3 production, Herbst, DeFrees & McLean (1987) made a theoretical study using *ab initio* quantum calculations of the reaction's potential surface. They concluded that the reaction possesses a large activation barrier and is not effective in ammonia synthesis. A consequence of this study is that NH_3 generated via the reaction between H_3^+ and N atoms has largely been discredited (e.g. Pineau des Forêts, Roueff & Flowers 1990). Two measurements have recently given cause for a re-examination of the relative importance of reaction (6) in ammonia synthesis. The first is that H_3^+ has been observed in the interstellar medium for the first time at roughly the densities expected from the models (Geballe & Oka 1996). The second is our laboratory measurement of reaction (6), which was found to be fast, having a rate coefficient $k = 4.5 \times 10^{-10}$ cm^3 s^{-1} at 300 K (Scott et al. 1997).

We comment here on the implications of these results.

*E-mail: m.mcewan@chem.canterbury.ac.nz (MJM)

Interstellar NH_3 synthesis

the reaction sequence (1)–(5) for the formation of NH_3 i the HK model there are three areas of difficulty. First, action (1) appears to be endothermic by about 1734 J ol^{-1} (Marquette, Rebrion & Rowe 1988), although in eir table of thermodynamic data Lias et al. (1988) list its dothermicity as 21 000 J mol^{-1}. Reaction (1) is clearly dothermic, and the question might be asked whether a rrier of about 1734 J mol^{-1} is sufficient to slow the reac- n down at the low temperatures of interstellar clouds and move production of ammonia via reaction (1) from con- ntion. This difficulty has been addressed by Herbst et al. 987), Yee, Lep & Dalgarno (1987), Galloway & Herbst 989) and Bourlot (1991), following a suggestion by dams, Smith & Millar (1984) that N^+ produced in the action

$$e^- + N_2 \rightarrow N^- + N + He \qquad (7)$$

ay have up to 0.14 eV of kinetic excitation. The effect of ie spin orbit state of N^- (Galloway & Herbst 1989) and the itio of ortho to para H_2 (Bourlot 1991) has been studied, id the consensus is that reaction (1) is sufficiently fast nder interstellar conditions to maintain an acceptable rate f production of NH_3 at temperatures down to 10 K. The ite coefficient of the reaction remains somewhat uncer- in, however, and values for the rate coefficient, under iterstellar conditions, between 10^{-18} and 10^{-13} cm^3 s^{-1} ave been proposed (Galloway & Herbst 1989); Millar, Far- uhar & Willacy (1997). Current models have assumed that, nder interstellar conditions, the rate coefficient for the eaction can be expressed by the 'crude' approximation $=1\times10^{-9}\exp(-85/T)$ cm^3 s^{-1} (Lee, Bettens & Herbst 996; Millar et al. 1997).

The second difficulty with the HK synthetic scheme 1)–(5) is reaction (4), which has a small activation barrier nd is slow at room temperature ($k=4.4\times10^{-13}$ cm^3 s^{-1}). lso, the rate coefficient decreases as T decreases, but eaches a minimum about 80 K and then increases again at ven lower temperatures due to tunnelling under the activa- ion barrier (Herbst et al. 1991). Again, given the high rela- ive abundance of H_2 and the known increase in rate oefficient at $T<80$ K, this reaction remains sufficiently ast not to act as an impedance to NH_3 production.

The third area of uncertainty concerns the products of lissociative recombination in reaction (5). This process has een examined in the laboratory, and a fractional H atom ontribution to the product distribution of ~1 was reported Adams et al. 1991). This implies that the NH_3+H product hannel is significant, although atomic hydrogen would also e generated if the $NH+H_2+H$ or NH_2+2H channels ere accessed during dissociative recombination. The letermination of a full branching ratio is required to resolve his ambiguity. Reaction (5) has also been the subject of everal theoretical studies. Both NH_3+H (Bates 1986, 987; Millar et al. 1988) and NH_2+H_2 (Herbst 1978; Bates 989) have been proposed as the predominant product hannels; however, the experimental data of Adams et al. 1991) indicate that the NH_2+H_2 channel is probably inor.

It has generally been assumed that H atom loss during issociative recombination is a reasonably efficient process (Bates 1991). However, recent measurements on the products of dissociative recombination of H_3O^+ show that the H_2O+H channel accounts for only 5 per cent of the product channels (Williams et al. 1996). Conflicting results have been reported by Anderson et al. (1996) in experiments carried out on a heavy-ion storage ring in which they measure a 33 per cent channel to H_2O+H. This discrepancy between the two measurements has yet to be resolved.

With these three areas of difficulty acknowledged, the HK synthesis has been included in most models as the preferred mechanism for NH_3 synthesis. We now compare production of NH_3 via the HK scheme with that initiated by the reaction between $H_3^+ + N$.

2.2 $H_3^+ + N$ or $N^+ + H_2$?

The relative rates of production of NH_3 initiated by reactions (1) and (6) lend themselves to easy comparison, as reactions (3)–(5) are common to both schemes. As reaction (2) is fast at 20 K, a simple comparison of the two synthetic schemes for NH_3 is achieved by comparing the relative rates of reactions (1) and (6), $R(1)$ and $R(6)$, under typical conditions. From the number densities computed by Lee et al. (1996) in their new standard model and shown in Table 1 we find the relative rates at 10 K, $R_6/R_1\sim6.3$, and at 50 K, $R_6/R_1\sim1.1$. Consequential changes to the number densities of ammonia and several other species (e.g. NH_2CN, HNC^+ and NH_2CN^+) also occur when the rate coefficient for reaction (6) is incorporated into standard models (Herbst, private communication).

Thus, if the observed rate coefficient of 4.5×10^{-10} cm^3 s^{-1} for reaction (6) does not change substantially with temperature (which is usually the case for exothermic bimolecular ion–molecule reactions dependent on charge-induced dipole interactions), then enhanced NH_3 production will

Table 1. Number densities evaluated by Lee et al. (1996) in their new standard model for steady-state conditions at 10 and 50 K relative to an H_2 density of 5×10^3 cm^{-3}. The calculated rates of reactions (1) and (6), R_1 and R_6 using these data are also shown.

Species/n_{H_2}	10 K	50 K
N	1.9×10^{-5}	6.6×10^{-6}
N^+	2.3×10^{-11}	9.7×10^{-14}
H_3^+	3.5×10^{-9}	6.6×10^{-9}
R_1[a]/(particle cm^{-3} s^{-1})	1.2×10^{-16}	4.4×10^{-16}
R_6[b]/(particle cm^{-3} s^{-1})	7.5×10^{-16}	4.9×10^{-16}

[a]Calculated using the rate coefficient for reaction (1) used in Lee et al. (1996) and Millar et al. (1997) of $k_1=1\times10^{-9}\exp(-85/T)$ cm^3 s^{-1}.
[b]Calculated using the rate coefficient measured at room temperature by Scott et al. (1997) of $k=4.5\times10^{-10}$ cm^3 s^{-1}; see text.

occur in models utilizing the $H_3^+ + N$ reaction. The Langevin collision rate for reaction (6) is 1.6×10^{-9} cm^3 s^{-1}. Production of NH_3 via reaction (6) may be the major source at temperatures around 10 K, with both mechanisms having equal roles around 50 K. We add a cautionary note, however. Should current estimates of the rate coefficient for reaction (1) at low temperature be too high, then the $H_3^+ + N$ mechanism will have the dominant role.

2.3 Why should $H_3^+ + N$ be fast?

The theoretical study of the $H_3^+ + N$ surface by Herbst et al. (1987) predicted that reaction (6) has a large activation barrier, and concluded that the reaction was unimportant. Their argument was based on the fact that since N has ^4S symmetry and H_3^+ has $^1A_1'$ symmetry, these reactants must collide on a surface that is characterized by quartet multiplicity. The reactants cannot access the lowest ($^2A_2''$) electronic state of NH_3^+. With these constraints dictated by spin conservation, Herbst et al. (1987) concluded that the pathways they examined, corresponding to three different entrance and exit channel geometries, all contained barriers. We note, however, that Ferguson (1983) and Federer et al. (1986) have observed a number of fast ion–N atom reactions which do not conserve spin. We are examining other possibilities for reaction pathways on the NH_3^+ potential surface in an endeavour to find a possible path.

3 CONCLUSIONS

The detection for the first time of H_3^+ in the interstellar medium (Geballe & Oka 1996) at about the densities expected from models provides support for an ion–molecule mechanism of formation for some molecules known to be present in interstellar clouds. The recent laboratory measurement of the fast reaction between $H_3^+ + N$ forming $NH_2^+ + H$ provides a significant new source of NH_3 in cold dark clouds.

ACKNOWLEDGMENTS

We thank Eric Herbst, Robert Maclagan and Leon Phillips for helpful discussions, and the Marsden Fund for financial support.

REFERENCES

Adams N. G., Smith D., Millar T. J., 1984, MNRAS, 211, 857
Adams N. G. et al., 1991, J. Chem. Phys., 94, 4852
Anderson L. H., Heber O., Kella D., Pedersen H. B., Vejby-Christensen L., Zajfman D., 1996, Phys. Rev. Lett., 77, 4891
Bates D. R., 1986, ApJ, 306, L45
Bates D. R., 1987, in Kingston A. E., ed., Modern Applications of Atomic and Molecular Processes. Plenum, New York, p. 1
Bates D. R., 1989, ApJ, 344, 531
Bates D. R., 1991, J. Phys. B, 24, 3267
Bourlot J. Le., 1991, A&A, 242, 235
Cheung A. C., Rank D. M., Townes C. H., Thornton D. D., Welch W. J., 1968, Phys. Rev. Lett., 21, 1701
Dalgarno A., 1975, in Ausloos, P., ed., Interaction between Ions and Molecules. Plenum Press, New York, p. 341
Federer W., Villinger H., Lindinger W., Ferguson E. E., 1986, Chem. Phys. Lett., 123, 12
Ferguson E. E., 1983, Chem. Phys. Lett., 99, 89
Galloway E. T., Herbst E., 1989, A&A, 211, 413
Geballe T. R., Oka T., 1996, Nat, 384, 334
Graedel T. E., Langer W. D., Frerking M. A., 1982, ApJS, 48, 321
Herbst E., 1978, ApJ, 222, 508
Herbst E., Klemperer W., 1973, ApJ, 185, 505
Herbst E., DeFrees D. J., McLean A. D., 1987, ApJ, 321, 898
Herbst E., DeFrees D. J., Talbi D., Pauzat F., Koch W., McLean A. D., 1991, J. Chem. Phys., 94, 7842
Huntress W. T., 1977, ApJS, 33, 495
Irvine W. M., Goldsmith P. F., Hjalmarson A., 1987, in Hollenbach D. J., Thronson H. A., eds, Interstellar Processes. Reidel, Dordrecht, p. 561
Lee H. H., Bettens R. P. A., Herbst E., 1996, A&AS, 119, 111
Lias S. G., Bartmess J. E., Liebman J. F., Holmes J. L., Levin R. D., Mallard W. G., 1988, J. Phys. Chem. Ref. Data, 17, Suppl. 1
Marquette J. B., Rebrion C., Rowe B. R., 1988, J. Chem. Phys., 89, 2041
Millar T. J., Leung C. M., Herbst E., 1987, A&A, 183, 109
Millar T. J., DeFrees D. J., McLean A. D., Herbst E., 1988, A&A, 194, 250
Millar T. J., Farquhar P. R. A., Willacy K., 1997, A&AS, 121, 139
Morris M., Zuckerman B., Palmer P., Turner B. E., 1973, ApJ, 186, 501
Pauls T. A., Wilson T. L., Bieging J. H., Martin R. N., 1983, A&A, 124, 23
Pineau des Forêts G., Roueff E., Flowers D. R., 1990, MNRAS, 244, 668
Scott G. B. I., Fairley D. A., Freeman C. G., McEwan M. J., 1997, Chem. Phys. Lett., 269, 88
Williams T. L., Adams N. G., Babcock L. M., Herd C. R., Geoghegan M., 1996, MNRAS, 282, 413
Yee J. H., Lepp S., Dalgarno A., 1987, MNRAS, 227, 461